Genetic diversity and phenotypic heterogeneity in *Staphylococcus aureus* populations

Dissertation

der Mathematisch-Naturwissenschaftlichen Fakultät

der Eberhard Karls Universität Tübingen

zur Erlangung des Grades eines

Doktors der Naturwissenschaften

(Dr. rer. nat.)

vorgelegt von

Shilpa Elizabeth George

aus Mumbai, Indien

Tübingen

2019

Gedruckt mit Genehmigung der Mathematisch-Naturwissenschaftlichen Fakultät der Eberhard Karls Universität Tübingen.

Tag der mündlichen Qualifikation:	11.12.2019
Dekan:	Prof. Dr. Wolfgang Rosenstiel
1. Berichterstatter:	Prof. Dr. Christiane Wolz
2. Berichterstatter:	Prof. Dr. Andreas Peschel
3. Berichterstatter:	Prof. Dr. Haike Antelmann

Erklärung

Ich erkläre hiermit, dass ich die zur Promotion eingereichte Arbeit selbständig verfasst, nur die angegebenen Quellen und Hilfsmittel benutzt und Stellen, die wörtlich oder inhaltlich nach den Werken anderer Autoren entnommen sind, als solche gekennzeichnet habe. Eine detaillierte Abgrenzung meiner eigenen Leistungen von den Beiträgen meiner Kooperationspartner habe ich in „Declaration of author contribution“ vorgenommen.

……..

Unterschrift
Tübingen,

For my family

TABLE OF CONTENTS

Summary

Bacteria adapt to rapidly changing environments by increasing intra-population diversity. This may be accomplished through either phenotypic heterogeneity between genetically identical cells or by acquiring mutations which increase genetic diversity. We studied both these strategies within the human pathogen *Staphylococcus aureus* to understand how heterogeneity may serve as a strategy critical to survival within the human host.

The capsular polysaccharide (CP) has been known to protect against phagocytosis, but also impedes adherence to endothelial cells and matrix proteins. In persistent human carriers, we found a distinct sub-population of nasal *S. aureus* to be CP positive. In vitro, *cap* expression is also heterogeneous and strongly growth phase dependent. This peculiar temporal and bistable expression is regulated at the promoter level by several transcriptional activators and repressors to result in phenotypic heterogeneity in CP. These regulators are further modulated by environmental changes such as salt stress or shifts in energy metabolism. While *cap* expression is primarily SigB dependent, the Agr quorum sensing system also acts as a positive regulator via inactivation of Rot. Furthermore, CodY, Sae and Rot act synergistically to repress *cap* expression. The high degree of noise in capsule regulation may thus be due to the noise propagated from its many regulators.

The quorum sensing (QS) Agr system of *S. aureus* is a social trait based on bacterial population density that orchestrates the timely expression of secreted toxins crucial for virulence. Paradoxically, Agr-defective mutants are known to be selected during infection. We studied the selection and fitness of *agr* mutants under infection-relevant conditions such as antibiotic stress and hypoxia. In vitro evolution and competition experiments showed that *agr* mutants readily accumulate in a process that is accelerated by ciprofloxacin, while the wild type is retained in the population at low numbers. Under aerobic growth, the Agr-controlled PSM toxins are produced. These are toxic for Staphylococci and thus select for *agr* mutants, which are non-producers. Thus, the Agr-imposed fitness cost is not due to a metabolic burden but due to the ROS-inducing capacity of the PSMs and RNAIII-regulated factors. Contrastingly, hypoxia favours maintenance of QS and even allows hyper-activation of the system without imposing a fitness burden. Under aerobic conditions, rapid

emergence of *agr* negative mutants may provide the population with a fitness advantage while hypoxia permits QS maintenance and even affords increased toxin production. We propose that changing oxygen environments encountered during infection not only alters the virulence potential but also the course of microbial evolution of the *S. aureus* community.[1]

[1] *Parts of the Summary has been published in:*

- Phenotypic heterogeneity and temporal expression of the capsular polysaccharide in *Staphylococcus aureus*.
  George SE, Nguyen T, Geiger T, Weidenmaier C, Lee JC, Liese J, Wolz C
  Molecular Microbiology 2015 Dec;98(6):1073-88. doi: 10.1111/mmi.13174.

- Oxidative stress drives the selection of quorum sensing mutants in the Staphylococcus aureus population.
  George SE, Hrubesch J, Breuing I, Vetter N, Korn N, Hennemann K, Bleul L, Willmann M, Ebner P, Götz F, Wolz C
  PNAS 2019 Sep 17;116(38):19145-19154. doi: 10.1073/pnas.1902752116

Zusammenfassung

Mit Hilfe ihrer von intra-populärer Diversität sind Bakterien in der Lage, sich an rasch ändernde Umweltbedingungen anzupassen. Dies kann durch phänotypische Heterogenität zwischen genetisch identischen Zellen oder Mutationen, die die genetische Diversität erhöhen, erreicht werden.

Um zu verstehen wie Heterogenität als Strategie ausschlaggebend für das Überleben im menschlichen Wirt kann, wurden beide Strategien im Humanpathogen *Staphylococcus aureus* untersucht.

Es ist bereits bekannt, dass die Polysaccharidkapsel (CP) vor Phagozytose schützt, gleichzeitig aber auch das Anhaften an Endothelzellen und Matrixproteine verhindert. Wir konnten zeigen, dass in Menschen, die nasal dauerhaft mit *S. aureus* besiedelt sind, eine CP-positive Subpopulation existiert. Die *cap* Expression ist i*n vitro* ebenfalls heterogen und stark abhängig von der Wachstumsphase. Diese eigenartige temporäre und bistabile Expression wird auf der Promoter-Ebene durch verschiedene Transkriptionsaktivatoren und –repressoren reguliert, woraus letztlich die phänotypische Heterogenität der Polysaccharidkapsel resultiert. Darüber hinaus werden diese Regulatoren durch sich ändernde Umwelteinflüsse wie Salzstress oder Veränderungen im Energiemetabolismus moduliert. Während die *cap* Expression hauptsächlich SigB-abhängig ist, agiert das Agr Quorum sensing System zusätzlich als positiver Regulator, indem es Rot inaktiviert. Zusätzlich agieren CodY, Sae und Rot synergistisch um die *cap* Expression zu reprimieren. Die Ursache für den hohen Grad an stochastischer Variation in der Regulation der Poysaccharidkapsel könnte demnach auf die Vielzahl an Regulatoren zurückzuführen sein.

Das Quorum sensing (QS) System Agr in *S. aureus* dient dazu die zeitlich Expression von sekretierten Toxinen die entscheiden für die Virulenz sind, basierend auf der Dichte der Bakterienpopulation, zu koordinieren. Es ist bekannt, das paradoxerweise Agr-defekte Mutanten während der Infektion selektiert werden. Wir haben die Selektion und Anpassung von *agr* Mutanten unter infektionsrelevanten Bedingungen wie Antibiotika-Stress und Hypoxie untersucht. *In vitro* Evolutions- und Kompetitionsexperimente konnten zeigen, das *agr* Mutanten mittels Ciprofloxacin sich schneller anhäufen, während der Wildtyp innerhalb der

Population in geringer Anzahl erhalten bleibt. Unter aerobem Wachstum werden die *agr*-regulierte PSM Toxine gebildet.

PSMs sind toxisch für Staphylokokken. Folglich üben sie einen Selektionsdruck aus und *agr* Mutanten, die keine PSMs mehr bilden, werden favorisiert. Somit sind die durch Agr entstandenen Anpassungsnachteile nicht auf eine Stoffwechsellast, sondern auf die ROS-induzierende Kapazität der PSMs und der RNAIII-regulierten Faktoren, zurückzuführen. Im Gegensatz dazu begünstigt Hypoxie die Aufrechterhaltung des QS und ermöglicht sogar eine Hyperaktivierung des Systems, ohne die Anpassungsfähigkeit zu beeinträchtigen. Unter aeroben Bedingungen kann das schnelle Auftreten von *agr*-negativen Mutanten der Population einen Fitnessvorteil verschaffen, während Hypoxie die Aufrechterhaltung des QS erlaubt und sogar eine erhöhte Toxinproduktion ermöglicht. Hiermit zeigen wir, dass die sich ändernde Sauerstoffversorgung während der Infektion nicht nur das Virulenzpotential, sondern auch den Verlauf der mikrobiellen Evolution der *S. aureus* Gemeinschaft verändert.

List of publications

- **Publication 1 (Research Article):**
  Phenotypic heterogeneity and temporal expression of the capsular polysaccharide in *Staphylococcus aureus*.
  George SE, Nguyen T, Geiger T, Weidenmaier C, Lee JC, Liese J, Wolz C
  Molecular Microbiology 2015 Dec;98(6):1073-88. doi: 10.1111/mmi.13174.

- **Publication 2 (Research Article):**
  Wall teichoic acids mediate increased virulence in *Staphylococcus aureus*.
  Wanner S, Schade J, Keinhörster D, Weller N, **George SE**, Kull L, Bauer J, Grau T, Winstel V, Stoy H, Kretschmer D, Kolata J, Wolz C, Bröker BM, Weidenmaier C
  Nature Microbiology 2017 Jan 23;2:16257. doi: 10.1038/nmicrobiol.2016.257.

- **Publication 3 (Research Article):**
  Inactivation of TCA cycle enhances *Staphylococcus aureus* persister cell formation in stationary phase.
  Wang Y, Bojer MS, **George SE**, Wang Z, Jensen PR, Wolz C, Ingmer H
  Scientific reports 2018 Jul 18;8(1):10849. doi: 10.1038/s41598-018-29123-0.

- **Publication 4 (Research Article):**
  Revisiting the regulation of the capsular polysaccharide biosynthesis gene cluster in *Staphylococcus aureus*.
  Keinhörster D, Salzer A, Duque-Jaramillo A, **George SE**, Marincola G, Lee JC, Weidenmaier C, Wolz C.
  Molecular Microbiology 2019 Jul 8. doi: 10.1111/mmi.14347.

- **Publication 5 (Review Article):**
  Function and regulation of *Staphylococcus aureus* wall teichoic acids and capsular polysaccharides.
  Keinhörster D, **George SE**, Weidenmaier C, Wolz C.
  Int J Med Microbiol. 2019 Jul 18:151333. doi: 10.1016/j.ijmm.2019.151333.

- **Publication 6 (Research Article):**
  Oxidative stress drives the selection of quorum sensing mutants in the *Staphylococcus aureus* population.
  George SE, Hrubesch J, Breuing I, Vetter N, Korn N, Hennemann K, Bleul L, Willmann M, Ebner P, Götz F, Wolz C
  PNAS 2019 Sep 17;116(38):19145-19154. doi: 10.1073/pnas.1902752116

Declaration of personal contribution to publications

- **Publication 1:** Phenotypic heterogeneity and temporal expression of the capsular polysaccharide in *Staphylococcus aureus*.
  I contributed to the design and execution of experiments. I performed and analysed all experiments with the exception of the ex vivo analysis of nasal swabs, cloning of the fluorescent vectors pJL53 and pCG318, and creation of quorum sensing constitutive and deletion mutants. I wrote the paper together with Christiane Wolz.

- **Publication 2:** Wall teichoic acids mediate increased virulence in *Staphylococcus aureus*.
  I participated in creating the *rot* mutants.

- **Publication 3:** Inactivation of TCA cycle enhances *Staphylococcus aureus* persister cell formation in stationary phase.
  I created the dual promoter- fluorescent reporter plasmid. I performed and analysed the promoter activity correlation experiments. I participated in writing and reviewing the manuscript.

- **Publication 4:** Revisiting the regulation of the capsular polysaccharide biosynthesis gene cluster in *Staphylococcus aureus*.
  I contributed to the conception and design of the study. I contributed to the acquisition, analysis and interpretation of the data. I developed tools and methods used in this study. This includes the design and creation of dual promoter-fluorescent reporter constructs and, microscopy and multi-plate reader techniques to evaluate fluorescence at the single cell and population level. I supervised the acquisition and processing of microscopy images.

- **Publication 5:** Function and regulation of *Staphylococcus aureus* wall teichoic acids and capsular polysaccharides.
  I participated in writing this review article and contributed figure 2.

- **Publication 6:** Oxidative stress drives the selection of quorum sensing mutants in the *Staphylococcus aureus* population.
  I contributed to the conception, design and execution of experiments. All experiments were performed or supervised and subsequently analysed by me. The cytotoxicity assay and western blot for aldolase was generated in collaboration with co-authors. I wrote the paper together with Christiane Wolz.

Introduction

Parts of this Introduction section have been published in:

- Phenotypic heterogeneity and temporal expression of the capsular polysaccharide in *Staphylococcus aureus*.
  George SE, Nguyen T, Geiger T, Weidenmaier C, Lee JC, Liese J, Wolz C
  Molecular Microbiology 2015 Dec;98(6):1073-88. doi: 10.1111/mmi.13174.

- Oxidative stress drives the selection of quorum sensing mutants in the Staphylococcus aureus population.
  George SE, Hrubesch J, Breuing I, Vetter N, Korn N, Hennemann K, Bleul L, Willmann M, Ebner P, Götz F, Wolz C
  PNAS 2019 Sep 17;116(38):19145-19154. doi: 10.1073/pnas.1902752116

Bacterial communities and intra-population heterogeneity

Bacteria are never alone despite being unicellular life forms, due to the alacrity with which they divide to conquer every ecological niche. While faced with a rapidly changing environment, bacteria have prospered because of the ability to adapt quickly to stress situations. From nutrient limitation to antibiotic antagonism – bacteria have evolved over the last 3.5 million years to efficiently prevail.

Often such adaptation involves spontaneous mutations wherein the resulting genetic variant possesses traits that improve fitness in the prevailing environment. Another adaptive response is phenotypic variability between individual cells within a genetically homogeneous population. Environmental changes that drive or fix such adaptation can range from variations in nutrient availability, oxygen tension and encounters with either predators or host defences. Heterogeneous adaptation may occur either; prior to or as a consequence of the environmental change (Davis & Isberg, 2016). The first instance has been described as bet-hedging in which pre-existing variability in the population ensures that a subset of individuals survive and propagate under any conditions (Veening et al, 2008). In the second instance, the environmental change might itself drive heterogeneity through an altered gene expression profile resulting in phenotypic variability, or a mutational event resulting in genetic diversity within the population.

Phenotypic heterogeneity

Phenotypic heterogeneity in otherwise genetically identical populations has been reported across bacterial genera inhabiting a variety of ecological niches. Several reasons have been proposed for why this behaviour has evolved (Ackermann, 2015).

In a strategy described as 'bistability', bacteria switch phenotypes to hedge their bets thereby ensuring population survival if the environment changes (Dubnau & Losick, 2006).

A well-studied example is the bistability of the competence system in *Bacillus subtilis* (Leisner et al, 2008; Maamar et al, 2007; Xi et al, 2013) wherein the transcriptional activator ComK is highly expressed in just 10-20% of cells in the bacterial population. This triggers the activation of over a 100 genes that permit transient competence whereby extracellular DNA is taken up and integrated into the bacterial genome. ComK is activated via quorum sensing and positively auto-regulates itself in a positive feedback loop (Maamar & Dubnau, 2005). Several molecular players act to fine-tune the protein levels of ComK relative to the threshold required for triggering competence. Transcription of *comK* is negatively regulated by the repressors AbrB, Rok and CodY (Hamoen et al, 2003; Hoa et al, 2002; Serror & Sonenshein, 1996) and positively regulated by DegU (Hamoen et al, 2000). Post-translationally, MecA binds free ComK and this complex is then processed by Clp-proteases (Prepiak & Dubnau, 2007). Degradation of ComK below a critical threshold signals an exit out of competence. However, ComS which is also regulated by quorum sensing competes with ComK for binding to MecA which releases ComK to positively regulate its own transcription again (Smits et al, 2005). Thus, a complex regulatory network functions at the transcriptional and post-translational level to signal the switch to competence in a sub-population of *Bacillus subtilis*.

In a second strategy different from that of 'bistability' detailed above, distinct sub-populations in bacterial biofilms 'specialize' at certain tasks and through division of labour cooperate for better survival of the community (Dragos et al, 2018). Moreover, while there are several instances of phenotypic heterogeneity that are unique and therefore restricted to specific bacterial species, some examples are widespread across genera. Antibiotic persistence is one such example which is prevalent among bacterial pathogens and has direct relevance to infection outcomes (Balaban et al, 2019). Here, a sub-population survives a bactericidal concentration of an antibiotic but cells regrown from such persisters are still sensitive to the antibiotic.

The root of most instances of phenotypic heterogeneity is the inherent fluctuation in the biochemical signals within individual cells. Such stochastic variation has been termed 'noise' (Balazsi et al, 2011; Bidnenko & Bidnenko, 2018; Eling & Morgan, 2019). Gene expression noise manifests into noise in protein copy numbers which directly impacts signal transduction within a given regulatory network. Expression noise may be due to intrinsic or extrinsic sources (Eldar & Elowitz, 2010; Elowitz et al, 2002; Kim & Jacobs-Wagner, 2018; Ozbudak et al, 2002; Sanchez et al, 2011; Swain et al, 2002; Tsimring, 2014) (Fig. 1). Intrinsic noise refers to intrinsically random nature of chemical reactions involved in transcription and translation while cell-to-cell variations in gene copy number, regulators, polymerases, and other global factors together comprise extrinsic noise. With the recent advancements in single-cell techniques, the description and understanding of cell-to-cell phenotypic variability within a bacterial population has become a major focus of research (Davis & Isberg, 2016; Leygeber et al, 2019).

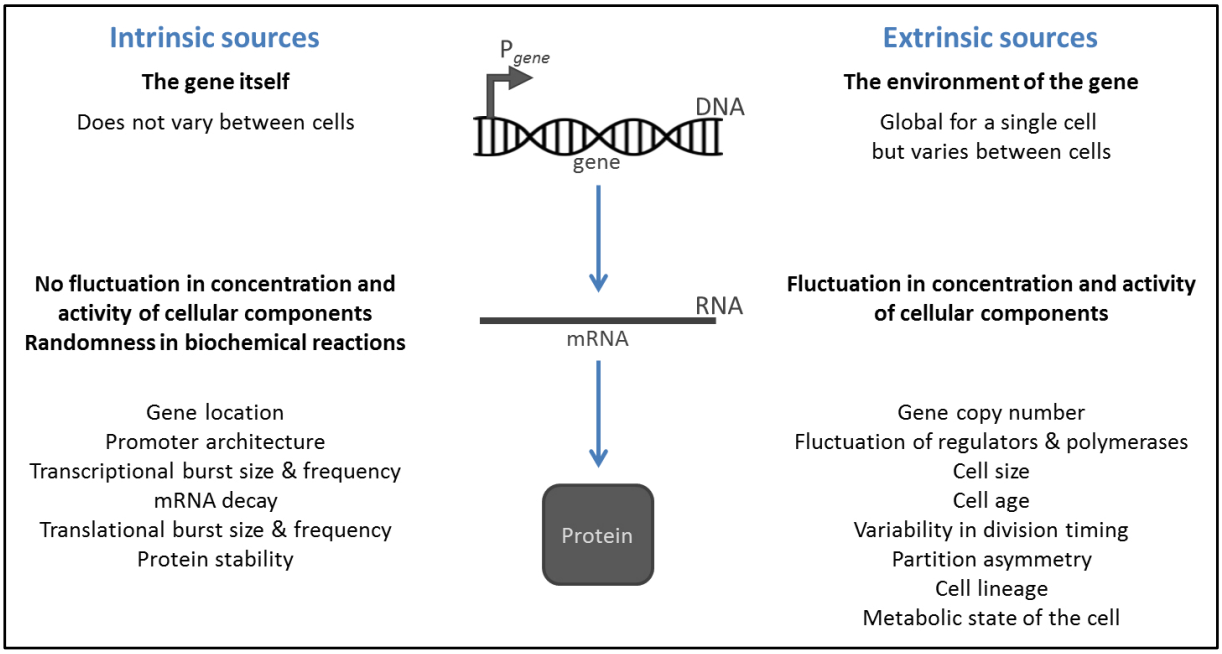

Figure 1: Noise in biological systems. Sources of noise may be intrinsic or extrinsic. Intrinsic sources are factors that pertain to the gene itself which does not vary between cells. Noise in this instance is due to random molecular events that influence biochemical reactions. Extrinsic sources are all the factors in the environment of the gene and therefore global for a given cell while still varying between cells. Noise in this instance is due to fluctuations in concentration and activity of cellular components as well as the metabolic state of the cell.

Genetic heterogeneity

Genetic divergence can occur due to random genetic drift or through a strong selection pressure to adapt; especially if a phenotypic response is unable to tide the bacterial population over the environmental change (Davis & Isberg, 2016; Ryall et

al, 2012). The bacterial genome is hard-wired to replicate its genome with high fidelity, however, mutation rates increase under strong selection pressures imposed by environmental stress (Hershberg, 2015; Ram & Hadany, 2014; Ryall et al, 2012). For example, bacterial pathogens often encounter genotoxic molecules such as reactive oxygen species (ROS) or reactive nitrogen species (RNS) while confronted with host defences during colonisation or infection (Fang et al, 2016). The inability of DNA repair mechanisms such as base excision repair (BER), nucleotide excision repair (NER) or mismatch repair (MMR) pathways to cope with the environmental insult gives way to error-prone repair associated with the SOS response and results in the accumulation of mutations (van der Veen & Tang, 2015). These mutations may subsequently be selected and maintained if suited to the changing environment as seen in the acquisition of antibiotic resistance in response to ROS insult (Dwyer et al, 2009). Interestingly, loss of function mutations in the MMR system which lead to the emergence of 'hypermutator' genotypes are often isolated in late stages of cystic fibrosis (CF) and are known to possess an increased resistance to antibiotics (Oliver & Mena, 2010). Two proteins LexA and RecA are central to the SOS response (Maslowska et al, 2019). Under normal conditions, the LexA transcriptional repressor binds to the promoter region of SOS genes; thereby preventing their expression. DNA damage results in the generation of single stranded DNA to which RecA binds to form the activated RecA nucleoprotein filament. The RecA filament subsequently induces auto-cleavage of the LexA repressor. There are about 40 genes known to be involved in SOS repair in *E. coli*. Most of these genes are involved in error-free DNA repair, including base excision repair (BER) and nucleotide excision repair (NER). If the DNA damage levels exceed the ability of error-free pathways to complete repair and restart replication, the mutagenic phase of SOS is triggered and mediated by error-prone DNA polymerases that replicate lesions in the template. The genes comprising the SOS regulon vary amongst bacterial species (Baharoglu & Mazel, 2014). There is only a single LexA-regulated polymerase identified among the 16 SOS genes identified in *S. aureus* (Cirz et al, 2007). Furthermore, several antibiotics can induce the SOS response. Persisters derived from fluoroquinolone treatment showed high SOS responses and subsequently a greater quantity of antibiotic resistant mutants (Barrett et al, 2019).

Gene amplification, either on the chromosome or via multicopy plasmids, is a strategy by which reversible genetic variation leads to increases in gene dosage of a beneficial gene (Andersson et al, 2015; Rodriguez-Beltran et al, 2018). In *Salmonella enterica*, a parental gene is amplified to a high copy number, and the amplified gene copies accumulate mutations that provide specialization and increased fitness (Nasvall et al, 2012). Selection subsequently maintains beneficial mutant alleles while the less-beneficial gene copies are allowed to be lost. Both tandem gene amplifications, as well as mutations such as single nucleotide polymorphisms (SNPs) and, insertions or deletions (indels) form the genetically encoded basis for antibiotic heteroresistance wherein a sub-population of bacterial cells possess reduced antibiotic susceptibility (Andersson et al, 2019). Chromosomal rearrangements resulting in reversible genomic instability was recently demonstrated to be the underlying mechanism of small-colony variant phenotypic switching in *S. aureus* (Guerillot et al, 2019).

Genetic heterogeneity within a clonal population is exemplified by the opportunistic pathogen *Pseudomonas aeruginosa*. During short-term growth in biofilm communities, *P. aeruginosa* undergoes considerable genetic variation to produce an 'insurance effect' (Boles et al, 2004) predicted to protect the community against adverse conditions. In chronic infections such as cystic fibrosis (CF), genetic variants of *P. aeruginosa* co-exist in the lung where quorum sensing defective LasR mutants are commonly isolated (Feltner et al, 2016). This diversity in the CF lung is often attributed to antibiotics, ROS and encounters with host defence (Malhotra et al, 2019). Quorum sensing (QS) in *Pseudomonas aeruginosa* has been well studied and consists of two acyl-homoserine lactone (AHL) systems, the LasRI and the Rh1RI systems and a third non-AHL QS system, the *Pseudomonas* quinolone signal (PQS). These QS systems control a variety of extracellular virulence factors such as proteases and exotoxins which are referred to as 'public goods'. Therefore, LasR mutants have been called 'cheaters' because they benefit from the proteases produced by the QS functional wild type sub-population without the cost of producing them (Sandoz et al, 2007; West et al, 2006).

Finally, both genetic and phenotypic strategies may act in synergy for optimal adaptation to environmental change. Stochastic phenotype switching has been described to facilitate or even speed up genetic evolution (Tadrowski et al, 2018) and

when natural selection acts on epigenetic variation in addition to genetic variation, populations adapt faster, and adaptive phenotypes can arise before any genetic changes occur (Klironomos et al, 2013).

Staphylococcus aureus – Does population heterogeneity enable dual lifestyles?

Among the pathogenic bacteria, *Staphylococcus aureus* is known for its dual lifestyle within the human host – as a relatively quiescent colonizer residing primarily in the nose or an aggressive pathogen whereby *S. aureus* is the leading cause of bacteremia and infective endocarditis as well as skin and soft tissue, pleuropulmonary, and device-related infections (Tong et al, 2015). The organism encounters a fluctuating environment in terms of nutrition, oxygen and pH at different sites of infection in the human host (Balasubramanian et al, 2017; Richardson et al, 2015). The ability to adapt to these diverse environments has been attributed to a formidable arsenal of virulence and immune-evasion mechanisms (Ferry et al, 2005) (Fig. 2). However, little is known about the role of population heterogeneity in the human pathogen *Staphylococcus aureus* (Garcia-Betancur & Lopez, 2019). Specifically how this might shape the colonization or infection potential of the pathogen has not been explored extensively. In the next section, phenotypic and genetic heterogeneity in the context of *S. aureus* will be introduced.

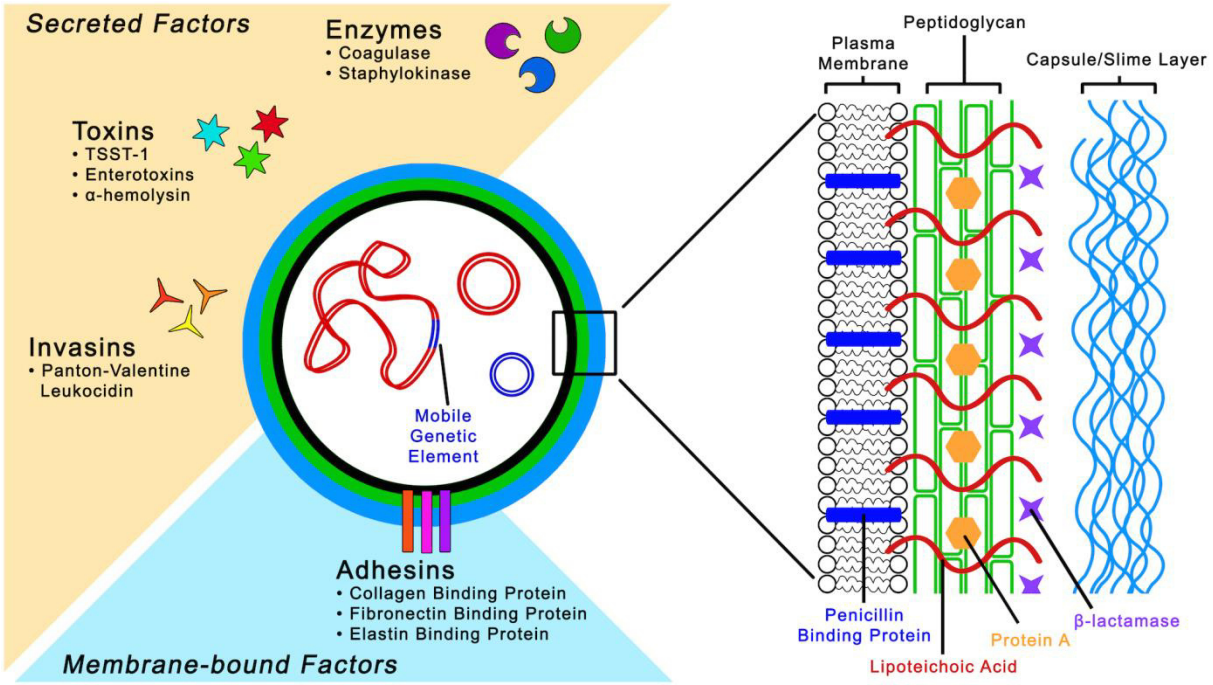

Figure 2: Virulence determinants of *Staphylococcus aureus*.
Staphylococcus aureus has a complex cell wall structure composed of a thick peptidoglycan layer and polysaccharide capsule. In addition, *S. aureus* possesses an elaborate arsenal of surface-associated and secreted virulence factors involved in toxin production, adherence to and invasion of host tissue, and immune evasion. (Kong & Johnson, 2016)

Phenotypic heterogeneity in capsular polysaccharide production

The capsular polysaccharide (CP) is an extracellular polysaccharide forming a thick layer as the outermost layer of the cell envelope. Most *S. aureus* strains contain either a *cap5A-P* or a *cap8A-P* gene cluster which encode enzymes for the most prevalent capsular serotypes, CP5 and CP8 respectively [Reviewed in, Weidenmaier & Lee, 2017 and publication no. 5 in this thesis: Keinhorster et al, 2019a]. The *cap5* and *cap8* gene clusters are almost identical differing only in the central genes *capHIJK* which bear little homology to each other and are type-specific. The *cap* operon is transcribed by one principal promoter (P_{cap}) in front of *capA* (Herbert et al, 2001; Sau et al, 1997). P_{cap} activity usually correlates with CP synthesis, indicating that regulation occurs predominantly on the transcriptional level.

The presence or absence of capsule in vivo has both been reported to be advantageous for *S. aureus* pathogenicity depending on the infection setting. Virulence studies using encapsulated and non-encapsulated *S. aureus* strains reveal that, depending on the animal model used, CP either enhances or attenuates virulence (O'Riordan & Lee, 2004; Tuchscherr et al, 2010). CP enhances virulence in murine models of bacteraemia (Thakker et al, 1998; Watts et al, 2005), septic arthritis (Nilsson et al, 1997), abscess formation (Portoles et al, 2001), and surgical wound infection (McLoughlin et al, 2006). In contrast, in mammary gland infections (Tuchscherr et al, 2005) and in catheter-induced endocarditis (Baddour et al, 1992; Nemeth & Lee, 1995) CP mutants are more virulent. This is likely because CPs are anti-phagocytic (Nanra et al, 2013; Thakker et al, 1998) but also inhibit the adherence of the underlying cell wall proteins to their specific target molecule, endothelial cells and/or matrix proteins (Pohlmann-Dietze et al, 2000; Risley et al, 2007). CP negative *S. aureus* strains are frequently isolated from patients with osteomyelitis, mastitis or cystic fibrosis, suggesting that loss of CP expression may be advantageous for *S. aureus* during chronic infection (Herbert et al, 1997; Lattar et al, 2009; Tuchscherr et al, 2010). Contrary to immune-evasion, the zwitterionic charge motif (ZPSs) of the capsular polysaccharide has been shown to stimulate CD4+ T cells through association with MHC-II (Kalka-Moll et al, 2002).

S. aureus is able to tightly control CP synthesis by various regulatory mechanisms in order to adapt to the changing infectious environments (O'Riordan & Lee, 2004). Heterogeneity of CP expression within a given bacterial culture was described by

immune labelling of bacteria using flow cytometry (Poutrel et al, 1997) and immunofluorescence (Pohlmann-Dietze et al, 2000) where only the non-encapsulated bacterial fraction was found to bind to endothelial cells (Pohlmann-Dietze et al, 2000). Such cell-cell phenotypic variation within the bacterial population may allow *S. aureus* to bet-hedge and thrive in diverse environments encountered in the human host.

Genetic diversity in quorum sensing Agr system

The virulence factors comprising the *S. aureus* virulon are regulated in a highly coordinated growth phase dependent manner. In staphylococci, a two-component quorum sensing system known as the *agr* (accessory gene regulator) system governs the expression of these virulence factors (Bronesky et al, 2016; Kavanaugh & Horswill, 2016; Novick & Geisinger, 2008; Wang & Muir, 2016). At high cell density, the expression of surface or cell wall associated virulence factors are generally repressed by Agr. However, secreted factors are induced by Agr. The well-studied *agr* locus is transcribed from two divergent promoters P2 and P3 (Fig. 3). The P2 transcript (RNAII) encodes Agr B, D, C and A. AgrB and AgrD combine to produce an autoinducing peptide (AIP) which is secreted out of the cell and acts as the ligand for AgrC. When the AIP accumulates at high cell density, it binds the membrane-bound histidine kinase AgrC, which auto-phosphorylates at a conserved histidine and transfers the phosphate group to an aspartate on the response regulator AgrA. Phosphorylated AgrA triggers transcription of its own operon (*agrBDCA*) as well as the divergently transcribed regulatory RNAIII from the adjacent P3 promoter. The haemolysins are under the control of RNAIII (Bronesky et al, 2016) and RNAIII itself also encodes a small peptide, δ-haemolysin, Hld (Janzon & Arvidson, 1990; Janzon et al, 1989). RNAIII as a regulatory RNA is the main effector of the Agr system. Regulation of several virulence genes is achieved indirectly through the global regulator Rot (repressor of toxins). Rot acts as a repressor of enterotoxin B (*seb*), alpha-toxin (*hla*), proteases encoded by the *spl* and *ssp* operons, and lipase (*geh*). Rot also acts as a positive regulator of some virulence factors such as Protein A. RNAIII binds *rot* mRNA to prevent its translation, thereby altering the expression of downstream genes.

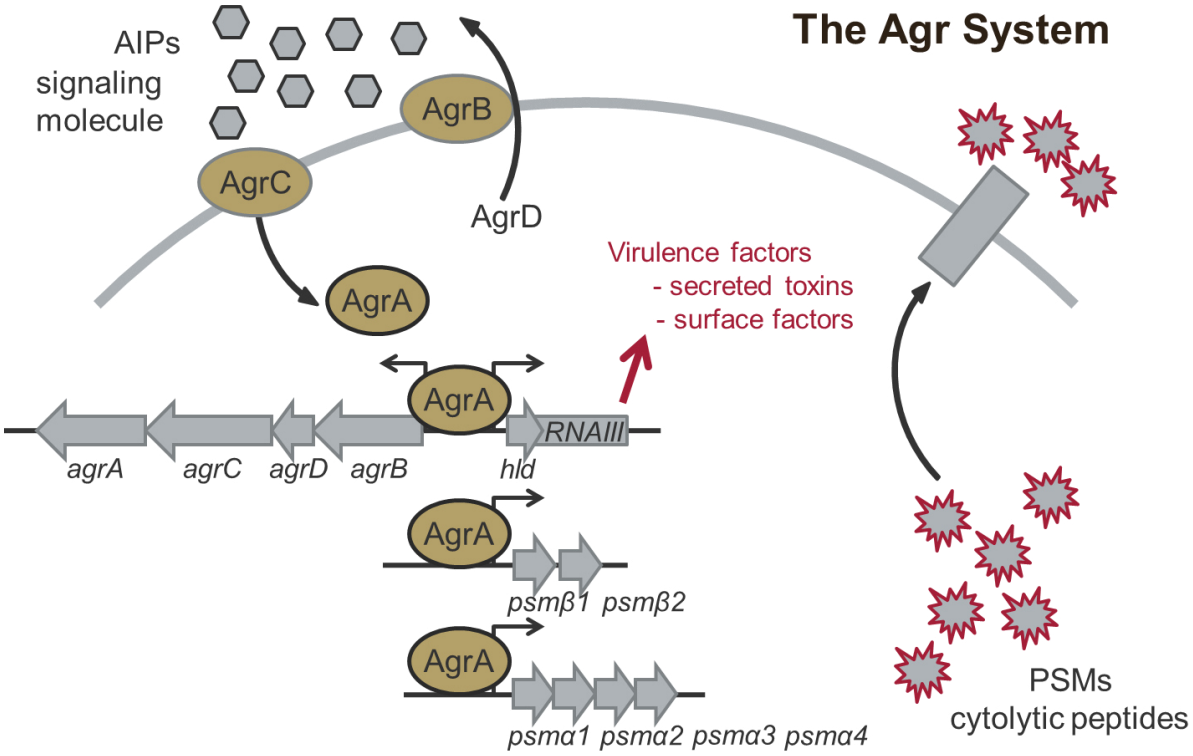

Figure 3: Quorum sensing in *Staphylococcus aureus* – The Agr system
The *agr* locus comprises the *agrBDCA* operon and the divergently transcribed RNAIII molecule which also encodes δ-haemolysin (Hld). The autoinducing peptide (AIP) is encoded by *agrD*. Accumulation of extracellular AIP results in auto-phosphorylation of the histidine kinase AgrC and phosphotransfer to the response regulator AgrA. Phosphorylated AgrA triggers transcription of its own operon (*agrBDCA*) as well as RNAIII. AgrA also binds to the promoters of the *psm* operons, *psmα* and *psmβ* coding for the PSMs; PSMα1-4 and PSMβ1-2 respectively.

The response regulator AgrA also binds to the promoters of the *psm* operons, *psmα* and *psmβ* coding for the phenol-soluble modulins; PSMα1-4 and PSMβ1-2 respectively (Fig. 3) (Queck et al, 2008). Hld and PSMs are a family of amphipathic, alpha-helical peptides that have multiple roles in staphylococcal pathogenesis and contribute a large extent to the pathogenic success of virulent staphylococci (Cheung et al, 2014). They are cytotoxic, stimulate inflammatory responses and contribute to biofilm dissemination (Peschel & Otto, 2013). However, PSMs and Hld may also interfere with bacteria. Hld and proteolytically processed derivatives of PSMα1 and PSMα2 possess antimicrobial activity against *Streptococccus pyogenes* (Cogen et al, 2010; Joo et al, 2011). They also interact with the producer's own membrane and promote the release of membrane vesicles from the cytoplasmic membrane via an increase of membrane fluidity (Schlatterer et al, 2018; Wang et al, 2018a). Recently, PSMs were also shown to reduce persister formation (Bojer et al, 2018; Xu et al, 2017). The antibacterial effect of PSMs is further supported by the necessity for the producer to protect itself from PSMs by the specific Pmt export system (Chatterjee et

al, 2013). Agr has been proven to be essential for virulence in several animal models (Le & Otto, 2015; Painter et al, 2014; Shopsin & Copin, 2018). Recently, Agr activity was also shown to be required for colonisation of the human gastro-intestinal tract (Piewngam et al, 2018). Many reports emphasize that Agr dependent factors such as α-haemolysin (Berube & Bubeck Wardenburg, 2013) and PSMs (Cheung et al, 2014) are major virulence determinants. Correspondingly, the highly virulent community-acquired methicillin-resistant *S. aureus* (caMRSA) strains such as MW2 and USA300 are characterized by high Agr activity (Wang et al, 2007). However, several lineages of healthcare-acquired MRSA (haMRSA) strains and many clinical isolates were shown to have low or no Agr activity (Shopsin & Copin, 2018; Wang et al, 2007). Agr-defective mutants also accumulate within the host e.g. during chronic infections (Goerke et al, 2000; Soong et al, 2015; Suligoy et al, 2018) or during persistent bacteraemia (Fowler et al, 2004; Giulieri et al, 2018; Young et al, 2017) and were even linked to higher mortality in bacteraemic patients (Schweizer et al, 2011). The use of certain antibiotics such as fluoroquinolones seems to select for *agr* mutants not only in vitro (Paulander et al, 2013; Schroder et al, 2013) but also during treatment (Butterfield et al, 2011). Of note, *agr* positive and *agr* negative strains often coexist in clinical samples (Goerke et al, 2007; Traber et al, 2008) or in animal models (He et al, 2019) suggesting that there are mechanisms at play keeping producer and cheater in balance. Thus, there is now compelling evidence for contrary roles of Agr during different stages of colonisation or infection. The selection pressures and mechanisms that shape the bacterial population; tilting either toward a net Agr function or dysfunction have not been defined.

Research objective

Staphylococcus aureus populations have been observed to undergo in vivo adaptation that employs both phenotypic and genotypic strategies (Fig. 4).

In previous work from our lab, immunofluorescence was used to determine whether S. *aureus* sampled from the noses of persistently-colonised human carriers were capsular polysaccharide positive. Only a sub-population of bacteria identified by fluorescence in-situ hybridization to be S. *aureus*, were found to be CP positive thus demonstrating phenotypic heterogeneity within the in vivo population (subsequently published in George et al, 2015).

Also in prior work from our lab, sputum samples from cystic fibrosis patients were plated on blood agar to reveal tremendous diversity between colonies with regard to haemolysis. The non-haemolytic population were identified to be genetic mutants in the quorum sensing system Agr (Goerke et al, 2007).

In this work, I have investigated both these strategies as exemplified by capsular polysaccharide synthesis and the accumulation of spontaneous quorum sensing mutants. The regulatory and environmental factors underpinning both observations were studied with the aim to understand the basis and subsequently the benefit in maintaining such heterogeneity within the population.

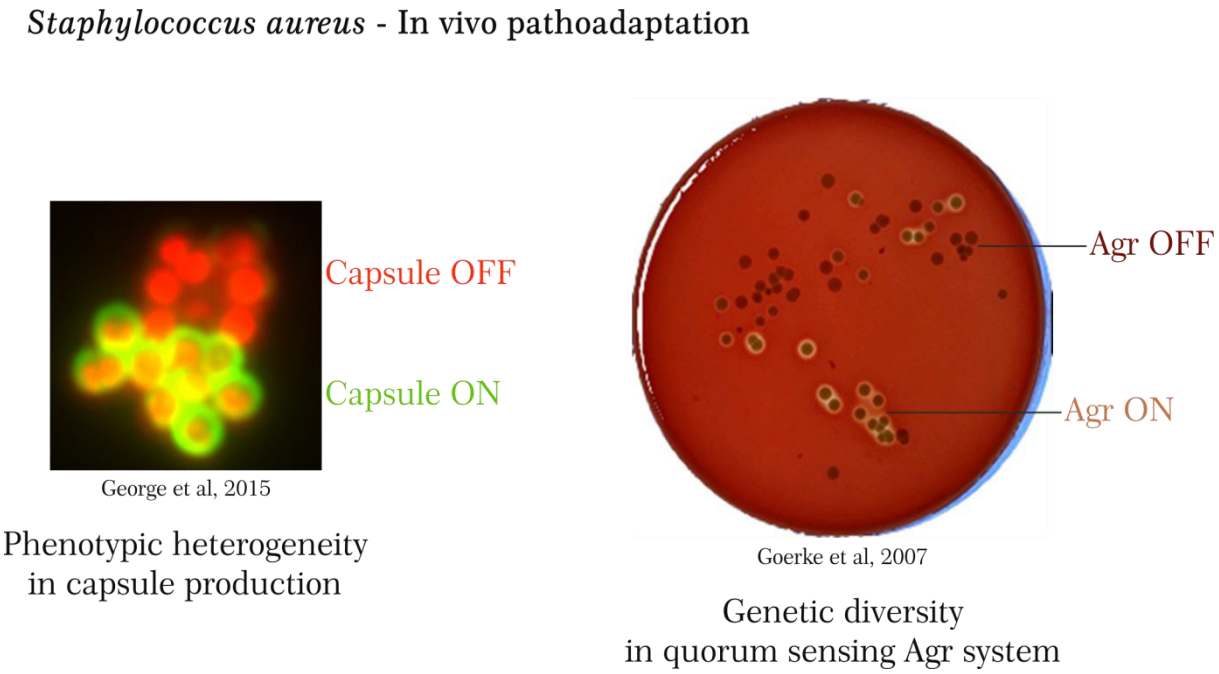

Figure 4: Heterogeneity within *Staphylococcus aureus* populations during in vivo pathoadaptation

Results and Discussion – I

Phenotypic heterogeneity and temporal expression of capsule

Parts of this Result and Discussion section have been published in:

- Phenotypic heterogeneity and temporal expression of the capsular polysaccharide in *Staphylococcus aureus*.
  George SE, Nguyen T, Geiger T, Weidenmaier C, Lee JC, Liese J, Wolz C
  Molecular Microbiology 2015 Dec;98(6):1073-88. doi: 10.1111/mmi.13174.
- Inactivation of TCA cycle enhances *Staphylococcus aureus* persister cell formation in stationary phase.
  Wang Y, Bojer MS, **George SE**, Wang Z, Jensen PR, Wolz C, Ingmer H
  Scientific reports 2018 Jul 18;8(1):10849. doi: 10.1038/s41598-018-29123-0.
- Revisiting the regulation of the capsular polysaccharide biosynthesis gene cluster in *Staphylococcus aureus*.
  Keinhörster D, Salzer A, Duque-Jaramillo A, **George SE**, Marincola G, Lee JC, Weidenmaier C, Wolz C.
  Molecular Microbiology 2019 Jul 8. doi: 10.1111/mmi.14347.
- Function and regulation of *Staphylococcus aureus* wall teichoic acids and capsular polysaccharides.
  Keinhörster D, **George SE**, Weidenmaier C, Wolz C.
  Int J Med Microbiol. 2019 Jul 18:151333. doi: 10.1016/j.ijmm.2019.151333.

Results:

Role of QS in temporal *cap* expression (George et al, Mol. Micro 2015)

Previous results showed that *S. aureus* sampled from the noses of persistently-colonised human carriers were CP positive. Moreover, only a sub-population of bacteria identified to be *S. aureus*, were found to be CP positive - even within a single cluster of bacteria. The individuals tested (A, B and C; George et al, 2015) were colonised with different *S. aureus* clones. This indicates that the heterogeneous expression of CP in vivo is a general feature of *S. aureus* and not related to a certain CP type or clonal complex.

The expression of *cap* was previously shown to be maximum in late growth phase and also dependent on the QS system, Agr (Dassy et al, 1993; Luong et al, 2002; Pohlmann-Dietze et al, 2000). We analysed whether the Agr system might be the primary trigger for the temporal and heterogeneous expression of CP synthesis within the bacterial population. We constructed strains in which the *agr* locus was either deleted or rendered constitutive independent of the autoinducing peptide AIP. First, RNAIII was expressed under an artificial *recA* promoter, from which the LexA binding motif was deleted (pRNAIII). The activation of this promoter was shown to be independent of the SOS response (Schroder et al, 2014) and is active mainly in

bacteria in the exponential phase of growth. In the second approach, a single point mutation was introduced in the native chromosomal *agrC* ($AgrC^{R238H}$) which rendered the enzyme constitutively active (Geisinger et al, 2009). For growth experiments, bacteria were grown in LB broth to an optical density at OD_{600} of 0.5 and then again diluted (1:10) to ensure that most bacteria entered the exponential growth phase. Bacteria were then analysed at an OD_{600} of 0.3 (T1) and after 2 h (T2,), 3 h (T3), 4 h (T4) or after growth overnight (T5) (Fig. 5A). The expression of the Agr effector molecule, RNAIII, from the different constructs was analysed by Northern blot. As intended, RNAIII expression was found to increase during growth in the WT, to decrease in the pRNAIII complemented *agr* mutant and to be constitutive in the $agrC^{R238H}$ mutant (Fig. 5B).

We next analysed whether *cap* expression correlated to RNAIII and/or the growth phase. At the indicated time points, *capA* mRNA was quantified by qRT-PCR (Fig. 5C). In all strains analysed *cap* expression significantly increased after bacteria had entered the mid-exponential growth phase. The *agr* mutant showed an 11-fold decrease of *cap* expression at T4 as compared with the wild type, indicating that RNAIII drives *cap* expression in the late growth phase. Of note also in the pRNAIII complemented *agr* mutant (early RNAIII expression), maximal cap expression was found at the mid to late exponential phase, T2 until T4, even though at these time points RNAIII is already severely diminished (Fig. 5B). Thus, the temporal expression of RNAIII and *cap* is not necessarily linked. This was further demonstrated in the constitutive $agrC^{R238H}$ strain in which maximum *cap* expression was again observed only in later growth phase. Thus, while RNAIII is required for optimal *cap* expression, additional factors must be involved to account for the strongly growth phase dependent expression.

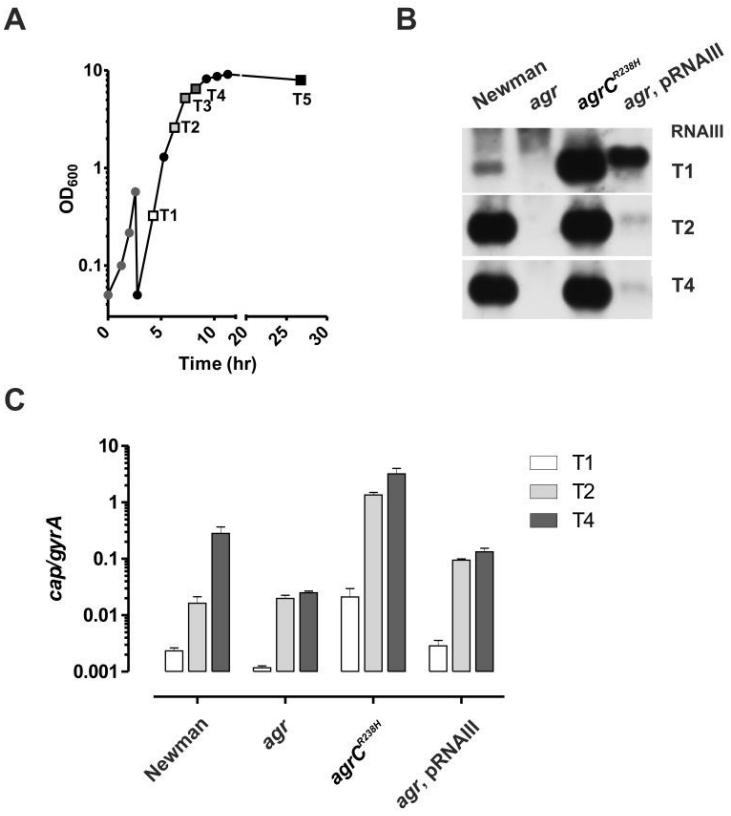

Figure 5: Influence of the Agr status on *cap* expression.
(A) Bacterial RNA was harvested at different growth phases (T1–T5 as shown here for strain Newman). Bacteria from exponential phase were again diluted to ensure that all bacteria entered exponential growth phase. Total RNA from strain Newman, the *agr* mutant (Newman-391), the constitutive *agrC*^{R238H} derivative (Newman-383) and *agr* mutant complemented with pRNAIII (Newman-363) was isolated at indicated time points (T1, T2, T4). (B) RNA was hybridised with digoxygenin-labelled probe specific for RNAIII, or (C) used for quantification of *cap* mRNA by qRT-PCR with reference to *gyrB*. The values are the mean ± SEM of three independent experiments.
(George et al, 2015)

Heterogeneity and correlation of promoter activities in single cells

(George et al, Mol. Micro 2015)

We analysed P_{RNAIII} and P_{cap} promoter activities simultaneously at the single-cell level using promoter-fluorescent protein fusions. The promoters were fused to the reporters' CFP - *cerulean* (CFP) or YFP - *venus* (YFP). To avoid artefacts due to multicopy effects, integration vectors were constructed which allowed the specific integration of the plasmid into the chromosomal *geh* locus or into the SaPI1 site. Both promoter reporter constructs were thus integrated into the chromosome, and the fluorescence expression in the WT and mutants was followed during growth. Analysis of dual reporter strains is illustrated in Fig. 6 in which P_{cap} activity appears yellow (YFP) and P_{RNAIII} activity blue (CFP). For quantification, we measured the fluorescence intensities of single bacteria (Fig. 6B). In the WT, P_{RNAIII} activity is only detectable after bacteria have entered the mid-exponential phase (T2). In the *agrC*^{R238H} strain, there was no significant difference in P_{RNAIII} activities between the different time points. In both strains, P_{cap} activity was found mainly in the stationary growth phase. To demonstrate the heterogeneity of promoter activities within the cultures, the fluorescence intensities (P_{RNAIII} activity versus P_{cap}) of 100 single bacteria were plotted (Fig. 6A). A wide range of P_{cap} activities (x-axes) was found in bacteria from the later growth phases. The corresponding P_{RNAIII} activity (y-axes) in contrast was largely uniform. In the wild type, most if not all bacteria were positive for P_{RNAIII} activity after the late-exponential growth phase (T4). In the *agrC*^{R238H} strain, bacteria are homogenously P_{RNAIII} positive throughout growth. Interestingly, within single bacteria, there was no detectable correlation between P_{cap} and P_{RNAIII} activities (Fig. 6A). After a certain threshold level of P_{RNAIII}, the P_{cap} activity is independent of *agr* and evidently determined by additional factors.

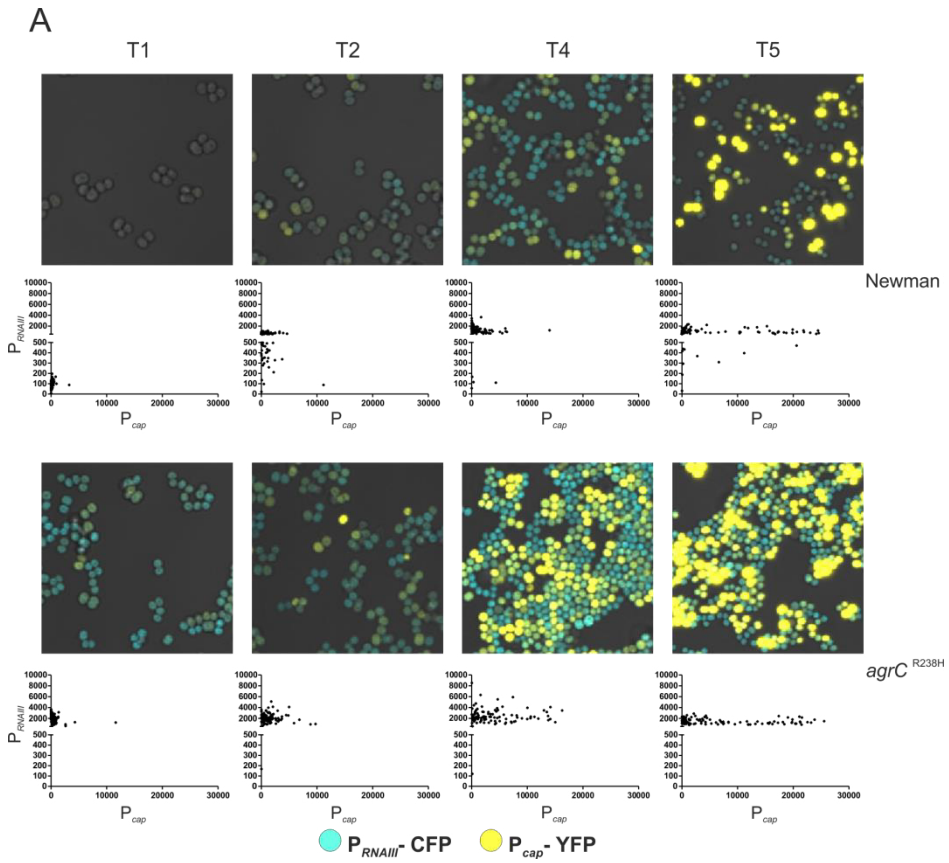

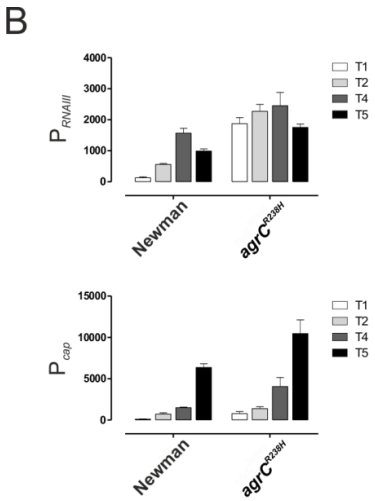

Figure 6: Influence of the Agr status on P_{RNAIII} and P_{cap} promoter activities.
(A) The P_{RNAIII} and P_{cap} promoters were cloned in front of *cfp* or *yfp* respectively and simultaneously integrated into the chromosome. Dual fluorescence expression was followed during growth in WT and the constitutive *agrC*^{R238H} strain at time T1-T5 (see Fig. 4A). P_{cap} promoter activity appears yellow and P_{RNAIII} activity blue. Correlation of the P_{RNAIII} and P_{cap} promoter activities of 100 bacteria each is shown below the images.
(B) For quantification, the mean fluorescence intensities of 100 single bacteria were measured. The mean ± SEM (of the mean intensities from single images) derived from three independent experiments is indicated.
(Modified from George et al, 2015)

Single cell transcription heterogeneity - smFISH (George et al, unpublished)

The heterogeneity on the P_{cap} promoter level could be confirmed by direct measurement of mRNA in single cells (Fig. 7). We adapted the single molecule FISH method from the protocol designed for gram-negative bacteria (Schreiber et al, 2016; Skinner et al, 2013) to detect mRNA in individual *S. aureus* cells. Fluorophore-labelled smFISH probes were designed to anneal to RNAIII and *cap* mRNA. Each pool of smFISH probes comprises up to 48 different oligos which are end-labelled

with a chemical dye. The fluorophores Quasar 570 (Cy3) and Quasar 670 (Cy5) were used to end-label the probe set for RNAIII and *cap* mRNA respectively. In early exponential phase, in wild type cells, there are no fluorescent mRNA 'spots' detected for RNAIII while there is a faint signal for *cap* mRNA. In the constitutively active *agrC*^{R238H} mutant, there are RNAIII signals in every cell in the population while only a few cells in the same population contain *cap* mRNA. There is some heterogeneity in the quantity of mRNA for RNAIII between cells which were not apparent using promoter-fluorescent protein fusion constructs. This may be due to the stability of fluorescent proteins which does not allow the monitoring of promoter-off states.

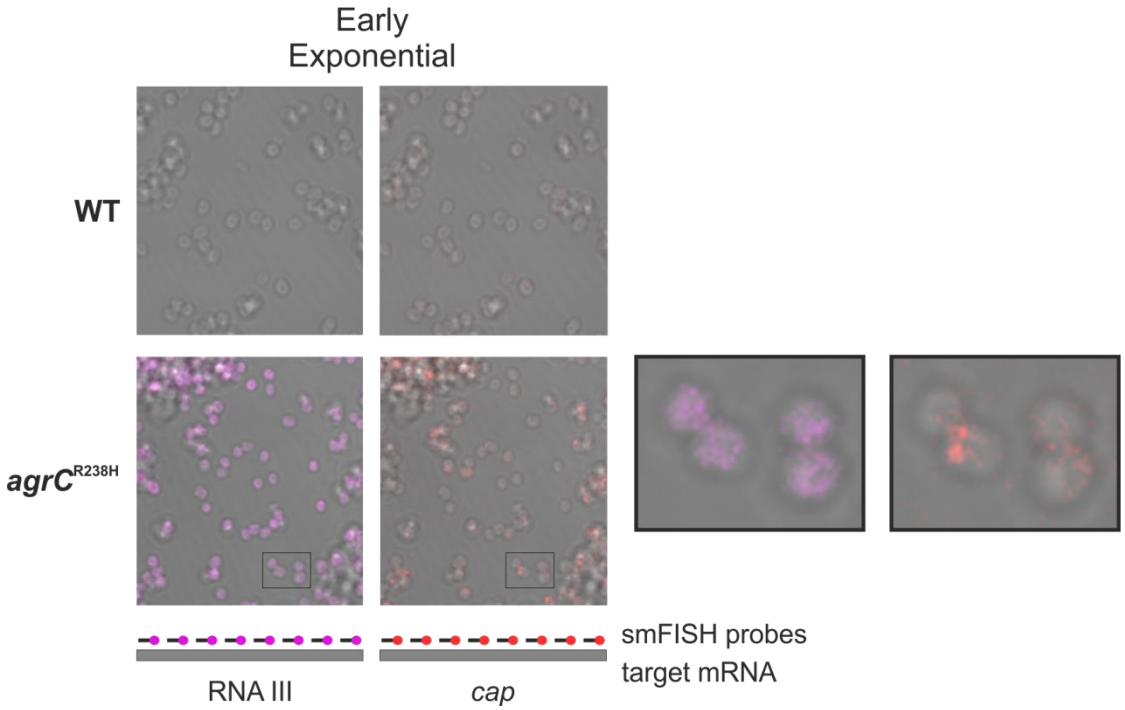

Figure 7: Single cell transcription heterogeneity measured by single molecule FISH
mRNA expression in single cells during early exponential growth (T1). mRNA in fixed and permeabilized cells were hybridised with fluorophore labelled DNA probe sets specific for RNAIII and *cap* mRNA (Quasar570 and Quasar670 respectively)
(George et al, unpublished)

Gene expression noise (George et al, unpublished)

We asked the question whether the noise in *cap* expression is primarily due to intrinsic or extrinsic sources (Eldar & Elowitz, 2010; Elowitz et al, 2002; Kim & Jacobs-Wagner, 2018; Ozbudak et al, 2002; Sanchez et al, 2011; Swain et al, 2002; Tsimring, 2014). Intrinsic noise refers to intrinsically random events pertaining to the gene itself such as genome location, promoter architecture, transcription and translation while cell-to-cell variations in the environment of the gene such as regulators, polymerases, and other global factors together comprise extrinsic noise

(Fig. 1). We cloned both CFP - *cerulean* and YFP- *venus* under the control of P_{cap} and measured the intensity of fluorescent signal in single cells over time. In such a dual promoter-reporter system, extrinsic sources of noise would be expected to affect both reporters equally and their signals would be expected to correlate in a given cell while an unequal amount of both reporters would be indicative of an intrinsic source of noise (Elowitz et al, 2002; Raj & van Oudenaarden, 2008). Intensities of YFP and CFP were determined using microbe J (Ducret et al, 2016) and the Pearson correlation coefficient between the two fluorescent signals were calculated. The positive correlation coefficient above 0.7 indicates that the noise in cap expression is to a large extent affected by the environment within the cell and therefore is mostly extrinsic (Fig. 8).

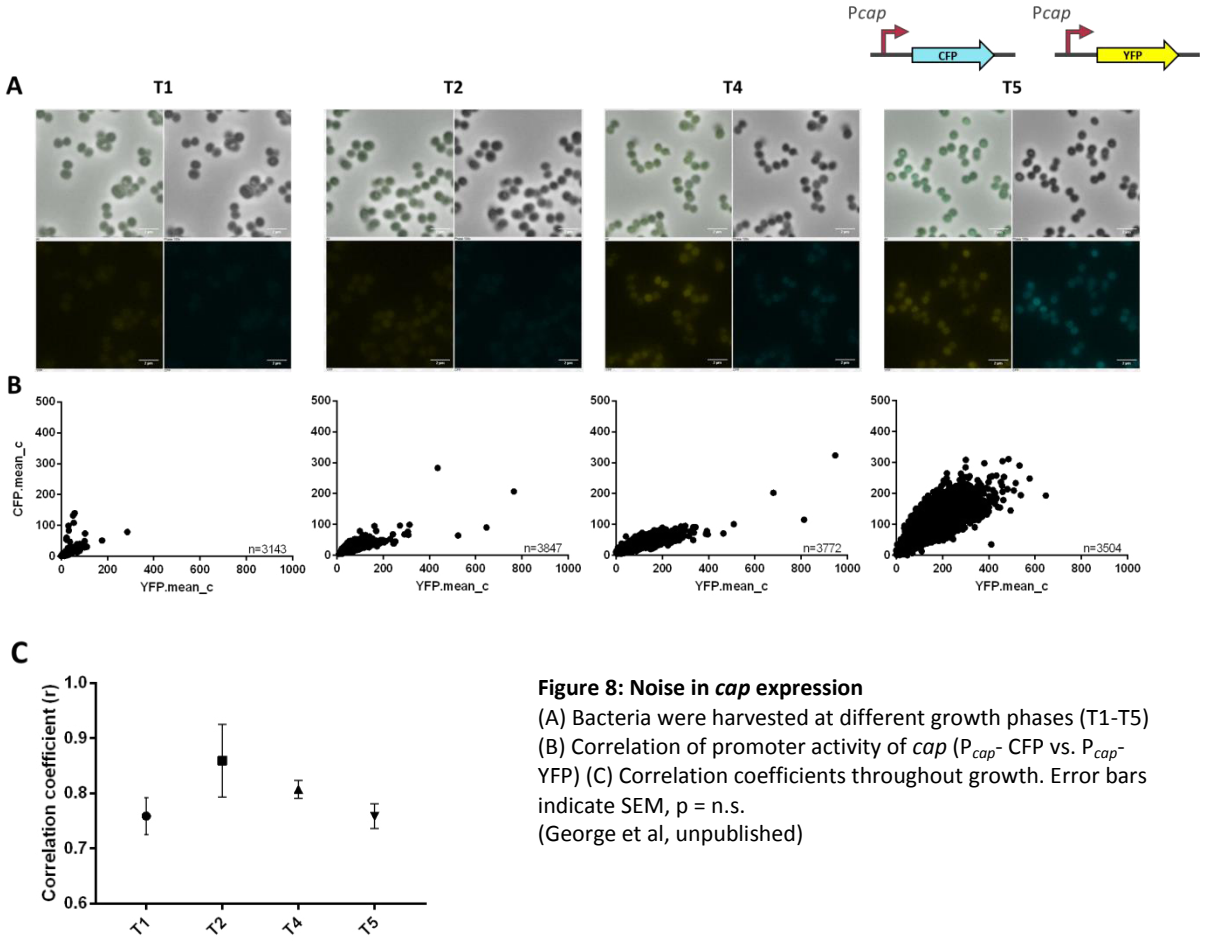

Figure 8: Noise in *cap* expression
(A) Bacteria were harvested at different growth phases (T1-T5) (B) Correlation of promoter activity of *cap* (P_{cap}- CFP vs. P_{cap}- YFP) (C) Correlation coefficients throughout growth. Error bars indicate SEM, p = n.s.
(George et al, unpublished)

Capsule production does not correlate with capsule promoter activity

(George et al. unpublished)

We developed a protocol by which the detection of fluorescent protein as a read out of promoter activity could be combined with detection of capsule production by

immunostaining. We investigated the correlation between P_{cap} activity and production of capsule (Fig. 9).

As expected, promoter activity preceded capsule synthesis. There was heterogeneity in both the P_{cap} YFP signal and the presence of capsule. Unexpectedly, there was no obvious correlation between the two signals.

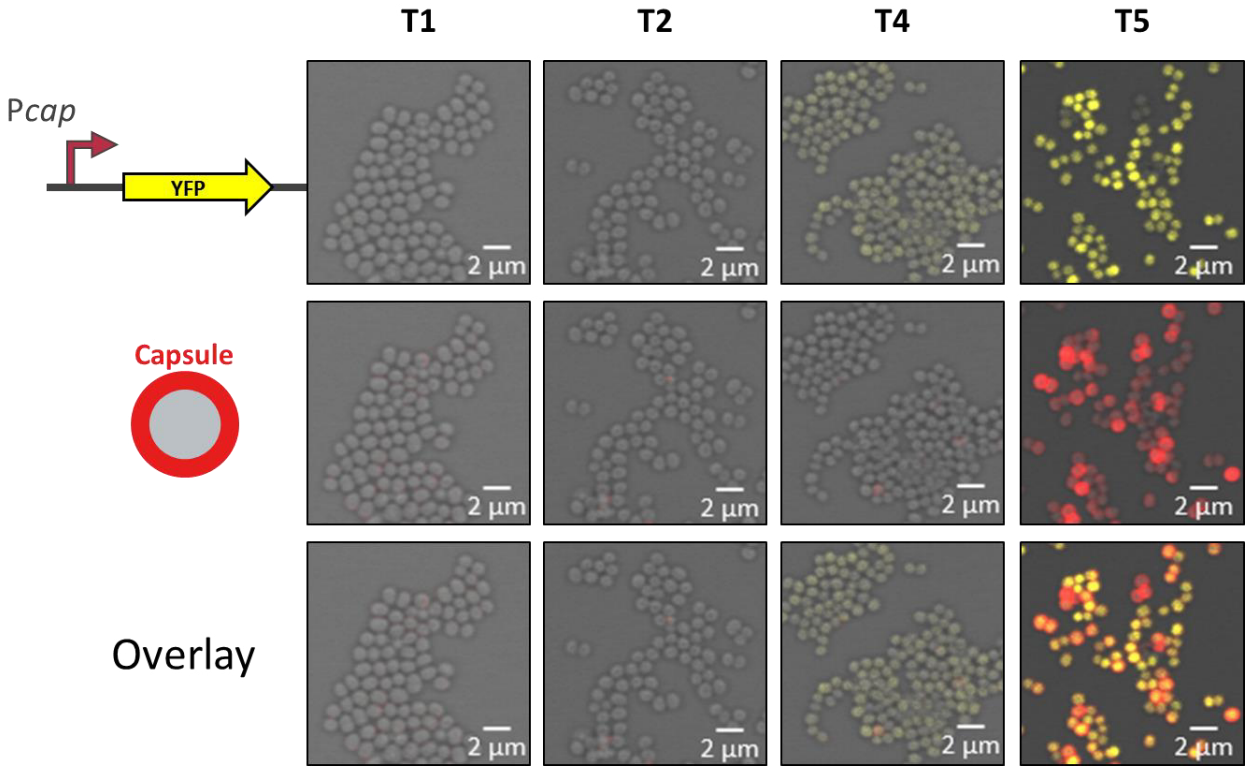

Figure 9: Promoter activity in Cap On-Off populations
Bacteria were harvested at different growth phases (T1-T5). P_{cap} promoter activity appears yellow. Capsule production was detected by immunofluorescence.
(George et al, unpublished)

Influence of Rot and other regulators

(George et al. Mol. Micro 2015 & unpublished; Keinhörster et al. Mol. Micro 2019)

We searched for candidate genes that may be involved in the characteristic CP expression (early Off/late Heterogen). We hypothesized that in early exponential growth phase, *cap* expression might be controlled by a repressor which becomes partially inactivated when bacteria enter a later growth phase. Furthermore, how RNAIII of the Agr system impacts *cap* expression was not clear. A *rot* mutant showed significantly enhanced *cap* expression and could restore *cap* expression in an *agr*-negative background as shown by CP immunofluorescence (Fig. 10) and qRT-PCR (Fig. 5A from George et al, 2015). The results support the hypothesis that RNAIII

inactivates the Rot repressor and that the effect of Rot on *cap* expression is downstream of RNAIII.

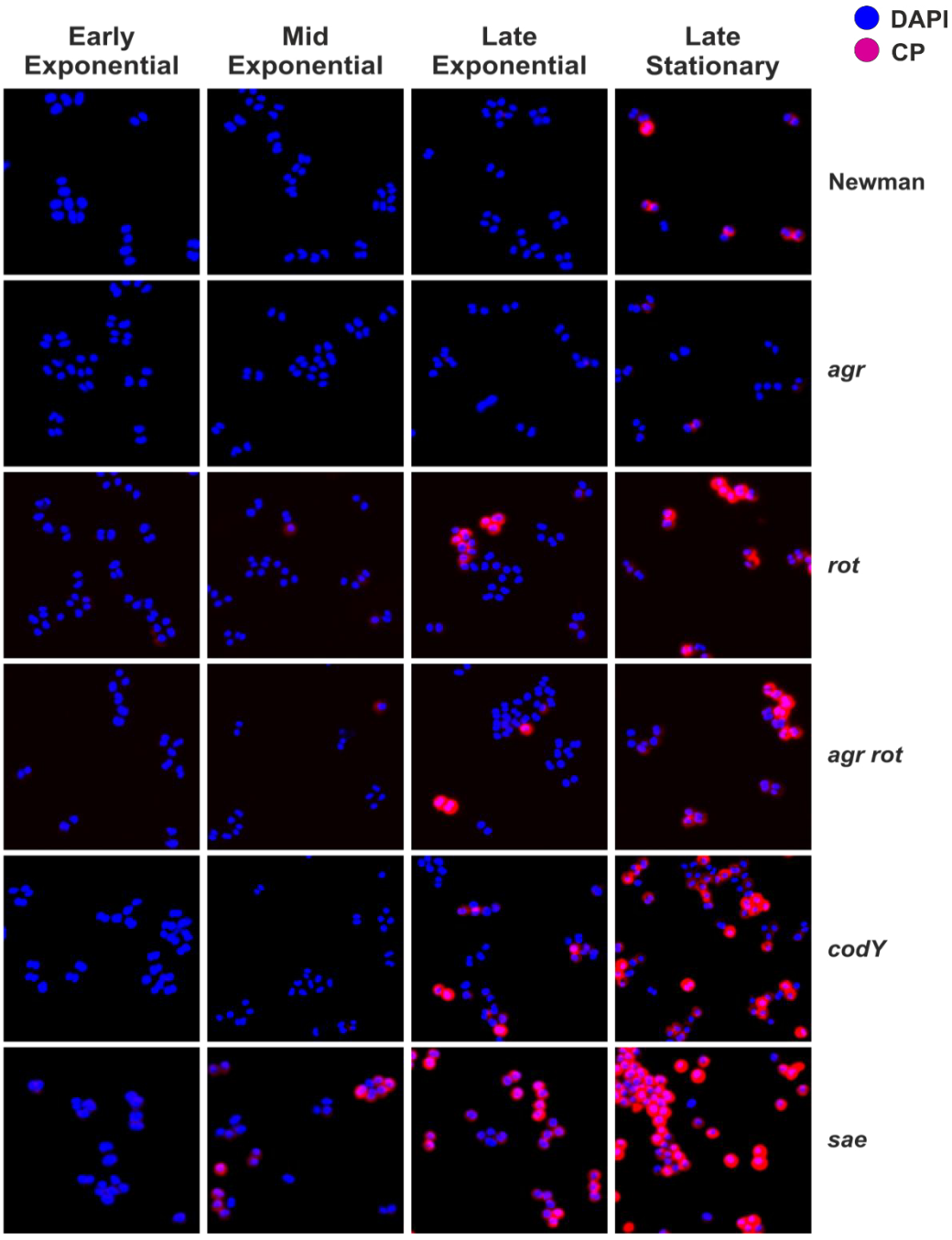

Figure 10: Temporal and heterogeneous synthesis of CP is influenced by different regulators.
CP was detected by immunofluorescence. *S. aureus* strain Newman and isogenic mutants grown in LB medium to the indicated growth phase (George et al, 2015; Keinhorster et al, 2019a).

The metabolic regulator CodY functions as a growth phase dependent repressor of the *cap* operon (Majerczyk et al, 2010; Pohl et al, 2009). Under conditions of low GTP or branched-chain amino acids, this repressor loses its DNA-binding activity leading to de-repression of target genes. We confirmed that CodY inhibits *cap* expression on the transcriptional level especially in bacteria in the mid exponential

phase (Fig. 6A from George et al, 2015). Also, CP positive bacteria were found at earlier time points compared with the wild type. However, the *codY* mutant still shows the early Off/ lateHeterogen expression (Fig. 10). The two-component system (TCS) SaeRS regulates several virulence factors including CP (Luong et al, 2011; Steinhuber et al, 2003).The *sae* mutant shows a significant increase in CP production (Fig. 10). These results underscore the impact of these repressors on *cap* expression. Further, a 'triple' mutant bearing a deletion in *rot* and *codY* along with down-regulation of *sae* shows CP- positive bacteria in early exponential phase (Fig. 11).

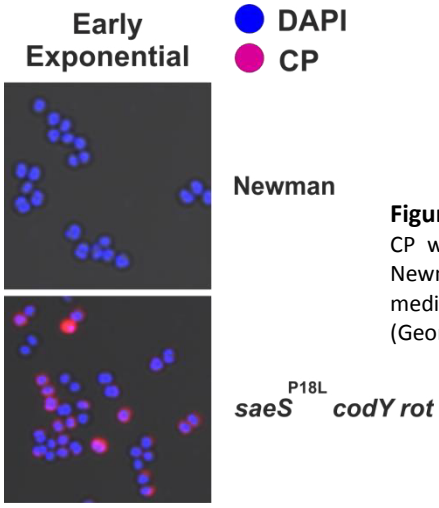

Figure 11: Additive effect of repressors on CP synthesis.
CP was detected by immunofluorescence. *S. aureus* strain Newman and isogenic mutant *saeS*^{P18L} *codY rot* grown in LB medium to early exponential growth phase.
(George et al, unpublished)

This suggests that these three regulators exert a significant additive effect with regard to *cap* repression to an extent that this mutant shows an early-On pattern of CP production. Besides these, there are several other regulators that have been shown to impact *cap* expression, many of which indirectly act through intertwined regulatory circuits (Fig. 12).

We recently mapped the repressive effect of Sae, CodY and Rot to an upstream region of the P_{cap} promoter (Keinhorster et al, 2019b). Also P_{cap} was found to be primarily SigB dependent and to a lesser extent also SigA dependent (Keinhorster et al, 2019b; Mader et al, 2016; Prados et al, 2016). The early-Off/late-Heterogenous *cap* expression is thus a consequence of SigB activity together with repression by Sae, CodY and Rot (Keinhorster et al, 2019b).

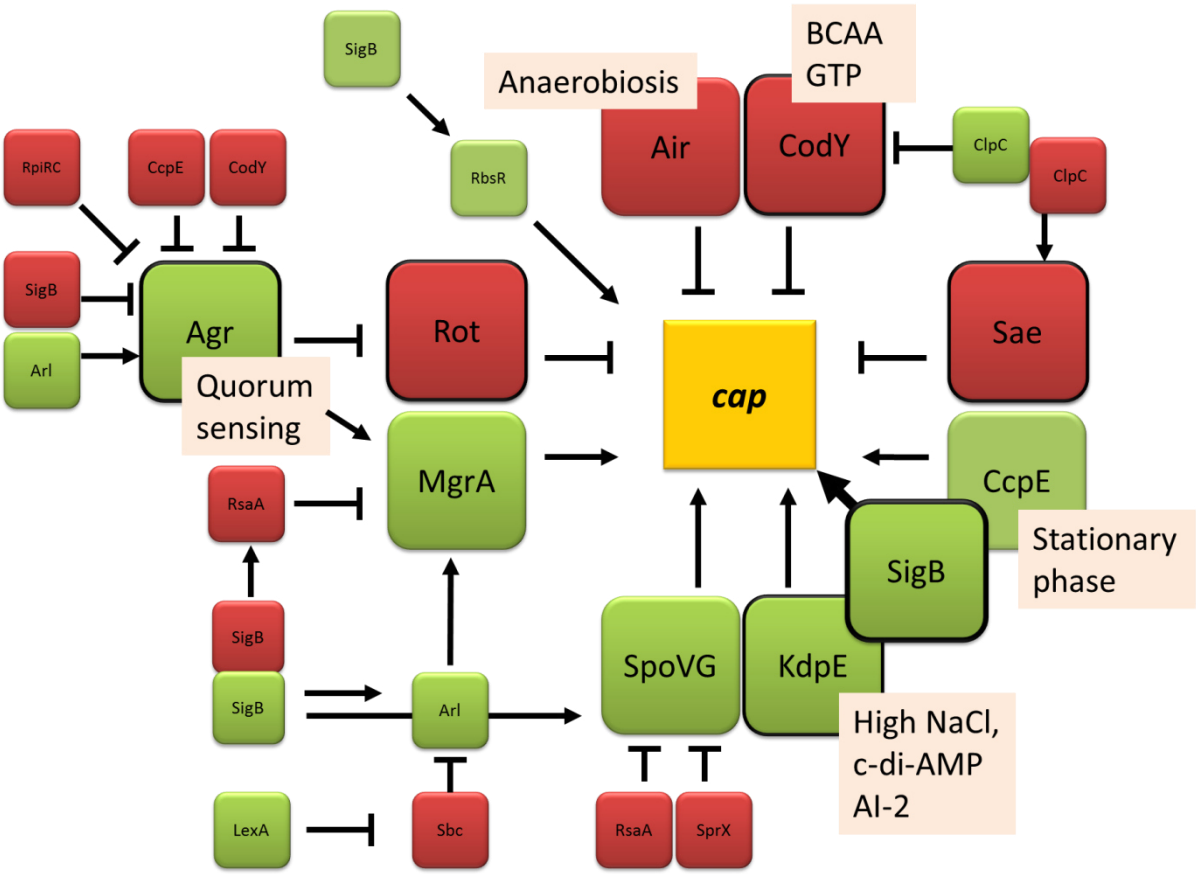

Figure 12: Activators and repressors involved in capsule regulation.
Overview of regulatory circuits which are known to impact *cap* expression. Green indicates an up-regulation, red a down-regulation effect on *cap* expression.
(Modified from George et al, 2015; Keinhorster et al, 2019b)

Influence of the environment (George et al. Mol. Micro 2015)

Several environmental factors also influence capsule synthesis. Environmental signals such as glucose, O_2 or high NaCl are transduced via regulatory systems CcpA (Seidl et al, 2006), Air (Sun et al, 2012a) and Kdp (Price-Whelan et al, 2013; Zhao et al, 2010) respectively. We analysed the impact of these conditions on CP expression and could confirm that glucose and anaerobiosis inhibit CP expression (Fig. 13). High NaCl in contrast results in enhanced CP expression presumably via Kdp.

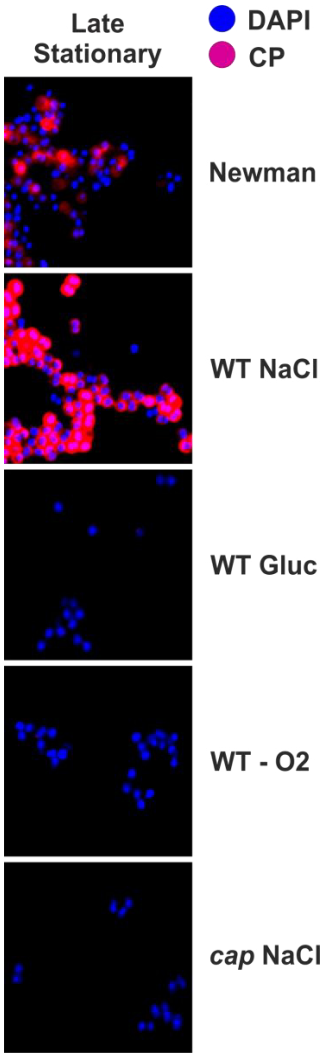

Figure 13: Influence of the environment
CP was detected by immunofluorescence. *S. aureus* strain Newman grown in LB supplemented without or with 2 M NaCl, 1% glucose or grown anaerobically. A *cap* mutant was included as negative control. (George et al, 2015)

Capsule as a stationary phase marker

(George et al. unpublished; Wang et al. Scientific Reports 2018)

In order to correlate promoter activities of different regulators to that of the capsule, we created a dual promoter – fluorescent protein fusion cassette which contains two tandem sequences each comprising a promoter of interest (P_{gene}) followed by a strong ribosomal binding site (RBS) and gene encoding either of the two fluorescent proteins gpVenus (YFP) or gpCerulean(CFP) (Keinhorster et al, 2019b; Wang et al, 2018b). Conlon et al showed that promoters of stationary phase genes such as *cap* and *arcA* were activated in cells that persist after antibiotic treatment and that persister cells were characterised by low ATP. Indeed lowering the ATP levels with arsenate activated P_{cap} (Conlon et al, 2016). We observed a rapid but transient increase in P_{cap} activity upon arsenate treatment (Fig. 14). The two strains tested, Newman and HG001 showed a different response to the same concentration of arsenate. While growth of HG001 was severely affected, P_{cap} was activated in just 1

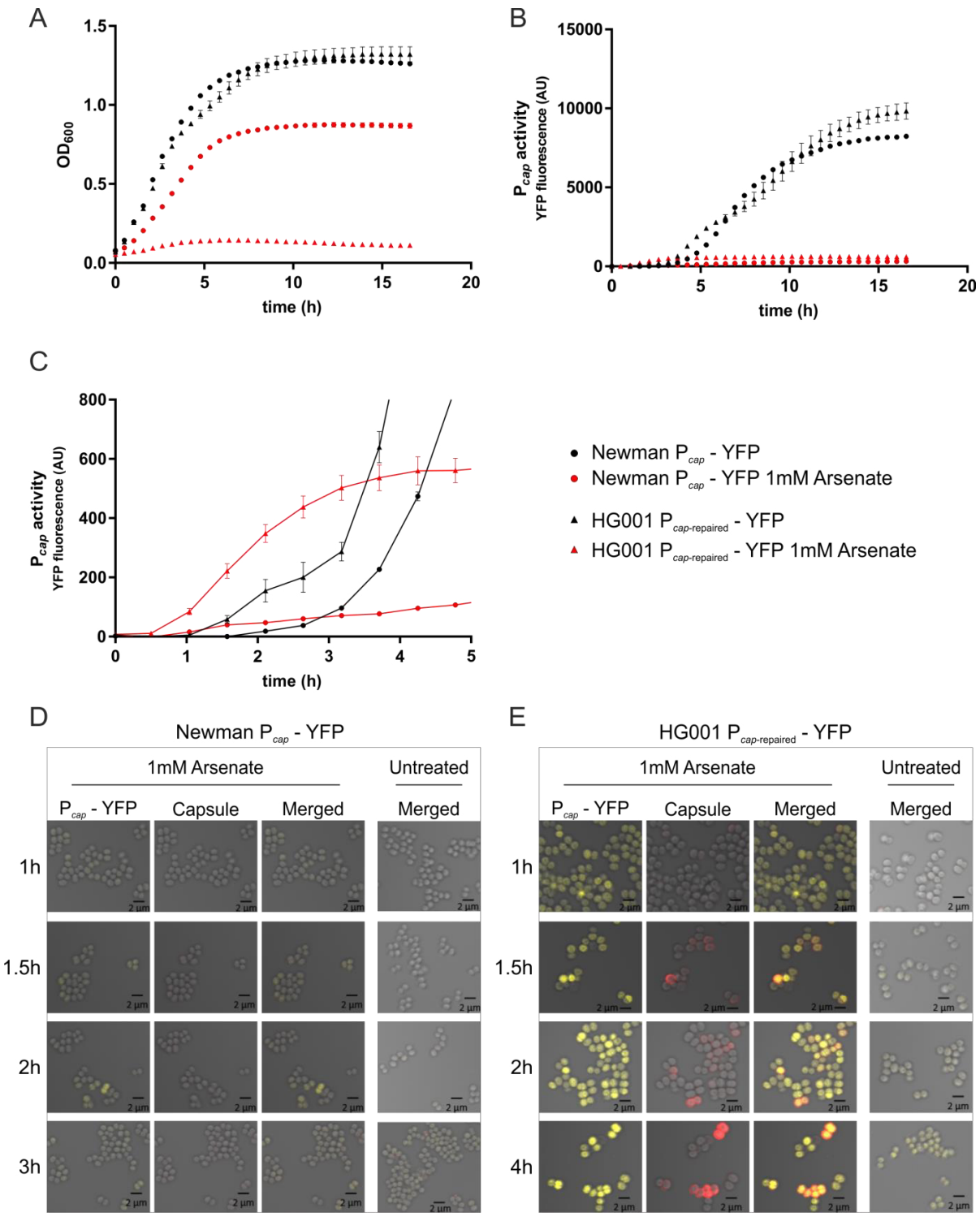

Figure 14: Effect of ATP depletion on P_{cap} activity and capsule production
Strains Newman and HG001 (P_{cap}-repaired) bearing plasmid containing P_{cap}-YFP were synchronised to OD_{600} 0.3 and then treated with 1mM Arsenate. (A, B, C) Subsequent growth and YFP fluorescence were monitored in a multiplate reader. (D, E) At designated time points, cultures were harvested and fixed. P_{cap} activity was measured by YFP intensity and capsule was detected by immunofluorescence. (George et al, unpublished)

hour after arsenate addition and remained active for about 3 hours. Untreated cells required as much as 4 hours to begin to show P_{cap} activity. Newman was not as affected by arsenate and also showed a smaller and transient increase in P_{cap} activity.

Since P_{cap} was identified as primarily a SigB-dependent promoter (Keinhorster et al, 2019b), we asked whether SigB responds to low cellular ATP levels. The P_{asp23} promoter is generally used as a marker for SigB activity. We could show that P_{asp23} activity increases in response to low cellular ATP levels induced by either arsenate or by CCCP (Fig. 15).

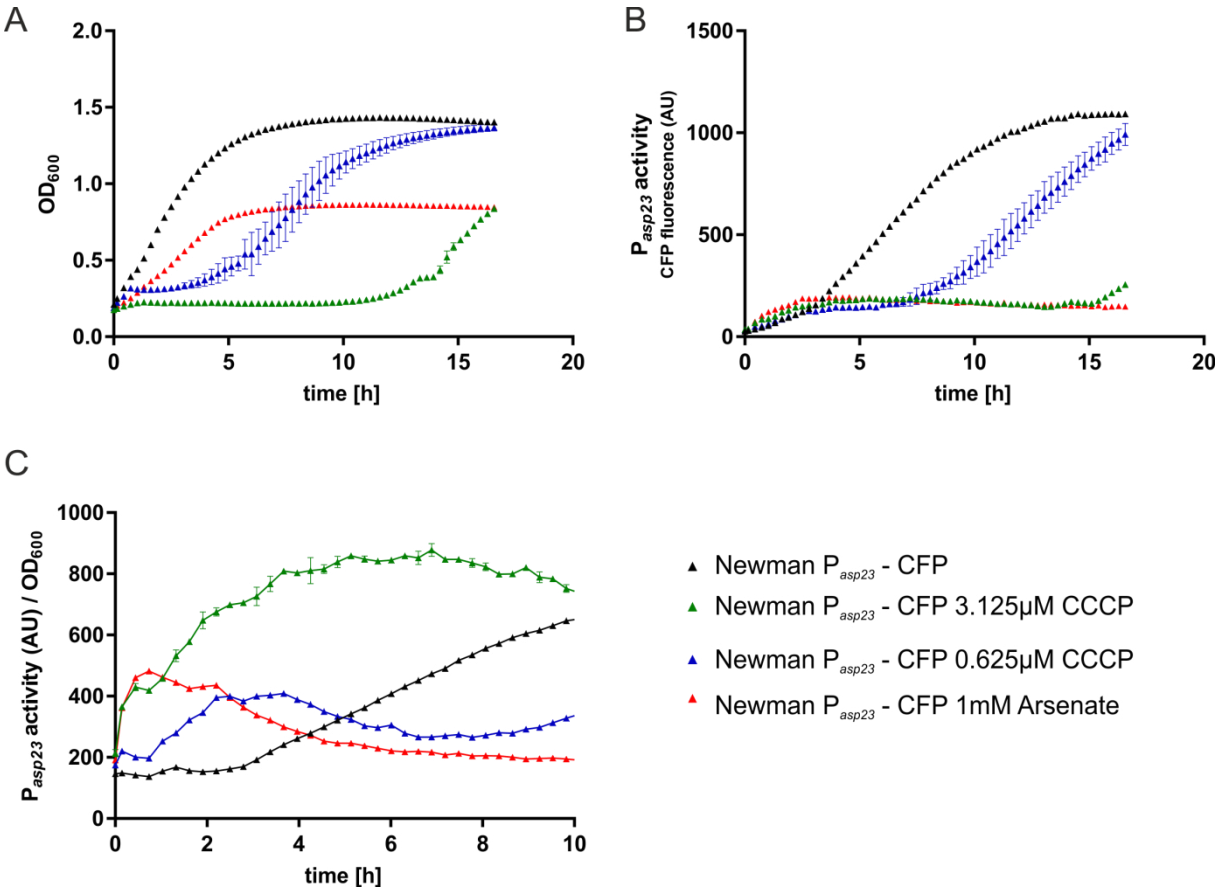

Figure 15: Effect of ATP depletion on P_{asp23} activity
Strains Newman bearing plasmid containing P_{asp23}-CFP were synchronised to OD_{600} 0.3 and then treated with 0.625µM, 3.125µM CCCP or 1mM Arsenate. (A) Growth and (B, C) CFP fluorescence were monitored in a multiplate reader.
(George et al, unpublished)

While evaluating the role of the TCA cycle in the formation of stationary phase persister cells, we monitored the gene expression of *sucA* simultaneously with that of P_{cap} in single cells by fusing the *sucA* promoter (P_{sucA}) to the CFP reporter gene in the dual promoter-reporter construct (Wang et al, 2018b)(Fig. 16). Expression of *sucA* was found to be high and heterogeneous in only the stationary phase and not in exponential phase. P_{sucA} activity on the single cell level seemed to correlate with P_{cap} activity in stationary phase. It was further proposed that *S. aureus* cells with low TCA cycle activity may be prone to form persisters.

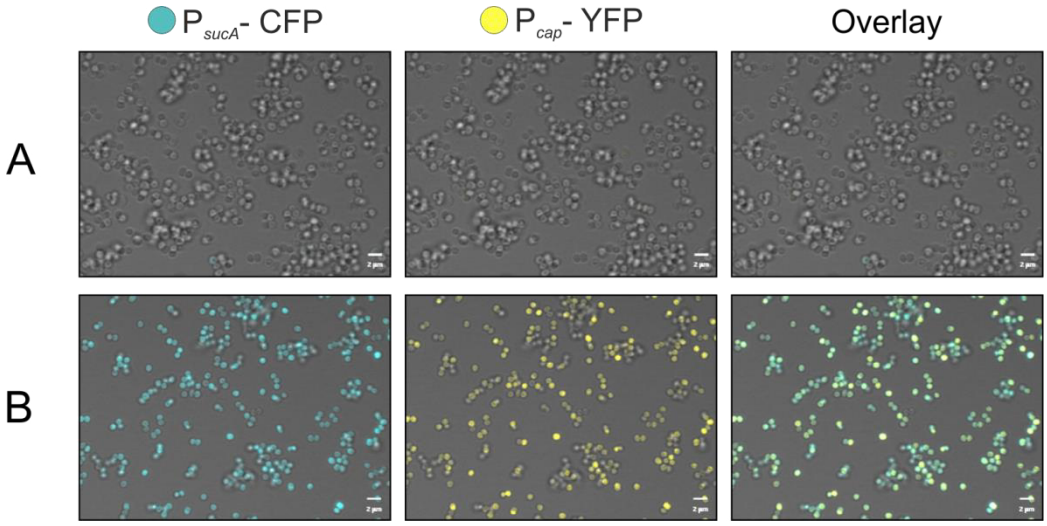

Figure 16: Expression of *sucA* in *S. aureus* Newman in exponential and stationary phase.
The fluorescence expression of both P_{sucA} (CFP) and P_{cap} (YFP) in strain Newman was monitored at (A) exponential and (B) stationary phase respectively.
(Wang et al, 2018b)

Discussion:

Bacterial individuality is not imposed by quorum sensing

The question of whether quorum sensing results in bacterial individuality has not been well addressed for peptide-based systems in Firmicutes. The expression of the regulatory RNAIII, transcribed from the P_{RNAIII} promoter, is driven by the prototypic quorum sensing system, Agr. Consequently, P_{RNAIII} is activated once bacteria reach a critical density (Fig. 5B). Here we show that most if not all bacteria activate P_{RNAIII} with little variation between single cells (Fig. 6A). Analysis of bacterial individuality imposed by quorum sensing systems of gram-negative model organisms such as *Pseudomonas* or *Vibrio* species show that in these organisms only a part of the bacterial population is responsive even in a homogenous environment or in confined micro-compartments (Anetzberger et al, 2012; Perez & Hagen, 2010; Pradhan & Chatterjee, 2014; Romilly et al, 2014). Indeed, heterogeneous activation of quorum sensing-related genes have been widely reported in gram-positive bacteria as well (Bettenworth et al, 2019). Therefore, the observed largely uniform P_{RNAIII} activity may be only true under conditions of a homogenous environment as analysed here. In vivo or in biofilms, small changes in the microenvironment are likely to modulate the quorum response. Expression of *agr* was shown to be non-uniform in biofilms and determines the specific structure of the biofilm (Periasamy et al, 2012). Recently, Garcia-Betancur et al. showed that the bimodal behaviour of the quorum sensing system in *S. aureus* regulates the differentiation into specialised cell types suited to either chronic or acute infections and that magnesium in the environment influenced the relative ratios of the two sub-populations (Garcia-Betancur et al, 2017). Under infectious conditions the Agr system is largely down-regulated e.g. through inactivation of the AIP signal (Goerke et al, 2000; Wright et al, 2005). Thus, whether RNAIII expression in vivo is more heterogeneous remains to be analysed.

Temporal and heterogeneous expression of capsule is governed by complex regulation

The *cap* operon is severely repressed in bacteria in the exponential growth phase (Fig. 5C). Here we clearly show that the strictly temporal *cap* expression is only partially mediated by quorum sensing via removal of Rot repression (Fig. 10, Fig. 5 in publication 1). In a *rot* mutant, *cap* expression is significantly increased. Moreover, in an *agr* negative background, *cap* expression could be restored by *rot* deletion.

However, constitutive activation of *agr* only resulted in an earlier onset of *cap* expression (Fig. 5C, Fig. 3 in publication 1). A similar result was obtained when analysing the *cap*- inhibitory system CodY (Figure 6 in publication 1). CodY leads to repression of the *cap* operon also in an *agr* negative background (Majerczyk et al, 2010; Pohl et al, 2009) but only partially impacts the temporal expression of *cap*. CodY is a typical metabolic sensor which in the presence of branched-chain amino acids and/or GTP binds to target genes usually resulting in gene repression. When nutrients become limited, CodY repression is relieved and target genes can be expressed. However, our results show that even simultaneous deletion of CodY and Rot only shifted the onset of *cap* expression to an earlier time point (late exponential). On the other hand, a Sae deletion alone resulted in an earlier onset of capsule synthesis (mid exponential phase). The SaeRS system is a two-component system that regulates the expression of several virulence factors and responds to external stimuli including host factors (Liu et al, 2016). We recently mapped the repressive effect of Sae, CodY and Rot to an upstream region of the P_{cap} promoter (Keinhorster et al, 2019b). Interestingly, in strain Newman the deletion of Rot and CodY coupled with only reducing Sae activity shifted capsule synthesis to the early exponential phase. This is in stark contrast to the temporal pattern of capsule production in wild type cells and confirms the additive effect of these three repressors.

However, in these mutant backgrounds capsule remains heterogeneous within the population. Heterogeneity was demonstrated at the CP synthesis level via immune-labelling as well as on the transcriptional level through promoter-fluorescent reporter fusions and direct detection of mRNA in single cells. We recently identified SigB as the main activator of capsule (Keinhorster et al, 2019b). SigB overexpression resulted in the loss of capsule heterogeneity in the stationary phase although the temporal pattern remained. Therefore, heterogeneity in SigB may be responsible for the heterogeneity of *cap* expression. Interestingly, SigB in other gram-positive organisms such as *Listeria monocytogenes* and *Bacillus subtilis* has been reported to be heterogeneous (Cabeen et al, 2017; Guldimann et al, 2017; Locke et al, 2011).

Noise in *cap* expression is mostly extrinsic

We show here that noise in *cap* expression is extrinsic based on the high degree of correlation within the same cell between CFP and YFP when driven by two identical *cap* promoters (Fig. 8). Interestingly, in cells that are P_{cap} ON, promoter activity is also variable suggesting high levels of transcription noise. Noise in protein levels was shown to be inversely dependent on the transcription rate but not the translation rate (Raj & van Oudenaarden, 2008). Quantifying mRNA at the single cell level shows that *cap* mRNA are low in abundance (Fig. 7) indicative of a low transcription rate which may explain the corresponding high noise in CP production. In *Bacillus subtilis*, the temporal regulation of *comK* transcription during stationary phase defines when transitions to the competent state may occur, and intrinsic noise in *comK* expression defines the rate at which cells become competent (Maamar et al, 2007). Lab-evolved synthetic promoters in *E. coli* exhibit low noise by default while natural promoters have high levels of noise (Wolf et al, 2015) suggesting that noise is a selected trait. Noisy promoters tend to be highly regulated by a number of transcription factors (Sharon et al, 2014; To & Maheshri, 2010; Wolf et al, 2015) which may themselves be noisy, and this noise necessarily propagates to their target genes (Pedraza & van Oudenaarden, 2005). Thus the noise characteristics of a gene sometimes reflect the dynamics of its modulators (Munsky et al, 2012) and the high noise in *cap* expression may be due to the noise propagation from the large number of regulators that are known to influence its expression (Fig. 12, Fig 17).

We monitored capsule production and P_{cap} activity over time. As expected, over time the promoter activity precedes synthesis of capsule (Fig. 9). However, once both signals were on at the population level, both were also heterogeneous wherein cells showed varying levels of both P_{cap} activity as well as CP. Unexpectedly, we did not see a correlation between P_{cap} activity and capsule. In instances where a given cell showed P_{cap}Off - CP On or P_{cap}On - CP Off, it could be a matter of timing wherein the promoter may have been active at a previous time point or that the cell may produce CP at a later time point. However, we could not exclude the possibility of post-transcriptional regulation. Post-transcriptional regulation in capsule synthesis was recently confirmed wherein rendering *cap* transcription constitutive from an early growth phase did not translate to corresponding CP production (Keinhorster et al, 2019b).

The different cell envelope components like CP, WTA and PG share the precursor UDP-D-GlcNAc (Keinhorster et al, 2019a; Weidenmaier & Lee, 2017). Further, their biosynthesis machineries converge at the membrane-anchored lipid carrier undecaprenyl-phosphate ($C_{55}P$) which is found in limited amounts and is recycled across the different synthesis cycles (Barreteau et al, 2009). Therefore the available pool of $C_{55}P$ has a direct effect on CP biosynthesis and the relative distribution and prioritization towards synthesis of the different cell wall components dictates the spatial and temporal regulation of these processes (Rausch et al, 2019). Furthermore, the CapAB tyrosine kinase complex through reversible phosphorylation controls several enzymatic checkpoints to balance the consumption of the essential precursors used in peptidoglycan biosynthesis. The Ser/Thr kinase PknB which can sense cellular lipid II levels negatively controls CP synthesis (Rausch et al, 2019).

The process of cell division also leads to inevitable single cell variation in the copy numbers of partitioned molecules at both the RNA and protein level (Fernandez-de-Cossio-Diaz et al, 2019; Huh & Paulsson, 2011). Fluctuations in protein levels in turn may persist over several generations leading to a 'molecular memory' of the given phenotype (van Boxtel et al, 2017). Another determinant for cell variability in some bacterial species is the age of the cell poles. Age-related asymmetric protein partitioning has been described in *E. coli*. Bakshi et al. described the non-diffusive partitioning of RNA polymerase wherein volume differences between two daughter cells will result in RNAP concentration differences (Bakshi et al, 2013). Thus, cell-to-cell variability in the RNAP concentration leads to heterogeneous protein expression across cells (Yang et al, 2014). Asymmetry of cell division results in asymmetric damage segregation as well. Baig et al. observed substantial division time asymmetry in growing microcolonies of *Staphylococcus aureus* whereby two daughter cells produced by one cell division show a difference in the time taken for further division (Baig et al, 2016). This asymmetry was further found to be cumulative suggesting that functional asymmetry in cell division can exist independently of the old pole-new pole axis in spherical organisms such as *S. aureus*. Therefore, several intrinsic and extrinsic factors may explain the noise in capsule production (Fig. 17).

Environmental factors cue production of capsule as a stationary phase marker

The temporal nature of *cap* expression has led to its designation as a stationary phase marker and an indicator of the metabolic status of the cell. Conlon and colleagues found P_{cap} activity to be enhanced in response to ATP depletion suggesting that *cap* expression is sensitive to and reports changes in energy status (Conlon et al, 2016). Further, low ATP was predictive of persister formation. Thereby, the stochastic entry into stationary phase as marked by capsule expression was correlated to a 100–1,000-fold increase in the likelihood of survival to antibiotic challenge. We found *cap* expression to correlate to TCA cycle genes which affect the persister phenotype (Fig. 16) (Wang et al, 2018b) and *S. aureus* cells with low TCA cycle activity were proposed to be prone to form persisters. This was recently reiterated by Zalis et al, wherein cells that have low levels of TCA cycle enzymes are more tolerant to antibiotics (Zalis et al, 2019). Thus the metabolic state of individual cells has a significant influence on antibiotic efficacy (Lopatkin et al, 2019).

Capsule positive cells may thus be considered to be a subset of the population that have transitioned into stationary phase 'earlier'. Whether this is due to switching between metabolic states as reported in *Bacillus* (Rosenthal et al, 2018) or to do with other sources of expression noise remains to be deciphered. CP synthesis is coupled to aerobic respiration, active TCA cycle and gluconeogenesis. These metabolic pathways are needed to generate the N-acetyl-glucosamine precursor (Sadykov et al, 2010). When glucose becomes limited, TCA activity, gluconeogenesis and *cap* expression become activated (Becher et al, 2009). However, it remains unclear how these metabolic circuits may result in the regulation of *cap* expression on the transcriptional level. Of note, all the experiments shown here were performed in LB medium without added glucose. The metabolic changes upon entry into stationary phase under such conditions without glucose are not well studied, but are presumably also linked to *cap* regulation. A small non-coding RNA, RsaI was recently found to be inhibited by high glucose concentrations in *S. aureus*. When glucose is consumed, RsaI expression is accompanied by a decreased transcription of genes involved in carbon catabolism pathway and an activation of genes involved in energy production, fermentation, and nitric oxide detoxification (Bronesky et al, 2019). The response of P_{cap} to low ATP levels is striking. Given that P_{cap} is primarily a SigB-dependent promoter, it would suggest that SigB in *S. aureus* is able to sense energy

stress. Indeed, preliminary data showed that P_{asp} activity which is often used as a proxy for SigB activity was also higher after arsenate treatment.

Interestingly, persister formation in *S. aureus* has also been associated with a prolonged lag times (Vulin et al, 2018). A recent study of starved *E. coli* showed that significant cell-to-cell heterogeneity in metabolism led to diverse growth phenotypes including dormancy (Simsek & Kim, 2018). In the organism *Klebsiella oxytoca*, environmental factors such as $NH_4(+)$ nutrient limitation was demonstrated to influence phenotypic heterogeneity in metabolism i.e. N_2 fixation (Schreiber et al, 2016). The N_2 fixation rate of single cells during $NH_4(+)$ limitation correlated positively with their growth rate after a shift to $NH_4(+)$ depletion, thus demonstrating the benefit of metabolic heterogeneity. Indeed, correlating capsule expression to growth characteristics at the individual cell level may shed more light on the metabolic heterogeneity within the population.

Noise in virulence gene expression is an important parameter for pathogenesis. In the food-borne pathogen *Listeria monocytogenes*, two major transcriptional regulators; alternative sigma factor B (σ^B) and the Positive Regulatory Factor A (PrfA) were found to be stochastically expressed at the single-cell level under different stress conditions (Guldimann et al, 2017; Utratna et al, 2012). Phenotypic heterogeneity was also observed in capsular polysaccharide of *Streptococcus pneumoniae* in the initial phase of infections (Hammerschmidt et al, 2005). A screen for promoters with high levels of phenotypic noise showed the highest level of phenotypic noise in promoters controlling flagellar synthesis in Salmonella (Freed et al, 2008). These examples serve to illustrate the considerable impact phenotypic heterogeneity has on virulence and infection outcomes in pathogenic bacteria. Non-genetic variability contributes significantly to the evolutionary success of bacteria by increasing fitness of the bacterial population. Phenotypic heterogeneity can now be understood to affect nearly all facets of bacterial physiology. The high noise in *cap* expression in *S. aureus* is yet another example of phenotypic heterogeneity playing a role in pathogenesis, thereby increasing the adaptive capacity of the population to survive fluctuating environments.

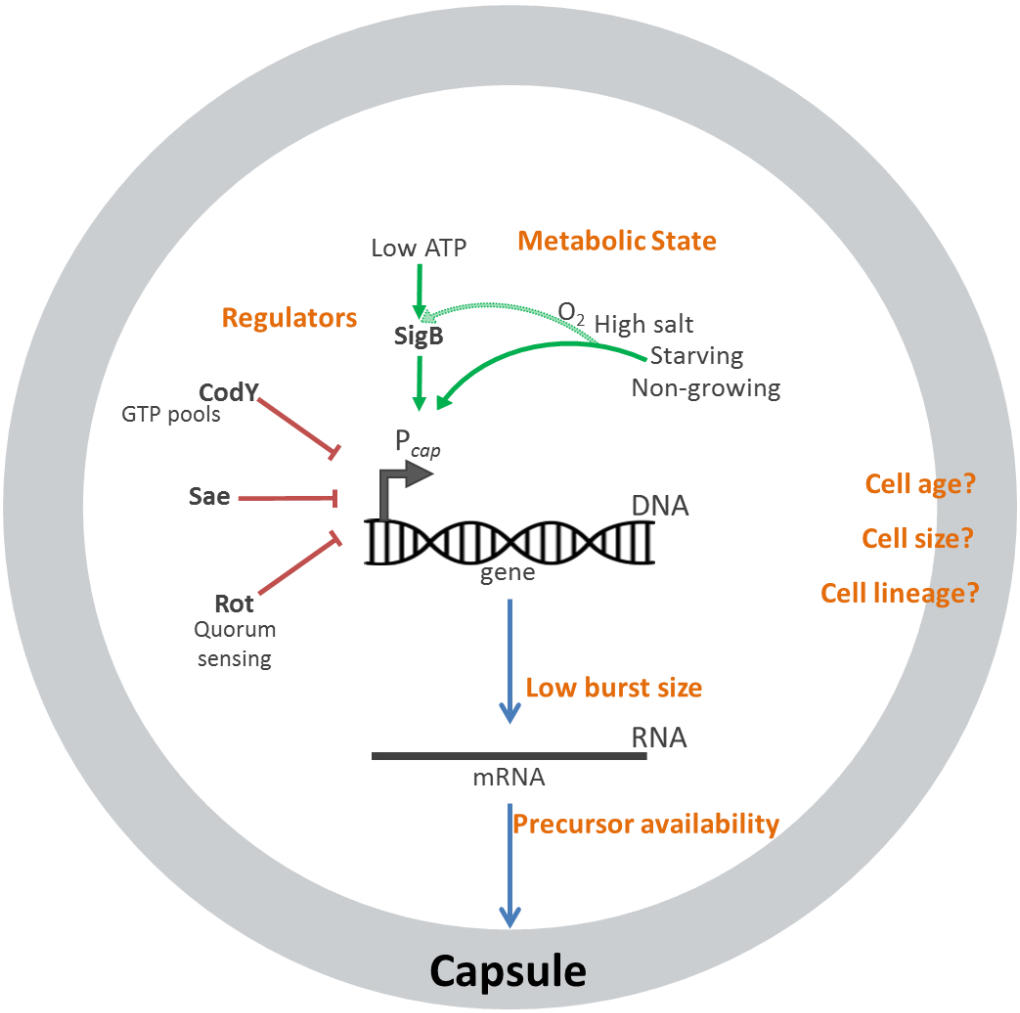

Figure 17: Noise in capsule expression and synthesis is multi-factorial. Several regulatory and environmental cues affect the noise in *cap* expression and capsule synthesis. These factors act on the transcriptional, post-transcriptional and metabolic level. Additional factors related to cell age, cell size and lineage may have a role as well.

Results and Discussion – II

Quorum sensing variants within *Staphylococcus aureus* populations

Parts of this Result and Discussion section have been published in:

- Oxidative stress drives the selection of quorum sensing mutants in the Staphylococcus aureus population.
  George SE, Hrubesch J, Breuing I, Vetter N, Korn N, Hennemann K, Bleul L, Willmann M, Ebner P, Götz F, Wolz C
  PNAS 2019 Sep 17;116(38):19145-19154. doi: 10.1073/pnas.1902752116

Results: (George et al, PNAS 2019)

Evolution of *agr* mutants in vitro

We set up an experimental system in which the selection of QS mutants can be monitored over time due to their characteristic non-haemolytic phenotype. We also employed ciprofloxacin, a known inducer of the SOS system to accelerate the mutation rate (Schroder et al, 2013). Cultures were transferred daily for 20 days in the presence or absence of sub-inhibitory concentrations of ciprofloxacin. While non-haemolytic variants accumulated readily in both treated and untreated cultures, ciprofloxacin accelerated the accumulation of variants (Fig. 18A, B). After only three transfers (Day 3), the non-haemolytic variant sub-population accounted for ~24% of the untreated cultures while in treated cultures, this sub-population accounted for ~65% of the total population. Interestingly, the wild type population did not get completely out-competed or lost from the population. Indeed, after 15 transfers both sub-populations seemed to reach a 'steady state' with about 10% of the wild type maintained.

Non-haemolytic variants isolated from independent cultures (42 isolates in total) after 3, 18 or 20 transfers were re-sequenced. All non-haemolytic variants were found to contain mutations within the *agr* locus (Fig. 18C), mostly within *agrA* and *agrC*. Interestingly, with the exception of one isolate that bore a large deletion spanning RNAIII/*hld* and *agrB*, we did not detect SNPs or indels in other loci that influence haemolysis i.e *hla*, *hld*, *psm, sae*. Thus, the Agr system imposes a strong fitness cost.

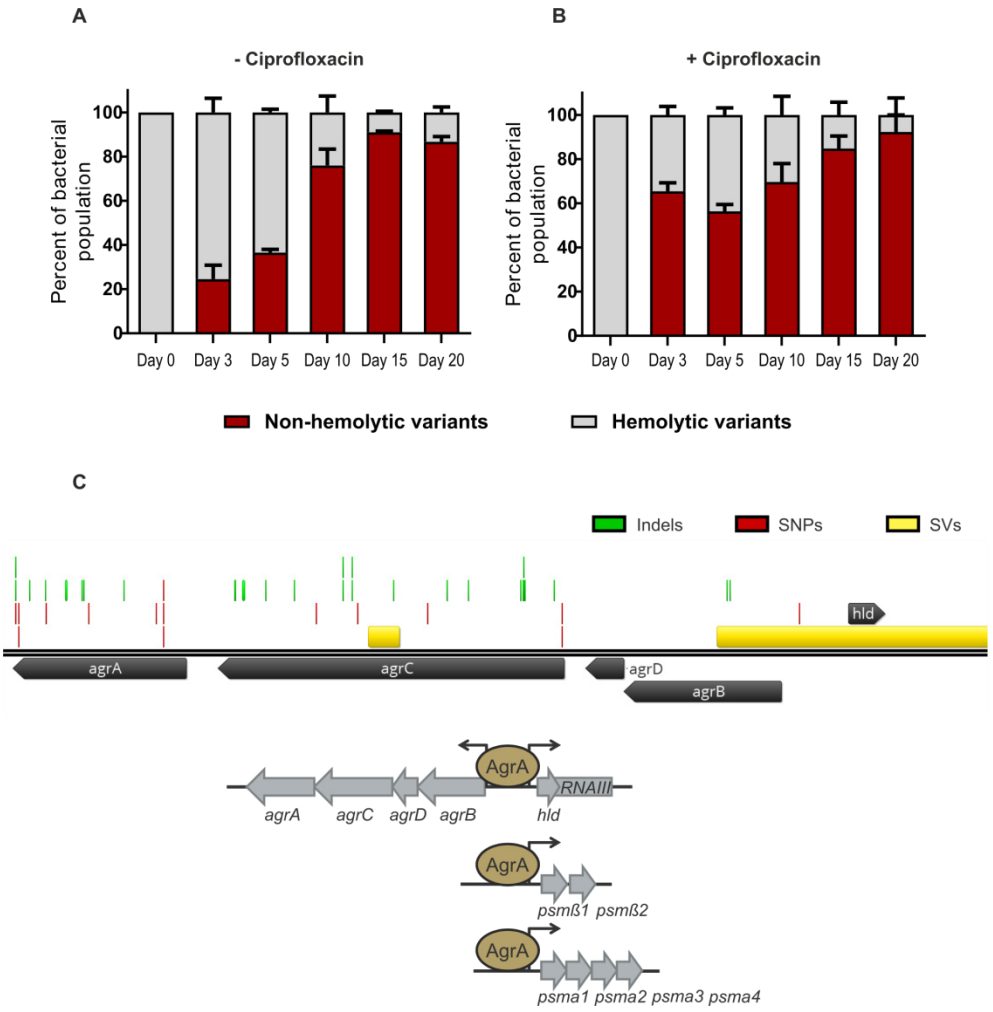

Figure 18: Evolution of *agr* mutants in vitro. Long term evolution of HG001 (A) without and (B) with sub-MIC of ciprofloxacin (0.125 µg/ml). Percentage of non-haemolytic and haemolytic sub-populations was determined based on colony phenotype on blood agar. (C) Representation of the mutations occurring within the *agr* locus after evolution in an aerobic environment. Mutations comprise single residue insertions or deletions (indels), single nucleotide polymorphisms (SNPs) or larger deletions i.e. structural variants (SVs).

Fitness advantage of *agr* mutants

We compared growth characteristics of the wild type against various *agr* mutants (Fig. 19A). We selected one representative *agr* deficient isolate which bore a single point mutation in AgrA^{R165H} without additional SNPs elsewhere in the genome. The point mutation lies in the C- terminal DNA-binding domain of AgrA and likely affects the ability to bind to target promoter regions. For comparison, we included an *agr*-deletion mutant in which the entire *agr*/RNAIII locus was deleted and also a strain in which a single amino-acid exchange in the histidine-kinase domain (AgrC^{R238H}) rendered the enzyme constitutively active (Geisinger et al, 2009; George et al, 2015). The *agr* mutants in which Agr function had been abrogated had similar growth rates as the wild type but differed in the final yield reached in stationary phase. This is in line with the understanding that quorum sensing and thereby Agr is active only once

the critical threshold of cell-density is reached. Accordingly, constitutive expression independent of quorum sensing should already impose a fitness cost in exponential phase. We could confirm that the growth of the constitutive *agrC*^{R238H} mutant (doubling time 31.36 ± 0.2139 min, n=3) is slightly retarded compared to wild type (doubling time 29.18 ± 0.5663 min, n=3; $p < 0.05$) (Fig. 19A). We postulated that in the constitutive *agrC*^{R238H} derivative, Agr should impose a higher burden thereby accelerating the accumulation of *agr* mutants. *agrC*^{R238H} cultures treated with ciprofloxacin accumulated non-haemolytic variants after fewer transfers compared to the wild type (Fig. 19B). After three transfers, the percentage of non-haemolytic variants that accumulated within the untreated *agrC*^{R238H} population was comparable to that in ciprofloxacin-treated wild type cultures and far exceeded that in untreated wild type cultures. Interestingly, in contrast to the long-term experiment using the wild type strain (Fig. 18A, B), the Agr-functional ancestor was not maintained in the *agrC*^{R238H} population as far as the limit of detection of the test system.

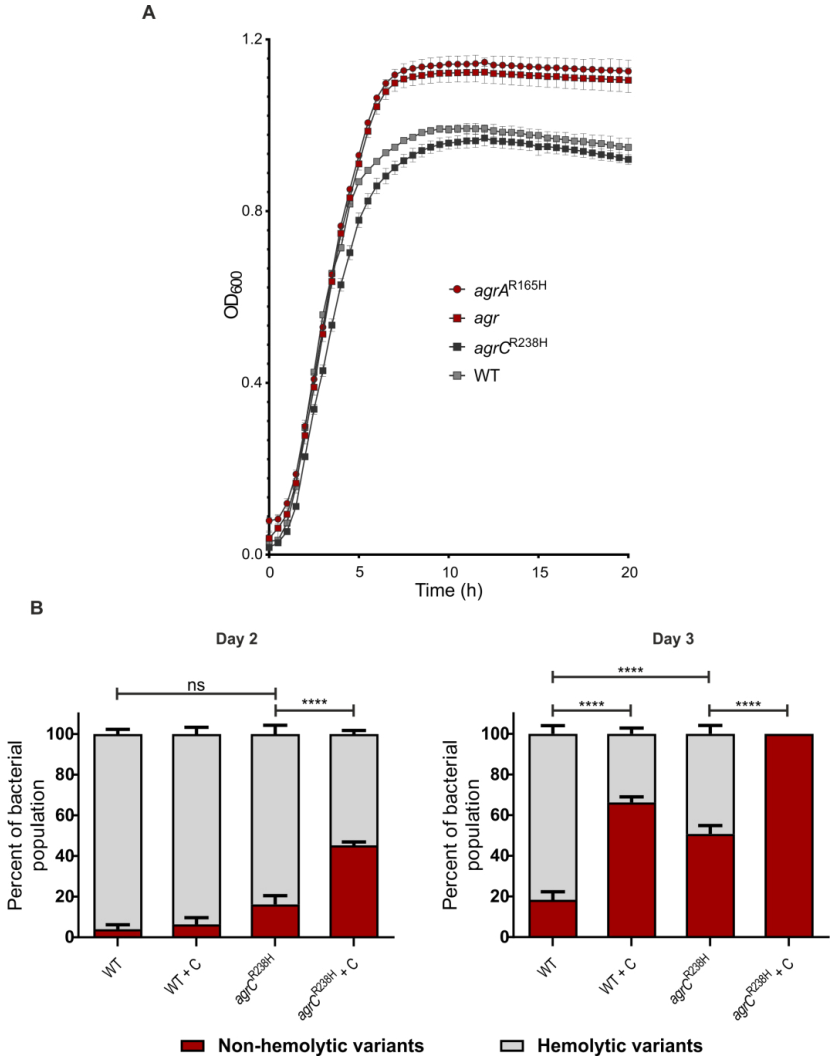

Figure 19: Fitness advantage of *agr* mutants. (A) Aerobic growth of HG001, *agr*, *agrC*^{R238H}, *agrA*^{R165H} in TSB. Error bars represent SD (n=3). (B) HG001 and *agrC*^{R238H} evolved for 2 and 3 days with and without sub-MIC of ciprofloxacin (0.125 µg/ml). Percentage of non-haemolytic and haemolytic sub-populations was determined based on colony phenotype on blood agar. Error bars indicate SEM (n = 3). Statistical significance determined by two-way ANOVA with Tukey's post-test. *P ≤ 0.05, **P ≤ 0.01, ***P ≤ 0.001, ****P ≤ 0.0001.

Fitness cost associated with the various nodes of the Agr system

The production of QS signalling molecules has been considered to be costly thereby imposing a metabolic burden (Keller & Surette, 2006; Ruparell et al, 2016). To test whether this holds true for staphylococcal AIPs, we created a signal non-producing *agrD* mutant. Such a mutant would be expected to have a fitness advantage relative to the wild type. We performed competition experiments between *agr* mutants (full-deletion or *agrD*) and the wild type. Strains were labelled with the fluorescent protein Venus and competed at a 1:1 ratio with the wild type labelled with the fluorescent protein Cerulean (Fig. 20A). After 2 sub-cultures, the percentage of wild type and mutant sub-populations were assessed. As expected, in the pairing with the *agr* full-deletion, the wild type was out-competed and the culture reached higher bacterial density. However, the *agrD* mutant did not out-compete the wild type. This shows that the *agrD* mutant was functionally complemented by the AIPs produced by the wild type and that the synthesis of AIP itself does not exert a fitness burden. Venus-labelled wild type in co-culture with wild type labelled with Cerulean remained in a stable 1:1 ratio and thus confirmed that the fitness traits of the competing strains was not influenced by either of the fluorescent proteins themselves.

Therefore, downstream consequences of Agr signalling must drive the selection of *agr* mutations. This might occur in possibly two ways: either through the production of the regulatory RNAIII, which is a key virulence determinant and controls the expression of several virulence and metabolic genes; or through the production of the cytolytic PSM peptides which are directly controlled by AgrA (Queck et al, 2008). To identify which specific node of the Agr system imposes the fitness disadvantage, we compared growth of mutants bearing deletions of either RNAIII or *psmα/psmβ* genes. Surprisingly, the *psm* deletion was sufficient to confer the same growth advantage as the complete *agr* deletion (Fig. 19A and 20B). Deletion of RNAIII had only a slight effect on growth compared to wild type. We next analysed the accumulation of non-haemolytic variants in these backgrounds. Of note, mutations in RNAIII or *psms* result in an altered haemolytic phenotype but are still clearly distinguishable from non-haemolytic *agr* mutants. Interestingly, both deletions abrogated the accumulation of non-haemolytic variants in bacterial populations (Fig. 20C). This was confirmed in a constitutive *agr*C^{R238H} background. No mutants

were selectable in a *psmα psmβ* double mutant. *psmα* deletion alone was sufficient to significantly reduce the accumulation of non-haemolytic variants (Fig. 20D), indicating that PSMα is more active compared to PSM*β*. In conclusion, the fitness advantage of an *agr* mutant can be attributed to the loss of PSMs and/or loss of RNAIII.

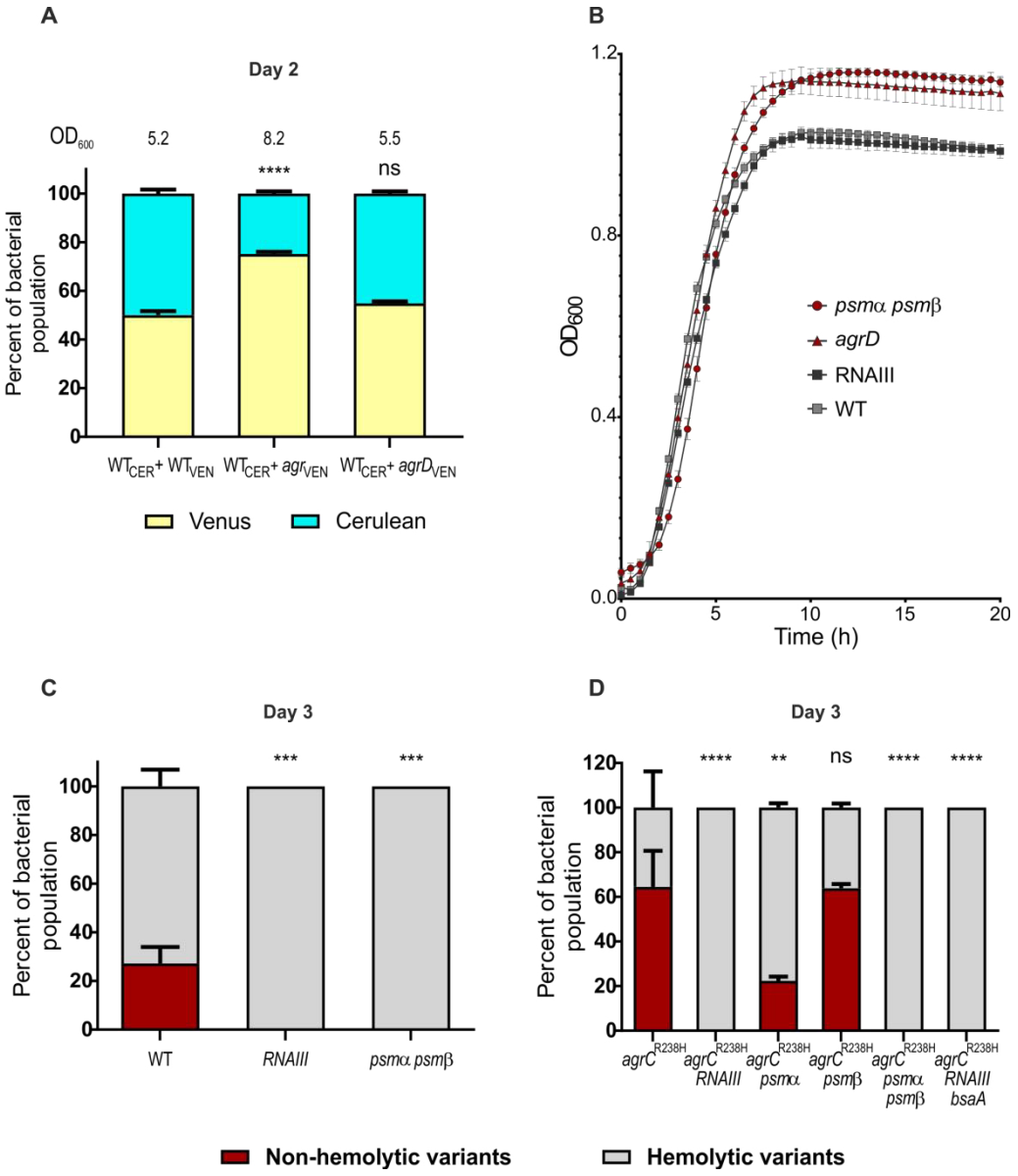

Figure 20: Fitness cost associated with the various nodes of the Agr system. (A) HG001 bearing P*sarA*-Cerulean was competed for 2 days with either *agr* or *agrD* bearing P*sarA*-Venus, starting at a ratio of 1:1. The final bacterial yield in each culture (OD_{600}) is indicated. Percentage of each bacterial sub-population was measured based on fluorescence. Error bars indicate SEM (n = 3). Statistical significance determined by one-way ANOVA with Tukey's post-test. Asterisks indicate statistical significance in comparison to the wild type population (WT_{CER} + WT_{VEN}). (B) Aerobic growth of HG001, *RNAIII*, *agrD* and *psmα psmβ* in TSB. Error bars represent SD (n=3). (C) HG001, *RNAIII* and *psmα psmβ* evolved for 3 days. Error bars indicate SEM (n = 5).. Asterisks indicate statistical significance in comparison to the wild type. (D) HG001 $agrC^{R238H}$, $agrC^{R238H}$ *RNAIII*, $agrC^{R238H}$ *psmα*, $agrC^{R238H}$ *psmβ*, $agrC^{R238H}$ *psmα psmβ* and $agrC^{R238H}$ *RNAIII bsaA* evolved for 3 days. Error bars indicate SEM (n = 3) Asterisks indicate statistical significance in comparison to the HG001 $agrC^{R238H}$. (C and D) Percentage of non-haemolytic and haemolytic sub-populations was determined based on colony phenotype on blood agar. Statistical significance determined by two-way ANOVA with Tukey's post-test. *P ≤ 0.05, **P ≤ 0.01, ***P ≤ 0.001, ****P ≤ 0.0001

Agr mutants are selected only under aerobic growth conditions

Different environmental cues are known to modulate Agr activity (Kavanaugh & Horswill, 2016). Oxygen concentrations vary greatly across different tissues (Carreau et al, 2011) affecting bacterial growth and signalling. There are conflicting results whether Agr is more (Wilde et al, 2015) or less (Stevens et al, 2017) active under hypoxia. We analysed the Agr-associated fitness cost under different oxygen conditions (Fig. 21A). Surprisingly, *agr* mutants did not accumulate in cultures transferred under low oxygen conditions. With 5-15% oxygen (microaerophilic), the mutation frequency was significantly decreased compared to normoxic conditions. Under hypoxic or anaerobic growth, non-haemolytic variants were not selected. We next performed a long-term evolution experiment under anaerobic conditions. Even after 20 transfers with ciprofloxacin, no *agr* mutants were detectable (Fig. 21B). To ascertain these observations, we performed a competition experiment under aerobic and anaerobic conditions wherein the wild type was competed with the streptomycin-resistant $agrA^{R165H}$ mutant starting at 1:1, 9:1 and 1:9 ratios (Fig. 21C, D; publication 6, SI Appendix Fig. S3). Within 20 transfers, the $agrA^{R165H}$ mutant accumulated rapidly under aerobic growth conditions irrespective of the initial ratio. Competition of a *psm* mutant or an RNAIII mutant with the wild type strain confirmed that both PSMs and RNAIII confer a fitness disadvantage over time (publication 6, SI Appendix Fig. S2). Under anaerobic growth, the relative starting ratios of wild type and $agrA^{R165H}$ mutant remained stable for 20 transfers (Fig. 21D). These results were unaltered in a competition experiment with the streptomycin-resistant wild type and an unmarked $agrA^{R165H}$ mutant (publication 6, SI Appendix Fig. S3). Thus, both evolution and competition experiments show that Agr imposes a fitness burden only under aerobic growth.

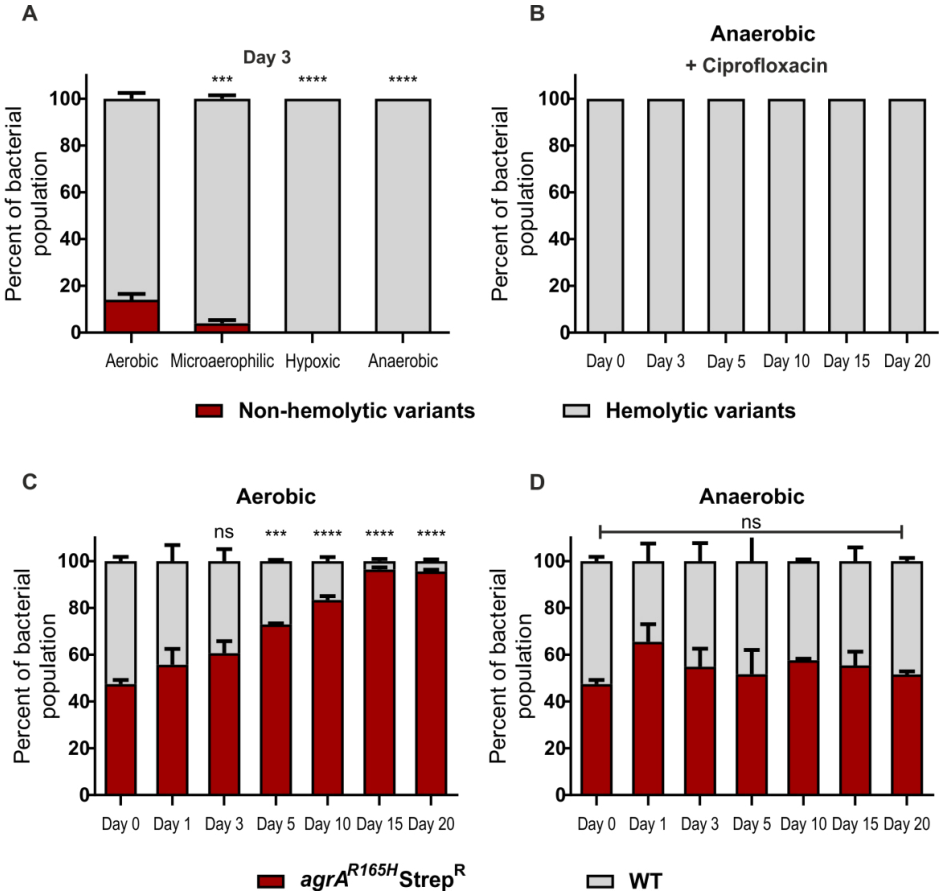

Figure 21: Agr mutants are selected only under aerobic growth conditions. (A) HG001 evolved for 3 days under aerobic, microaerophilic, hypoxic and anaerobic environments. Error bars indicate SEM (n=3). Asterisks indicate statistical significance in comparison to the aerobic condition. (B) Long term evolution of HG001 under anaerobic conditions with ciprofloxacin (C and D) HG001 was competed for 20 days with streptomycin-resistant *agrA*^{R165H}, starting at a ratio of 1:1 under (C) aerobic or (D) anaerobic conditions. Percentage of each bacterial sub-population was determined based on colony phenotype on blood agar. Error bars indicate SEM (n = 3). Asterisks indicate statistical significance in comparison to Day 0. Statistical significance determined by (A) two-way ANOVA (C and D) repeated measures two-way ANOVA with Tukey's post-test. *P ≤ 0.05, **P ≤ 0.01, ***P ≤ 0.001, ****P ≤ 0.0001.

Increased Agr activity in low oxygen environments

Growth under hypoxic conditions resulted in significantly lower final bacterial densities. However, the *agr* mutant no longer has a growth advantage under hypoxia (Fig. 22A). We reasoned that perhaps due to the lower cell density, the quorum sensing system might just not be active under low oxygen conditions. In contrast to this assumption we found that Agr activity is even higher under hypoxic conditions. This was shown on the transcriptional level wherein both the Agr target genes; *RNAIII* and *psmα* were significantly increased throughout growth under hypoxia compared to aerobic conditions (Fig. 22B). Interestingly, the transcription of *pmt* coding for the PSM transporter was not significantly influenced by hypoxia (publication 6, SI Appendix Fig. S4).

Next we analysed whether the increased transcription of *RNAIII* and *psmα* is accompanied by Agr dependent changes in haemolysis. Increased expression of

haemolysis could be verified after anaerobic growth on blood agar plates (Fig. 22C). The haemolytic zone relative to the size of single colonies was significantly higher ($p < 0.005$) in anaerobic (20.3 ± 5.002) compared to aerobic (4.204 ± 0.2803) grown bacteria. Moreover, under hypoxia the RNAIII encoded peptide Hld was found to be more abundant in the supernatants (Fig. 22D) consistent with the increased transcription of RNAIII. The release of cytoplasmic proteins and lipoproteins into the extracellular milieu was shown previously to be dependent on PSMs (Ebner et al, 2017; Hanzelmann et al, 2016). Accordingly, fewer proteins are detectable in the supernatants of the *psm* mutant (Fig. 22E). Of note, this effect was mainly seen under hypoxia. There was also increased level of the cytoplasmic protein aldolase in the secretome under hypoxia (Fig. 22D). Aldolase was previously used as marker protein for excretion of cytoplasmic proteins (Ebner et al, 2017).

These data demonstrate that Agr activity is clearly higher under hypoxia without imposing a fitness cost. Furthermore, the data indicate that metabolic burden imposed by the synthesis of RNAIII or PSMs does not explain the fitness differences. If this were the case, we would expect the fitness differences between wild type and *agr* mutants under hypoxia to be higher and not lower. To solve this conundrum, we speculated that PSMs may be inactivated under hypoxic conditions e.g. through proteolytic cleavage and thus cannot impose a selection pressure. We therefore tested the cytotoxicity of bacterial culture supernatants on THP1 cells (Fig. 22F). There was a significant increase in cytotoxicity of supernatants from wild type and RNAIII mutants grown under hypoxia. This was abrogated in a *psmαβ* mutant, indicating that PSMs produced under hypoxia are not inactive with regard to their cytotoxic effects.

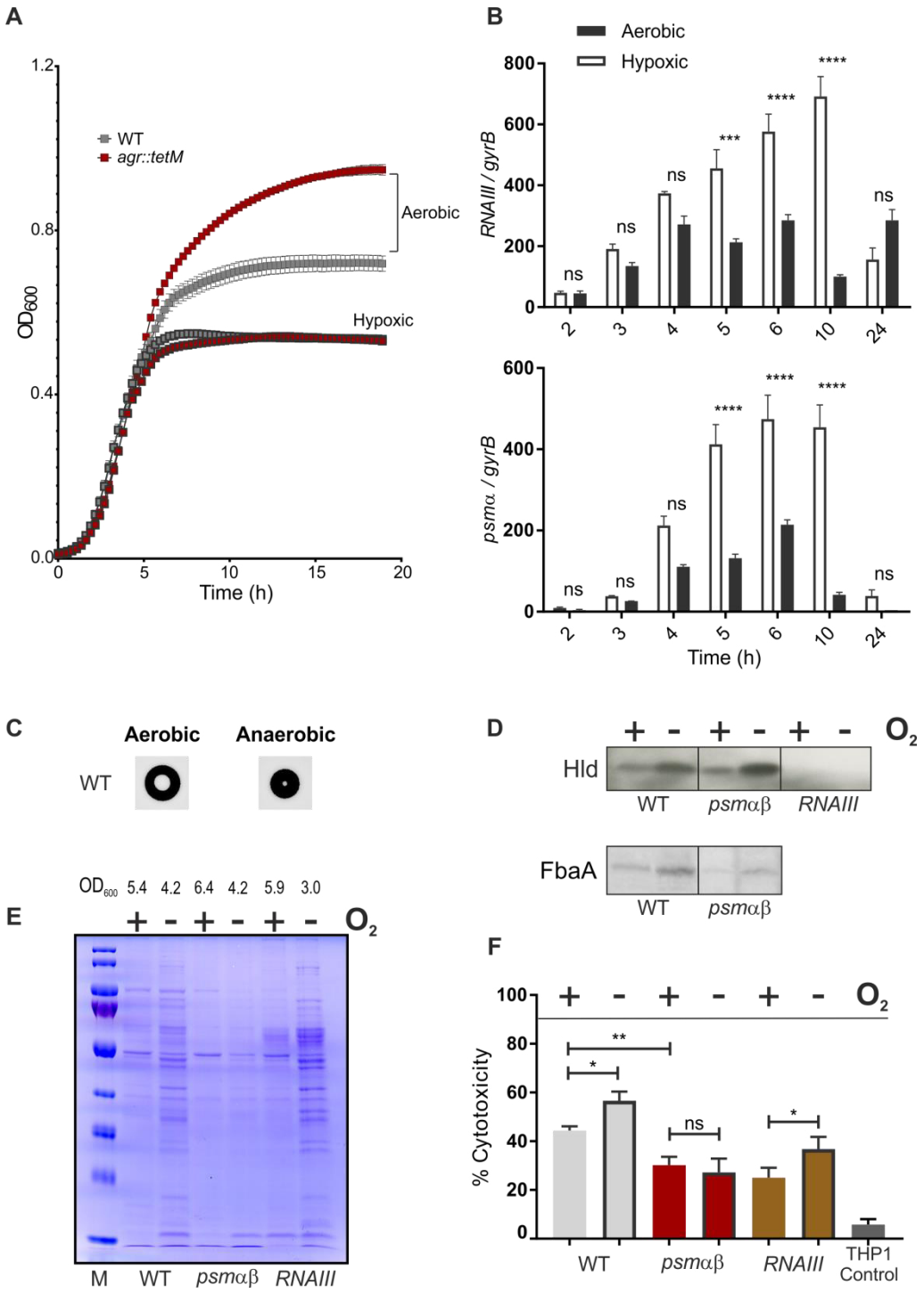

Figure 22: Increased Agr activity in low oxygen environments. (A) Growth of HG001 and *agr::tetM* under aerobic and hypoxic environments. Error bars represent SD (n=3). (B) Bacteria were harvested at different time-points (2, 3, 4, 5, 6, 10, 24 h) during growth. Total RNA from strain HG001 was isolated. *RNAIII* or *psmα* mRNA was quantified by qRT-PCR with reference to *gyrB*. Error bars indicate SEM (n = 3). Statistical significance determined by repeated measures two-way ANOVA with Bonferroni's post-test. (C) Colony morphology and haemolysis zone of HG001 grown on blood agar under aerobic and anaerobic environments (D, E and F) Bacterial supernatants from cultures (HG001, *psmα psmβ*, RNAIII) grown either aerobically or under hypoxic conditions were analysed by (D) Western blot for delta-haemolysin (Hld) and aldolase (FbaA) and (E) SDS-PAGE for extracellular proteome (loading control for western blots). The final bacterial yield in each culture (OD_{600}) is indicated. (F) Bacterial supernatants were analysed for cytotoxic potential against THP1 macrophages. Percent cytotoxicity shown was normalised to the Triton control. Error bars indicate SD (n = 6). Statistical significance determined by one-way ANOVA with Tukey's post-test. *P ≤ 0.05, **P ≤ 0.01, ***P ≤ 0.001, ****P ≤ 0.0001.

PSMs induce ROS and possess antimicrobial activity under aerobic conditions

We next hypothesized that the bacterial cells are themselves not susceptible to PSMs under low O_2. In an aerobic environment PSMα3 resulted in a concentration-dependent growth defect wherein as low as 10 μg/ml affected bacterial yield; while up to 50 μg/ml had no effect under hypoxia (Fig. 23A). Therefore, under hypoxia the Agr system is highly active with increased secretion of toxic PSMs. However, bacteria seem to be protected from their antimicrobial effects under these conditions.

We speculated that PSMs may induce ROS under aerobic conditions contributing to the toxicity. Indeed we found significantly higher levels of ROS in the wild type compared to the *psmαβ* or *agr* mutant (Fig. 23B). Thus, under hypoxia cytotoxic PSM production is enhanced without harming the producer suggesting that the selection of *agr* mutants under aerobic conditions is to avoid PSM-mediated ROS production. Indeed, addition of 2,2'-bipyridyl and thiourea to block hydroxyl radical accumulation, could completely prevent selection of *agr* mutants in the constitutive *agrC*^{R238H} background (Fig. 23C).

However, we also found that RNAIII deletion was sufficient to prevent selection of *agr* mutants, (Fig. 20C) although ROS production was comparable to the wild type (Fig. 23B). The glutathione peroxidase BsaA was reported to be de-repressed in *agr* mutants thus enabling bacteria to survive oxidative stress (Sun et al, 2012b). We therefore tested whether *bsaA* deletion would increase the selection pressure in an RNAIII mutant (Fig. 20D). However, this was not the case. Moreover, we could not confirm that *agrA* or RNAIII deletion significantly increases *bsaA* expression under our growth conditions (publication 6, SI Appendix Fig. S6). Taken together, these results suggest that other RNAIII-regulated factors are involved in the protective effect against ROS in an RNAIII mutant.

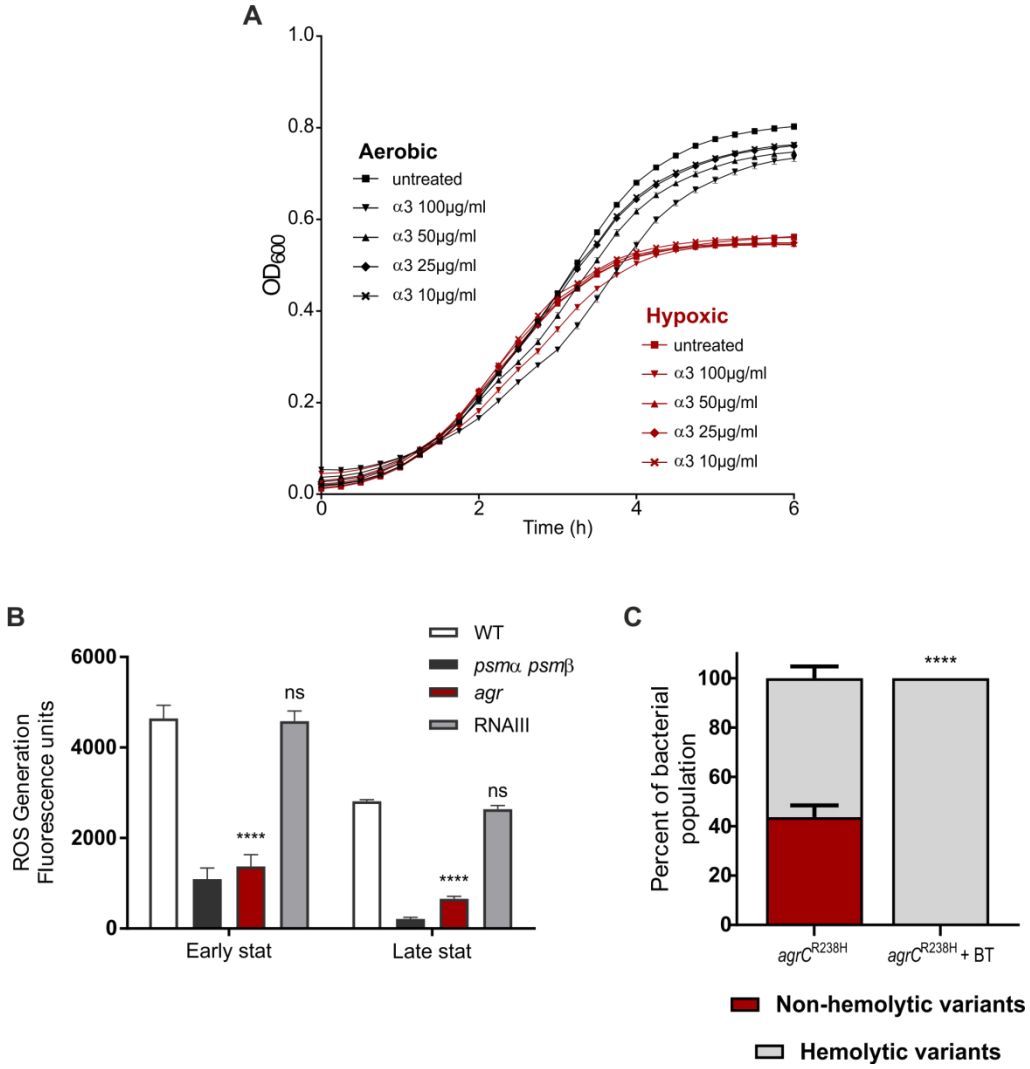

Figure 23: PSMs induce ROS and possess antimicrobial activity under aerobic conditions. (A) Different concentrations of PSMα3 (100, 50, 25, 10 µg/ml) was added to bacterial cultures of HG001 *agr*. Growth under aerobic and hypoxic environment was monitored. Error bars indicate SEM (n = 3). Bacterial yield compared to the untreated control was significant only under aerobic growth (****P ≤ 0.0001) and not under hypoxia (B) Early and late stationary phase cultures of HG001, *psmα psmβ*, *agr* and RNAIII were compared for ROS levels. Error bars indicate SEM (n = 3). Asterisks indicate statistical significance in comparison to HG001. (C) HG001 *agrC*^{R238H} evolved for 3 days in the presence of antioxidants (1mM 2,2'-bipyridyl and 100mM thiourea). Percentage of non-haemolytic and haemolytic sub-populations was determined based on colony phenotype on blood agar. Error bars indicate SEM (n = 3). Asterisks indicate statistical significance in comparison to the HG001 *agrC*^{R238H}. Statistical significance determined by (A) one-way ANOVA with Tukey's post-test (B) and (C) two-way ANOVA with Bonferroni's post-test. *P ≤ 0.05, **P ≤ 0.01, ***P ≤ 0.001, ****P ≤ 0.0001.

Discussion: (George et al, PNAS 2019)

The social trait of QS sensing in proteobacteria has been widely studied and, depending on the model organism analysed, different mechanisms to balance the relationship between QS positive bacteria and QS negative cheaters has been discovered (Abisado et al, 2018; Asfahl & Schuster, 2017; Whiteley et al, 2017). To gain insight into such processes in peptide-based QS systems, we employed evolution and competition experiments. We investigated conditions and factors driving the evolution and selection of QS-negative *S. aureus* mutants and found the anti-microbial activity of the QS dependent PSMs to be a major driver for the evolution of QS mutants. Thus, a QS-controlled gene product, PSMα, can drive the selection of QS mutants. This demarcates the Agr system from other QS systems that are described to have evolved mechanisms to avoid cheating (Asfahl & Schuster, 2017; Wang et al, 2015).

Fitness advantage of *agr* mutants

We show that under aerobic conditions *agr* mutants possess a fitness advantage and grow to higher cell densities compared to the wild type. A*gr* mutants were shown to out-compete the wild type consistent with previous in vitro (Paulander et al, 2013) and in vivo reports (Pollitt et al, 2014). Interestingly, the wild type is not lost from the population, but remains in the culture at low numbers (Fig. 18). This is likely because the AIP concentration falls below the threshold for Agr activation. Accordingly, a constitutive AIP producer in which AIP synthesis is uncoupled from QS is lost from the population after prolonged co-culture (Fig. 19B). When producers are scarce, the auto-regulatory properties of the system restrict AgrA activity and thereby maintain the producer in the population (publication 6, SI Appendix Fig. S1). Other mechanisms to inactivate Agr during infection e.g. through haemoglobin (Pynnonen et al, 2011), lipoproteins (Hall et al, 2013), oxidants (Rothfork et al, 2004) or microbial interference (Paharik et al, 2017; Piewngam et al, 2018; Williams et al, 2019) may similarly function to maintain producer-cheater homeostasis.

QS fitness cost is not due to metabolic burden

It was proposed that the fitness advantage of QS mutants is due to the costs associated with producing QS signal and/or the regulated public goods (Asfahl &

Schuster, 2017; Keller & Surette, 2006; Ruparell et al, 2016). The metabolic cost to just produce AIP in *S. aureus* was estimated to be high with 184 ATP for a single AgrD preprotein AIP (Keller & Surette, 2006). However, our data show that that the fitness advantage of *agr* mutants is independent of the assumed metabolic burden. First, an AIP non-producer showed a fitness advantage in monoculture but interestingly not in competition with an AIP producer. Thus, AIP synthesis itself does not impose a fitness burden. Secondly, the syntheses of down-stream targets (public goods) are also unlikely to drive evolution of *agr* mutants based on the metabolic burden to produce them. This is based on our observation that under anaerobic conditions, significantly more public goods such as PSMs or RNAIII regulated factors are synthesized (Fig. 22). However, under this specific condition the increased Agr activity has no impact on the fitness monitored either by growth (Fig. 22A) or in competition experiments (Fig. 21D). Of note, also for other QS systems experimental evidence for the assumption that QS cheaters arise because of the metabolic cost is limited (Ruparell et al, 2016) and warrants revisiting. This observation conforms to the idea that the function and not production of a factor downstream of QS signalling imposes the fitness burden under aerobic conditions.

Increased Agr activity under hypoxia

Here we demonstrated that Agr activity is increased during hypoxic growth, despite lower bacterial cell densities. Hypoxia results in significantly enhanced transcription of the main AgrA targets (RNAIII and *psm*), Hld synthesis, PSM-mediated protein release and cell toxicity (Fig. 22). The results confirm recent data from Wilde et al, 2015. It has been shown that oxidising conditions induce disulphide bond formation of AgrA involving the conserved cysteine Cys-199 (Sun et al, 2012b). Of note, the same residue also reacts with nitric oxide (Urbano et al, 2018). Both oxidation and S-nitrosylation of Cys-199 were shown to inhibit DNA-binding of AgrA to its cognate promoters. Therefore, under aerobic conditions AgrA function might be partially inhibited through oxidation.

Agr/PSM does not impose a fitness cost under hypoxia due to a diminished ROS formation

Under aerobic conditions, the fitness cost could be linked to PSM expression. Under hypoxia the higher level of PSMs does not affect fitness since bacteria are protected

from the anti-microbial activity of PSMs. We could further show that PSM synthesis results in increased ROS formation (Fig. 23B). This explains the fitness burden of *psm* positive strains under aerobic conditions only. However, it does not explain the fitness advantage of the RNAIII mutant. *AgrA* mutants were previously found to be more resistant towards certain kinds of oxidative stress which was linked to higher expression of the glutathione peroxidase BsaA (Kumar et al, 2017; Sun et al, 2012b). The role of BsaA could not be confirmed here. However, other ROS protective factors might be up-regulated in the RNAIII mutant to compensate for PSM toxicity.

Role of Agr QS In vivo

Several epidemiological and virulence studies indicate that Agr activity is required only under certain infection settings (He et al, 2019; Shopsin & Copin, 2018). Nevertheless, Agr activity is maintained in most colonising isolates despite the obvious fitness disadvantage. This indicates that on the population level several mechanisms may have evolved to maintain the balance. The Agr-system was found to be inactive during nose colonisation (Burian et al, 2010), possibly due to Agr interference imposed by other Staphylococci (Williams et al, 2019) in the skin microbiome. Many of the globally spreading haMRSA strains are characterised by low Agr activity (Wang et al, 2007) which could also be seen as a strategy to avoid *agr* mutant selection.

Aerobic growth conditions and the clinically-relevant quinolone antibiotic, ciprofloxacin accelerates the selection of *agr* mutants. Ciprofloxacin leads to induction of the SOS response and thus an increased mutation rate. However, ciprofloxacin might also favour *agr* mutations because they are better adapted to survive oxidative stress imposed by the antibiotic (Kumar et al, 2017). Thus, ROS formation by the bacterium's own products (PSMs), ciprofloxacin or other infection-related stresses such as phagocytosis may favour the selection of QS mutants. PSMs have been shown to disrupt membrane potential via depolarisation (Ebner et al, 2017) which might be a trigger for ROS accumulation. Bacteria have evolved mechanisms to dampen Agr activity under such conditions by e.g. AgrA oxidation/nitrosylation (Sun et al, 2012b; Urbano et al, 2018) or inactivation of the AIP (Rothfork et al, 2004). Hypoxic conditions in contrast favour the maintenance of

the wild type population and even allow the hyper-activation of the system without imposing a fitness burden.

S. aureus is a major skin pathogen and the oxygen-driven tuning of the Agr system might be especially of importance to provide the pathogen with different features beneficial for disease progression (Fig. 24). Under high O_2 conditions like at the skin surface, *agr* mutants are selected (Soong et al, 2015) and one may also speculate that this might be the source for *agr* mutants often found in bactaeremic patients (Fowler et al, 2004; Giulieri et al, 2018; Young et al, 2017). On the other hand, Agr activity is crucial for pathogenicity in skin abscesses (He et al, 2019). Here, *S. aureus* is entrapped in a hypoxic environment in which the bacteria can now afford to increase Agr activity without the accompanied fitness disadvantage. The increase in Agr-regulated toxins such as PSMs may thus function to facilitate escape from the abscess. In this manner the environmental oxygen might act to alter the bacterial perception of a self-inflicted insult such as the PSMs in order to change the course of microbial evolution.

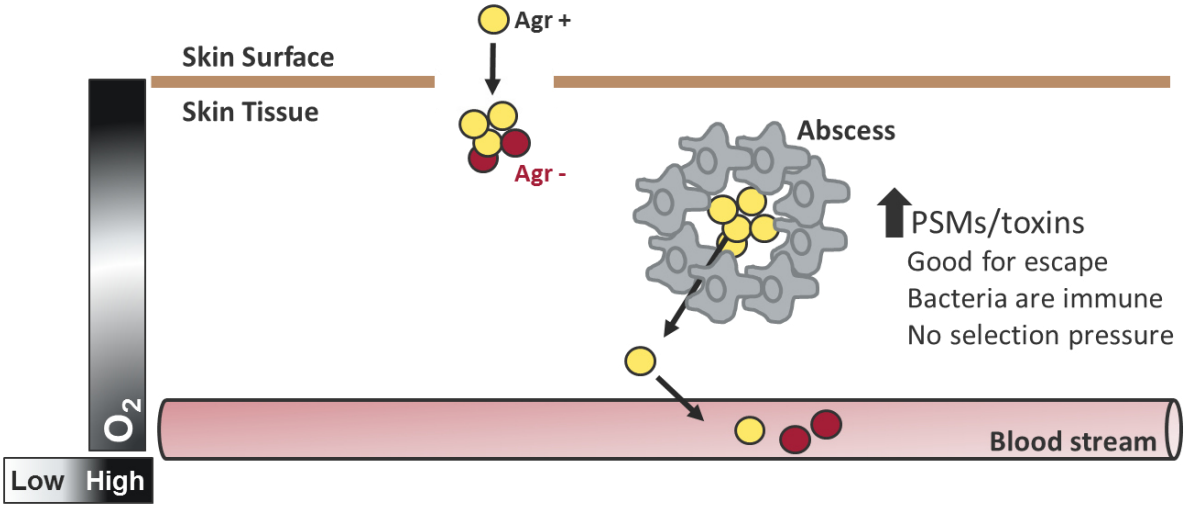

Figure 24: Oxygen drives mutations during *S. aureus* infection. Higher oxygen at the skin surface and in superficial tissues may drive the selection of *agr* mutants which subsequently have a fitness advantage over the wild type sub-population. High levels of Agr are necessary and even afforded during abscess infections to allow bacteria to escape host defences. The relatively higher oxygen levels in the blood may again select for spontaneous *agr* mutants. *S. aureus* may thus utilize or dispense with Agr function depending on the host environment.

Conclusions and future perspectives

In this work, we investigated both phenotypic and genetic heterogeneity within clonal populations of the human pathogen *Staphylococcus aureus*.

Capsule synthesis is a striking example of phenotypic heterogeneity wherein *cap* expression and synthesis follows a strict temporal pattern over growth. At the same time, only a few cells in a given population produce capsule. This peculiar temporal and bistable expression is tightly regulated by a vast number of intrinsic and extrinsic cues pertaining to either the genetic circuit itself or the environment that the circuit is embedded in. We have delineated several factors that operate on the promoter level thereby controlling *cap* expression, from promoter architecture to several transcriptional activators and repressors. These activators and repressors are in turn acted upon by environmental changes in nutrition, energy and even social behaviour. This is illustrated by our finding that SigB as a potent activator of *cap* expression is able to sense and respond to energy stress. Furthermore, the high noise in *cap* expression may be due to the noise propagation from its many regulators. Thus, heterogeneity in SigB may be partly responsible for the heterogeneity of *cap* expression. Post-transcriptionally, capsule synthesis also depends on freely available cell wall precursors that must be diverted away from the production of other cell wall components such as wall teichoic acids (WTA) and peptidoglycan (PG). The high level of inherent noise in capsule regulation may thus be due to a convergence of all these factors.

The conclusions in this work were reached by observing single cells at discrete time points i.e. across snapshots of the growing population (Thomas, 2019). To gain a better understanding of how all the intrinsic and extrinsic sources of noise might combine to result in a phenotype, we would need to study the real time dynamics of single cell behaviour under defined growth conditions. Microfluidic platforms coupled with low stability fluorescent reporters would allow us to connect promoter on and off states with single-cell growth parameters such as cell age, size, interdivision times and lineage history making it possible to answer whether cellular hysteresis or epigenetic memory plays a role (Kaiser et al, 2018; Roemhild et al, 2018; Veening et al, 2008). Furthermore, constitutive promoters may be able to report on growth rates as well as the inherent stochasticity in the system. Metabolic

sensors for ATP, pH as well as photo convertible reporters coupled to constitutive promoters may prove to be useful tools as well (Lobas et al, 2019; Seiß et al, 2019). Finally, studying the response of the single cell to shifts in the environment such as oxygen gradients and energy, pH or salt stress would help us understand population behaviour in the 'real' world such as during colonization or infection in the human host.

In a second example of heterogeneity, we sought to answer why quorum sensing genetic mutants rapidly arise in an infecting population although quorum sensing has been classically considered to be essential for virulence. The genetic diversity of infecting *S. aureus* populations has been widely reported for a variety of infection settings though most notoriously in the cystic fibrosis lung. We show that quorum sensing is costly for the bacterium not because of a metabolic burden but rather due to the production of the potent PSM toxins. However, this cost is perceived only under aerobiosis. Under low oxygen conditions, possibly such as that encountered in abscesses, bacteria can easily afford this cost to an extent that even upregulation of the QS system does not select for spontaneous *agr* mutants. This oxygen dependent sensitivity to self-produced PSMs allows the bacteria to wield the QS system to its advantage – shutting it down via genetic mutations when it is more important to increase population fitness and turning it up when encountering host defences. Our study highlights the significant influence the environment has on the behaviour and pathogenic potential of *S. aureus*. Recently, microbiome and metabolome maps of explanted lungs from cystic fibrosis patients revealed that chemical environments differ greatly between patients and within the lungs in the same individual (Melnik et al, 2019). This underscores how the chemical environment may shape bacterial interactions and vice versa.

S. aureus thus shows great genomic and regulatory versatility. In the short term phenotypic heterogeneity as demonstrated by capsule synthesis serves to bet-hedge changes in environment. In the long term, genetic variation allows committed adaptation to a specific niche. This versatility however does not bode well for patient outcomes in the clinic especially for the young and immune-compromised because then in spite of the resistance mounted against the bacterium, a sub-population may always be able to 'escape'. Phenotypic heterogeneity may in some instances foreshadow lasting genetic change. This is especially true in the case of antibiotic

tolerance and persistence paving the way for genetically ingrained antibiotic resistance (Dengler Haunreiter et al, 2019; Dhar & McKinney, 2007; Levin-Reisman et al, 2017). Finally, the interplay between both genetic and phenotypic adaptation strategies will shape the course of evolution.

References

Abisado RG, Benomar S, Klaus JR, Dandekar AA, Chandler JR (2018) Bacterial Quorum Sensing and Microbial Community Interactions. *mBio* **9**

Ackermann M (2015) A functional perspective on phenotypic heterogeneity in microorganisms. *Nature reviews Microbiology* **13:** 497-508

Andersson DI, Jerlstrom-Hultqvist J, Nasvall J (2015) Evolution of new functions de novo and from preexisting genes. *Cold Spring Harbor perspectives in biology* **7**

Andersson DI, Nicoloff H, Hjort K (2019) Mechanisms and clinical relevance of bacterial heteroresistance. *Nature reviews Microbiology* **17:** 479-496

Anetzberger C, Schell U, Jung K (2012) Single cell analysis of *Vibrio harveyi* uncovers functional heterogeneity in response to quorum sensing signals. *BMC microbiology* **12:** 209

Asfahl KL, Schuster M (2017) Social interactions in bacterial cell-cell signaling. *FEMS microbiology reviews* **41:** 92-107

Baddour LM, Lowrance C, Albus A, Lowrance JH, Anderson SK, Lee JC (1992) *Staphylococcus aureus* microcapsule expression attenuates bacterial virulence in a rat model of experimental endocarditis. *The Journal of infectious diseases* **165:** 749-753

Baharoglu Z, Mazel D (2014) SOS, the formidable strategy of bacteria against aggressions. *FEMS microbiology reviews* **38:** 1126-1145

Baig U, Sunny R, Watve M, Lele U (2016) Cumulative cell division time asymmetry in Staphyloccus aureus. *Matters (Zurich)*

Bakshi S, Dalrymple RM, Li W, Choi H, Weisshaar JC (2013) Partitioning of RNA polymerase activity in live Escherichia coli from analysis of single-molecule diffusive trajectories. *Biophysical journal* **105:** 2676-2686

Balaban NQ, Helaine S, Lewis K, Ackermann M, Aldridge B, Andersson DI, Brynildsen MP, Bumann D, Camilli A, Collins JJ, Dehio C, Fortune S, Ghigo JM, Hardt WD, Harms A, Heinemann M, Hung DT, Jenal U, Levin BR, Michiels J, Storz G, Tan MW, Tenson T, Van Melderen L, Zinkernagel A (2019) Definitions and guidelines for research on antibiotic persistence. *Nature reviews Microbiology* **17:** 441-448

Balasubramanian D, Harper L, Shopsin B, Torres VJ (2017) Staphylococcus aureus pathogenesis in diverse host environments. *Pathogens and disease* **75**

Balazsi G, van Oudenaarden A, Collins JJ (2011) Cellular decision making and biological noise: from microbes to mammals. *Cell* **144:** 910-925

Barreteau H, Magnet S, El Ghachi M, Touze T, Arthur M, Mengin-Lecreulx D, Blanot D (2009) Quantitative high-performance liquid chromatography analysis of the pool levels of undecaprenyl phosphate and its derivatives in bacterial membranes. *J Chromatogr B Analyt Technol Biomed Life Sci* **877:** 213-220

Barrett TC, Mok WWK, Murawski AM, Brynildsen MP (2019) Enhanced antibiotic resistance development from fluoroquinolone persisters after a single exposure to antibiotic. *Nature communications* **10:** 1177

Becher D, Hempel K, Sievers S, Zuhlke D, Pane-Farre J, Otto A, Fuchs S, Albrecht D, Bernhardt J, Engelmann S, Volker U, van Dijl JM, Hecker M (2009) A proteomic view of an important human

pathogen--towards the quantification of the entire *Staphylococcus aureus* proteome. *PloS one* **4:** e8176

Berube BJ, Bubeck Wardenburg J (2013) Staphylococcus aureus alpha-toxin: nearly a century of intrigue. *Toxins* **5:** 1140-1166

Bettenworth V, Steinfeld B, Duin H, Petersen K, Streit WR, Bischofs I, Becker A (2019) Phenotypic Heterogeneity in Bacterial Quorum Sensing Systems. *Journal of molecular biology*

Bidnenko E, Bidnenko V (2018) Transcription termination factor Rho and microbial phenotypic heterogeneity. **64:** 541-546

Bojer MS, Lindemose S, Vestergaard M, Ingmer H (2018) Quorum Sensing-Regulated Phenol-Soluble Modulins Limit Persister Cell Populations in Staphylococcus aureus. *Frontiers in microbiology* **9:** 255

Boles BR, Thoendel M, Singh PK (2004) Self-generated diversity produces "insurance effects" in biofilm communities. *Proceedings of the National Academy of Sciences of the United States of America* **101:** 16630-16635

Bronesky D, Desgranges E, Corvaglia A, François P, Caballero CJ, Prado L, Toledo-Arana A, Lasa I, Moreau K, Vandenesch F, Marzi S, Romby P, Caldelari I (2019) A multifaceted small RNA modulates gene expression upon glucose limitation in Staphylococcus aureus. *The EMBO journal* **38:** e99363

Bronesky D, Wu Z, Marzi S, Walter P, Geissmann T, Moreau K, Vandenesch F, Caldelari I, Romby P (2016) Staphylococcus aureus RNAIII and Its Regulon Link Quorum Sensing, Stress Responses, Metabolic Adaptation, and Regulation of Virulence Gene Expression. *Annual review of microbiology* **70:** 299-316

Burian M, Wolz C, Goerke C (2010) Regulatory adaptation of *Staphylococcus aureus* during nasal colonization of humans. *PloS one* **5:** e10040

Butterfield JM, Tsuji BT, Brown J, Ashley ED, Hardy D, Brown K, Forrest A, Lodise TP (2011) Predictors of agr dysfunction in methicillin-resistant Staphylococcus aureus (MRSA) isolates among patients with MRSA bloodstream infections. *Antimicrobial agents and chemotherapy* **55:** 5433-5437

Cabeen MT, Russell JR, Paulsson J, Losick R (2017) Use of a microfluidic platform to uncover basic features of energy and environmental stress responses in individual cells of Bacillus subtilis. *PLoS genetics* **13:** e1006901

Carreau A, El Hafny-Rahbi B, Matejuk A, Grillon C, Kieda C (2011) Why is the partial oxygen pressure of human tissues a crucial parameter? Small molecules and hypoxia. *Journal of cellular and molecular medicine* **15:** 1239-1253

Chatterjee SS, Joo HS, Duong AC, Dieringer TD, Tan VY, Song Y, Fischer ER, Cheung GY, Li M, Otto M (2013) Essential Staphylococcus aureus toxin export system. *Nature medicine* **19:** 364-367

Cheung GY, Joo HS, Chatterjee SS, Otto M (2014) Phenol-soluble modulins--critical determinants of staphylococcal virulence. *FEMS microbiology reviews* **38:** 698-719

Cirz RT, Jones MB, Gingles NA, Minogue TD, Jarrahi B, Peterson SN, Romesberg FE (2007) Complete and SOS-mediated response of *Staphylococcus aureus* to the antibiotic ciprofloxacin. *Journal of bacteriology* **189:** 531-539

Cogen AL, Yamasaki K, Sanchez KM, Dorschner RA, Lai Y, MacLeod DT, Torpey JW, Otto M, Nizet V, Kim JE, Gallo RL (2010) Selective antimicrobial action is provided by phenol-soluble modulins derived from Staphylococcus epidermidis, a normal resident of the skin. *The Journal of investigative dermatology* **130:** 192-200

Conlon BP, Rowe SE, Gandt AB, Nuxoll AS, Donegan NP, Zalis EA, Clair G, Adkins JN, Cheung AL, Lewis K (2016) Persister formation in Staphylococcus aureus is associated with ATP depletion. *Nature microbiology* **1:** 16051

Dassy B, Hogan T, Foster TJ, Fournier JM (1993) Involvement of the accessory gene regulator (agr) in expression of type 5 capsular polysaccharide by Staphylococcus aureus. *Journal of general microbiology* **139 Pt 6:** 1301-1306

Davis KM, Isberg RR (2016) Defining heterogeneity within bacterial populations via single cell approaches. *BioEssays : news and reviews in molecular, cellular and developmental biology* **38:** 782-790

Dengler Haunreiter V, Boumasmoud M, Haffner N, Wipfli D, Leimer N, Rachmuhl C, Kuhnert D, Achermann Y, Zbinden R, Benussi S, Vulin C, Zinkernagel AS (2019) In-host evolution of Staphylococcus epidermidis in a pacemaker-associated endocarditis resulting in increased antibiotic tolerance. *Nature communications* **10:** 1149

Dhar N, McKinney JD (2007) Microbial phenotypic heterogeneity and antibiotic tolerance. *Current opinion in microbiology* **10:** 30-38

Dragos A, Kiesewalter H, Martin M, Hsu CY, Hartmann R, Wechsler T, Eriksen C, Brix S, Drescher K, Stanley-Wall N, Kummerli R, Kovacs AT (2018) Division of Labor during Biofilm Matrix Production. *Current biology : CB* **28:** 1903-1913.e1905

Dubnau D, Losick R (2006) Bistability in bacteria. *Molecular microbiology* **61:** 564-572

Ducret A, Quardokus EM, Brun YV (2016) MicrobeJ, a tool for high throughput bacterial cell detection and quantitative analysis. *Nature microbiology* **1:** 16077

Dwyer DJ, Kohanski MA, Collins JJ (2009) Role of reactive oxygen species in antibiotic action and resistance. *Current opinion in microbiology* **12:** 482-489

Ebner P, Luqman A, Reichert S, Hauf K, Popella P, Forchhammer K, Otto M, Gotz F (2017) Non-classical Protein Excretion Is Boosted by PSMalpha-Induced Cell Leakage. *Cell reports* **20:** 1278-1286

Eldar A, Elowitz MB (2010) Functional roles for noise in genetic circuits. *Nature* **467:** 167

Eling N, Morgan MD (2019) Challenges in measuring and understanding biological noise. **20:** 536-548

Elowitz MB, Levine AJ, Siggia ED, Swain PS (2002) Stochastic gene expression in a single cell. *Science* **297:** 1183-1186

Fang FC, Frawley ER, Tapscott T, Vazquez-Torres A (2016) Bacterial Stress Responses during Host Infection. *Cell host & microbe* **20:** 133-143

Feltner JB, Wolter DJ, Pope CE, Groleau MC, Smalley NE, Greenberg EP, Mayer-Hamblett N, Burns J, Deziel E (2016) LasR Variant Cystic Fibrosis Isolates Reveal an Adaptable Quorum-Sensing Hierarchy in Pseudomonas aeruginosa. **7**

Fernandez-de-Cossio-Diaz J, Mulet R, Vazquez A (2019) Cell population heterogeneity driven by stochastic partition and growth optimality. *Scientific reports* **9:** 9406

Ferry T, Perpoint T, Vandenesch F, Etienne J (2005) Virulence determinants in Staphylococcus aureus and their involvement in clinical syndromes. *Current infectious disease reports* **7:** 420-428

Fowler VG, Jr., Sakoulas G, McIntyre LM, Meka VG, Arbeit RD, Cabell CH, Stryjewski ME, Eliopoulos GM, Reller LB, Corey GR, Jones T, Lucindo N, Yeaman MR, Bayer AS (2004) Persistent bacteremia due to methicillin-resistant Staphylococcus aureus infection is associated with agr dysfunction and

low-level in vitro resistance to thrombin-induced platelet microbicidal protein. *The Journal of infectious diseases* **190:** 1140-1149

Freed NE, Silander OK, Stecher B, Bohm A, Hardt WD, Ackermann M (2008) A simple screen to identify promoters conferring high levels of phenotypic noise. *PLoS genetics* **4:** e1000307

Garcia-Betancur JC, Goni-Moreno A, Horger T, Schott M, Sharan M, Eikmeier J, Wohlmuth B, Zernecke A, Ohlsen K, Kuttler C, Lopez D (2017) Cell differentiation defines acute and chronic infection cell types in Staphylococcus aureus. *eLife* **6**

Garcia-Betancur JC, Lopez D (2019) Cell Heterogeneity in Staphylococcal Communities. *Journal of molecular biology*

Geisinger E, Muir TW, Novick RP (2009) *agr* receptor mutants reveal distinct modes of inhibition by staphylococcal autoinducing peptides. *Proceedings of the National Academy of Sciences of the United States of America* **106:** 1216-1221

George SE, Nguyen T, Geiger T, Weidenmaier C, Lee JC, Liese J, Wolz C (2015) Phenotypic heterogeneity and temporal expression of the capsular polysaccharide in Staphylococcus aureus. *Molecular microbiology* **98:** 1073-1088

Giulieri SG, Baines SL, Guerillot R, Seemann T, Goncalves da Silva A, Schultz M, Massey RC, Holmes NE, Stinear TP, Howden BP (2018) Genomic exploration of sequential clinical isolates reveals a distinctive molecular signature of persistent Staphylococcus aureus bacteraemia. *Genome medicine* **10:** 65

Goerke C, Campana S, Bayer MG, Doring G, Botzenhart K, Wolz C (2000) Direct quantitative transcript analysis of the agr regulon of Staphylococcus aureus during human infection in comparison to the expression profile in vitro. *Infection and immunity* **68:** 1304-1311

Goerke C, Gressinger M, Endler K, Breitkopf C, Wardecki K, Stern M, Wolz C, Kahl BC (2007) High phenotypic diversity in infecting but not in colonizing *Staphylococcus aureus* populations. *Environmental microbiology* **9:** 3134-3142

Guerillot R, Kostoulias X, Donovan L, Li L, Carter GP, Hachani A, Vandelannoote K, Giulieri S, Monk IR, Kunimoto M, Starrs L, Burgio G, Seemann T, Peleg AY, Stinear TP, Howden BP (2019) Unstable chromosome rearrangements in Staphylococcus aureus cause phenotype switching associated with persistent infections. *Proceedings of the National Academy of Sciences of the United States of America*

Guldimann C, Guariglia-Oropeza V, Harrand S, Kent D, Boor KJ, Wiedmann M (2017) Stochastic and Differential Activation of σB and PrfA in Listeria monocytogenes at the Single Cell Level under Different Environmental Stress Conditions. *Frontiers in Microbiology* **8**

Hall PR, Elmore BO, Spang CH, Alexander SM, Manifold-Wheeler BC, Castleman MJ, Daly SM, Peterson MM, Sully EK, Femling JK, Otto M, Horswill AR, Timmins GS, Gresham HD (2013) Nox2 modification of LDL is essential for optimal apolipoprotein B-mediated control of agr type III Staphylococcus aureus quorum-sensing. *PLoS pathogens* **9:** e1003166

Hammerschmidt S, Wolff S, Hocke A, Rosseau S, Muller E, Rohde M (2005) Illustration of pneumococcal polysaccharide capsule during adherence and invasion of epithelial cells. *Infection and immunity* **73:** 4653-4667

Hamoen LW, Kausche D, Marahiel MA, van Sinderen D, Venema G, Serror P (2003) The Bacillus subtilis transition state regulator AbrB binds to the -35 promoter region of comK. *FEMS microbiology letters* **218:** 299-304

Hamoen LW, Van Werkhoven AF, Venema G, Dubnau D (2000) The pleiotropic response regulator DegU functions as a priming protein in competence development in Bacillus subtilis. *Proceedings of the National Academy of Sciences of the United States of America* **97:** 9246-9251

Hanzelmann D, Joo HS, Franz-Wachtel M, Hertlein T, Stevanovic S, Macek B, Wolz C, Gotz F, Otto M, Kretschmer D, Peschel A (2016) Toll-like receptor 2 activation depends on lipopeptide shedding by bacterial surfactants. *Nature communications* **7:** 12304

He L, Le KY, Khan BA (2019) Resistance to leukocytes ties benefits of quorum sensing dysfunctionality to biofilm infection. **4:** 1114-1119

Herbert S, Newell SW, Lee C, Wieland KP, Dassy B, Fournier JM, Wolz C, Doring G (2001) Regulation of *Staphylococcus aureus* type 5 and type 8 capsular polysaccharides by $CO_{(2)}$. *Journal of bacteriology* **183:** 4609-4613

Herbert S, Worlitzsch D, Dassy B, Boutonnier A, Fournier JM, Bellon G, Dalhoff A, Doring G (1997) Regulation of *Staphylococcus aureus* capsular polysaccharide type 5: CO2 inhibition in vitro and in vivo. *The Journal of infectious diseases* **176:** 431-438

Hershberg R (2015) Mutation--The Engine of Evolution: Studying Mutation and Its Role in the Evolution of Bacteria. *Cold Spring Harbor perspectives in biology* **7:** a018077

Hoa TT, Tortosa P, Albano M, Dubnau D (2002) Rok (YkuW) regulates genetic competence in Bacillus subtilis by directly repressing comK. *Molecular microbiology* **43:** 15-26

Huh D, Paulsson J (2011) Non-genetic heterogeneity from stochastic partitioning at cell division. *Nature genetics* **43:** 95-100

Janzon L, Arvidson S (1990) The role of the delta-lysin gene (hld) in the regulation of virulence genes by the accessory gene regulator (agr) in Staphylococcus aureus. *The EMBO journal* **9:** 1391-1399

Janzon L, Lofdahl S, Arvidson S (1989) Identification and nucleotide sequence of the delta-lysin gene, hld, adjacent to the accessory gene regulator (agr) of Staphylococcus aureus. *Molecular & general genetics : MGG* **219:** 480-485

Joo HS, Cheung GY, Otto M (2011) Antimicrobial activity of community-associated methicillin-resistant Staphylococcus aureus is caused by phenol-soluble modulin derivatives. *The Journal of biological chemistry* **286:** 8933-8940

Kaiser M, Jug F, Julou T, Deshpande S, Pfohl T, Silander OK, Myers G, van Nimwegen E (2018) Monitoring single-cell gene regulation under dynamically controllable conditions with integrated microfluidics and software. *Nature communications* **9:** 212

Kalka-Moll WM, Tzianabos AO, Bryant PW, Niemeyer M, Ploegh HL, Kasper DL (2002) Zwitterionic polysaccharides stimulate T cells by MHC class II-dependent interactions. *Journal of immunology (Baltimore, Md : 1950)* **169:** 6149-6153

Kavanaugh JS, Horswill AR (2016) Impact of Environmental Cues on Staphylococcal Quorum Sensing and Biofilm Development. *The Journal of biological chemistry* **291:** 12556-12564

Keinhorster D, George SE, Weidenmaier C, Wolz C (2019a) Function and regulation of Staphylococcus aureus wall teichoic acids and capsular polysaccharides. *International journal of medical microbiology : IJMM* **309:** 151333

Keinhorster D, Salzer A, Duque-Jaramillo A, George SE, Marincola G, Lee JC, Weidenmaier C, Wolz C (2019b) Revisiting the regulation of the capsular polysaccharide biosynthesis gene cluster in Staphylococcus aureus. *Molecular microbiology*

Keller L, Surette MG (2006) Communication in bacteria: an ecological and evolutionary perspective. *Nature Reviews Microbiology* **4:** 249

Kim S, Jacobs-Wagner C (2018) Effects of mRNA Degradation and Site-Specific Transcriptional Pausing on Protein Expression Noise. *Biophys J* **114:** 1718-1729

Klironomos FD, Berg J, Collins S (2013) How epigenetic mutations can affect genetic evolution: model and mechanism. *BioEssays : news and reviews in molecular, cellular and developmental biology* **35:** 571-578

Kong EF, Johnson JK (2016) Community-Associated Methicillin-Resistant Staphylococcus aureus: An Enemy amidst Us. **12:** e1005837

Kumar K, Chen J, Drlica K, Shopsin B (2017) Tuning of the Lethal Response to Multiple Stressors with a Single-Site Mutation during Clinical Infection by Staphylococcus aureus. *mBio* **8**

Lattar SM, Tuchscherr LP, Caccuri RL, Centron D, Becker K, Alonso CA, Barberis C, Miranda G, Buzzola FR, von Eiff C, Sordelli DO (2009) Capsule expression and genotypic differences among *Staphylococcus aureus* isolates from patients with chronic or acute osteomyelitis. *Infection and immunity* **77:** 1968-1975

Le KY, Otto M (2015) Quorum-sensing regulation in staphylococci-an overview. *Frontiers in microbiology* **6:** 1174

Leisner M, Stingl K, Frey E, Maier B (2008) Stochastic switching to competence. *Current opinion in microbiology* **11:** 553-559

Levin-Reisman I, Ronin I, Gefen O (2017) Antibiotic tolerance facilitates the evolution of resistance. **355:** 826-830

Leygeber M, Lindemann D, Sachs CC, Kaganovitch E, Wiechert W, Noh K, Kohlheyer D (2019) Analyzing Microbial Population Heterogeneity-Expanding the Toolbox of Microfluidic Single-Cell Cultivations. *Journal of molecular biology*

Liu Q, Yeo WS, Bae T (2016) The SaeRS Two-Component System of Staphylococcus aureus. *Genes* **7**

Lobas MA, Tao R, Nagai J, Kronschläger MT, Borden PM, Marvin JS, Looger LL, Khakh BS (2019) A genetically encoded single-wavelength sensor for imaging cytosolic and cell surface ATP. *Nature communications* **10:** 711

Locke JC, Young JW, Fontes M, Hernandez Jimenez MJ, Elowitz MB (2011) Stochastic pulse regulation in bacterial stress response. *Science (New York, NY)* **334:** 366-369

Lopatkin AJ, Stokes JM, Zheng EJ, Yang JH, Takahashi MK, You L, Collins JJ (2019) Bacterial metabolic state more accurately predicts antibiotic lethality than growth rate. *Nature microbiology*

Luong T, Sau S, Gomez M, Lee JC, Lee CY (2002) Regulation of *Staphylococcus aureus* capsular polysaccharide expression by *agr* and *sar*A. *Infection and immunity* **70:** 444-450

Luong TT, Sau K, Roux C, Sau S, Dunman PM, Lee CY (2011) *Staphylococcus aureus* ClpC divergently regulates capsule via *sae* and *codY* in strain newman but activates capsule via *codY* in strain UAMS-1 and in strain Newman with repaired *saeS*. *Journal of bacteriology* **193:** 686-694

Maamar H, Dubnau D (2005) Bistability in the *Bacillus subtilis* K-state (competence) system requires a positive feedback loop. *Molecular microbiology* **56:** 615-624

Maamar H, Raj A, Dubnau D (2007) Noise in gene expression determines cell fate in Bacillus subtilis. *Science* **317:** 526-529

Mader U, Nicolas P, Depke M, Pane-Farre J, Debarbouille M, van der Kooi-Pol MM, Guerin C, Derozier S, Hiron A, Jarmer H, Leduc A, Michalik S, Reilman E, Schaffer M, Schmidt F, Bessieres P,

Noirot P, Hecker M, Msadek T, Volker U, van Dijl JM (2016) Staphylococcus aureus Transcriptome Architecture: From Laboratory to Infection-Mimicking Conditions. *PLoS genetics* **12:** e1005962

Majerczyk CD, Dunman PM, Luong TT, Lee CY, Sadykov MR, Somerville GA, Bodi K, Sonenshein AL (2010) Direct targets of CodY in *Staphylococcus aureus*. *Journal of bacteriology* **192:** 2861-2877

Malhotra S, Hayes D, Jr., Wozniak DJ (2019) Cystic Fibrosis and Pseudomonas aeruginosa: the Host-Microbe Interface. *Clinical microbiology reviews* **32**

Maslowska KH, Makiela-Dzbenska K, Fijalkowska IJ (2019) The SOS system: A complex and tightly regulated response to DNA damage. *Environ Mol Mutagen* **60:** 368-384

McLoughlin RM, Solinga RM, Rich J, Zaleski KJ, Cocchiaro JL, Risley A, Tzianabos AO, Lee JC (2006) CD4+ T cells and CXC chemokines modulate the pathogenesis of *Staphylococcus aureus* wound infections. *Proceedings of the National Academy of Sciences of the United States of America* **103:** 10408-10413

Melnik AV, Vazquez-Baeza Y, Aksenov AA, Hyde E, McAvoy AC, Wang M, da Silva RR, Protsyuk I, Wu JV, Bouslimani A, Lim YW, Luzzatto-Knaan T, Comstock W, Quinn RA, Wong R, Humphrey G, Ackermann G, Spivey T, Brouha SS, Bandeira N, Lin GY, Rohwer F, Conrad DJ, Alexandrov T, Knight R, Dorrestein PC, Garg N (2019) Molecular and Microbial Microenvironments in Chronically Diseased Lungs Associated with Cystic Fibrosis. *mSystems* **4**

Munsky B, Neuert G, van Oudenaarden A (2012) Using gene expression noise to understand gene regulation. *Science (New York, NY)* **336:** 183-187

Nanra JS, Buitrago SM, Crawford S, Ng J, Fink PS, Hawkins J, Scully IL, McNeil LK, Aste-Amezaga JM, Cooper D, Jansen KU, Anderson AS (2013) Capsular polysaccharides are an important immune evasion mechanism for Staphylococcus aureus. *Human vaccines & immunotherapeutics* **9:** 480-487

Nasvall J, Sun L, Roth JR, Andersson DI (2012) Real-time evolution of new genes by innovation, amplification, and divergence. *Science (New York, NY)* **338:** 384-387

Nemeth J, Lee JC (1995) Antibodies to capsular polysaccharides are not protective against experimental *Staphylococcus aureus* endocarditis. *Infection and immunity* **63:** 375-380

Nilsson IM, Lee JC, Bremell T, Ryden C, Tarkowski A (1997) The role of staphylococcal polysaccharide microcapsule expression in septicemia and septic arthritis. *Infection and immunity* **65:** 4216-4221

Novick RP, Geisinger E (2008) Quorum sensing in staphylococci. *Annual review of genetics* **42:** 541-564

O'Riordan K, Lee JC (2004) *Staphylococcus aureus* capsular polysaccharides. *Clinical microbiology reviews* **17:** 218-234

Oliver A, Mena A (2010) Bacterial hypermutation in cystic fibrosis, not only for antibiotic resistance. *Clinical microbiology and infection : the official publication of the European Society of Clinical Microbiology and Infectious Diseases* **16:** 798-808

Ozbudak EM, Thattai M, Kurtser I, Grossman AD, van Oudenaarden A (2002) Regulation of noise in the expression of a single gene. *Nature genetics* **31:** 69-73

Paharik AE, Parlet CP, Chung N, Todd DA, Rodriguez EI, Van Dyke MJ, Cech NB, Horswill AR (2017) Coagulase-Negative Staphylococcal Strain Prevents Staphylococcus aureus Colonization and Skin Infection by Blocking Quorum Sensing. *Cell host & microbe* **22:** 746-756.e745

Painter KL, Krishna A, Wigneshweraraj S, Edwards AM (2014) What role does the quorum-sensing accessory gene regulator system play during Staphylococcus aureus bacteremia? *Trends in microbiology* **22**

Paulander W, Nissen Varming A, Baek KT, Haaber J, Frees D, Ingmer H (2013) Antibiotic-mediated selection of quorum-sensing-negative Staphylococcus aureus. *mBio* **3:** e00459-00412

Pedraza JM, van Oudenaarden A (2005) Noise propagation in gene networks. *Science (New York, NY)* **307:** 1965-1969

Perez PD, Hagen SJ (2010) Heterogeneous response to a quorum-sensing signal in the luminescence of individual *Vibrio fischeri*. *PloS one* **5:** e15473

Periasamy S, Joo HS, Duong AC, Bach TH, Tan VY, Chatterjee SS, Cheung GY, Otto M (2012) How *Staphylococcus aureus* biofilms develop their characteristic structure. *Proceedings of the National Academy of Sciences of the United States of America* **109:** 1281-1286

Peschel A, Otto M (2013) Phenol-soluble modulins and staphylococcal infection. *Nature reviews Microbiology* **11:** 667-673

Piewngam P, Zheng Y, Nguyen TH, Dickey SW, Joo HS, Villaruz AE, Glose KA, Fisher EL, Hunt RL, Li B, Chiou J, Pharkjaksu S, Khongthong S, Cheung GYC, Kiratisin P, Otto M (2018) Pathogen elimination by probiotic Bacillus via signalling interference. *Nature* **562:** 532-537

Pohl K, Francois P, Stenz L, Schlink F, Geiger T, Herbert S, Goerke C, Schrenzel J, Wolz C (2009) CodY in *Staphylococcus aureus*: a regulatory link between metabolism and virulence gene expression. *Journal of bacteriology* **191:** 2953-2963

Pohlmann-Dietze P, Ulrich M, Kiser KB, Doring G, Lee JC, Fournier JM, Botzenhart K, Wolz C (2000) Adherence of *Staphylococcus aureus* to endothelial cells: influence of capsular polysaccharide, global regulator *agr*, and bacterial growth phase. *Infection and immunity* **68:** 4865-4871

Pollitt EJG, West SA, Crusz SA, Burton-Chellew MN, Diggle SP (2014) Cooperation, Quorum Sensing, and Evolution of Virulence in Staphylococcus aureus. *Infection and immunity* **82:** 1045-1051

Portoles M, Kiser KB, Bhasin N, Chan KH, Lee JC (2001) Staphylococcus aureus Cap5O has UDP-ManNAc dehydrogenase activity and is essential for capsule expression. *Infection and immunity* **69:** 917-923

Poutrel B, Rainard P, Sarradin P (1997) Heterogeneity of cell-associated CP5 expression on *Staphylococcus aureus* strains demonstrated by flow cytometry. *Clinical and diagnostic laboratory immunology* **4:** 275-278

Pradhan BB, Chatterjee S (2014) Reversible non-genetic phenotypic heterogeneity in bacterial quorum sensing. *Molecular microbiology* **92:** 557-569

Prados J, Linder P, Redder P (2016) TSS-EMOTE, a refined protocol for a more complete and less biased global mapping of transcription start sites in bacterial pathogens. *BMC genomics* **17:** 849

Prepiak P, Dubnau D (2007) A peptide signal for adapter protein-mediated degradation by the AAA+ protease ClpCP. *Mol Cell* **26:** 639-647

Price-Whelan A, Poon CK, Benson MA, Eidem TT, Roux CM, Boyd JM, Dunman PM, Torres VJ, Krulwich TA (2013) Transcriptional profiling of *Staphylococcus aureus* during growth in 2 M NaCl leads to clarification of physiological roles for Kdp and Ktr K+ uptake systems. *mBio* **4**

Pynnonen M, Stephenson RE, Schwartz K, Hernandez M, Boles BR (2011) Hemoglobin promotes Staphylococcus aureus nasal colonization. *PLoS pathogens* **7:** e1002104

Queck SY, Jameson-Lee M, Villaruz AE, Bach TH, Khan BA, Sturdevant DE, Ricklefs SM, Li M, Otto M (2008) RNAIII-independent target gene control by the *agr* quorum-sensing system: insight into the evolution of virulence regulation in *Staphylococcus aureus*. *Mol Cell* **32:** 150-158

Raj A, van Oudenaarden A (2008) Nature, nurture, or chance: stochastic gene expression and its consequences. *Cell* **135:** 216-226

Ram Y, Hadany L (2014) Stress-induced mutagenesis and complex adaptation. *Proceedings Biological sciences* **281**

Rausch M, Deisinger JP, Ulm H, Muller A, Li W, Hardt P, Wang X, Li X, Sylvester M, Engeser M, Vollmer W, Muller CE, Sahl HG, Lee JC, Schneider T (2019) Coordination of capsule assembly and cell wall biosynthesis in Staphylococcus aureus. *Nature communications* **10:** 1404

Richardson AR, Somerville GA, Sonenshein AL (2015) Regulating the Intersection of Metabolism and Pathogenesis in Gram-positive Bacteria. *Microbiology spectrum* **3**

Risley AL, Loughman A, Cywes-Bentley C, Foster TJ, Lee JC (2007) Capsular polysaccharide masks clumping factor A-mediated adherence of *Staphylococcus aureus* to fibrinogen and platelets. *The Journal of infectious diseases* **196:** 919-927

Rodriguez-Beltran J, Hernandez-Beltran JCR, DelaFuente J, Escudero JA, Fuentes-Hernandez A, MacLean RC (2018) Multicopy plasmids allow bacteria to escape from fitness trade-offs during evolutionary innovation. **2:** 873-881

Roemhild R, Gokhale CS, Dirksen P, Blake C, Rosenstiel P, Traulsen A, Andersson DI, Schulenburg H (2018) Cellular hysteresis as a principle to maximize the efficacy of antibiotic therapy. *Proceedings of the National Academy of Sciences* **115:** 9767-9772

Romilly C, Lays C, Tomasini A, Caldelari I, Benito Y, Hammann P, Geissmann T, Boisset S, Romby P, Vandenesch F (2014) A non-coding RNA promotes bacterial persistence and decreases virulence by regulating a regulator in *Staphylococcus aureus*. *PLoS pathogens* **10:** e1003979

Rosenthal AZ, Qi Y, Hormoz S, Park J, Li SH, Elowitz MB (2018) Metabolic interactions between dynamic bacterial subpopulations. *eLife* **7**

Rothfork JM, Timmins GS, Harris MN, Chen X, Lusis AJ, Otto M, Cheung AL, Gresham HD (2004) Inactivation of a bacterial virulence pheromone by phagocyte-derived oxidants: new role for the NADPH oxidase in host defense. *Proceedings of the National Academy of Sciences of the United States of America* **101:** 13867-13872

Ruparell A, Dubern JF, Ortori CA, Harrison F, Halliday NM, Emtage A, Ashawesh MM, Laughton CA, Diggle SP, Williams P, Barrett DA, Hardie KR (2016) The fitness burden imposed by synthesising quorum sensing signals. *Scientific reports* **6:** 33101

Ryall B, Eydallin G, Ferenci T (2012) Culture history and population heterogeneity as determinants of bacterial adaptation: the adaptomics of a single environmental transition. *Microbiology and molecular biology reviews : MMBR* **76:** 597-625

Sadykov MR, Mattes TA, Luong TT, Zhu Y, Day SR, Sifri CD, Lee CY, Somerville GA (2010) Tricarboxylic acid cycle-dependent synthesis of Staphylococcus aureus Type 5 and 8 capsular polysaccharides. *Journal of bacteriology* **192:** 1459-1462

Sanchez A, Garcia HG, Jones D, Phillips R, Kondev J (2011) Effect of Promoter Architecture on the Cell-to-Cell Variability in Gene Expression. *PLoS computational biology* **7:** e1001100

Sandoz KM, Mitzimberg SM, Schuster M (2007) Social cheating in Pseudomonas aeruginosa quorum sensing. *Proceedings of the National Academy of Sciences* **104:** 15876

Sau S, Bhasin N, Wann ER, Lee JC, Foster TJ, Lee CY (1997) The *Staphylococcus aureus* allelic genetic loci for serotype 5 and 8 capsule expression contain the type-specific genes flanked by common genes. *Microbiology* **143 (Pt 7):** 2395-2405

Schlatterer K, Beck C, Hanzelmann D, Lebtig M, Fehrenbacher B, Schaller M, Ebner P, Nega M, Otto M, Kretschmer D, Peschel A (2018) The Mechanism behind Bacterial Lipoprotein Release: Phenol-Soluble Modulins Mediate Toll-Like Receptor 2 Activation via Extracellular Vesicle Release from Staphylococcus aureus. *mBio* **9**

Schreiber F, Littmann S, Lavik G, Escrig S, Meibom A, Kuypers MM, Ackermann M (2016) Phenotypic heterogeneity driven by nutrient limitation promotes growth in fluctuating environments. *Nat Microbiol* **1:** 16055

Schroder W, Bernhardt J, Marincola G, Klein-Hitpass L, Herbig A, Krupp G, Nieselt K, Wolz C (2014) Altering gene expression by aminocoumarins: the role of DNA supercoiling in *Staphylococcus aureus*. *BMC genomics* **15:** 291

Schroder W, Goerke C, Wolz C (2013) Opposing effects of aminocoumarins and fluoroquinolones on the SOS response and adaptability in Staphylococcus aureus. *The Journal of antimicrobial chemotherapy* **68:** 529-538

Schweizer ML, Furuno JP, Sakoulas G, Johnson JK, Harris AD, Shardell MD, McGregor JC, Thom KA, Perencevich EN (2011) Increased mortality with accessory gene regulator (agr) dysfunction in Staphylococcus aureus among bacteremic patients. *Antimicrobial agents and chemotherapy* **55:** 1082-1087

Seidl K, Stucki M, Ruegg M, Goerke C, Wolz C, Harris L, Berger-Bachi B, Bischoff M (2006) Staphylococcus aureus CcpA affects virulence determinant production and antibiotic resistance. *Antimicrobial agents and chemotherapy* **50:** 1183-1194

Seiß EA, Krone A, Formaglio P, Goldmann O, Engelmann S, Schraven B, Medina E, Müller AJ (2019) Longitudinal proliferation mapping in vivo reveals NADPH oxidase-mediated dampening of Staphylococcus aureus growth rates within neutrophils. *Scientific reports* **9:** 5703-5703

Serror P, Sonenshein AL (1996) Interaction of CodY, a novel *Bacillus subtilis* DNA-binding protein, with the dpp promoter region. *Molecular microbiology* **20:** 843-852

Sharon E, van Dijk D, Kalma Y, Keren L, Manor O, Yakhini Z, Segal E (2014) Probing the effect of promoters on noise in gene expression using thousands of designed sequences. *Genome research* **24:** 1698-1706

Shopsin B, Copin R (2018) Staphylococcus aureus Adaptation During Infection. In *Antimicrobial Resistance in the 21st Century*, Fong IW, Shlaes D, Drlica K (eds), pp 431-459. Cham: Springer International Publishing

Simsek E, Kim M (2018) The emergence of metabolic heterogeneity and diverse growth responses in isogenic bacterial cells. *Isme j* **12:** 1199-1209

Skinner SO, Sepulveda LA, Xu H, Golding I (2013) Measuring mRNA copy number in individual Escherichia coli cells using single-molecule fluorescent in situ hybridization. *Nat Protoc* **8:** 1100-1113

Smits WK, Eschevins CC, Susanna KA, Bron S, Kuipers OP, Hamoen LW (2005) Stripping Bacillus: ComK auto-stimulation is responsible for the bistable response in competence development. *Molecular Microbiology* **56:** 604-614

Soong G, Paulino F, Wachtel S, Parker D, Wickersham M, Zhang D, Brown A, Lauren C, Dowd M, West E, Horst B, Planet P, Prince A (2015) Methicillin-resistant Staphylococcus aureus adaptation to human keratinocytes. *mBio* **6**

Steinhuber A, Goerke C, Bayer MG, Doring G, Wolz C (2003) Molecular architecture of the regulatory Locus sae of Staphylococcus aureus and its impact on expression of virulence factors. *Journal of bacteriology* **185:** 6278-6286

Stevens E, Laabei M, Gardner S, Somerville GA, Massey RC (2017) Cytolytic toxin production by Staphylococcus aureus is dependent upon the activity of the protoheme IX farnesyltransferase. *Scientific reports* **7:** 13744

Suligoy CM, Lattar SM, Noto Llana M, Gonzalez CD, Alvarez LP, Robinson DA, Gomez MI, Buzzola FR, Sordelli DO (2018) Mutation of Agr Is Associated with the Adaptation of Staphylococcus aureus to the Host during Chronic Osteomyelitis. *Frontiers in cellular and infection microbiology* **8:** 18

Sun F, Ji Q, Jones MB, Deng X, Liang H, Frank B, Telser J, Peterson SN, Bae T, He C (2012a) AirSR, a [2Fe-2S] cluster-containing two-component system, mediates global oxygen sensing and redox signaling in *Staphylococcus aureus*. *Journal of the American Chemical Society* **134:** 305-314

Sun F, Liang H, Kong X, Xie S, Cho H, Deng X, Ji Q, Zhang H, Alvarez S, Hicks LM, Bae T, Luo C, Jiang H, He C (2012b) Quorum-sensing agr mediates bacterial oxidation response via an intramolecular disulfide redox switch in the response regulator AgrA. *Proceedings of the National Academy of Sciences of the United States of America* **109:** 9095-9100

Swain PS, Elowitz MB, Siggia ED (2002) Intrinsic and extrinsic contributions to stochasticity in gene expression. *Proceedings of the National Academy of Sciences of the United States of America* **99:** 12795-12800

Tadrowski AC, Evans MR, Waclaw B (2018) Phenotypic Switching Can Speed up Microbial Evolution. *Scientific reports* **8:** 8941

Thakker M, Park JS, Carey V, Lee JC (1998) *Staphylococcus aureus* serotype 5 capsular polysaccharide is antiphagocytic and enhances bacterial virulence in a murine bacteremia model. *Infection and immunity* **66:** 5183-5189

Thomas P (2019) Intrinsic and extrinsic noise of gene expression in lineage trees. *Scientific reports* **9:** 474

To TL, Maheshri N (2010) Noise can induce bimodality in positive transcriptional feedback loops without bistability. *Science (New York, NY)* **327:** 1142-1145

Tong SY, Davis JS, Eichenberger E, Holland TL, Fowler VG, Jr. (2015) Staphylococcus aureus infections: epidemiology, pathophysiology, clinical manifestations, and management. *Clinical microbiology reviews* **28:** 603-661

Traber KE, Lee E, Benson S, Corrigan R, Cantera M, Shopsin B, Novick RP (2008) agr function in clinical Staphylococcus aureus isolates. *Microbiology* **154:** 2265-2274

Tsimring LS (2014) Noise in biology. *Rep Prog Phys* **77:** 026601

Tuchscherr L, Loffler B, Buzzola FR, Sordelli DO (2010) *Staphylococcus aureus* adaptation to the host and persistence: role of loss of capsular polysaccharide expression. *Future microbiology* **5:** 1823-1832

Tuchscherr LP, Buzzola FR, Alvarez LP, Caccuri RL, Lee JC, Sordelli DO (2005) Capsule-negative *Staphylococcus aureus* induces chronic experimental mastitis in mice. *Infection and immunity* **73:** 7932-7937

Urbano R, Karlinsey JE, Libby SJ, Doulias PT, Ischiropoulos H, Warheit-Niemi HI, Liggitt DH, Horswill AR, Fang FC (2018) Host Nitric Oxide Disrupts Microbial Cell-to-Cell Communication to Inhibit Staphylococcal Virulence. *Cell host & microbe* **23:** 594-606.e597

Utratna M, Cosgrave E, Baustian C, Ceredig R, O'Byrne C (2012) Development and optimization of an EGFP-based reporter for measuring the general stress response in Listeria monocytogenes. *Bioengineered bugs* **3:** 93-103

van Boxtel C, van Heerden JH, Nordholt N, Schmidt P, Bruggeman FJ (2017) Taking chances and making mistakes: non-genetic phenotypic heterogeneity and its consequences for surviving in dynamic environments. *Journal of the Royal Society, Interface* **14**

van der Veen S, Tang CM (2015) The BER necessities: the repair of DNA damage in human-adapted bacterial pathogens. *Nature reviews Microbiology* **13:** 83-94

Veening JW, Smits WK, Kuipers OP (2008) Bistability, epigenetics, and bet-hedging in bacteria. *Annual review of microbiology* **62:** 193-210

Vulin C, Leimer N, Huemer M, Ackermann M, Zinkernagel AS (2018) Prolonged bacterial lag time results in small colony variants that represent a sub-population of persisters. *Nature communications* **9:** 4074

Wang B, Muir TW (2016) Regulation of Virulence in Staphylococcus aureus: Molecular Mechanisms and Remaining Puzzles. *Cell chemical biology* **23:** 214-224

Wang M, Schaefer AL, Dandekar AA, Greenberg EP (2015) Quorum sensing and policing of Pseudomonas aeruginosa social cheaters. *Proceedings of the National Academy of Sciences of the United States of America* **112:** 2187-2191

Wang R, Braughton KR, Kretschmer D, Bach TH, Queck SY, Li M, Kennedy AD, Dorward DW, Klebanoff SJ, Peschel A, DeLeo FR, Otto M (2007) Identification of novel cytolytic peptides as key virulence determinants for community-associated MRSA. *Nature medicine* **13:** 1510-1514

Wang X, Thompson CD, Weidenmaier C, Lee JC (2018a) Release of Staphylococcus aureus extracellular vesicles and their application as a vaccine platform. *Nature communications* **9:** 1379

Wang Y, Bojer MS, George SE, Wang Z, Jensen PR, Wolz C, Ingmer H (2018b) Inactivation of TCA cycle enhances Staphylococcus aureus persister cell formation in stationary phase. *Scientific reports* **8:** 10849

Watts A, Ke D, Wang Q, Pillay A, Nicholson-Weller A, Lee JC (2005) *Staphylococcus aureus* strains that express serotype 5 or serotype 8 capsular polysaccharides differ in virulence. *Infection and immunity* **73:** 3502-3511

Weidenmaier C, Lee JC (2017) Structure and Function of Surface Polysaccharides of Staphylococcus aureus. In *Staphylococcus aureus: Microbiology, Pathology, Immunology, Therapy and Prophylaxis*, Bagnoli F, Rappuoli R, Grandi G (eds), pp 57-93. Cham: Springer International Publishing

West SA, Griffin AS, Gardner A, Diggle SP (2006) Social evolution theory for microorganisms. *Nature reviews Microbiology* **4:** 597-607

Whiteley M, Diggle SP, Greenberg EP (2017) Progress in and promise of bacterial quorum sensing research. *Nature* **551:** 313-320

Wilde AD, Snyder DJ, Putnam NE, Valentino MD, Hammer ND, Lonergan ZR, Hinger SA, Aysanoa EE, Blanchard C, Dunman PM, Wasserman GA, Chen J, Shopsin B, Gilmore MS, Skaar EP, Cassat JE (2015) Bacterial Hypoxic Responses Revealed as Critical Determinants of the Host-Pathogen Outcome by TnSeq Analysis of Staphylococcus aureus Invasive Infection. *PLoS pathogens* **11:** e1005341

Williams MR, Costa SK, Zaramela LS, Khalil S, Todd DA, Winter HL, Sanford JA, O'Neill AM, Liggins MC, Nakatsuji T, Cech NB, Cheung AL, Zengler K, Horswill AR, Gallo RL (2019) Quorum sensing

between bacterial species on the skin protects against epidermal injury in atopic dermatitis. *Science translational medicine* **11:** eaat8329

Wolf L, Silander OK, van Nimwegen E (2015) Expression noise facilitates the evolution of gene regulation. *Elife* **4**

Wright JS, 3rd, Jin R, Novick RP (2005) Transient interference with staphylococcal quorum sensing blocks abscess formation. *Proceedings of the National Academy of Sciences of the United States of America* **102:** 1691-1696

Xi H, Duan L, Turcotte M (2013) Point-cycle bistability and stochasticity in a regulatory circuit for Bacillus subtilis competence. *Mathematical biosciences* **244:** 135-147

Xu T, Wang XY, Cui P, Zhang YM, Zhang WH, Zhang Y (2017) The Agr Quorum Sensing System Represses Persister Formation through Regulation of Phenol Soluble Modulins in Staphylococcus aureus. *Frontiers in microbiology* **8:** 2189

Yang S, Kim S, Rim Lim Y, Kim C, An HJ, Kim JH, Sung J, Lee NK (2014) Contribution of RNA polymerase concentration variation to protein expression noise. *Nature communications* **5:** 4761

Young BC, Wu CH, Gordon NC, Cole K, Price JR, Liu E, Sheppard AE, Perera S, Charlesworth J, Golubchik T, Iqbal Z, Bowden R, Massey RC, Paul J, Crook DW, Peto TE, Walker AS, Llewelyn MJ, Wyllie DH, Wilson DJ (2017) Severe infections emerge from commensal bacteria by adaptive evolution. *eLife* **6**

Zalis EA, Nuxoll AS, Manuse S, Clair G, Radlinski LC, Conlon BP, Adkins J, Lewis K (2019) Stochastic Variation in Expression of the Tricarboxylic Acid Cycle Produces Persister Cells. *mBio* **10:** e01930-01919

Zhao L, Xue T, Shang F, Sun H, Sun B (2010) *Staphylococcus aureus* AI-2 quorum sensing associates with the KdpDE two-component system to regulate capsular polysaccharide synthesis and virulence. *Infection and immunity* **78:** 3506-3515

Appendix: Accepted Publications

Publication 1 (Research Article):

Phenotypic heterogeneity and temporal expression of the capsular polysaccharide in *Staphylococcus aureus*.

George SE, Nguyen T, Geiger T, Weidenmaier C, Lee JC, Liese J, Wolz C

Molecular Microbiology 2015 Dec;98(6):1073-88. doi: 10.1111/mmi.13174.

Publication 2 (Research Article):

Wall teichoic acids mediate increased virulence in *Staphylococcus aureus*.

Wanner S, Schade J, Keinhörster D, Weller N, **George SE**, Kull L, Bauer J, Grau T, Winstel V, Stoy H, Kretschmer D, Kolata J, Wolz C, Bröker BM, Weidenmaier C

Nature Microbiology 2017 Jan 23;2:16257. doi: 10.1038/nmicrobiol.2016.257.

Publication 3 (Research Article):

Inactivation of TCA cycle enhances *Staphylococcus aureus* persister cell formation in stationary phase.

Wang Y, Bojer MS, **George SE**, Wang Z, Jensen PR, Wolz C, Ingmer H

Scientific reports 2018 Jul 18;8(1):10849. doi: 10.1038/s41598-018-29123-0.

Publication 4 (Research Article):

Revisiting the regulation of the capsular polysaccharide biosynthesis gene cluster in *Staphylococcus aureus*.

Keinhörster D, Salzer A, Duque-Jaramillo A, **George SE**, Marincola G, Lee JC, Weidenmaier C, Wolz C.

Molecular Microbiology 2019 Jul 8. doi: 10.1111/mmi.14347.

Publication 5 (Review Article):

Function and regulation of *Staphylococcus aureus* wall teichoic acids and capsular polysaccharides.

Keinhörster D, **George SE**, Weidenmaier C, Wolz C.

Int J Med Microbiol. 2019 Jul 18:151333. doi: 10.1016/j.ijmm.2019.151333.

Publication 6 (Research Article):

Oxidative stress drives the selection of quorum sensing mutants in the *Staphylococcus aureus* population.

George SE, Hrubesch J, Breuing I, Vetter N, Korn N, Hennemann K, Bleul L, Willmann M, Ebner P, Götz F, Wolz C

PNAS 2019 Sep 17;116(38):19145-19154. doi: 10.1073/pnas.1902752116

Publication 1

Phenotypic heterogeneity and temporal expression of the capsular polysaccharide in *Staphylococcus aureus*.

George SE, Nguyen T, Geiger T, Weidenmaier C, Lee JC, Liese J, Wolz C

Molecular Microbiology 2015 Dec;98(6):1073-88. doi: 10.1111/mmi.13174.

Molecular Microbiology (2015) 98(6), 1073–1088 ■
doi:10.1111/mmi.13174
First published online 25 September 2015

Phenotypic heterogeneity and temporal expression of the capsular polysaccharide in *Staphylococcus aureus*

Shilpa E. George,[1] Tran Nguyen,[1,2] Tobias Geiger,[1†] Christopher Weidenmaier,[1] Jean C. Lee,[3] Jan Liese[1] and Christiane Wolz[1*]

[1]*Interfaculty Institute of Microbiology and Infection Medicine, University of Tübingen, Tübingen, Germany.*
[2]*Centre for Infection Research (DZIF), Partner Site Tübingen, Tübingen, Germany.*
[3]*Channing Laboratory, Brigham and Women's Hospital, Harvard Medical School, Boston, MA 02115, USA.*

Summary

Bacteria respond to ever-changing environments through several adaptive strategies. This includes mechanisms leading to a high degree of phenotypic variability within a genetically homogeneous population. In *Staphylococcus aureus*, the capsular polysaccharide (CP) protects against phagocytosis, but also impedes adherence to endothelial cells and/or matrix proteins. We analysed the regulation of core biosynthesis genes (*capA-P*) necessary for CP synthesis using single-cell assays (immunofluorescence and promoter-activity). In persistent human carriers, we found a distinct subpopulation of nasal *S. aureus* to be CP positive. *In vitro*, *cap* expression is also heterogeneous and strongly growth-phase dependent. We asked whether this peculiar expression pattern (earlyOff/lateHeterogen) is orchestrated by the quorum system Agr. We show that the Agr-driven effector molecule RNAIII promotes *cap* expression largely via inactivation of the repressor Rot. High NaCl, deletion of CodY or Sae also resulted in higher *cap* expression but did not change the earlyOFF/lateHeterogen expression pattern. Activity of the quorum system itself is largely homogenous and does not account for the observed heterogeneity of *cap* expression or the strictly growth phase dependent expression. Our findings are in contrast to the prevailing view that quorum sensing is the main driving force for virulence gene expression when bacterial cell densities increase.

Accepted 21 August, 2015. *For correspondence. E-mail christiane.wolz@med.uni-tuebingen.de; Tel. (+49) 7071 2980187; Fax (+49) 7071 295165. †Present address: Department of Microbial Pathogenesis, Yale University School of Medicine, New Haven, CT 06536, USA.

© 2015 John Wiley & Sons Ltd

Introduction

Staphylococcus aureus causes a variety of infections in humans but also asymptomatically colonises the noses of healthy individuals. Pathogenicity beyond toxinoses is considered multifactorial and due to the joint synergy of different secreted factors, cell surface proteins and polysaccharides. *S. aureus* is equipped with enzymes necessary for the synthesis of at least two extracellular polysaccharides, the capsular polysaccharide (CP) and the polysaccharide intercellular adhesin (PIA). Almost all *S. aureus* strains contain either a *cap5A-P* or a *cap8A-P* gene cluster encoding enzymes for the most prevalent capsular serotypes, CP5 and CP8 respectively. Staphylococcal CPs have been shown to possess anti-phagocytic properties, allowing the bacterium to persist in the blood and tissues of infected hosts (Thakker *et al.*, 1998). The *cap5* and *cap8* gene clusters are chromosomally allelic. The 12 flanking genes are almost identical, whereas the central genes *capHIJK* bear little homology to each other and are type specific.

Staphylococcus aureus is able to tightly control CP synthesis by various regulatory mechanisms in order to adapt to the changing infectious environments (O'Riordan and Lee, 2004). Furthermore, only some bacteria from a given population seem to express CP on their surface (e.g. to avoid phagocytosis), whereas at the same time the un-encapsulated subpopulation might be better suited for adherence to endothelial cells and/or matrix proteins. Heterogeneity of CP expression within a given bacterial culture was previously described by immune labelling of bacteria using either flow cytometry (Poutrel *et al.*, 1997) or immunofluorescence (Pohlmann-Dietze *et al.*, 2000). Furthermore, only the non-encapsulated bacterial fraction was found to bind to endothelial cells (Pohlmann-Dietze *et al.*, 2000). This kind of cell-to-cell variation may be part of a general mechanism to provide better adaptability of the entire population. With the recent advancements in single-cell techniques, the description and understanding of cell-to-cell phenotypic variability within a bacterial population, sometimes termed non-genetic individuality, has become a major focus of research (Dubnau and Losick, 2006;

Davidson and Surette, 2008; Veening *et al*., 2008; Balazsi *et al*., 2011; Munsky *et al*., 2012; Ryall *et al*., 2012). The underlying mechanisms leading to noise in gene expression are diverse, ranging from stochastic fluctuation of biological processes, regulatory feedback loops to complex self-perpetuating DNA methylation patterns (Ben-Jacob and Schultz, 2010; Casadesus and Low, 2013). It was also suggested that at least for some organisms, quorum sensing systems drive the heterogeneity in a clonal population (Perez and Hagen, 2010; Garmyn *et al*., 2011; Anetzberger *et al*., 2012; Pradhan and Chatterjee, 2014). Non-genetic individuality in bacteria has especially been described for key differentiation events such as sporulation, competence and biofilm development. However, cell-to-cell variability with regard to cell-wall glycopolymer biosynthesis or peptide-based quorum sensing systems has rarely been studied.

Studying CP production and/or *cap* expression on the population level shows that CP expression is highly influenced by several environmental factors including the inhibition by glucose, CO_2, or anaerobiosis (O'Riordan and Lee, 2004). Both of the *cap* operons, (*cap5* and *cap8*) are similarly regulated and transcribed by one principal promoter (P_{cap}) in front of *capA* (Sau *et al*., 1997; Herbert *et al*., 2001). Usually P_{cap} activity correlates with CP synthesis, indicating that regulation occurs predominantly on the transcriptional level (Meier *et al*., 2007; Jansen *et al*., 2013; Hartmann *et al*., 2014; Romilly *et al*., 2014). Different environmental cues are signalled via the activity of several largely interactive regulatory systems composed of transcriptional factors CodY (Pohl *et al*., 2009; Majerczyk *et al*., 2010), CcpE (Ding *et al*., 2014; Hartmann *et al*., 2014), MgrA (Gupta *et al*., 2013; Romilly *et al*., 2014), SpoVG (Schulthess *et al*., 2009b) RpiR (Zhu *et al*., 2011), SbcDC (Chen *et al*., 2007) or two-component regulatory systems Kdp (Zhao *et al*., 2010), Air (Sun *et al*., 2012), Sae (Steinhuber *et al*., 2003; Luong *et al*., 2011) and Agr (Dassy *et al*., 1993; Pohlmann-Dietze *et al*., 2000; Luong *et al*., 2002). A central player in the network is the quorum sensing system Agr composed of the *agrBDCA* operon and the divergently transcribed RNAIII molecule (Novick and Geisinger, 2008; Thoendel *et al*., 2011). The autoinducing peptide (AIP), encoded by *agrD*, induces autophosphorylation of the histidine-kinase AgrC with subsequent phosphotransfer to the response regulator AgrA. Phosphorylated AgrA triggers transcription of its own operon (*agrBDCA*) as well as the divergently transcribed regulatory RNAIII. RNAIII has the unique property of acting both as an mRNA that encodes the δ-hemolysin peptide, and as a critical regulator. RNAIII represses the synthesis of early expressed genes coding for coagulase, protein A, or the repressor of toxins (Rot) at the post transcriptional level. Most commonly, RNAIII functions as an anti-sense RNA that anneals to target mRNAs. The formed complexes result in the repression of translation initiation and in rapid mRNA degradation triggered by RNase III (Boisset *et al*., 2007). *Cap* expression is highly dependent on Agr activity (Dassy *et al*., 1993; Pohlmann-Dietze *et al*., 2000; Luong *et al*., 2002) and clinical CP negative strains were found to lack Agr function (Cocchiaro *et al*., 2006; Fischer *et al*., 2014). So far the mechanism by which the Agr-RNAIII system affects *cap* expression has not been elucidated.

Here we used single-cell assays to show that *cap* expression and CP synthesis is heterogeneous and strongly growth-phase dependent. We asked whether this peculiar expression pattern (earlyOff/lateHeterogen) is dictated by the quorum system Agr. We showed that CP synthesis as well as P_{cap} activity is dependent on the Agr-RNAIII system. The mechanism by which the regulatory RNAIII promotes P_{cap} activity was found to be largely due to RNAIII-mediated inactivation of the repressor Rot. However, activity of the quorum sensing system is largely uniform and does not account for the observed high degree of heterogeneity of *cap* expression. Surprisingly, the strictly temporal expression of CP in the late growth phase is also independent of the Agr-Rot system.

Results

A distinct subpopulation of bacteria produces CP in vivo

Previously we demonstrated that Agr-RNAIII expression is very low during *S. aureus* colonisation of the human nose while an intermediate level of *cap* expression is detectable (Burian *et al*., 2012). To ascertain whether *S. aureus* bacteria are encapsulated during nose colonisation, we used immunofluorescence to detect CP in *S. aureus* sampled by nasal swab from persistently colonised carriers. Results from three individuals are depicted in Fig. 1. Two representative images are shown for each individual. *S. aureus* was identified by fluorescence in-situ hybridisation (FISH). Only a subpopulation of the bacteria identified as *S. aureus* were found to be CP positive. Coexistence of CP positive and CP negative bacteria was observed even within a single cluster of bacteria. The three individuals (A, B and C) were colonised with different *S. aureus* clones: A: spa-type t1239, CP8, agr-type 3a, CC30; B: spa-type t1071, CP5, agr-type 2, CC15; C: spa-type t4309, CP8, ST3236 respectively. This indicates that the heterogeneous expression of CP *in vivo* is a general feature of *S. aureus* and not related to a certain CP type or clonal complex.

The role of quorum sensing for temporal cap *expression*

It was previously shown that *cap* expression is maximal during the late growth phase and also depends on the quorum sensing system, Agr (Dassy *et al*., 1993;

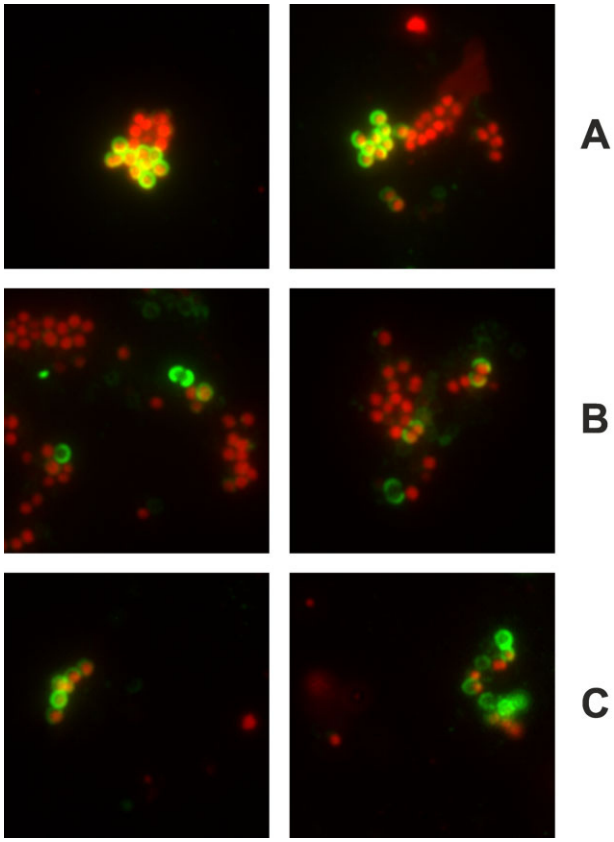

Fig. 1. Heterogeneous CP expression during *S. aureus* colonisation of the human nose.
For *ex vivo* analysis, nasal swabs from carriers were processed and spotted onto glass slides. *S. aureus* were identified by *in situ* hybridisation with peptide nucleic acid (PNA) probes targeting *S. aureus* 16S rRNA (red) followed by immunofluorescence to detect CP5 and CP8 antigen (green). From each of the three persistently colonised human volunteers (A, B and C), two images are illustrated.

Pohlmann-Dietze *et al.*, 2000; Luong *et al.*, 2002). We analysed whether the Agr system might be the primary trigger for the temporal and heterogeneous expression of CP synthesis. To this end, we constructed strains in which the *agr* locus is either deleted or in which the regulatory RNAIII is expressed independent of the autoinducing peptide, AIP. First, RNAIII was expressed under an artificial *recA* promoter, from which the LexA binding motif was deleted (pRNAIII). The activation of this promoter was shown to be independent of the SOS response (Schroder *et al.*, 2014) and is mainly active in bacteria in the exponential phase of growth. In the second approach, a single point mutation was introduced in the native chromosomal *agrC*. The resulting single amino-acid exchange in the histidine-kinase domain ($AgrC^{R238H}$) rendered the enzyme constitutively active (Geisinger *et al.*, 2009). For growth experiments, bacteria were grown in Luria-Bertani (LB) broth to an optical density at OD_{600} of 0.5 and then again diluted (1:10) to ensure that most bacteria entered the exponential growth phase. Bacteria were then analysed at an OD_{600} of 0.3 (T1) and after 2 h (T2,), 3 h (T3), 4 h (T4) or after growth overnight (T5) (Fig. 2A). There was no significant difference in growth between the strains analysed (Fig. S1).

The expression of the Agr effector molecule, RNAIII, from the different constructs was analysed by Northern blot. The results confirmed the intended differences in the temporal RNAIII expression pattern of the manipulated strains (Fig. 2B): RNAIII expression was found to increase during growth in the wild type, to decrease in the pRNAIII complemented *agr* mutant and to be constitutive in the $agrC^{R238H}$ mutant.

We next analysed whether *cap* expression correlated to RNAIII and/or the growth phase. At the indicated time points, *capA* mRNA was quantified by qRT-PCR (Fig. 2C). In all strains analysed *cap* expression significantly increased after bacteria had entered the mid-exponential growth phase. The *agr* mutant showed an 11-fold decrease of *cap* expression at T4 as compared with the wild type, indicating that RNAIII drives *cap* expression in the late growth phase. Of note also in the pRNAIII complemented *agr* mutant (early RNAIII expression), maximal *cap* expression was found at the mid to late exponential phase, T2 until T4, even though at these time points RNAIII is already severely diminished (Fig. 2B). Thus, the temporal expression of RNAIII and *cap* is not necessarily linked. This was further demonstrated in the constitutive $agrC^{R238H}$ strain in which maximum *cap* expression was again observed only in the later growth phase. Thus, while RNAIII is required for optimal *cap* expression, additional factors must be involved to account for the strongly growth phase dependent expression in the later growth phase. This is supported by the finding that the residual *cap* expression detected in the *agr* mutant also increases during growth.

Quorum sensing is not responsible for earlyOff/lateHeterogen CP synthesis

We next analysed the impact of quorum sensing on CP synthesis at the single cell level. For this purpose, we assessed CP synthesis by immunofluorescence (Fig. 3). The specificity of the CP signal was assessed by analysis of *cap*, *spa* (coding for protein A) and *cap/spa* mutants (Fig. S2). In the wild type, CP positive bacteria are only detectable in the late stationary phase (T5, Fig. 3). In the $agrC^{R238H}$ strain, CP positive bacteria were already detectable at T4. However, independent of the *agr* status, only a subpopulation of the bacteria appeared CP positive.

We next analysed whether the CP positive bacteria accumulate more CP upon further growth. Quantitative analysis revealed that the mean fluorescence per positive bacterium was elevated in bacteria from the late stationary phase (T5) compared to that of the mid or late expo-

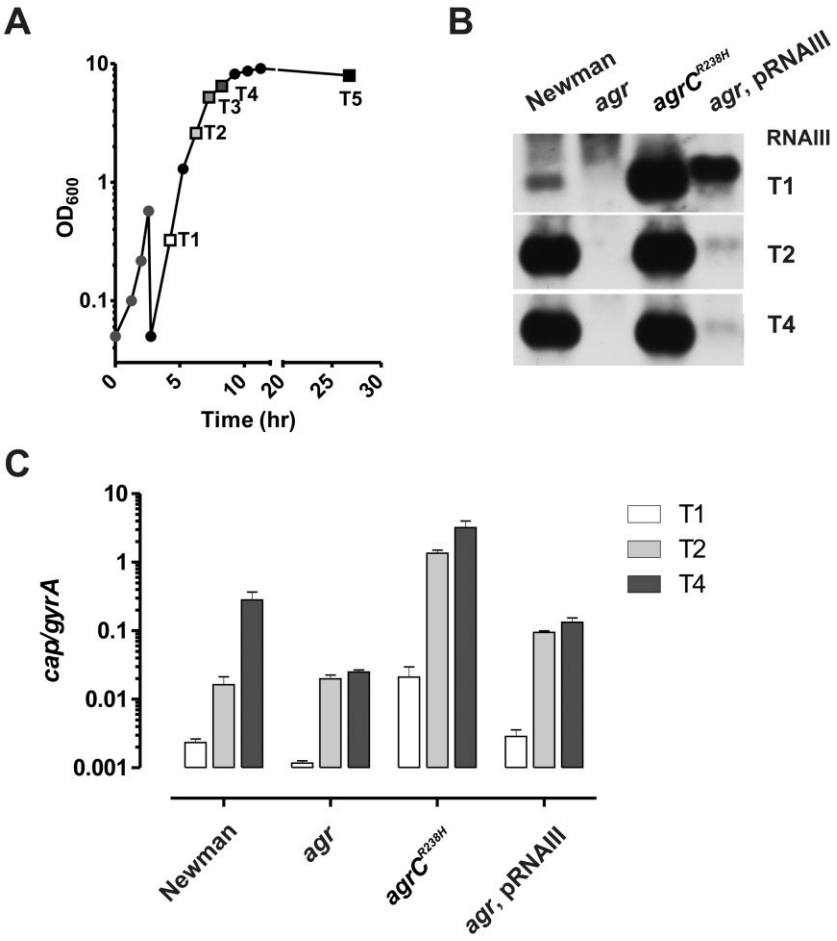

Fig. 2. Influence of the Agr status on *cap* expression.
(A) Bacterial RNA was harvested at different growth phases (T1–T5 as shown here for strain Newman). Bacteria from exponential phase were again diluted to ensure that all bacteria entered exponential growth phase. Total RNA from strain Newman, the *agr* mutant (Newman-391), the constitutive *agrC*^{R238H} derivative (Newman-383) and *agr* mutant complemented with pRNAIII (Newman-363) was isolated at indicated time points (T1, T2, T4). RNA was hybridised with digoxygenin-labelled probe specific for RNAIII (B), or used for quantification of *cap* mRNA (C) by qRT-PCR with reference to *gyrB*. The values are the mean ± SEM of three independent experiments.

nential phase (T2) (Fig. 3B). This was true for all strains analysed suggesting that once a certain expression threshold is crossed the bacteria continuously accumulate CP material on their surface. The regulatory RNAIII only partially contributes to this threshold effect, by shifting the onset of CP detection to the earlier growth phase. However, the earlyOff/lateHeterogen CP expression pattern is not mediated by RNAIII.

Heterogeneity and correlation of P_{RNAIII} and P_{cap} promoter activities in single cells

The correlation of *cap* mRNA and CP indicates that CP synthesis is mainly regulated at the transcriptional level. To support this, we analysed P_{RNAIII} and P_{cap} promoter-activities simultaneously at the single-cell level using promoter-fluorescent protein fusions. To avoid artefacts due to multicopy effects, integration vectors were constructed based on a cassette-based shuttle vector system. The staphylococcal replicon was replaced by attachment sites that allowed the specific integration of the plasmid into the chromosomal *geh* locus or into the SaPI1 site. The vectors were also modified to contain either the fluorescence reporter genes *cer* (blue variant of gfpmut2) or *yfp* (yellow variant of gfpmut2), and TetM or ErmC encoding resistance cassettes for selection. Both promoter reporter constructs were integrated into the chromosome, and the fluorescence expression in the wild type and mutants was followed during growth. Analysis of dual reporter strains is illustrated in Fig. 4 in which P_{cap} activity appears yellow (YFP) and P_{RNAIII} activity blue (Cer). For quantification, we measured the fluorescence intensities of single bacteria (Fig. 4). The mean intensities across three independent experiments (Fig. 4B) strongly mirror the results obtained by qRT-PCR and CP immunofluorescence (Fig. 2C and Fig. 3). In the wild type, P_{RNAIII} activity is only detectable after bacteria have entered the mid-exponential phase (T2). In the *agrC*^{R238H} strain, there was no significant difference in P_{RNAIII} activities between the different sampling times. In both strains, P_{cap} activity was found mainly in the stationary growth phase.

To demonstrate the heterogeneity of promoter activities within the cultures, the fluorescence intensities (P_{RNAIII} activity versus P_{cap}) of 100 single bacteria were plotted (Fig. 4A). A wide range of P_{cap} activities (*x*-axes) was found in bacteria from the later growth phases. The

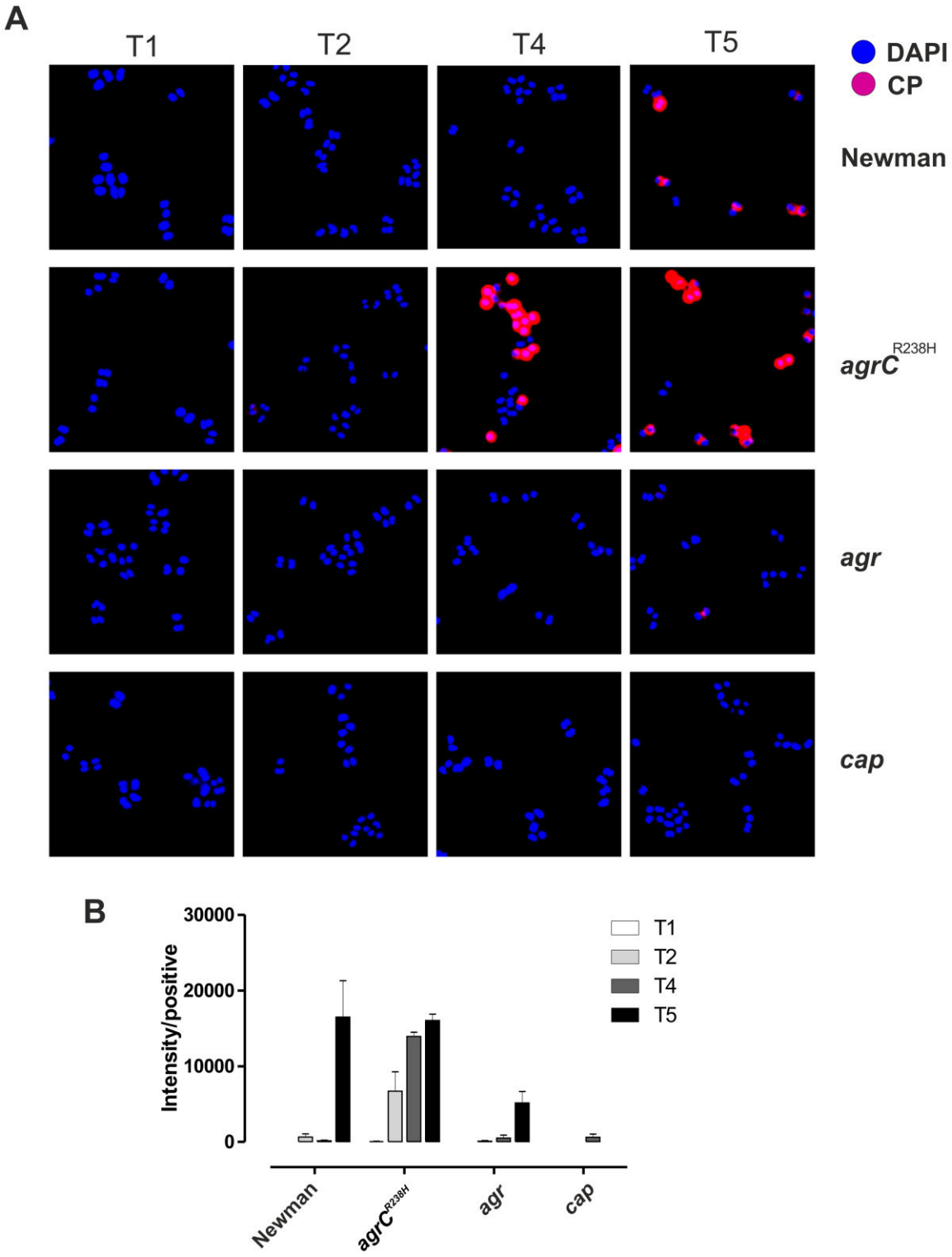

Fig. 3. Influence of the Agr status on CP synthesis.
A. Detection of CP on bacteria from different growth phases (see Fig. 2A). Strains Newman, the constitutive *agrC*^{R238H} derivative (Newman-383), the *agr* mutant (Newman-391) and the *cap* mutant (Newman-132) were grown to defined growth phase T1–T5 (see Fig. 2A) and CP detected by immunofluorescence.
B. CP positive bacteria were determined from at least three independent cultures using mean fluorescence of the *cap* mutant as threshold. The mean intensities of the positive bacterial fractions derived from three independent cultures are indicated.

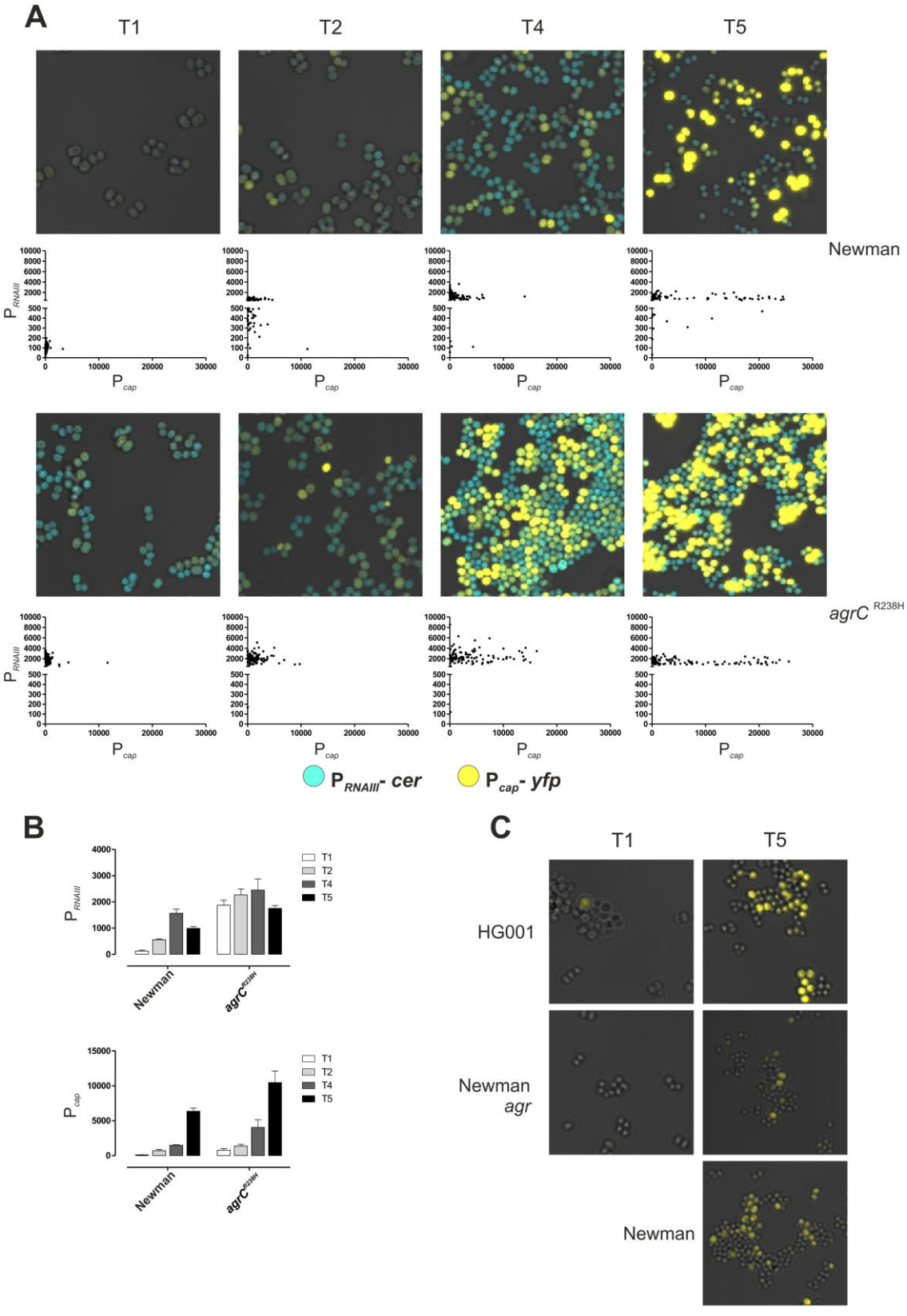
A
T1
T2
T4
T5
Newman
agrC R238H
P RNAIII
P cap
P RNAIII- cer
P cap- yfp
B
T1
T2
T4
T5
Newman
agrC R238H
C
T1
T5
HG001
Newman agr
Newman

Fig. 4. Influence of the Agr status on P_{RNAIII} and P_{cap} promoter activities.
A. The P_{RNAIII} and P_{cap} promoters were cloned in front of *cer* or *yfp* respectively and simultaneously integrated into the chromosome. Dual fluorescence expression was followed during growth in wild type and the constitutive *agrC*^{R238H} strain at time T1-T5 (see Fig. 2A). P_{cap} promoter activity appears yellow and P_{RNAIII} activity blue. Correlation of the P_{RNAIII} and P_{cap} promoter activities of 100 bacteria each is shown below the images. There is high variation in fluorescence intensities of P_{cap} activity especially at the later growth phase in both strains analysed.
B. For quantification, the mean fluorescence intensities of 100 single bacteria were measured. The mean ± SEM (of the mean intensities from single images) derived from three independent experiments is indicated.
C. The P_{cap}-*yfp* promoter fusion plasmid was integrated into strain HG001 and the *agr* mutant of strain Newman. Fluorescence expression was followed during growth at time T1 and T5.

corresponding P_{RNAIII} activity (*y*-axes) in contrast was largely uniform. In the wild type, a shift towards higher P_{RNAIII} activity was detectable during growth, and most if not all bacteria were positive after the late-exponential growth phase (T4). In the *agrC*^{R238H} strain, bacteria are homogenously P_{RNAIII} positive throughout growth. We next asked whether the P_{cap} promoter activity correlates with P_{RNAIII} activity within a single bacterium. Interestingly, no correlation between P_{cap} and P_{RNAIII} activities was detectable (Fig. 4A). After a certain threshold level of P_{RNAIII}, the P_{cap} activity is independent of *agr* and evidently determined by additional factors.

In an *agr* negative strain, P_{cap} promoter activity was detectable in some bacteria from the late growth phase (Fig. 4C). We further analysed whether the earlyOff/lateHeterogen expression of P_{cap} is also detectable in another strain background. Therefore, the P_{cap}-reporter was transduced into the prototypic strain HG001 (an *rsbU*-repaired derivative of 8325-4). The expression pattern was similar to that observed in strain Newman (Fig. 4C).

Rot mediates the RNAIII-dependent cap *regulation but is not responsible for the earlyOff/lateHeterogen CP expression pattern*

In the search for candidate genes that may be involved in the peculiar CP expression pattern (earlyOff/lateHeterogen), we hypothesised that at the early exponential growth phase *cap* expression might be controlled by a repressor that becomes partially inactivated when bacteria enter a later growth phase. Furthermore, how regulatory RNAIII impacts *cap* expression was not clear. For other RNAIII target genes, it has been proposed that RNAIII acts via the inactivation of the transcriptional factor Rot (Boisset *et al*., 2007). We could show that this is also true for *cap* regulation. First, a *rot* mutant showed significantly enhanced *cap* expression and could restore *cap* expression in an *agr*-negative background as shown by qRT-PCR (Fig. 5A) and CP immunofluorescence (Fig. 5B). The results support the hypothesis that RNAIII inactivates the Rot repressor and that the effect of Rot on *cap* expression is downstream of RNAIII. We also analysed P_{cap} promoter activity in the *rot* mutant background (Fig. 5C). The growth phase dependent trend of P_{cap} expression was found to be similar to that detected in the *agrC*^{R238H} strain further supporting the notion that the RNAIII mediated effect on *cap* regulation is via Rot. Thus, RNAIII-mediated inactivation of Rot is the main mechanism by which the quorum sensing system impacts *cap* expression. However, the earlyOff/lateHeterogen expression pattern was still detectable in the *rot* mutant, and thus Rot does not account for this phenotype.

CodY-mediated cap *regulation*

The metabolic regulator CodY functions as a growth phase-dependent repressor of the *cap* operon (Pohl *et al*., 2009; Majerczyk *et al*., 2010). Under conditions of low GTP or branched-chain amino acids, this repressor loses its DNA-binding activity leading to de-repression of target genes. Here we analysed whether the mutation in *codY* would result in early activation of *cap* expression. We confirmed that CodY inhibits *cap* expression on the transcriptional level especially in bacteria in the mid exponential phase (Fig. 6A). Also, CP positive bacteria were found at earlier time points compared with the wild type. However, the *codY* mutant still shows the earlyOff/lateHeterogen expression (Fig. 6B). We next asked whether inactivation of both *cap* repressors (Rot and CodY) would eventually lead to early/homogenous expression. The effect of *codY* and *rot* mutation was found to be additive, but the general earlyOff/lateHeterogen *cap* expression pattern remained.

Impact of other regulators and growth conditions for cap *expression*

There are several other regulators that were shown to impact *cap* expression, many of which act indirectly through intertwined regulatory circuits (summarised in Fig. S3). Previously, the impact of the transcriptional regulators SpoVG, sigma factor B, Arl and CcpE were analysed using immunofluorescence (Meier *et al*., 2007; Schulthess *et al*., 2009a; Hartmann *et al*., 2014). Mutations in these regulators led to a decrease in CP expression. Here, we included *sae* in our analysis (Fig. S4). The *sae* mutant shows a significant increase in CP expression in line with previous results (Steinhuber *et al*., 2003;

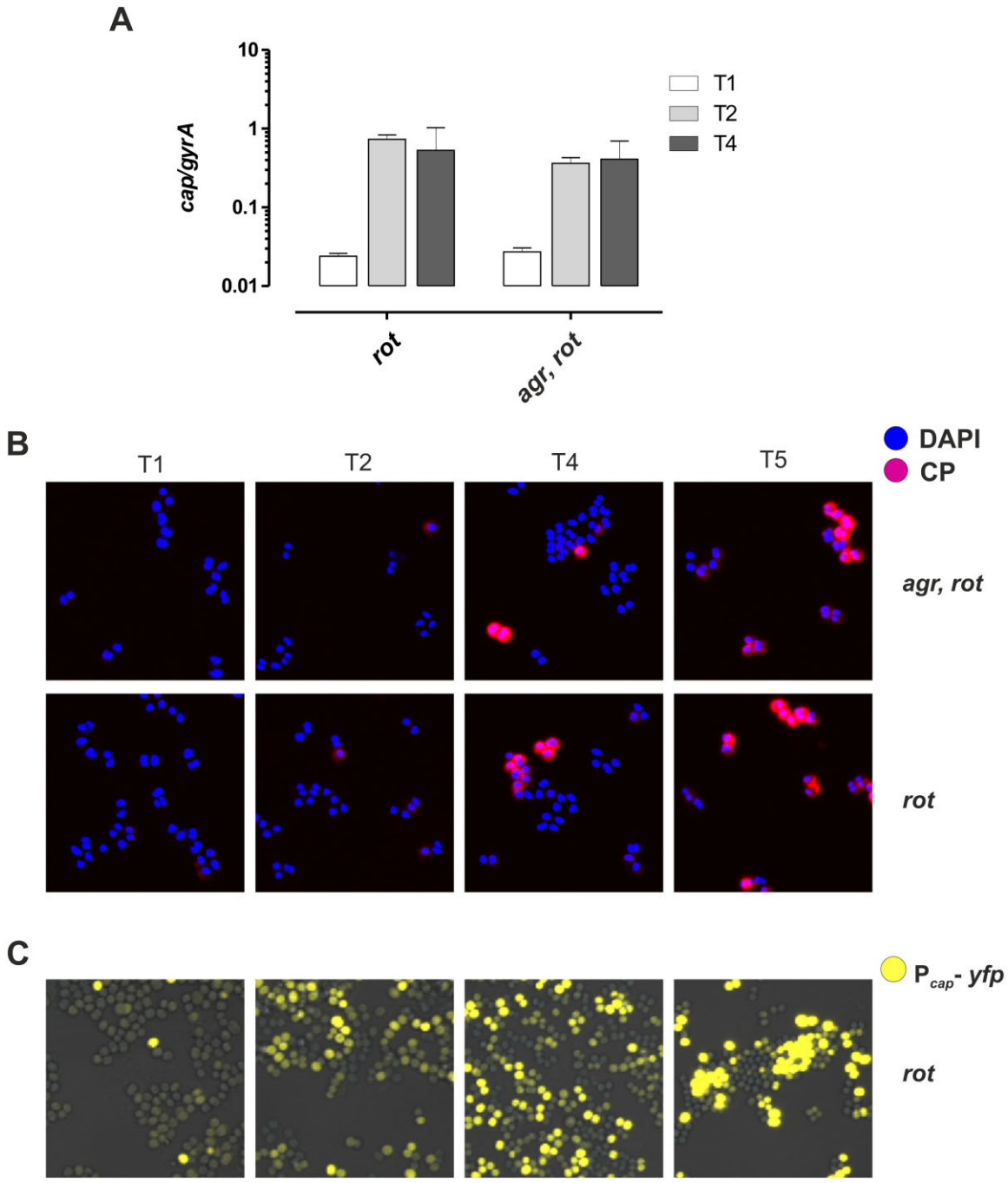

Fig. 5. Influence of Rot on *cap* expression and CP synthesis.
Bacteria were harvested at different growth phases (T1–T5, see Fig. 2A).
A. *cap* mRNA was quantified by qRT-PCR with reference to *gyrB*. For comparison with wild type, see Fig. 2C (results shown in Fig. 2B, 2C and 5A were acquired from the same experiment).
B. Detection of CP by immunofluorescence in *rot* and *rot agr* mutants. For comparison with wild type, see Fig. 3A (results shown in Fig. 3 and 5B were acquired from the same experiment).
C. P_{cap} promoter activity (P_{cap}-*yfp* integrated into *geh*) in the *rot* mutant during growth. For comparison with wild type, see Fig. 4A (results shown in Fig. 4A and 5C were acquired from the same experiment).

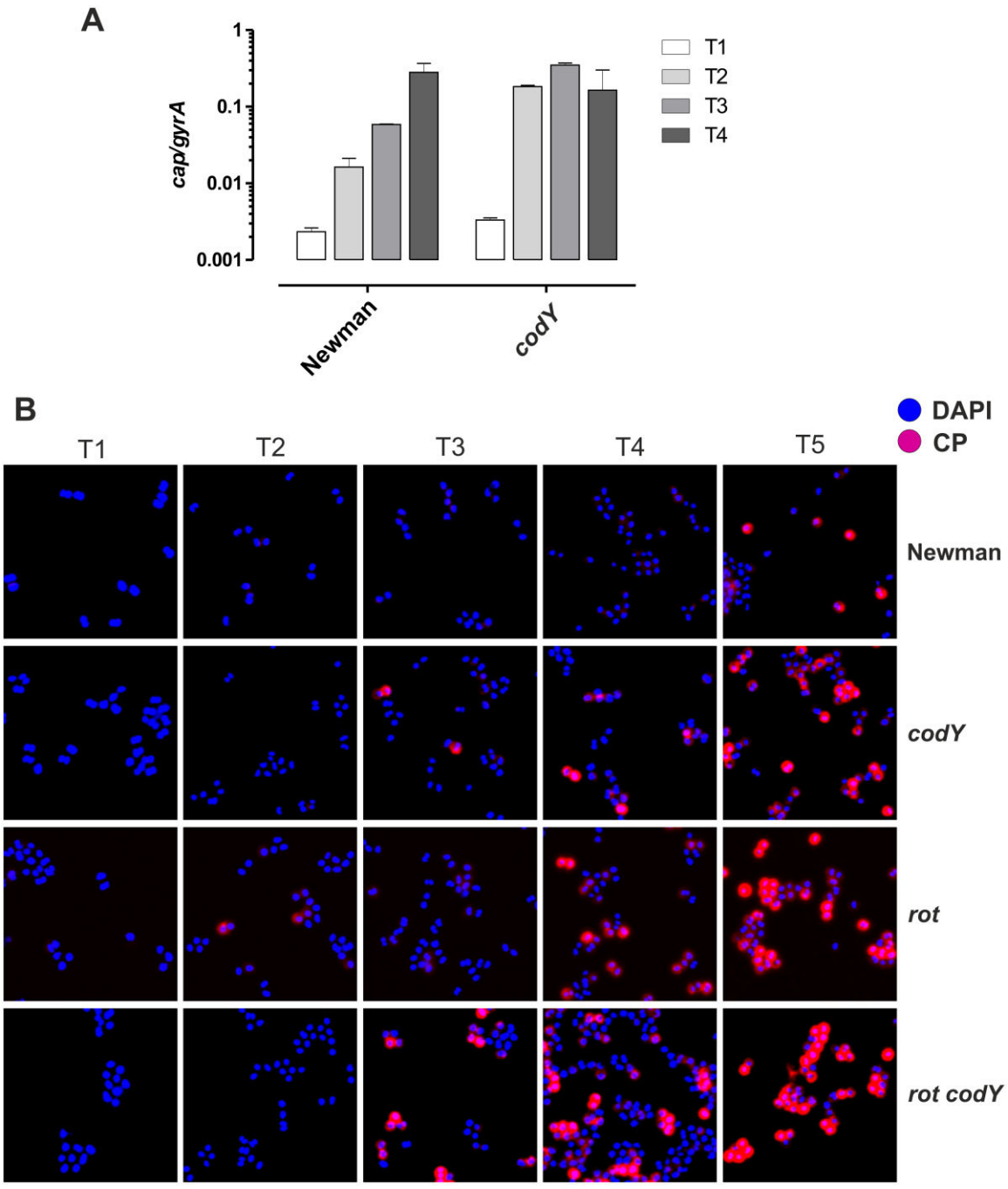

Fig. 6. Influence of CodY on *cap* expression and CP synthesis.
Bacteria were harvested at different growth phases (T1–T5, see Fig. 2A).
A. *cap* mRNA was quantified by qRT-PCR with reference to *gyrB*.
B. Detection of CP by immunofluorescence in strain Newman and its *codY* mutant.

Luong *et al*., 2011). However, in the *sae* mutant CP expression was still found to be earlyOff/lateHeterogen. Environmental signals such as glucose, O_2 or high NaCl are transduced via regulatory systems CcpA (Seidl *et al*., 2006), Air (Sun *et al*., 2012) and Kdp (Zhao *et al*., 2010; Price-Whelan *et al*., 2013) respectively. We analysed the impact of these environmental conditions on CP expression (Fig. S5) and could confirm that glucose and anaerobiosis inhibits CP expression. High NaCl in contrast results in enhanced CP expression presumably via Kdp. However, CP expression was also earlyOff/lateHeterogen under the inducing high NaCl conditions. Taken together,

we confirmed that CP expression is tightly controlled by various regulatory systems and environmental conditions. However, so far none of the signals/regulators analysed can account for the peculiar earlyOff/lateHeterogen expression pattern.

Discussion

Individuality not imposed by quorum sensing

The question of whether quorum sensing results in bacterial individuality has not been well addressed for peptide-based systems in Firmicutes. The expression of the regulatory RNAIII, transcribed from the P_{RNAIII} promoter, is driven by the prototypic quorum sensing system, Agr. Consequently, P_{RNAIII} is activated once bacteria reach a critical density. Here we show that most if not all bacteria activate P_{RNAIII} with little variation between single cells. This is in line with previous results in which bacteria were isolated in small droplets and shown to react with an all or none response to the AIP (Carnes *et al.*, 2010). Analysis of bacterial individuality imposed by quorum sensing systems of Gram-negative model organisms such as *Pseudomonas* or *Vibrio* species show strong evidence that in these organisms only a part of the bacterial population is responsive even in a homogenous environment or in confined micro-compartments (Perez and Hagen, 2010; Anetzberger *et al.*, 2012; Pradhan and Chatterjee, 2014; Romilly *et al.*, 2014). In Firmicutes, quorum sensing differs in many ways from those employed in proteobacteria. In particular, the AIP has to be actively exported and signal perceived by membrane bound sensor histidine-kinases (Novick and Geisinger, 2008; Thoendel *et al.*, 2011). Also the integration with other regulatory systems is highly diverse between species. The interaction often implies several positive and negative feedback loops, which determine the noise level of the output signals (Long *et al.*, 2009; Tu *et al.*, 2010).

The observed largely uniform P_{RNAIII} activity may be only true under conditions of a homogenous environment as analysed here. *In vivo* or in biofilms, small changes in the microenvironment are likely to modulate the quorum response. Recent data showed that *agr* expression is non-uniform in biofilms and determines the specific structure of the biofilm (Periasamy *et al.*, 2012). Under infectious conditions the Agr system is largely downregulated, e.g. through inactivation of the AIP signal (Goerke *et al.*, 2000; Wright *et al.*, 2005). Thus, whether RNAIII expression *in vivo* is more heterogeneous remains to be analysed.

Temporal expression of cap

The *cap* operon is severely repressed in bacteria in the exponential growth phase (Becher *et al.*, 2009). Here we clearly show that the strictly temporal *cap* expression is only partially mediated by quorum sensing (Fig. 7) via removal of Rot repression. In a *rot* mutant, *cap* expression is significantly increased. Moreover, in an *agr* negative background *cap* expression could be restored by *rot* deletion. However, constitutive activation of *agr* only resulted in an earlier onset of *cap* expression. A similar result was obtained when analysing the *cap*-inhibitory system CodY. CodY leads to repression of the *cap* operon also in an *agr* negative background (Pohl *et al.*, 2009; Majerczyk *et al.*, 2010) but only partially impacts the temporal expression of *cap*. CodY is a typical metabolic sensor which, in the presence of branched-chain amino acids and/or GTP, binds to target genes usually resulting in gene repression. When nutrients become limited, CodY repression is relieved and target genes can be expressed. However, our results show that even simultaneous deletion of CodY and Rot only shifted the onset of *cap* expression to an earlier time point. Therefore, as yet undefined regulatory circuits must account for the strictly temporal expression of *cap*. Such mechanisms may also account for the temporal expression in the late growth phase of other virulence genes such as *hla* coding for α-hemolysin (Vandenesch *et al.*, 1991). Metabolic sensors may be involved in such a regulation. CP synthesis is coupled to aerobic respiration, active TCA cycle and gluconeogenesis. These metabolic pathways are needed to generate the N-acetyl-glucosamine precursor (Sadykov *et al.*, 2010). When

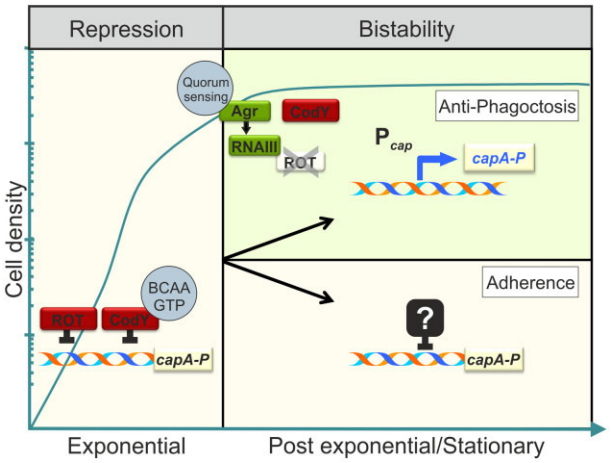

Fig. 7. Temporal and bistable expression of *cap*. During exponential growth, *cap* expression is tightly repressed through the repressors Rot, CodY and additional factors. Upon entry into post-exponential growth phase, the quorum sensing system Agr leads to inactivation of Rot and partial relief of *cap* repression. The CodY ligands GTP and/or BCAA (branched-chain amino acids) become limited in the later growth phase which also adds to the relief of *cap* repression. However, even in the stationary phase, *cap* remains strongly repressed in a part of the population. High degree of heterogeneity in *cap* expression at the single cell level is evident in wild type, *rot* and *codY* mutant strains.

glucose becomes limited, TCA activity, gluconeogenesis and *cap* expression become activated (Becher *et al.*, 2009). However, it remains unclear how these metabolic circuits may result in the regulation of *cap* expression on the transcriptional level. Of note, all the experiments shown here are performed in LB medium without added glucose. The metabolic changes upon entry into stationary phase under such conditions without glucose are not well studied but are presumably also linked to *cap* regulation.

Heterogeneity of cap *expression*

Here we show that *cap* expression is highly heterogeneous. Only a part of the population produces detectable CP when bacteria enter stationary phase. This was not only shown in artificial *in vitro* cultures but also in bacteria from human nares. We assume that heterogeneity of CP expression has evolved to supply the bacterial population with better adaptability during infection/colonisation. CP synthesis is not always advantageous for the bacteria. Virulence studies using encapsulated and non-encapsulated *S. aureus* strains reveal that, depending on the animal model used, CP either enhances or attenuates virulence (O'Riordan and Lee, 2004; Tuchscherr *et al.*, 2010). In murine models of bacteraemia (Thakker *et al.*, 1998; Watts *et al.*, 2005), septic arthritis (Nilsson *et al.*, 1997), abscess formation (Portoles *et al.*, 2001) and surgical wound infection (McLoughlin *et al.*, 2006), CP enhances virulence. In contrast, in mammary gland infections (Tuchscherr *et al.*, 2005) and in catheter-induced endocarditis (Baddour *et al.*, 1992; Nemeth and Lee, 1995) CP mutants are more virulent. This may be attributed to the finding that CPs are anti-phagocytic but also inhibit the binding of the underlying cell-wall proteins to their specific target molecule (Pohlmann-Dietze *et al.*, 2000; Risley *et al.*, 2007). It was also demonstrated that CP negative *S. aureus* strains are frequently isolated from patients with osteomyelitis, mastitis or cystic fibrosis, suggesting that loss of CP expression may be advantageous for *S. aureus* during chronic infection (Herbert *et al.*, 1997; Lattar *et al.*, 2009; Tuchscherr *et al.*, 2010).

There are now more studies supporting the view that noise in virulence gene expression is an important parameter for pathogenesis. A recent unbiased screen for promoters with high levels of phenotypic noise showed the highest level of phenotypic noise in promoters controlling flagellar synthesis in Salmonella (Freed *et al.*, 2008). Very recently it was also demonstrated in *E. coli* that expression noise is a tuneable parameter, with different gene regulatory architectures giving rise to different, but predictable, patterns of expression noise (Jones *et al.*, 2014). It was concluded that noise is an evolutionary accessible phenotypic parameter and not merely stochastic. Similar mechanisms may account for the observed heterogeneity of CP expression in *Streptococcus pneumoniae* (Hammerschmidt *et al.*, 2005). The high noise in *cap* expression described here is another example of evolved heterogeneity playing a role in pathogenesis, possibly by providing better fitness of the bacterial population during infection/colonisation.

Experimental procedures

Bacterial strains and growth conditions

Strains and plasmids are listed in Table S1. Strains were grown in Luria–Bertani medium (low salt) with appropriate antibiotics in the overnight culture (3 μg ml^{-1} tetracycline, 10 μg ml^{-1} erythromycin or 10 μg ml^{-1} chloramphenicol). Bacteria were subsequently diluted to an initial optical density at OD_{600} of 0.05 (without antibiotics), grown to an OD_{600} of 0.5, again diluted (1:10) and grown to OD_{600} of 0.3 (T1) or for additional 2 h (T2, OD_{600} ~ 2.6), 3 h (T3, OD_{600} ~ 5.2), 4 h (T4, OD_{600} ~ 6.5) or 16 h (T5, OD_{600} ~ 8). To study the impact of glucose, O_2 or high NaCl, strains were grown as described above; however, at the second subculture, they were grown in LB supplemented with 1% glucose, 2M NaCl or under anaerobiosis using the AnaeroGen gas pack (Thermo Scientific). Typing of colonising isolates were performed using established methods for *cap*, *agr*, (Goerke *et al.*, 2005), *spa* (Harmsen *et al.*, 2003) and MLST (Enright *et al.*, 2000).

Strain construction

All plasmids and oligonucleotides are listed in Tables S1 and S2 respectively. Cloning of pCG363: The *recA* promoter with deletion of the LexA binding site was amplified using oligonucleotides PstI-recapfor and PstIIrecaprev from pCG298 (Schröder *et al.*, 2013) and cloned into the PstI site of the integration vector pLL39 [59] resulting in pCG339. RNAIII was amplified with oligonucleotides BamHI-RNAIII-for and SalIIRNA-III-rev3 and cloned into the BamHI-SalII restricted pCG339 vector to generate pCG363. pCG363 was electroporated into CYL316 [60] and transduced into strain Newman using phage phi11. Plasmid stability was verified after growth to stationary phase. Cultures were serially diluted and plated on blood agar plates. Colonies were picked on plates containing chloramphenicol. All analysed colonies were still chloramphenicol resistant indicating that the plasmid was not lost during the experiment. The *agrBCDA-hld* deletion mutant (Newman-391) was obtained using the temperature-sensitive shuttle vector pBASE6 (Geiger *et al.*, 2012). Total deletion was introduced by overlapping PCR employing the oligonucleotides, Gibsonbaseagrdeletion-U and Gibsonbaseagrdeletion-L. The obtained amplicon was cloned into pBASE6 using Gibson assembly. The resulting plasmid pCG391 was transformed into the restriction-deficient strain RN4220 and transduced into *S. aureus* strain Newman. Mutagenesis was performed as described elsewhere (Bae and Schneewind, 2006). The deletion was verified by PCR with oligonucleotides spanning the deletion region. The *agr*-constitutive strain Newman-383 was constructed by site-directed mutagenesis. Part of the *agr* operon was amplified with oligonucleotides agr2434 and agrAdigrev and cloned into the

EcoRI/SalI restricted pBASE6 vector. Single base pair mutation was achieved by site-directed mutagenesis (SDM Q5 Kit) according to the instruction of the manufacturer (New England Biolabs) using the oligonucleotides agrCconstQ5for and agrCconstQ5rev. Sequence-verified pCG383 was electroporated into RN4220 and transduced into strain Newman. Mutagenesis was performed as described before (Bae and Schneewind, 2006). The mutagenesis was verified by sequencing of the amplicon generated with oligonucleotides spanning the *agrC* region (Agrhld1418for and Agr83252266rev).

The single-copy fluorescence reporter plasmid pJL53 is based on pRN7145 (Charpentier *et al*., 2004), which harbours the SaPI1-attS cassette for integration into the chromosome. The pT181 replicon was removed from this plasmid to facilitate chromosomal integration, and then a fragment from pJL-agr-CER (Liese *et al*., 2013) containing *gpcer* (encoding gpCerulean) under control of the P_{RNAIII} promoter was cloned into the multicloning site to generate pJL53. pJL93 was constructed by replacing the *ermC* resistance cassettes from pJL-sar-VEN (Liese *et al*., 2013), by the *tet(M)* cassette from pCN36 (Charpentier *et al*., 2004). For alternative integration vectors, the pT181cop-wt replicon of pJL93 was replaced by the attL54 site, the attachment site for bacteriophage L54a that integrates into the chromosome located within *geh*. Att54L was amplified from pCL84 (Lee *et al*., 1991) (oligonucleotides NarattL54-for and ApaattL54-rev) and cloned into the NarI-ApaI restricted vectors pJL93 resulting in pCG295. The P_{cap}-promoter was amplified (oligonucleotides spHI-cap8for, capP8-rev), and the amplicon cloned into the SphI-EcoRI restricted pCG295 plasmid resulting in pCG318. The down-stream oligonucleotide capP8-rev was chosen to generate a cap promoter fragment with mutated RBS and frameshift mutation of the native start codon. The plasmids were electroporated into strain CYL316 and transduced into different *S. aureus* strains.

RNA isolation and quantification

For transcript analysis, approximately 10^9 *S. aureus* cells were lysed in 1 ml TRIzol reagent (Life Technologies, Germany) with 0.5 ml of zirconia-silica beads (0.1 mm diameter) in a high-speed homogeniser. RNA was isolated as described in the instructions provided by the manufacturer of TRIzol (Life Technologies). Northern blot analysis was performed as described (Goerke *et al*., 2000). qRT-PCR to quantify *cap* and *gyr* mRNAs were performed using the Quanti Fast SYBR-Green RT-PCR kit (Qiagen) and standard curves generated using 10-fold serial dilutions (10^4 to 10^8 copies) of specific *in vitro* transcribed RNA standard molecules (Burian *et al*., 2010). The number of copies of each sample transcript was determined with the aid of the LightCycler software and the *cap* mRNA expressed in reference to copies of *gyrB*.

Immunofluorescence for specific detection of CP5 and CP8

Bacteria were centrifuged, washed in 1× PBS and diluted to OD_{600} of 0.1 and 10 µl spotted onto glass slides (with 10 reaction zones, Medco, München). After heat fixation, Protein A was blocked by incubation with pre-adsorbed human serum (diluted 1:10 in 1× PBS/0.1 % Tween 20) for 1 h. The serum was depleted for *S. aureus* specific antibodies using a protein A deficient strain (Newman *Δspa::ermC*). Briefly, 10^{10} bacteria from an overnight culture were re-suspended in 1 ml of pooled human serum and incubated for 1 h on ice. After centrifugation (5000 *g*, 3 min), the serum supernatant was again incubated with 10^{10} bacteria for 1 h on ice and the serum supernatant filter-sterilised (0.45 µm). After blocking, the slides were washed thrice for 5 min each with 20 µl PBS/Tween 20 followed by incubation with rabbit serum raised against CP5 (1 h, diluted 1:200 in PBS/Tween 20). Antiserum was obtained by immunising rabbits with whole killed encapsulated $CP5^+$ or $CP8^+$ bacteria. The sera were rendered CP specific by absorption with strain Wood 46 (protein A deficient) and isogenic acapsular mutant strains (Watts *et al*., 2005; McLoughlin *et al*., 2006) that were trypsinised to remove protein A. The slides were washed thrice with PBS/Tween 20 followed by incubation with the secondary antibody (diluted 1:200 in PBS/Tween 20, 1 h). Secondary antibodies were either AlexaFluor488-conjugated F(ab)2 goat anti-rabbit IgG (Invitrogen), or Cy3-conjugated F(ab)2 goat-anti-rabbit IgG (Dianova, Hamburg). Following three washes with PBS/Tween 20, bacteria were stained for 5 min at room temperature with 4, 6-diamidino-2-phenylindol (DAPI, 2 mg l^{-1}; Sigma-Aldrich, Munich, Germany). Each slide was finally mounted using fluorescence mounting medium (DAKO). The specificity of CP detection was verified using reference strains Becker (CP8), Newman (CP5), Newman *Δspa::ermC* and the CP negative strains, Newman-132 and strain 8325-4.

Monitoring of P_{cap} and P_{RNAIII} activity

Approximately 10^8 bacteria diluted in 1× PBS were harvested into 24 well cell culture plates (Greiner bio-one) lined with round 12 mm diameter coverslips. Culture supernatant was removed after centrifugation at 600 *g* for 5 mins. Following a 1× PBS wash, bacteria were fixed with 400 µl of 4% paraformaldehyde (room temperature, 15 min). Subsequent to another 1× PBS wash, coverslips were mounted onto slides with fluorescence mounting medium (DAKO).

Coupled in situ *hybridisation and immunofluorescence for detection of CP on* S. aureus *in nasal specimens*

Healthy volunteers were classified as persistent carriers of *S. aureus* when at least three consecutive nasal swab cultures were positive for *S. aureus*. For *ex vivo* analysis of CP in these carriers, nasal swabs were collected and immediately immersed into 500 µl 1× PBS. After rigourous vortexing, the detached bacteria were pelleted (5000 *g*, 4 min) and re-suspended in 50 µl of PBS. Ten microliters was spotted onto glass slides (marked with 10 reaction zones, Medco, München) and air dried. Slides were rinsed in 50%, 80% and 99% ethanol for 3 min each for sample fixation. Fluorescence in-situ hybridisation (FISH) was performed as described previously (Oliveira *et al*., 2002). Briefly, bacteria were incubated with approximately 20 µl of hybridisation solution (10% dextran sulphate, 10 mM NaCl, 30% formamide, 0.1% sodium pyrophosphate, 0.2% polyvinylpyrrolidone, 0.2% Ficoll, 5 mM

disodium EDTA, 1% Triton X-100, 50 mM Tris-HCl, pH 7.5) containing 500 nM Cy3-labeled peptide nucleic acid probe (GCTTCTCGTCCGTTC) targeting *S. aureus* 16S rRNA (Panagene Daejeon, Korea). The slides were incubated for 90 min at 55°C in a 50 ml reaction tube (Falcon), in which a wet filter paper was applied to avoid desiccation. Following hybridisation, the slides were immersed in pre-warmed 5 mM Tris (pH 10), 15 mM NaCl, 0.1% Triton X-100 in a water bath at 55°C and incubated for a total of 30 min with a buffer change every 10 min. Air-dried slides were subjected to immunofluorescence to detect CP (as described above) but using a mixture of rabbit serum raised against CP5 and CP8 (1:200 dilution in PBS, Tween 20) as primary antibodies and Alexa488-F(ab)2, goat anti-rabbit-IgG (Invitrogen probes) as secondary antibody.

Image acquisition, processing and quantification

Image acquisition was performed in the confocal mode of an inverted Zeiss LSM 710 NLO microscope equipped with a spectral detector and employing a Zeiss Plan-Apochromat 63×/1.40 oil DIC M27 objective. The following excitation wavelengths, laser sources and detection spectra were used for the immunofluorescence experiments: DAPI: 405 nm/diode laser/410–567 nm; Cy3: 561 nm/DPSS laser/566–702 nm. For the promoter activity experiments, gpCerulean: 405 nm/diode laser/454–516 nm; gpYFP: 514 nm/argon laser/519–621 nm. Images were exported in the different channels or overlays as 16-bit tagged image files for further analysis. Overlays were batch processed for intensity and colour balance using Corel draw.

Quantification of the fluorescence of single bacteria was performed using the single channel images on the MetaVue™ Research Imaging System (Molecular Devices). For immunofluorescence quantification, from each image 40 bacteria as detected by DAPI were randomly selected and the regions transferred to the corresponding Cy3-labelled image. Integrated intensities of single bacteria were measured after subtracting the mean intensity obtained from the *cap* mutant Newman-132. For quantification of promoter activity, bacteria were selected based on phase contrast images and the regions transferred to the corresponding gpCerulean and gpYFP images. The integrated intensities of 100 single bacteria were analysed per image.

Ethics statement

Nose swabs were taken from healthy volunteers in strict accordance with the institutional guidelines, according to the Declaration of Helsinki. The protocol was approved by the Institutional Review Board of the University of Tübingen. Written informed consent was received from all participants.

Acknowledgements

This work was funded by the Deutsch Forschungsgemeinschaft through SFB766 to CWo and CWe and the GRK1708 to CWo. TN received stipends from the Centre for Infection Research (DZIF) and intramural funding of the 'Interdisziplinäres Zentrum für Klinische Forschung' (IZKF) of the medical faculty, Tübingen. We thank Isabell Samp, Vittoria Bisanzio, Natalya Korn and Nenad Katava for excellent technical assistance. The mutant NE386 from the Nebraska library was obtained through the Network on Antimicrobial Resistance in *Staphylococcus aureus* (NARSA) program supported under NIAID NIH Contact No. HHSN272200700055C.

References

Anetzberger, C., Schell, U., and Jung, K. (2012) Single cell analysis of *Vibrio harveyi* uncovers functional heterogeneity in response to quorum sensing signals. *BMC Microbiol* **12:** 209.

Baddour, L.M., Lowrance, C., Albus, A., Lowrance, J.H., Anderson, S.K., and Lee, J.C. (1992) *Staphylococcus aureus* microcapsule expression attenuates bacterial virulence in a rat model of experimental endocarditis. *J Infect Dis* **165:** 749–753.

Bae, T., and Schneewind, O. (2006) Allelic replacement in *Staphylococcus aureus* with inducible counter-selection. *Plasmid* **55:** 58–63.

Balazsi, G., van Oudenaarden, A., and Collins, J.J. (2011) Cellular decision making and biological noise: from microbes to mammals. *Cell* **144:** 910–925.

Becher, D., Hempel, K., Sievers, S., Zuhlke, D., Pane-Farre, J., Otto, A., *et al.* (2009) A proteomic view of an important human pathogen – towards the quantification of the entire *Staphylococcus aureus* proteome. *PLoS ONE* **4:** e8176.

Ben-Jacob, E., and Schultz, D. (2010) Bacteria determine fate by playing dice with controlled odds. *Proc Natl Acad Sci USA* **107:** 13197–13198.

Boisset, S., Geissmann, T., Huntzinger, E., Fechter, P., Bendridi, N., Possedko, M., *et al.* (2007) *Staphylococcus aureus* RNAIII coordinately represses the synthesis of virulence factors and the transcription regulator Rot by an antisense mechanism. *Genes Dev* **21:** 1353–1366.

Burian, M., Wolz, C., and Goerke, C. (2010) Regulatory adaptation of *Staphylococcus aureus* during nasal colonization of humans. *PLoS ONE* **5:** e10040.

Burian, M., Grumann, D., Holtfreter, S., Wolz, C., Goerke, C., and Broker, B.M. (2012) Expression of staphylococcal superantigens during nasal colonization is not sufficient to induce a systemic neutralizing antibody response in humans. *Eur J Clin Microbiol Infect Dis* **31:** 251–256.

Carnes, E.C., Lopez, D.M., Donegan, N.P., Cheung, A., Gresham, H., Timmins, G.S., and Brinker, C.J. (2010) Confinement-induced quorum sensing of individual *Staphylococcus aureus* bacteria. *Nat Chem Biol* **6:** 41–45.

Casadesus, J., and Low, D.A. (2013) Programmed heterogeneity: epigenetic mechanisms in bacteria. *J Biol Chem* **288:** 13929–13935.

Charpentier, E., Anton, A.I., Barry, P., Alfonso, B., Fang, Y., and Novick, R.P. (2004) Novel cassette-based shuttle vector system for gram-positive bacteria. *Appl Environ Microbiol* **70:** 6076–6085.

Chen, Z., Luong, T.T., and Lee, C.Y. (2007) The sbcDC locus mediates repression of type 5 capsule production as part of the SOS response in *Staphylococcus aureus*. *J Bacteriol* **189:** 7343–7350.

Cocchiaro, J.L., Gomez, M.I., Risley, A., Solinga, R., Sordelli,

D.O., and Lee, J.C. (2006) Molecular characterization of the capsule locus from non-typeable *Staphylococcus aureus*. *Mol Microbiol* **59:** 948–960.

Dassy, B., Hogan, T., Foster, T.J., and Fournier, J.M. (1993) Involvement of the accessory gene regulator (agr) in expression of type 5 capsular polysaccharide by *Staphylococcus aureus*. *J Gen Microbiol* **139** (Part 6): 1301–1306.

Davidson, C.J., and Surette, M.G. (2008) Individuality in bacteria. *Annu Rev Genet* **42:** 253–268.

Ding, Y., Liu, X., Chen, F., Di, H., Xu, B., Zhou, L., *et al*. (2014) Metabolic sensor governing bacterial virulence in *Staphylococcus aureus*. *Proc Natl Acad Sci USA* **111:** E4981–E4990.

Dubnau, D., and Losick, R. (2006) Bistability in bacteria. *Mol Microbiol* **61:** 564–572.

Enright, M.C., Day, N.P., Davies, C.E., Peacock, S.J., and Spratt, B.G. (2000) Multilocus sequence typing for characterization of methicillin-resistant and methicillin-susceptible clones of *Staphylococcus aureus*. *J Clin Microbiol* **38:** 1008–1015.

Fischer, J., Lee, J.C., Peters, G., and Kahl, B.C. (2014) Acapsular clinical *Staphylococcus aureus* isolates lack *agr* function. *Clin Microbiol Infect* **20:** O414–O417.

Freed, N.E., Silander, O.K., Stecher, B., Bohm, A., Hardt, W.D., and Ackermann, M. (2008) A simple screen to identify promoters conferring high levels of phenotypic noise. *PLoS Genet* **4:** e1000307.

Garmyn, D., Gal, L., Briandet, R., Guilbaud, M., Lemaitre, J.P., Hartmann, A., and Piveteau, P. (2011) Evidence of autoinduction heterogeneity via expression of the Agr system of *Listeria monocytogenes* at the single-cell level. *Appl Environ Microbiol* **77:** 6286–6289.

Geiger, T., Francois, P., Liebeke, M., Fraunholz, M., Goerke, C., Krismer, B., *et al*. (2012) The stringent response of *Staphylococcus aureus* and its impact on survival after phagocytosis through the induction of intracellular PSMs expression. *PLoS Pathog* **8:** e1003016.

Geisinger, E., Muir, T.W., and Novick, R.P. (2009) *agr* Receptor mutants reveal distinct modes of inhibition by staphylococcal autoinducing peptides. *Proc Natl Acad Sci USA* **106:** 1216–1221.

Goerke, C., Campana, S., Bayer, M.G., Doring, G., Botzenhart, K., and Wolz, C. (2000) Direct quantitative transcript analysis of the agr regulon of *Staphylococcus aureus* during human infection in comparison to the expression profile *in vitro*. *Infect Immun* **68:** 1304–1311.

Goerke, C., Esser, S., Kummel, M., and Wolz, C. (2005) *Staphylococcus aureus* strain designation by agr and cap polymorphism typing and delineation of agr diversification by sequence analysis. *Int J Med Microbiol* **295:** 67–75.

Gupta, R.K., Alba, J., Xiong, Y.Q., Bayer, A.S., and Lee, C.Y. (2013) MgrA activates expression of capsule genes, but not the alpha-toxin gene in experimental *Staphylococcus aureus* endocarditis. *J Infect Dis* **208:** 1841–1848.

Hammerschmidt, S., Wolff, S., Hocke, A., Rosseau, S., Muller, E., and Rohde, M. (2005) Illustration of pneumococcal polysaccharide capsule during adherence and invasion of epithelial cells. *Infect Immun* **73:** 4653–4667.

Harmsen, D., Claus, H., Witte, W., Rothganger, J., Turnwald, D., and Vogel, U. (2003) Typing of methicillin-resistant *Staphylococcus aureus* in a university hospital setting by using novel software for spa repeat determination and database management. *J Clin Microbiol* **41:** 5442–5448.

Hartmann, T., Baronian, G., Nippe, N., Voss, M., Schulthess, B., Wolz, C., *et al*. (2014) The catabolite control protein E (CcpE) affects virulence determinant production and pathogenesis of *Staphylococcus aureus*. *J Biol Chem* **289:** 29701–29711.

Herbert, S., Worlitzsch, D., Dassy, B., Boutonnier, A., Fournier, J.M., Bellon, G., *et al*. (1997) Regulation of *Staphylococcus aureus* capsular polysaccharide type 5: CO2 inhibition in vitro and in vivo. *J Infect Dis* **176:** 431–438.

Herbert, S., Newell, S.W., Lee, C., Wieland, K.P., Dassy, B., Fournier, J.M., *et al*. (2001) Regulation of *Staphylococcus aureus* type 5 and type 8 capsular polysaccharides by $CO_{(2)}$. *J Bacteriol* **183:** 4609–4613.

Jansen, A., Szekat, C., Schroder, W., Wolz, C., Goerke, C., Lee, J.C., *et al*. (2013) Production of capsular polysaccharide does not influence *Staphylococcus aureus* vancomycin susceptibility. *BMC Microbiol* **13:** 65.

Jones, D.L., Brewster, R.C., and Phillips, R. (2014) Promoter architecture dictates cell-to-cell variability in gene expression. *Science* **346:** 1533–1536.

Lattar, S.M., Tuchscherr, L.P., Caccuri, R.L., Centron, D., Becker, K., Alonso, C.A., *et al*. (2009) Capsule expression and genotypic differences among *Staphylococcus aureus* isolates from patients with chronic or acute osteomyelitis. *Infect Immun* **77:** 1968–1975.

Lee, C.Y., Buranen, S.L., and Ye, Z.H. (1991) Construction of single-copy integration vectors for *Staphylococcus aureus*. *Gene* **103:** 101–105.

Liese, J., Rooijakkers, S.H., van Strijp, J.A., Novick, R.P., and Dustin, M.L. (2013) Intravital two-photon microscopy of host-pathogen interactions in a mouse model of *Staphylococcus aureus* skin abscess formation. *Cell Microbiol* **15:** 891–909.

Long, T., Tu, K.C., Wang, Y., Mehta, P., Ong, N.P., Bassler, B.L., and Wingreen, N.S. (2009) Quantifying the integration of quorum-sensing signals with single-cell resolution. *PLoS Biol* **7:** e68.

Luong, T., Sau, S., Gomez, M., Lee, J.C., and Lee, C.Y. (2002) Regulation of *Staphylococcus aureus* capsular polysaccharide expression by *agr* and *sar*A. *Infect Immun* **70:** 444–450.

Luong, T.T., Sau, K., Roux, C., Sau, S., Dunman, P.M., and Lee, C.Y. (2011) *Staphylococcus aureus* ClpC divergently regulates capsule via *sae* and *codY* in strain newman but activates capsule via *codY* in strain UAMS-1 and in strain Newman with repaired *saeS*. *J Bacteriol* **193:** 686–694.

McLoughlin, R.M., Solinga, R.M., Rich, J., Zaleski, K.J., Cocchiaro, J.L., Risley, A., *et al*. (2006) CD4+ T cells and CXC chemokines modulate the pathogenesis of *Staphylococcus aureus* wound infections. *Proc Natl Acad Sci USA* **103:** 10408–10413.

Majerczyk, C.D., Dunman, P.M., Luong, T.T., Lee, C.Y., Sadykov, M.R., Somerville, G.A., *et al*. (2010) Direct targets of CodY in *Staphylococcus aureus*. *J Bacteriol* **192:** 2861–2877.

Meier, S., Goerke, C., Wolz, C., Seidl, K., Homerova, D., Schulthess, B., *et al*. (2007) sigmaB and the sigmaB-

dependent arlRS and yabJ-spoVG loci affect capsule formation in *Staphylococcus aureus*. *Infect Immun* **75:** 4562–4571.

Munsky, B., Neuert, G., and van Oudenaarden, A. (2012) Using gene expression noise to understand gene regulation. *Science* **336:** 183–187.

Nemeth, J., and Lee, J.C. (1995) Antibodies to capsular polysaccharides are not protective against experimental *Staphylococcus aureus* endocarditis. *Infect Immun* **63:** 375–380.

Nilsson, I.M., Lee, J.C., Bremell, T., Ryden, C., and Tarkowski, A. (1997) The role of staphylococcal polysaccharide microcapsule expression in septicemia and septic arthritis. *Infect Immun* **65:** 4216–4221.

Novick, R.P., and Geisinger, E. (2008) Quorum sensing in staphylococci. *Annu Rev Genet* **42:** 541–564.

O'Riordan, K., and Lee, J.C. (2004) *Staphylococcus aureus* capsular polysaccharides. *Clin Microbiol Rev* **17:** 218–234.

Oliveira, K., Procop, G.W.,Wilson, D.,Coull, J., and Stender, H. (2002) Rapid identification of Staphylococcus aureus directly from blood cultures by fluorescence in situ hybridization with peptide nucleic acid probes. *J Clin Microbiol* **40:** 247–251.

Perez, P.D., and Hagen, S.J. (2010) Heterogeneous response to a quorum-sensing signal in the luminescence of individual *Vibrio fischeri*. *PLoS ONE* **5:** e15473.

Periasamy, S., Joo, H.S., Duong, A.C., Bach, T.H., Tan, V.Y., Chatterjee, S.S., *et al*. (2012) How *Staphylococcus aureus* biofilms develop their characteristic structure. *Proc Natl Acad Sci USA* **109:** 1281–1286.

Pohl, K., Francois, P., Stenz, L., Schlink, F., Geiger, T., Herbert, S., *et al*. (2009) CodY in *Staphylococcus aureus*: a regulatory link between metabolism and virulence gene expression. *J Bacteriol* **191:** 2953–2963.

Pohlmann-Dietze, P., Ulrich, M., Kiser, K.B., Doring, G., Lee, J.C., Fournier, J.M., *et al*. (2000) Adherence of *Staphylococcus aureus* to endothelial cells: influence of capsular polysaccharide, global regulator *agr*, and bacterial growth phase. *Infect Immun* **68:** 4865–4871.

Portoles, M., Kiser, K.B., Bhasin, N., Chan, K.H., and Lee, J.C. (2001) *Staphylococcus aureus* Cap5O has UDP-ManNAc dehydrogenase activity and is essential for capsule expression. *Infect Immun* **69:** 917–923.

Poutrel, B., Rainard, P., and Sarradin, P. (1997) Heterogeneity of cell-associated CP5 expression on *Staphylococcus aureus* strains demonstrated by flow cytometry. *Clin Diagn Lab Immunol* **4:** 275–278.

Pradhan, B.B., and Chatterjee, S. (2014) Reversible non-genetic phenotypic heterogeneity in bacterial quorum sensing. *Mol Microbiol* **92:** 557–569.

Price-Whelan, A., Poon, C.K., Benson, M.A., Eidem, T.T., Roux, C.M., Boyd, J.M., *et al*. (2013) Transcriptional profiling of *Staphylococcus aureus* during growth in 2 M NaCl leads to clarification of physiological roles for Kdp and Ktr K+ uptake systems. *mBio* **4**(4)**:** e00407–13.

Risley, A.L., Loughman, A., Cywes-Bentley, C., Foster, T.J., and Lee, J.C. (2007) Capsular polysaccharide masks clumping factor A-mediated adherence of *Staphylococcus aureus* to fibrinogen and platelets. *J Infect Dis* **196:** 919–927.

Romilly, C., Lays, C., Tomasini, A., Caldelari, I., Benito, Y., Hammann, P., *et al*. (2014) A non-coding RNA promotes bacterial persistence and decreases virulence by regulating a regulator in *Staphylococcus aureus*. *PLoS Pathog* **10:** e1003979.

Ryall, B., Eydallin, G., and Ferenci, T. (2012) Culture history and population heterogeneity as determinants of bacterial adaptation: the adaptomics of a single environmental transition. *Microbiol Mol Biol Rev* **76:** 597–625.

Sadykov, M.R., Mattes, T.A., Luong, T.T., Zhu, Y., Day, S.R., Sifri, C.D., *et al*. (2010) Tricarboxylic acid cycle-dependent synthesis of *Staphylococcus aureus* Type 5 and 8 capsular polysaccharides. *J Bacteriol* **192:** 1459–1462.

Sau, S., Bhasin, N., Wann, E.R., Lee, J.C., Foster, T.J., and Lee, C.Y. (1997) The *Staphylococcus aureus* allelic genetic loci for serotype 5 and 8 capsule expression contain the type-specific genes flanked by common genes. *Microbiology* **143** (Part 7): 2395–2405.

Schroder, W., Bernhardt, J., Marincola, G., Klein-Hitpass, L., Herbig, A., Krupp, G., *et al*. (2014) Altering gene expression by aminocoumarins: the role of DNA supercoiling in *Staphylococcus aureus*. *BMC Genomics* **15:** 291.

Schröder, W., Goerke, C., and Wolz, C. (2013) Opposing effects of aminocoumarins and fluoroquinolones on the SOS response and adaptability in *Staphylococcus aureus*. *J Antimicrob Chemother* **68:** 529–538.

Schulthess, B., Meier, S., Homerova, D., Goerke, C., Wolz, C., Kormanec, J., *et al*. (2009a) Functional characterization of the sigmaB-dependent yabJ-spoVG operon in *Staphylococcus aureus:* role in methicillin and glycopeptide resistance. *Antimicrob Agents Chemother* **53:** 1832–1839.

Schulthess, B., Meier, S., Homerova, D., Goerke, C., Wolz, C., Kormanec, J., *et al*. (2009b) Functional characterization of the σB-dependent *yabJ-spoVG* operon in *Staphylococcus aureus*: role in methicillin and glycopeptide resistance. *Antimicrob Agents Chemother* **53:** 1832–1839.

Seidl, K., Stucki, M., Ruegg, M., Goerke, C., Wolz, C., Harris, L., *et al*. (2006) *Staphylococcus aureus* CcpA affects virulence determinant production and antibiotic resistance. *Antimicrob Agents Chemother* **50:** 1183–1194.

Steinhuber, A., Goerke, C., Bayer, M.G., Doring, G., and Wolz, C. (2003) Molecular architecture of the regulatory Locus *sae* of *Staphylococcus aureus* and its impact on expression of virulence factors. *J Bacteriol* **185:** 6278–6286.

Sun, F., Ji, Q., Jones, M.B., Deng, X., Liang, H., Frank, B., *et al*. (2012) AirSR, a [2Fe-2S] cluster-containing two-component system, mediates global oxygen sensing and redox signaling in *Staphylococcus aureus*. *J Am Chem Soc* **134:** 305–314.

Thakker, M., Park, J.S., Carey, V., and Lee, J.C. (1998) *Staphylococcus aureus* serotype 5 capsular polysaccharide is antiphagocytic and enhances bacterial virulence in a murine bacteremia model. *Infect Immun* **66:** 5183–5189.

Thoendel, M., Kavanaugh, J.S., Flack, C.E., and Horswill, A.R. (2011) Peptide signaling in the staphylococci. *Chem Rev* **111:** 117–151.

Tu, K.C., Long, T., Svenningsen, S.L., Wingreen, N.S., and Bassler, B.L. (2010) Negative feedback loops involving small regulatory RNAs precisely control the *Vibrio harveyi*

quorum-sensing response. *Mol Cell* **37:** 567–579.
Tuchscherr, L., Loffler, B., Buzzola, F.R., and Sordelli, D.O. (2010) *Staphylococcus aureus* adaptation to the host and persistence: role of loss of capsular polysaccharide expression. *Future Microbiol* **5:** 1823–1832.
Tuchscherr, L.P., Buzzola, F.R., Alvarez, L.P., Caccuri, R.L., Lee, J.C., and Sordelli, D.O. (2005) Capsule-negative *Staphylococcus aureus* induces chronic experimental mastitis in mice. *Infect Immun* **73:** 7932–7937.
Vandenesch, F., Kornblum, J., and Novick, R.P. (1991) A temporal signal, independent of agr, is required for hla but not spa transcription in *Staphylococcus aureus*. *J Bacteriol* **173:** 6313–6320.
Veening, J.W., Smits, W.K., and Kuipers, O.P. (2008) Bistability, epigenetics, and bet-hedging in bacteria. *Annu Rev Microbiol* **62:** 193–210.
Watts, A., Ke, D., Wang, Q., Pillay, A., Nicholson-Weller, A., and Lee, J.C. (2005) *Staphylococcus aureus* strains that express serotype 5 or serotype 8 capsular polysaccharides differ in virulence. *Infect Immun* **73:** 3502–3511.
Wright, J.S., 3rd, Jin, R., and Novick, R.P. (2005) Transient interference with staphylococcal quorum sensing blocks abscess formation. *Proc Natl Acad Sci USA* **102:** 1691–1696.
Zhao, L., Xue, T., Shang, F., Sun, H., and Sun, B. (2010) *Staphylococcus aureus* AI-2 quorum sensing associates with the KdpDE two-component system to regulate capsular polysaccharide synthesis and virulence. *Infect Immun* **78:** 3506–3515.
Zhu, Y., Nandakumar, R., Sadykov, M.R., Madayiputhiya, N., Luong, T.T., Gaupp, R., *et al*. (2011) RpiR homologues may link *Staphylococcus aureus* RNAIII synthesis and pentose phosphate pathway regulation. *J Bacteriol* **193:** 6187–6196.

Supporting information

Additional supporting information may be found in the online version of this article at the publisher's web-site.

Phenotypic Heterogeneity and Temporal Expression of the Capsular Polysaccharide in *Staphylococcus aureus*, Molecular Microbiology, George et al.

Supplementary Information:

Table S1. Strains and plasmids. Description of the bacterial strains and plasmids used.

Table S2. Oligonucleotides. Description of the oligonucleotides used.

Supporting figure S1. Growth curves.

Supporting figure S2. Control for specificity of CP detection by immunofluorescence. Strains were grown to defined growth phase T1-T5 (see Fig. 2A) and CP detected by immunofluorescence.

Supporting figure S3. Overview of regulatory circuits which are known to impact *cap* expression. Green indicates an up-regulation, red a down-regulation effect on *cap* expression.

Supporting figure S4. Influence of *sae* on CP synthesis. Bacteria were harvested at different growth phases (T1-T5, see Fig. 2A). Detection of CP by immunofluorescence in Newman and *sae* mutants.

Supporting figure S5. Influence of glucose, O_2 or high NaCl on CP synthesis. Strain Newman grown in LB supplemented with 1% glucose, 2M NaCl or under anaerobiosis. Bacteria were harvested at different growth phases as indicated (T1-T5, see Fig. 2A). Detection of CP by immunofluorescence.

Table S1: Strains and Plasmids

Strains	Description	Reference
One Shot, TOP10	Competent *E. coli* for plasmid transformation	Invitrogen
RN4220	Restriction-deficient *S. aureus* strain	(Kreiswirth et al., 1983)
CYL316	RN4220 with L54a integrase gene cloned plasmid vector (pYL112ð19)	(Lee et al., 1991)
RN9011	RN4220 with, SAPI1integrase gene cloned in plasmid vector (ppRN7023)	(Charpentier et al., 2004)
NE386	USA300, *rot*:: *bursa aurealis*, Nebraska Transposon Mutant Library	(Fey et al., 2013)
HG001	*rsbU*-repaired derivative of RN1 (=8325)	(Herbert et al., 2010)
Newman	Wild-type	(Duthie and Lorenz, 1952)
Newman-132	pMUTIN integrated into capsule promoter P*cap*	(Jansen et al., 2013)
Newman-*rot*	Newman *rot*:: *bursa aurealis*	This work
ALC355	Newman, Δ*agr*::*tetM*	(Wolz et al., 1996)
ALC355, *rot*	Newman, Δ*agr*::*tetM*, *rot*:: *bursa aurealis*	This work
Newman-391	Newman, Δ*agr*, markerless deletion of *agrBDCA* and *hld*	This work
Newman-363	Newman, Δ*agr-hld* (Newman-391), complemented with RNAIII expression vector pCG363	This work
Newman-383	Newman with constitutive on *agrC, agrC*^{R238H}	This work
Newman-21	Newman *ΔcodY::tet(M)*	(Pohl et al., 2009)
Newman-21, *rot*	Newman *ΔcodY::tet(M), rot:: bursa aurealis*	
Newman-29	Newman *ΔsaePQRS::kan*	(Mainiero et al., 2010)
Newman, *spa*	Newman *Δspa::ermC*	This work
Newman-132 *spa*	Newman pMUTIN integrated into capsule promoter P*cap*; *Δspa::ermC*	This work

Plasmids	Description	Reference
pLL39	Single copy vector, integrates into *geh*	(Luong and Lee, 2007)

pCG 298	*recA* with deleted LexA binding motif (14 bp) cloned in pCR4blunt-topo	(Schroder et al., 2014)
pCG339	*recA* promoter with deleted LexA binding motif cloned into PstI site of pLL39, allows early phase expression in *S. aureus*	This work
pCG363	RNAIII cloned into BamHI/SalI site of pCG339	This work
pBASE6	Suicide mutagenesis vector	(Geiger et al., 2012)
pCG391	pBASE6 vector with flanking regions of *agr*-locus	This work
pCG383	pBASE6 vector *agrC*-mutation *, agrC*^{R238H}	This work
pJL53	Integration vector, P_{RNAIII}-*gpcer*, SaPI1-attS, *ermC*	This work
pJL93	$P1_{sar}$-*yfp*, pT181cop-wt repC, *tetM*	This work
pCG295	Integration vector, JL93, with replacement of pT181cop-wt repC by attL54 attachment site, *tetM*	This work
pCG318	pCG295 replacement of $P1_{sar}$ with P_{cap}, attL54, *tetM*	This work

References

Charpentier, E., Anton, A.I., Barry, P., Alfonso, B., Fang, Y., and Novick, R.P. (2004) Novel cassette-based shuttle vector system for gram-positive bacteria. *Appl Environ Microbiol* **70**: 6076-6085.

Duthie, E.S., and Lorenz, L.L. (1952) Staphylococcal coagulase; mode of action and antigenicity. *J Gen Microbiol* **6**: 95-107.

Fey, P.D., Endres, J.L., Yajjala, V.K., Widhelm, T.J., Boissy, R.J., Bose, J.L., and Bayles, K.W. (2013) A genetic resource for rapid and comprehensive phenotype screening of nonessential *Staphylococcus aureus* genes. *MBio* **4**: e00537-00512.

Geiger, T., Francois, P., Liebeke, M., Fraunholz, M., Goerke, C., Krismer, B. et al. (2012) The stringent response of *Staphylococcus aureus* and its impact on survival after phagocytosis through the induction of intracellular PSMs expression. *PLoS Pathog* **8**: e1003016.

Herbert, S., Ziebandt, A.K., Ohlsen, K., Schafer, T., Hecker, M., Albrecht, D. et al. (2010) Repair of global regulators in *Staphylococcus aureus* 8325 and comparative analysis with other clinical isolates. *Infect Immun* **78**: 2877-2889.

Jansen, A., Szekat, C., Schroder, W., Wolz, C., Goerke, C., Lee, J.C. et al. (2013) Production of capsular polysaccharide does not influence *Staphylococcus aureus* vancomycin susceptibility. *BMC Microbiol* **13**: 65.

Kreiswirth, B.N., Lofdahl, S., Betley, M.J., O'Reilly, M., Schlievert, P.M., Bergdoll, M.S., and Novick, R.P. (1983) The toxic shock syndrome exotoxin structural gene is not detectably transmitted by a prophage. *Nature* **305**: 709-712.

Lee, C.Y., Buranen, S.L., and Ye, Z.H. (1991) Construction of single-copy integration vectors for *Staphylococcus aureus*. *Gene* **103**: 101-105.

Luong, T.T., and Lee, C.Y. (2007) Improved single-copy integration vectors for *Staphylococcus aureus*. *J Microbiol Methods* **70**: 186-190.

Mainiero, M., Goerke, C., Geiger, T., Gonser, C., Herbert, S., and Wolz, C. (2010) Differential target gene activation by the *Staphylococcus aureus* two-component system saeRS. *J Bacteriol* **192**: 613-623.

Pohl, K., Francois, P., Stenz, L., Schlink, F., Geiger, T., Herbert, S. et al. (2009) CodY in *Staphylococcus aureus*: a regulatory link between metabolism and virulence gene expression. *J Bacteriol* **191**: 2953-2963.

Schroder, W., Bernhardt, J., Marincola, G., Klein-Hitpass, L., Herbig, A., Krupp, G. et al. (2014) Altering gene expression by aminocoumarins: the role of DNA supercoiling in *Staphylococcus aureus*. *BMC Genomics* **15**: 291.

Wolz, C., McDevitt, D., Foster, T.J., and Cheung, A.L. (1996) Influence of *agr* on fibrinogen binding in *Staphylococcus aureus* Newman. *Infect Immun* **64**: 3142-3147.

Table S2: Oligonucleotides

Description/Purpose	Template	Name*	Sequence
agr deletion	USA300 JE2	Gibsonbaseagrdeletion-U	ATTACGCCCCGCCCTGCCACTCATCGCAGTGCAGCGGAATTCCGGAGCTCTACTTATGTGACCCAACTTATCTG
		Gibsonbaseagrdeletion-L	TCTGCAGGCATGCAAGCTTGATATCGTCGACAGATCTGCGCGCTAGCCCGGGGATAACGCTGAAGATTT
DIG PCR for RNAIII detection	Col	agrU1028	ATCTATTTTTGGGGATGTTA
		agr1436	CGACACAGTGAACAAATTC
gyr-qt RT PCR	USA300 JE2	gyr297-U	TTAGTGTGGGAAATTGTCGATAAT
		gyr574-L	AGTCTTGTGACAATGCGTTTACA
cap-qt RT PCR		capAs	CAAATTCCGAAGATTATGAGTTTGGA
		capAR	TTGAATTGAACCCAATACAGGCA
pCG363	HG001	BamHI-RNAIII-for	GGGGGATCCCAGTAAGAACCCATTTCGCCCTT
		SalIIRNA III-rev3	GGGGTCGACAGATCACAGAGATGTGATGG
pCG339	pCG298	PstI-recapfor-	GGGGCTGCAGATGATGGTATTACTAATGGTGC
		PstIIrecaprev.	GGGGCTGCAGAGCGAGACCTCCTAATTGAAATTGCTA
AttL54-cloning	pCL84	NarIattL54-for	GGGGGGCGCCAAGGGCAGATTATTTGAA
		ApaIattL54-rev	GGGGGGGCCCAAAATGGACAGAGAGTT
For constitutive agrC^{H238H} mutant	Newman	EcoRIagrCconstfor	GGGGGAATTCTTTGTTGATTATGACTTCGC
		SalIagrCconst2rev	GGGGTCGACACATTCACATCCTTATGG
	agrC-pBASE6	agrCconstQ5for	AGTTCCATCATGATTATGTC
		agrCconstQ5rev	TGCGCATTTCGTTGTTGATA
	Newman-383	Agrhld1418for	GAATTTGTTCACTGTGTCG
		Agr83252266rev	CATTTTTTAATTCACGCGTC
Cap-promoter	Newman	spHI-cap8for	CCCGCATGCCTAATCCTAAAGAAGCACTAA
		capP8-rev	TTAAGAATTCGTACTTTCCAATATTTACCTC
Geh integration control	Integrants	pCG295rechts	AACTGATTTTCCCTCTATTA
		scv2.1	TGTGCCATGATAACAGCACG
SaPI integration control	Integrants	SAPI_int_for	CATTAACTTGAGGGAGTGGG
		SAPI_int_rev	GGCAGAGGCCATATATCTG

Fig. S1

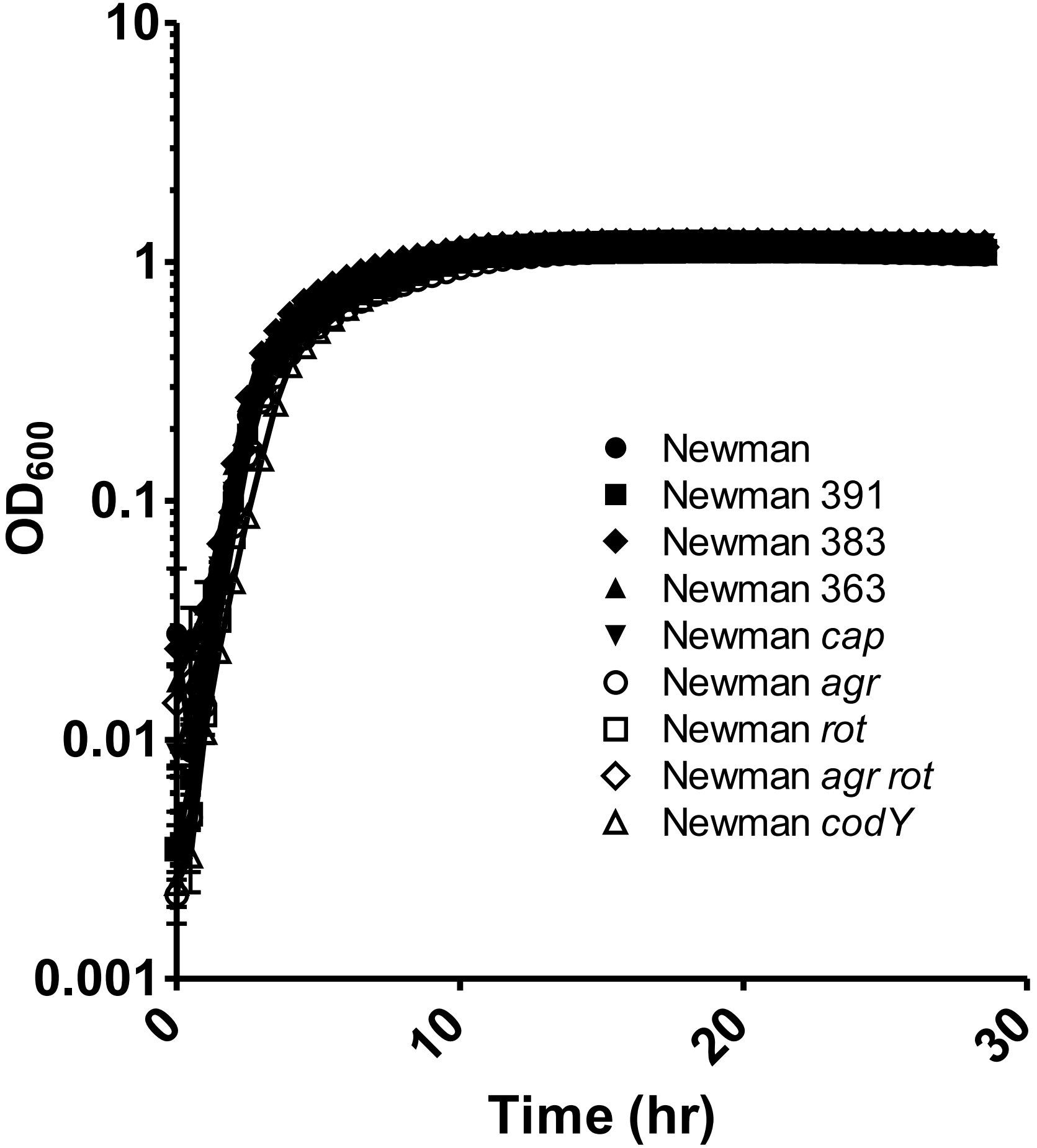
10
1
0.1
0.01
0.001
OD600
0
10
20
30
Time (hr)
Newman
Newman 391
Newman 383
Newman 363
Newman cap
Newman agr
Newman rot
Newman agr rot
Newman codY

Fig. S2

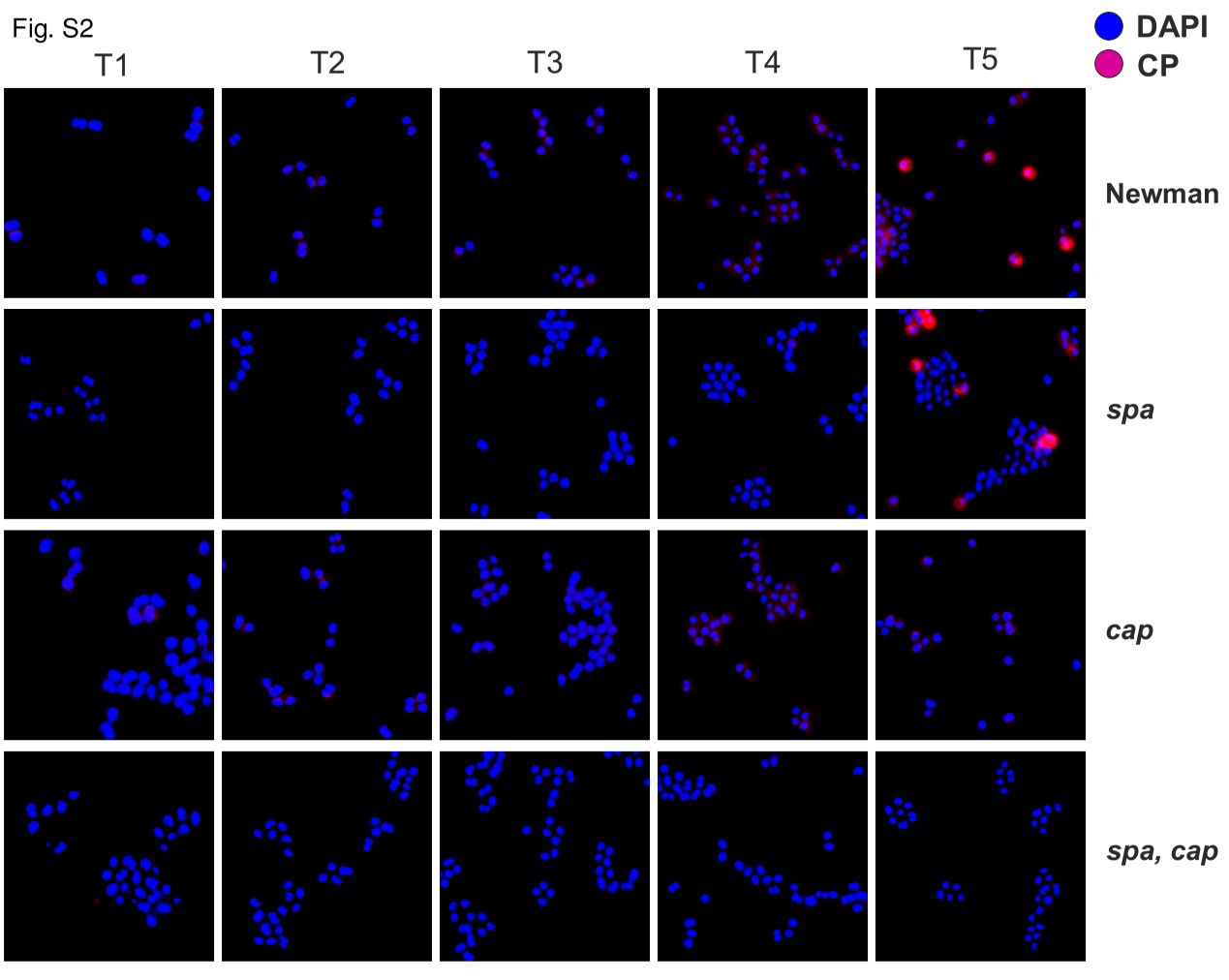

Fig. S3

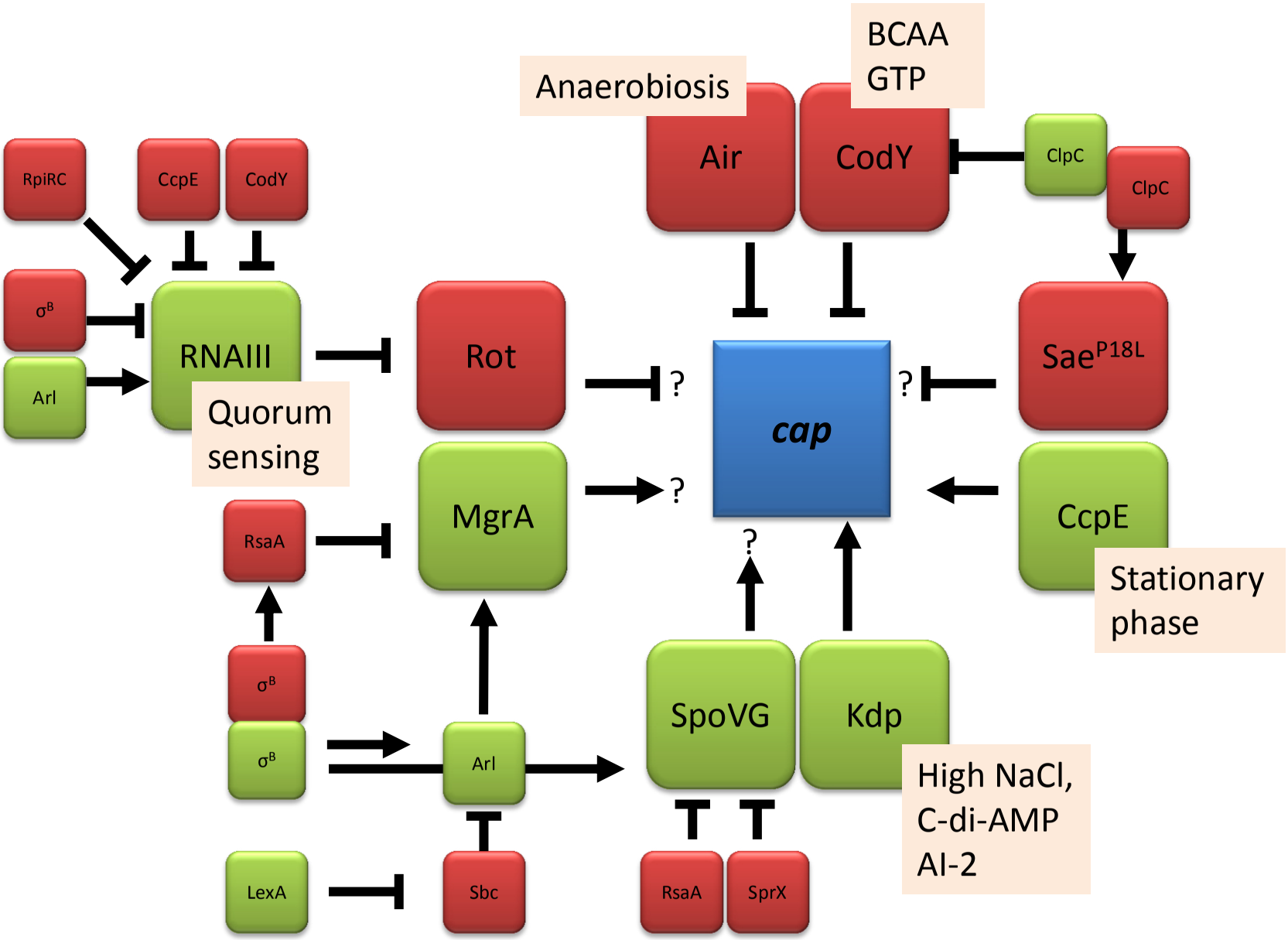
Anaerobiosis
BCAA
GTP
Air
CodY
ClpC
ClpC
RpiRC
CcpE
CodY
σB
Arl
RNAIII
Quorum
sensing
Rot
MgrA
RsaA
σB
σB
Arl
LexA
Sbc
?
?
?
?
cap
Sae P18L
CcpE
Stationary
phase
SpoVG
Kdp
RsaA
SprX
High NaCl,
C-di-AMP
AI-2

Fig. S4

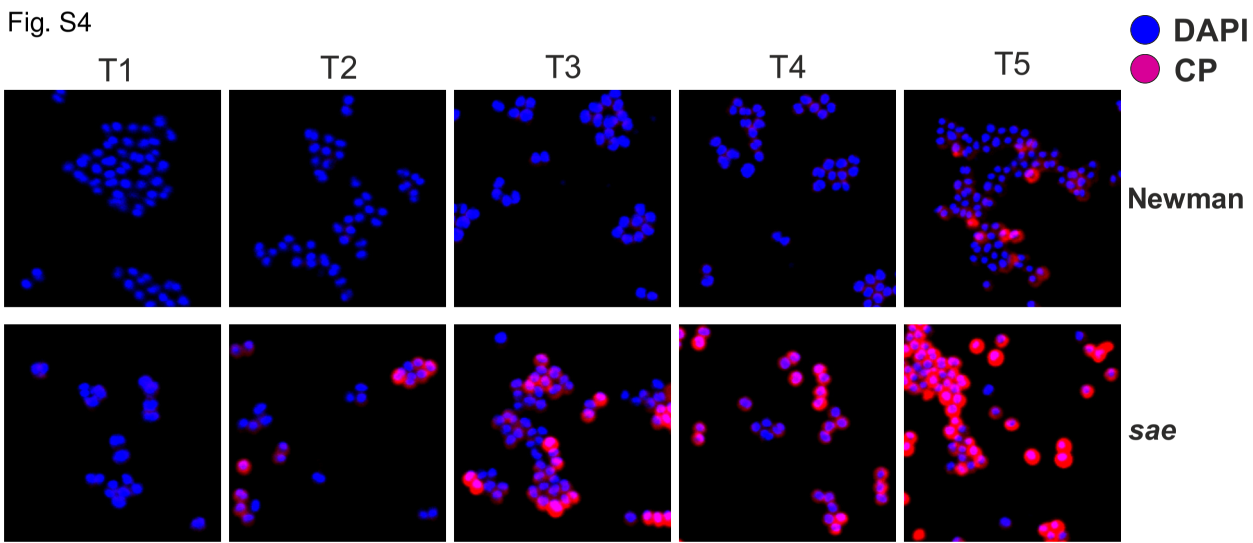

Fig. S5

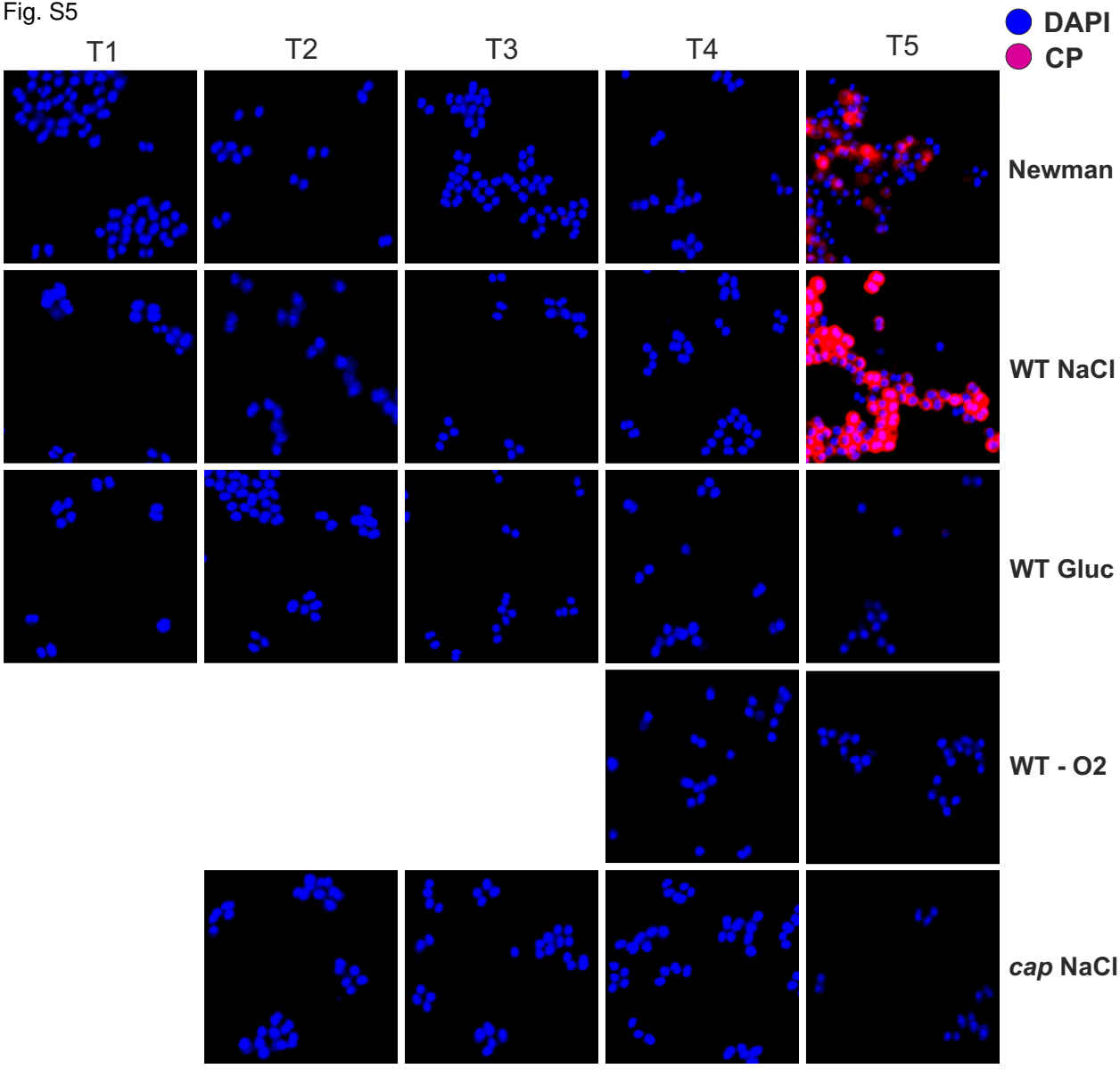

Publication 2

Wall teichoic acids mediate increased virulence in *Staphylococcus aureus*.

Wanner S, Schade J, Keinhörster D, Weller N, **George SE**, Kull L, Bauer J, Grau T, Winstel V, Stoy H, Kretschmer D, Kolata J, Wolz C, Bröker BM, Weidenmaier C

Nature Microbiology 2017 Jan 23;2:16257. doi: 10.1038/nmicrobiol.2016.257.

nature microbiology

ARTICLES

PUBLISHED: 23 JANUARY 2017 | VOLUME: 2 | ARTICLE NUMBER: 16257

Wall teichoic acids mediate increased virulence in *Staphylococcus aureus*

Stefanie Wanner[1†], Jessica Schade[1†], Daniela Keinhörster[1], Nicola Weller[1], Shilpa E. George[1], Larissa Kull[1], Jochen Bauer[1], Timo Grau[1], Volker Winstel[2], Henriette Stoy[1], Dorothee Kretschmer[1], Julia Kolata[3], Christiane Wolz[1], Barbara M. Bröker[4] and Christopher Weidenmaier[1,5*]

Community-associated methicillin-resistant *Staphylococcus aureus* (CA-MRSA) are the cause of a severe pandemic consisting primarily of skin and soft tissue infections. The underlying pathomechanisms have not been fully understood and we report here a mechanism that plays an important role for the elevated virulence of CA-MRSA. Surprisingly, skin abscess induction in an animal model was correlated with the amount of a major cell wall component of *S. aureus*, termed wall teichoic acid (WTA). CA-MRSA exhibited increased cell-wall-associated WTA content (WTA^{high}) and thus were more active in inducing abscess formation via a WTA-dependent and T-cell-mediated mechanism than *S. aureus* strains with a WTA^{low} phenotype. We show here that WTA is directly involved in *S. aureus* strain-specific virulence and provide insight into the underlying molecular mechanisms that could guide the development of novel anti-infective strategies.

Community-associated methicillin-resistant *Staphylococcus aureus* (CA-MRSA) strains pose a serious threat due to their rapid epidemic spread and their enormous virulence potential, which exceeds that of traditional hospital-associated strains (HA-MRSA)[1]. Skin and soft tissue infections (SSTIs) are the most common CA-MRSA infections, and 50–75% of patients present with abscesses[2]. Less frequent are lethal infections such as sepsis or necrotizing pneumonia[3–7]. In the USA, USA300 isolates are primarily responsible for the ongoing CA-MRSA epidemics[8–10], having replaced earlier USA400 isolates[11]. The success of CA-MRSA strains appears to be due to a unique combination of genetic factors that enable the bacteria to evade the human host defence systems[12–18]. However, the relative role of virulence factors in CA-MRSA virulence is still under debate[19–22]. More recent findings suggest that the cytolytic phenol-soluble modulin PSMα peptides[23–25], which are responsible for increased neutrophil killing capacity, the cytolysin α-toxin[20,24,26,27], as well as the global virulence regulator (termed accessory gene regulator (Agr)[28]) play key roles in CA-MRSA virulence in different experimental skin infection models. It has been demonstrated that the global virulence gene regulator Agr exerts strict control over PSM expression[29] and that the cytolytic PSMα peptides are produced in large amounts by CA-MRSA strains[23,30] as a consequence of high Agr activity[30]. The *agr* four-gene operon encodes a typical autoactivation circuit[31] and makes use of a regulatory RNA, RNAIII, as its effector[32,33]. In this study, we present evidence for a novel important factor in CA-MRSA virulence. Until now the focus has largely been on toxins and a putative pathogenicity island termed the 'arginine catabolic mobile element' (ACME)[34–36]. However, the impact of cell wall components has not been studied so far. Here, we introduce a novel concept of staphylococcal strain-specific virulence that includes a major cell wall glycopolymer. Cell wall teichoic acid (WTA) is a zwitterionic, secondary cell wall polymer of *S. aureus* that has important functions in bacterial physiology[37] as well as in *S. aureus* colonization and infection[38–41]. WTA is one of the most abundant surface determinants of *S. aureus* and has recently attracted major attention as a target structure for novel anti-infective strategies[42] and antibiotics[43–48]. The WTA of *S. aureus* is composed of ~40 ribitol phosphate repeating units modified with *N*-acetylglucosamine and D-alanine[49,50] (Supplementary Fig. 1). Negatively charged phosphate groups in the repeating unit and ester-linked D-alanine residues are responsible for the zwitterionic charge of WTA. We have demonstrated previously that the zwitterionic WTA of *S. aureus* activates CD4$^+$ T cells via a major histocompatibility complex (MHC) II-dependent mechanism, which modulates the development of skin abscesses in a mouse model[51] at the early stages of abscess formation. Given that CA-MRSA is the predominant cause of SSTIs, we focus here on the role of WTA in CA-MRSA skin infections and demonstrate that the WTA content in cell wall fractions from highly pathogenic CA-MRSA strains such as USA300 (LAC) and MW2 (USA400) is significantly elevated compared to less virulent patient isolates (103), HA-MRSA (USA500) or laboratory strains (SA113). We termed these phenotypes WTA^{high} and WTA^{low}, respectively, and describe here the underlying regulatory mechanisms and the impact on skin-infection-related virulence in a mouse model.

Results

Highly pathogenic CA-MRSA strains exhibit elevated WTA content in their cell walls compared to less pathogenic strains. We analysed the cell wall composition of several *S. aureus* strains that share the same ribitol–WTA structure and biosynthetic pathways (Supplementary Figs 1–3) with respect to amounts of WTA. When we determined the WTA content of the cell wall fractions, we found that the highly pathogenic CA-MRSA strains MW2 and USA300, as well as clinical isolate 103 (superantigen-free,

[1]Department of Medicine, Interfacultary Institute for Microbiology and Infection Medicine (IMIT), University of Tübingen, Elfriede-Aulhorn Straße 6, 72076 Tübingen, Germany. [2]Department of Microbiology, University of Chicago, Chicago, Illinois 60637, USA. [3]Medical Microbiology, UMC Utrecht, Heidelberglaan 100, 3584CX Utrecht, The Netherlands. [4]Department of Immunology, University Medicine Greifswald, Ferdinand-Sauerbruch-Straße DZ7, 17475 Greifswald, Germany. [5]German Center for Infection Research (DZIF), Partner Site Tübingen, 72076 Tübingen, Germany. †These authors contributed equally to this work. *e-mail: christopher.weidenmaier@med.uni-tuebingen.de

© 2017 Macmillan Publishers Limited, part of Springer Nature. All rights reserved.

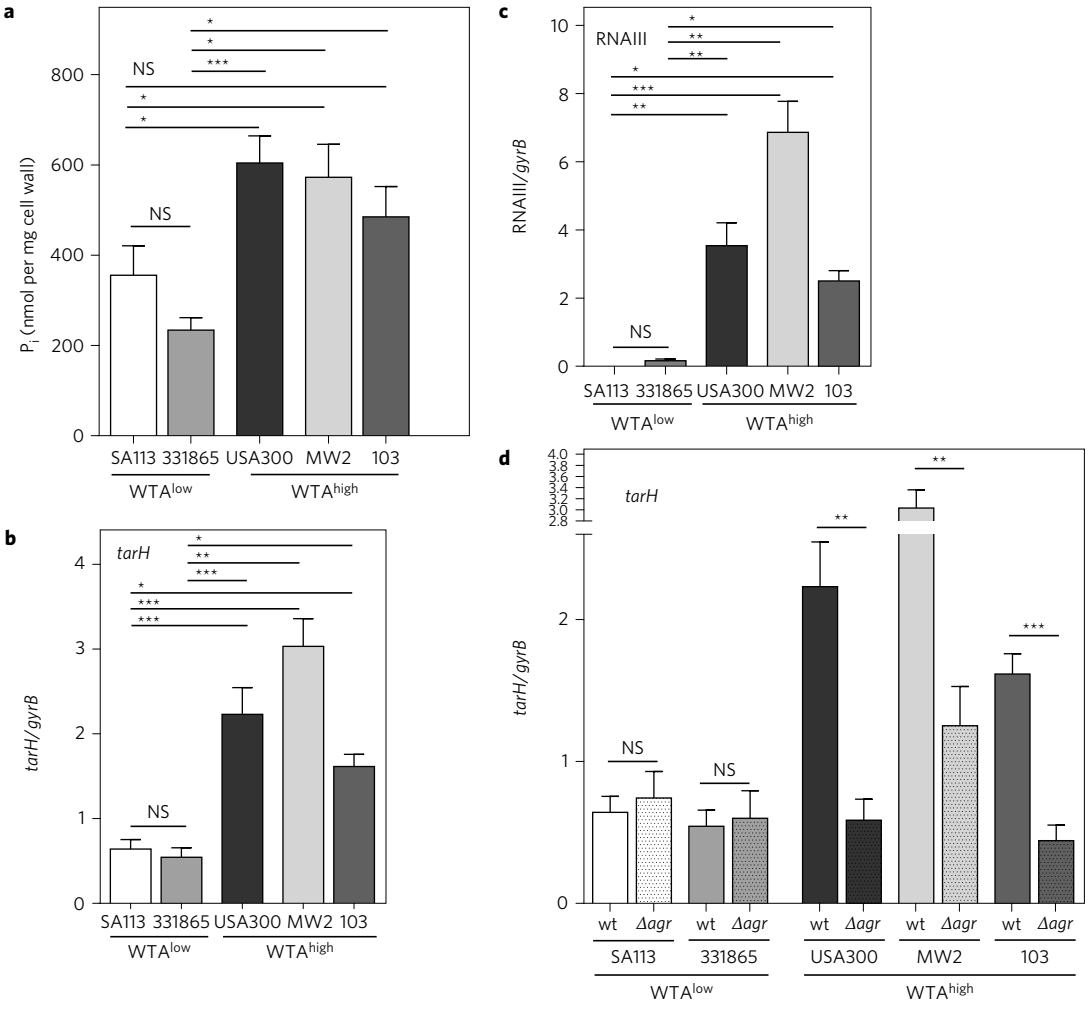

Figure 1 | Amounts of WTA in the cell wall fractions of *S. aureus* strains and transcriptional analysis by qRT–PCR. a, The amount of WTA per mg of cell wall preparation was determined with a colorimetric assay and is depicted as nmol inorganic phosphorus (P_i) per mg cell wall dry weight. CA-MRSA strains USA300 and MW2 (as well as clinical, superantigen-free isolate 103) were compared to non-CA-MRSA strains (SA113, and clinical, superantigen-free isolate 331865). Shown are means ± s.e.m. for $n = 8$–11 independent WTA isolations. *P* values for multiple comparisons were determined by one-way ANOVA with Tukey's post-test. $^*P < 0.05$, $^{**}P < 0.01$, $^{***}P < 0.0001$. NS, not significant. **b**, Transcriptional analysis of the WTA biosynthesis gene *tarH* from *in vitro* cultures grown to stationary phase in WTA^{high} strains (MW2, USA300, 103) and WTA^{low} strains (SA113, 331865). The expression of transcripts was quantified relative to the transcription of gyrase (copies of *tarH* per copy of *gyrB*). Shown are means ± s.e.m., $n = 6$ independent experiments. *P* values for multiple comparisons were determined by one-way ANOVA with Tukey's post-test. $^*P < 0.05$, $^{**}P < 0.01$, $^{***}P < 0.0001$. **c**, Transcriptional analysis of RNAIII, the downstream regulator of the global virulence Agr regulon. WTA^{high} strains (MW2, USA300, 103) and WTA^{low} strains (SA113, 331865) were grown to stationary phase. Transcripts were quantified relative to the transcription of gyrase (copies of RNAIII per copy of *gyrB*). Shown are means ± s.e.m., $n = 6$ independent experiments. *P* values for multiple comparisons were determined by one-way ANOVA with Tukey's post-test. $^*P < 0.05$, $^{**}P < 0.01$, $^{***}P < 0.0001$. **d**, Transcriptional analysis of the WTA biosynthesis gene *tarH*. *In vitro* cultures of WTA^{high}, WTA^{high} *Δagr* mutant, WTA^{low} and WTA^{low} *Δagr* mutant strains were grown to stationary phase. Transcripts were quantified relative to the transcription of gyrase (copies of *tarH* per copy of *gyrB*). Shown are means ± s.e.m., $n = 6$ independent experiments. Statistically significant differences between WTA^{high} and WTA^{low} and their respective *Δagr* mutant strains were determined by Student's *t*-test. $^*P < 0.05$, $^{**}P < 0.01$, $^{***}P < 0.001$.

included as a control for superantigen activity; see section beginning with 'Cell wall fractions'), exhibited elevated WTA content in their cell wall fractions compared to laboratory strain SA113 and clinical isolate 331865 (superantigen-free, included as a control for superantigen activity). We grouped the isolates as WTA^{high} (MW2, USA300, 103) and WTA^{low} (SA113, 331865) strains (Fig. 1a).

The WTA^{high} phenotype is mediated by overexpression of the *tarH* gene. To understand the mechanisms underlying the WTA^{high} and WTA^{low} phenotypes, we quantified the expression of genes involved in WTA biosynthesis using quantitative real-time–polymerase chain reaction (qRT–PCR) of *in vitro* cultures. The WTA biosynthesis genes *tarO*, *tarA*, *tarK*, *tarL*, *tarG* and *tarH* (Supplementary Figs 2 and 3) were analysed in the logarithmic and stationary growth phases (Fig. 1 and Supplementary Figs 4 and 5). Only *tarH* transcription was significantly increased in WTA^{high} strains (MW2, USA300, 103) compared to WTA^{low} strains (SA113, 331865). This effect was only observed in the stationary growth phase (Fig. 1b) (transcriptional analyses for *tarH* in logarithmic and *tarO*, *tarA* in stationary and logarithmic growth phases are shown in Supplementary Fig. 4, and for *tarK* and *tarL* in Supplementary Fig. 5a,b, respectively). *tarH* encodes for the energizing part of the two-component ABC transporter (*TarGH*), which facilitates WTA translocation across the membrane[52,53]. Because we detected decreased tarK expression in MW2, we also analysed a potential

© 2017 Macmillan Publishers Limited, part of Springer Nature. All rights reserved.

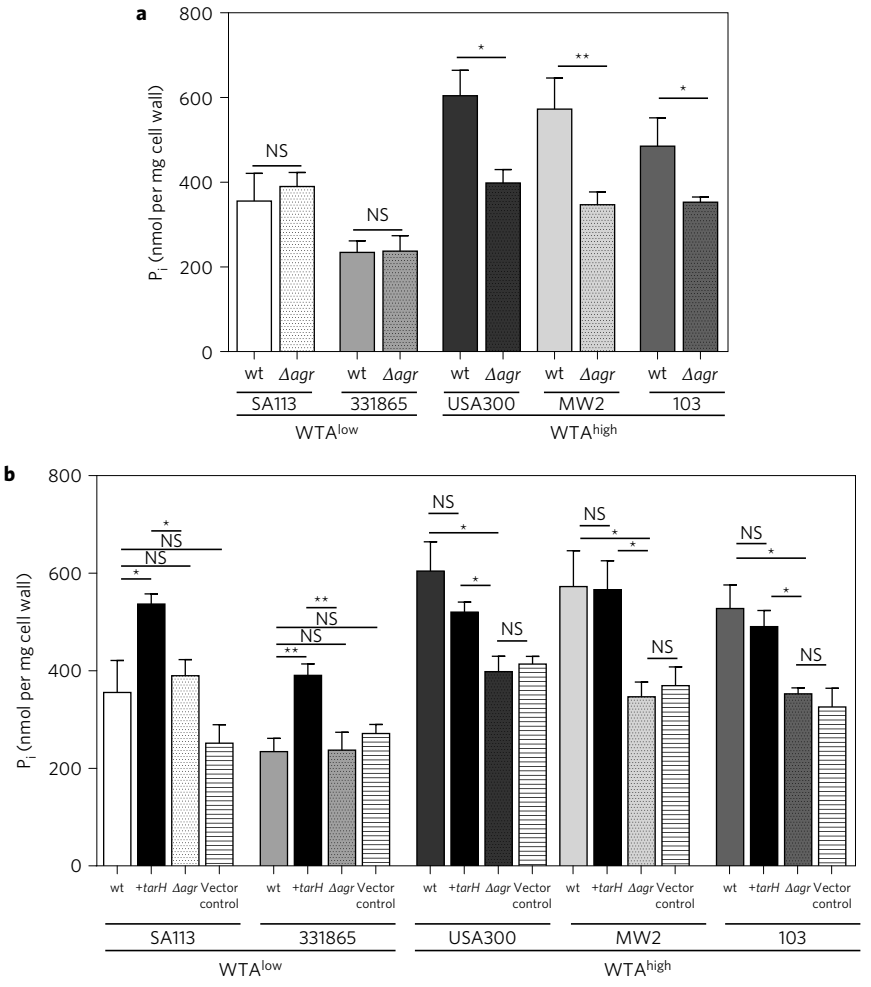

Figure 2 | Agr-dependent control of WTA content in the staphylococcal cell wall. a, Content of WTA in the cell wall of WTA^{high} (MW2, USA300, 103), WTA^{high} *Δagr* mutant (MW2*Δagr*, USA300*Δagr*, 103*Δagr*), WTA^{low} (SA113, 331865) and WTA^{low} *Δagr* mutant (SA113*Δagr*, 331865*Δagr*) strains**.** The amount of WTA per mg cell wall preparation was determined with a colorimetric assay (WTA amount is depicted as nmol inorganic phosphorus (P_i) per mg cell wall dry weight). Shown are means ± s.e.m. for $n = 8$–11 independent WTA isolations. Statistically significant differences between WTA^{high} and WTA^{low} and their respective *Δagr* mutant strains were determined by Student's *t*-test. $^*P < 0.05$, $^{**}P < 0.01$, $^{***}P < 0.001$. **b**, Content of WTA in the cell wall fractions of WTA^{high}, WTA^{high} *Δagr* mutant and WTA^{low} strains after *tarH* overexpression. Overexpression of *tarH* in expression vector pRB474 (under control of a constitutive promoter) was tested in WTA^{low} strains SA113 and 331865. Expression vector pRB474 alone was used as a negative (vector) control. The amount of WTA per mg cell wall preparation was determined with a colorimetric assay. Shown are means ± s.e.m. for $n = 8$–12 independent WTA isolations. *P* values for multiple comparisons were determined by one-way ANOVA with Tukey's post-test for each strain. $^*P < 0.05$, $^{**}P < 0.01$, $^{***}P < 0.001$.

chain length variation in the WTA polymer. However, WTA PAGE analysis (Supplementary Fig. 4a) of polymer isolated from stationary-phase cells did not reveal significant differences in polymer lengths between WTA^{high} and WTA^{low} strains.

The WTA^{high} phenotype depends on a highly active Agr regulon. The Agr system has been linked to staphylococcal pathogenesis in a subcutaneous abscess infection model[54], and is known to increase the expression of virulence factors during the transition from the late-exponential to stationary growth phase *in vitro*[55,56]. To test whether the Agr system is differentially expressed in WTA^{high} and WTA^{low} strains, we measured the expression of the primary transcript RNAIII in the stationary growth phase by qRT–PCR. All WTA^{high} strains possessed an intact Agr regulon and produced high levels of RNAIII. One of the WTA^{low} strains was a naturally occurring functional *agr*-deletion mutant (SA113), while the other produced low levels of RNAIII (Fig. 1c).

To test whether the agr system is involved in the differential regulation of the WTA biosynthesis gene *tarH*, we compared *agr*-deletion mutants (Supplementary Table 1) with their corresponding isogenic wild type (wt) by qRT–PCR. In WTA^{high} strains, *tarH* expression in *Δagr* mutants was significantly decreased compared to the WTA^{high} wt strains. In contrast, there was no difference in *tarH* expression between WTA^{low} *Δagr* mutants and their wt strains (Fig. 1d).

To validate the role of Agr in WTA biosynthesis, we quantified the WTA content of WTA^{high} and WTA^{low} strains and their *Δagr* mutants with a colorimetric assay. WTA content correlated with *tarH* expression levels and was significantly reduced in WTA^{high} *Δagr* mutants. Conversely, WTA^{low} *Δagr* mutants and WTA^{low} wt strains showed no difference in WTA content. WTA^{high} *Δagr* mutants demonstrated the same WTA content as both wt and *Δagr* mutants in the WTA^{low} strain background (Fig. 2a). This is evidence for a distinct role for the Agr system in WTA biosynthesis regulation in WTA^{high} strains. Moreover, there appears to be a correlation between loss of Agr function and the reduced expression of *tarH* in WTA^{low} strains. In line with these results, we found that an HA-MRSA strain (USA 500) that exhibited low agr-activity (Supplementary Fig. 6a) also exhibited low *tarH* expression (Supplementary Fig. 6b) and therefore a WTA^{low} phenotype (Supplementary Fig. 6c) when compared to WTA^{high} CA-MRSA strain USA300.

© 2017 Macmillan Publishers Limited, part of Springer Nature. All rights reserved.

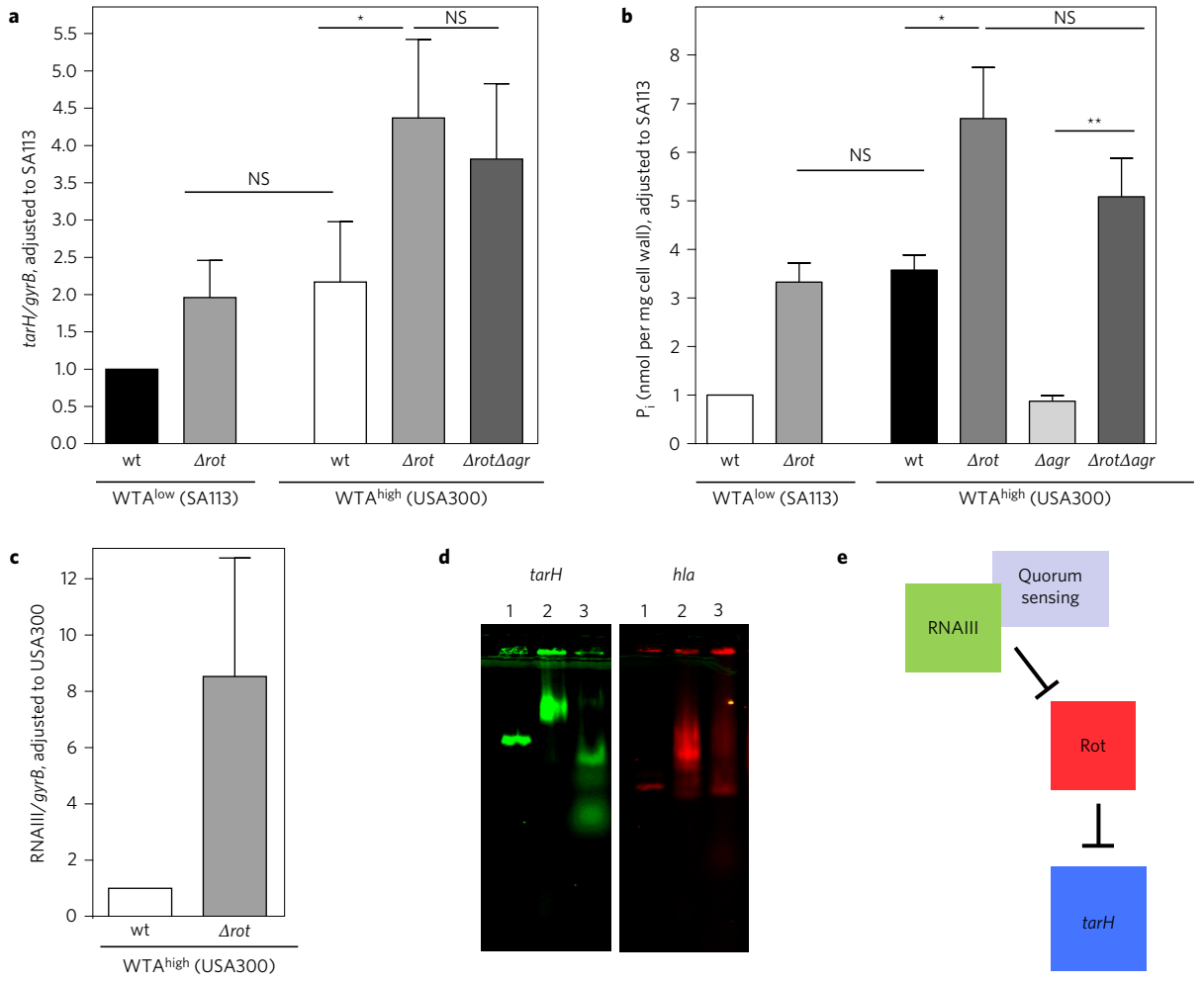

Figure 3 | Rot controls *tarH* expression and WTA biosynthesis downstream of RNAIII. a, Transcription analysis of the WTA biosynthesis gene *tarH* from *in vitro* cultures grown to stationary phase. Expression of transcripts was quantified relative to the transcription of gyrase (copies of *tarH* per copy of *gyrB*) and adjusted to SA113 (expression of SA113 in each independent experiment was set to 1). Shown are means ± s.e.m., $n = 8$ independent experiments. *P* values for multiple comparisons were determined by one-way ANOVA with Bonferroni's post-test. $^{*}P < 0.05$. **b**, Content of WTA in the cell wall of WTA^{high} (USA300), WTA^{high} *Δrot* mutant (USA300*Δrot*), WTA^{low} (SA113) and WTA^{low} *Δagr* mutant (SA113*Δagr*) strains. Amount of WTA per mg cell wall preparation was determined with a colorimetric assay (WTA amount is depicted as nmol inorganic phosphorus (P_i) per mg cell wall dry weight) and adjusted to SA113 (WTA amount of SA113 in each independent experiment was set to 1). Shown are means ± s.e.m., $n = 6$ independent experiments. *P* values for multiple comparisons were determined by one-way ANOVA with Bonferroni's post-test. $^{*}P < 0.05$, $^{**}P < 0.01$. **c**, Transcription analysis of RNAIII in WTA^{high} and WTA^{high} *Δrot S. aureus* in stationary-phase cultures. Expression of the RNAIII transcript was quantified relative to the transcription of gyrase (copies of RNAIII per copy of *gyrB*) and adjusted to wt WTA^{high}. Shown are means ± s.e.m., $n = 8$ independent experiments. **d**, LI-COR Odyssey-based gel-shift assays with cell extracts and *tarH* promoter (green). Rot binding to the promoter was visualized with cell extracts from a Rot-expressing USA300 strain lacking *agr* (lane 2) and an isogenic *rot* mutant (lane 3). Lane 1 contains the promoter fragment without cell extract as a control. The *hla* promoter (red) was used as a positive control. Rot binding to the *hla* promoter was visualized with cell extracts from a Rot-expressing USA300 strain lacking *agr* (lane 2) and an isogenic *rot* mutant (lane 3). Lane 1 contains the promoter fragment without cell extract as a control. Shown is a representative example of $n = 3$ independent experiments. **e**, The *tarH* regulatory cascade; *tarH* is under negative control of a repressor termed 'repressor of toxins' (Rot). Rot mRNA stability is controlled by RNAIII and at high RNAIII levels Rot-mediated repression is relaxed.

Transcriptional control of *tarH* by the repressor of toxins, a major downstream regulator of the Agr system. The repressor of toxins (Rot) is a major effector downstream of *agr*[56] and acts as a transcriptional regulator of an array of genes. Rot mRNA stability is negatively affected by RNAIII and therefore RNAIII mediates derepression of Rot-regulated genes[57]. When we measured *tarH* expression in WTA^{high} and WTA^{low} wt and *rot* mutants, we found a significant impact of *rot* on t*arH* expression (Fig. 3a). In fact, a WTA^{low} rot mutant exhibited the same *tarH* expression level as a WTA^{high} wt. In addition, the *rot* mutation alleviated the strong decrease of *tarH* expression found in an *agr* mutant (see Fig. 2). In fact, the *rot agr* double mutant exhibited similarly elevated levels of *tarH* expression as a *rot* mutant alone. When we measured the amounts of WTA in the cell walls of WTA^{high} and WTA^{low} wt and *rot* mutants (Fig. 3b), we found that WTA amounts correlated with a *rot*-dependent *tarH* expression pattern. A WTA^{low} *rot* mutant exhibited an elevated amount of WTA that was comparable to the WTA amount detected in a WTA^{high} wt. The *rot* mutation increased the WTA amounts in the WTA^{high} background even further, and in a *rot agr* double mutant the *agr* mutation phenotype was completely alleviated. Interestingly, when we measured RNAIII levels in the WTA^{high} background in the wt and *rot* mutant we found that the absence of *rot* severely increased the levels of RNAIII (Fig. 3c). This indicates a direct interplay between *rot* mRNA and RNAIII and an altered steady state for RNAIII when Rot is missing. To

© 2017 Macmillan Publishers Limited, part of Springer Nature. All rights reserved.

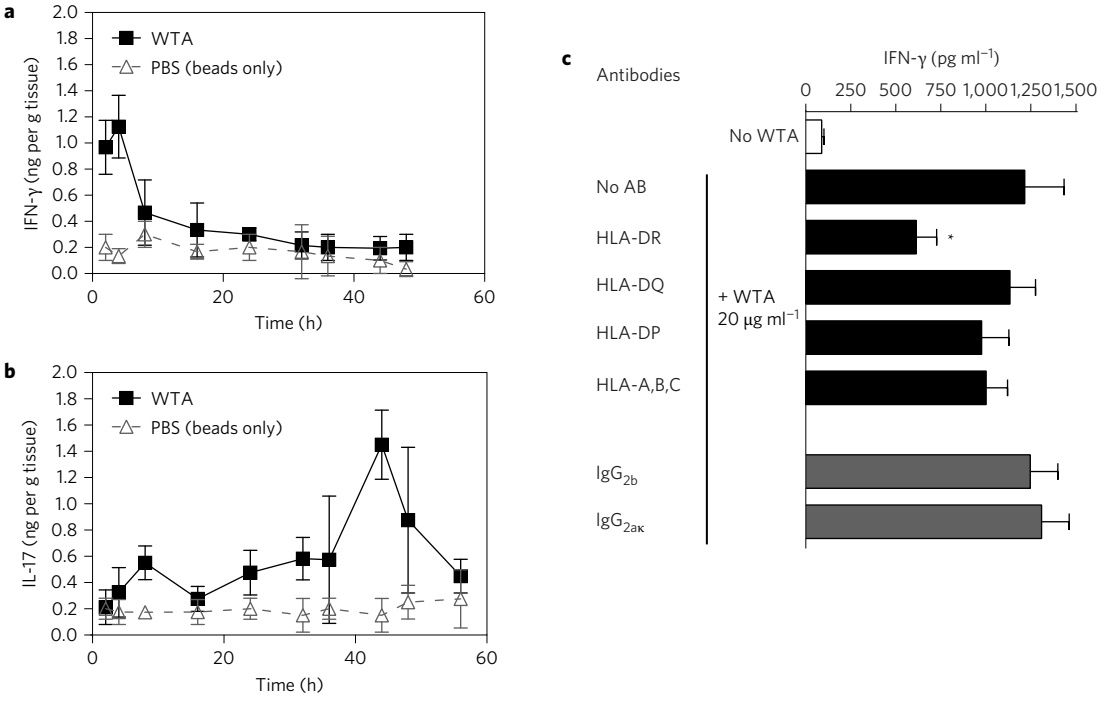

Figure 4 | MHC II-dependent cytokine secretion of WTA-stimulated T cells during skin abscess formation. a,**b**, Skin abscesses were induced by injecting 20 μg of purified wt *S. aureus* WTA mixed with cytodex beads into the flanks of mice. Abscesses were excised, and the amounts of IFN-γ per gram of abscess tissue (**a**) and IL-17 per gram of abscess tissue (**b**) were measured by ELISA; $n = 6$ (three mice per time point with two abscesses per mouse). For controls dextran beads in PBS without WTA were used. Results are expressed as means ± s.d. **c**, WTA activates human T cells to produce IFN-γ in an MHC II-dependent mechanism. Total mononuclear cells, such as APCs, were pre-incubated with blocking Abs (2 μg ml^{-1}) to the MHC II molecules HLA-DR, HLA-DP and HLA-DQ or MHC I molecules HLA-A, HLA-B and HLA-C and appropriate isotype control Abs for 1 h before the addition of CD4$^+$ T cells. Co-cultures of the APCs (1×10^5) and CD4$^+$ T cells (1×10^5) were then stimulated with 20 μg ml^{-1} WTA for 72 h. IFN-γ levels in the supernatants were then quantified by ELISA. The HLA-DR Ab significantly reduced IFN-γ production. Results are expressed as means ± s.e.m. for $n = 6$ independent experiments. *P* values for comparisons with no Ab were determined by one-way ANOVA with Dunnett's post-test. *$P < 0.05$.

demonstrate Rot binding to the *tarH* promoter region we performed gel-shift assays (Fig. 3d). Cell extracts from a Rot-expressing strain (in the USA300 *agr* mutant to ensure high Rot levels) mediated a clear shift of the promoter fragment when run in an agarose gel, while a cell extract from an isogenic strain lacking Rot was not able to mediate such a shift and the promoter fragment was partially degraded. A promoter fragment of the *hla* gene, which is Rot-repressed[59], was used and showed a similar shift.

In addition, when we measured WTA expression over time (Supplementary Fig. 7), we found that WTA amounts increased during logarithmic growth and peaked in the stationary growth phase. In line with an RNAIII and *rot*-dependent mechanism, this effect was more pronounced in a WTA^{high} wt strain when compared to a WTA^{low} strain, and the WTA^{high} phenotype only became evident at the onset of the stationary phase. Taken together, we conclude a regulatory cascade that involves high RNAIII levels, a more efficient Rot mRNA degradation and thus a more efficient Rot derepression on the *tarH* promoter level than the molecular mechanism behind the WTA^{high} phenotype (Fig. 3e).

Overexpression of *tarH* in WTA^{low} strains can restore the WTA^{high} phenotype. We hypothesized that high *tarH* expression leads to the WTA^{high} phenotype due to increased translocation of WTA molecules. We therefore tested whether the WTA^{high} phenotype could be restored in WTA^{low} strains by overexpressing the *tarH* gene in WTA^{low} strain SA113 from the plasmid vector 474 (Supplementary Fig. 8). The *tarH* gene was put under the control of a promoter encoded on plasmid pRB474 (Supplementary Table 1). Overexpression of *tarH* in the WTA^{low} (SA113 pRB474+ *tarH*) strain indeed induced the WTA^{high} phenotype (Fig. 2b). As indicated above, *tarH* gene expression in WTA^{high} *Δagr* mutants was reduced to the level of WTA^{low} strains. We therefore used the *tarH* overexpression vector in WTA^{high} *Δagr* mutants (103*Δagr* pRB474+*tarH*, MW2*Δagr* pRB474+*tarH*, USA300*Δagr* pRB474 +*tarH*) and were able to restore the WTA^{high} phenotype. In contrast, transformation with the empty plasmid pRB474 (SA113 pRB474, 331865 pRB474, 103*Δagr* pRB474, MW2*Δagr* pRB474, USA300*Δagr* pRB474) did not affect WTA levels in any *S. aureus* strain (Fig. 2b).

WTA induces interferon-γ at the onset of skin abscess formation and IL-17 at the late stages of abscess formation. We have seen before that self-clearing, non-lesion-forming subcutaneous abscesses, induced by WTA, depend on CD4$^+$ T cells[51], and we wanted to elucidate the hallmark cytokines involved in this process. Abscess formation was induced by injecting WTA mixed with cytodex beads into the flanks of mice. We measured interferon-γ (IFN-γ) and interleukin 17 (IL-17) production in the abscess by enzyme-linked immunosorbent assay (ELISA) at different time points (Fig. 4) and detected strong IFN-γ production only in the very early phases of abscess formation (Fig. 4a), while IL-17 showed only weak production at early time points (Fig. 4b) and peaked at later time points that coincided with abscess clearing.

We have seen before that mouse and human T cells are activated by WTA-presenting APCs (antigen-presenting cells) in an MHC II-dependent manner[51]. To demonstrate the MHC II dependency of the IFN-γ response after WTA-induced CD4$^+$ T cell (human T cells) activation *in vitro*, we tested whether IFN-γ production could be inhibited in the presence of blocking

© 2017 Macmillan Publishers Limited, part of Springer Nature. All rights reserved.

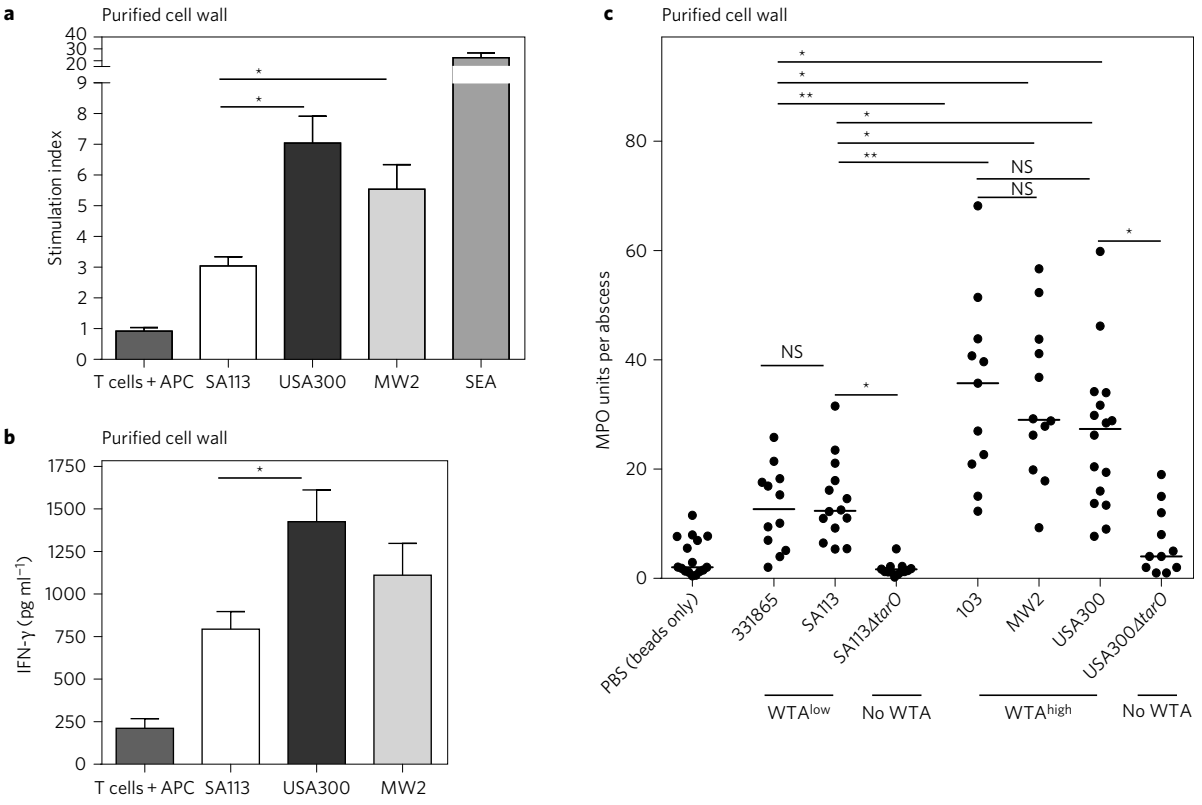

Figure 5 | Induction of T-cell-dependent IFN-γ secretion and abscess formation by cell wall fractions. a, T cell proliferation assay with highly pure, protein-free cell wall fractions. Cell wall fractions isolated from highly pathogenic CA-MRSA strains (MW2, USA300) were incubated with APCs (1×10^5) and T cells (2×10^5) for 6 days. *S. aureus* enterotoxin A (SEA) was used as a positive control (2 ng ml^{-1}). Cell wall fractions from CA-MRSA strains (MW2, USA300) induce T cell proliferation more efficiently than cell wall fractions from MSSA and the laboratory *S. aureus* strain SA113. Results are expressed as means ± s.e.m. for $n = 5$ independent experiments. *P* values for comparisons with SA113 were determined by one-way ANOVA with Dunnett's post-test. *$P < 0.05$. **b**, Measurement of T-cell-dependent IFN-γ expression. A T cell proliferation assay with cell wall fractions was performed. Cell wall fractions isolated from MW2 and USA300 (CA-MRSA) induce T-cell-dependent IFN-γ expression more efficiently than cell wall fractions from SA113 (MSSA, laboratory strain) ($n = 5$). T cells and APCs were incubated with cell wall preparations for 72 h. IFN-γ secretion was determined by ELISA. Results are expressed as the means ± s.e.m. for $n = 5$ independent experiments. *P* values for comparisons with SA113 were determined by one-way ANOVA with Dunnett's post-test. *$P < 0.05$. **c**, Abscess formation induced by cell wall fractions monitored via a myeloperoxidase (MPO) assay. Cell wall fractions from the CA-MRSA strains USA300, MW2 and the superantigen-free clinical isolate 103 induce abscesses more efficiently than cell wall fractions from laboratory strain SA113 and superantigen-free clinical isolate 331865. MPO is a marker of inflammation in abscess tissue. Twenty micrograms of cell wall were injected into the flanks of mice, and abscesses were extracted. MPO activity was measured in an enzymatic assay. Shown is a dot-blot with medians, with each dot representing a single abscess (two abscesses per mouse). *P* values for multiple comparisons were determined by one-way ANOVA with Bonferroni's post-test. *$P < 0.05$, **$P < 0.01$.

antibodies (Abs) against the MHC II molecules HLA-DR, HLA-DP and HLA-DQ or the MHC I molecules HLA-A, HLA-B and HLA-C and isotype control Abs. We were able to inhibit IFN-γ production significantly by adding an HLA-DR blocking Ab (Fig. 4c). Antibodies to HLA-DP, HLA-A, HLA-B or HLA-C and their respective isotype controls showed no effect. The experiment revealed that WTA activates human T cells to produce IFN-γ via an MHC II-dependent mechanism.

Cell wall fractions from highly pathogenic WTA^{high} strains induce T cell proliferation, IFN-γ secretion, and skin abscess formation more efficiently than cell wall fractions isolated from WTA^{low} strains. To compare the ability of highly pure, protein-free cell wall fractions isolated from the pathogenic CA-MRSA strains MW2 and USA300 and a less virulent methicillin-sensitive *Staphylococcus aureus* (MSSA) laboratory strain (SA113) to activate T cells and induce IFN-γ production, we cultured human CD4$^+$ T cells with irradiated APCs and cell wall fractions. Cell wall fractions from CA-MRSA strains MW2 and USA300 provoked stronger T cell proliferation (Fig. 5a) and induced stronger IFN-γ secretion than cell wall fractions from the laboratory strain SA113 (Fig. 5b).

We then tested the ability of purified cell wall fractions to induce abscess formation in mice. Protein-free, highly pure cell wall fractions were derived from the highly virulent CA-MRSA strains MW2, USA300, the superantigen-free clinical isolate 103, as well as the less virulent *S. aureus* strains SA113 and 331865 (superantigen-free clinical isolate), and were used in a skin abscess mouse model. Abscess-inducing activity was quantified by measuring neutrophil accumulation at the infection site with a myeloperoxidase (MPO) assay[51]. Cell wall fractions from highly virulent (WTA^{high}) *S. aureus* strains induced strong MPO activity, whereas cell wall fractions from the less virulent (WTA^{low}) *S. aureus* isolates were significantly less active (Fig. 5c). To test whether WTA amounts alone affect the induction of abscess formation, we injected different amounts of purified WTA and found that MPO activity indeed depends on the amount of WTA injected subcutaneous (s.c.) into the flanks of mice (Supplementary Fig. 9). To exclude the possibility that WTA tailoring modifications[58] (D-ala, GlcNAc) contribute to cell-wall-mediated abscess formation, we assessed the expression of the *dlt* operon, which is responsible for WTA D-alanylation[59], and the two *N*-acetylglucosaminyl-transferases (TarM and TarS), which are responsible for WTA modification with α- or β-GlcNAc,

© 2017 Macmillan Publishers Limited, part of Springer Nature. All rights reserved.

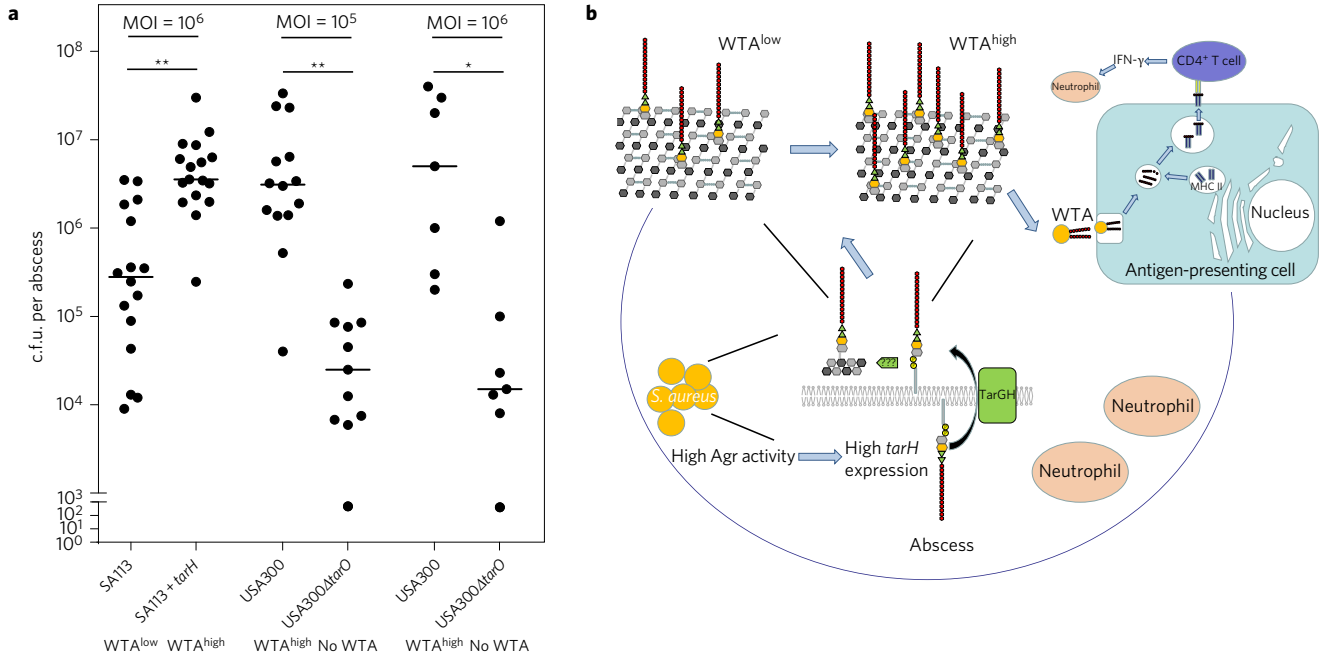

Figure 6 | Skin abscess formation with whole bacterial cells and model for WTA-mediated strain-specific virulence. a, To induce abscess formation, 10^6–10^5 colony-forming units (c.f.u.) of living bacterial cells (*S. aureus* SA113 (WTA^{low}), SA113 pRB*tarH* (*tarH* overexpression plasmid which facilitates a WTA^{high} phenotype), USA300 (WTA^{high}) and USA300Δ*tarO* (lacks all WTA)) were mixed with cytodex beads and injected s.c. into the flanks of mice. After 48 h, the mice were euthanized, and each abscess was excised, homogenized and cultured quantitatively. In the case of USA300, we found dermonecrosis at a higher multiplicity of infection (MOI of 10^6) and therefore included an MOI of 10^5 where defined abscesses can be excised. Shown is a dot-blot with medians, with each dot representing a single abscess (two abscesses per mouse). Pairwise *P* values were determined by *t*-test with Welch correction. $^*P < 0.05$, $^{**}P < 0.01$. **b**, Model for the impact of WTA on strain-specific virulence. In CA-MRSA, cell WTA incorporation into the peptidoglycan is significantly elevated. This WTA^{high} phenotype depends on the specific upregulation of *tarH* expression by the global virulence regulator Agr, which exhibits intrinsically high activity in CA-MRSA. WTA^{high} cell walls are able to stimulate T-cell-dependent IFN-γ production at the onset of abscess formation more efficiently than cell walls with lower WTA amounts. This mechanism plays an important role in modulation of early abscess development.

respectively[60] (Supplementary Figs 1 and 2). We could detect differences in the expression of the GlcNAc transferases in the tested strains (Supplementary Fig. 10). WTA^{low} strain SA113 exhibited expression of both *tarM* (Supplementary Fig. 10a) and *tarS* (Supplementary Fig. 10b) expression. Compared to SA113 and another HA-MRSA, WTA^{low} strain (USA500), the WTA^{high} strain USA300 clearly exhibited elevated levels of *tarM* mRNA (Supplementary Fig. 10a). All three strains also exhibited *tarS* expression (elevated in USA300 only). In contrast, MW2 (WTA^{high}) showed very low *tarM* mRNA levels and moderate *tarS* levels. Strains 331865 (WTA^{low}) and 103 (WTA^{high}) only expressed *tarS* in considerable amounts (Supplementary Fig. 10b), but *tarS* mRNA levels were severely decreased compared to SA113. In line with these results, USA 300 exhibited a slightly, albeit not statistically significant, increased amount of GlcNAc in its WTA when compared to SA113, while 331865 and 103 showed very low GlcNAc levels (Supplementary Fig. 11). We then assessed the impact of WTA GlcNAc modification on abscess formation. To that end, we compared cell wall fractions isolated from USA300 wt and an isogenic mutant lacking both TarM and TarS in the s.c. abscess model (Supplementary Fig 12). We could not detect a significant impact on abscess induction when both GlcNAc modifications were missing from WTA. In addition, WTA^{low} cell wall isolated from an HA-MRSA strain (USA500) exhibited a significantly lower abscess-inducing capacity when compared to USA300 cell wall. When we compared whole, live bacteria in the abscess model (Supplementary Fig. 13), we again detected no significant phenotype in the *tarM/S* mutant, while the WTA^{low} strain USA500 was clearly a less efficient abscess inducer. In addition, when we injected purified WTA together with live bacterial cells of the two WTA^{low} strains SA113 and USA500 (HA-MRSA), the colony-forming units (c.f.u.) recovered after 48 h were significantly increased and the WTA^{low} strains exhibited a phenotype that was comparable to USA300 (CA-MRSA). With respect to D-alanine modifications, we could not detect differences in the expression of the *dlt* operon (Supplementary Fig. 10c), nor in the D-alanine levels of isolated WTA (Supplementary Fig. 11), from all tested strains.

Overexpression of *tarH* in WTA^{low} strains increases the ability to induce skin abscess formation, comparable to WTA^{high} strain USA300. Finally, we compared the ability of strain SA113, with and without the *tarH* overexpression plasmid (which leads to a WTA^{high} phenotype), to induce abscess formation (Fig. 6a). When we used whole bacterial cells in the s.c. abscess model, the *tarH* plasmid-harbouring strain demonstrated an increased capacity to induce abscess formation. This was in line with the elevated abscess induction observed with USA300. To test if WTA has an impact on abscess formation in the highly pathogenic USA300 background, we used an isogenic mutant lacking all WTA molecules (USA300Δ*tarO*). This mutant exhibited a significantly reduced ability to induce abscess formation when compared to the WTA^{high} wt USA300. Furthermore, when we overexpressed *tarH* in an additional WTA^{low} strain background (HA-MRSA USA500), we could again detect an increased ability to induce s.c. abscesses in the flanks of mice (Supplementary Fig. 14).

Discussion

Here, we have demonstrated a novel role for the zwitterionic cell wall polymer WTA in *S. aureus* strain-specific virulence. Our data indicate that increased expression of the late-phase WTA biosynthesis gene *tarH* leads to a WTA^{high} phenotype in CA-MRSA,

© 2017 Macmillan Publishers Limited, part of Springer Nature. All rights reserved.

which is characterized by significantly elevated amounts of WTA in the cell wall. Surprisingly, we found that the WTA^{high} phenotype exhibited by CA-MRSA is connected to the quorum sensing system Agr. It has been reported previously that this global virulence regulator system is highly active in CA-MRSA strains[22,28,61]. Indeed, we found highly active Agr in all WTA^{high} strains, while WTA^{low} strains showed weak Agr activity or even a functionally inactive *agr* regulon. In WTA^{high} strains an excess of WTA in the cell wall is achieved by Agr-dependent over-expression of a *tarH* that encodes a possible bottleneck enzyme in WTA biosynthesis. The mature WTA polymer is exported by the TarG/H transporter and TarH constitutes the energizing ATPase unit of the ABC transporter. The coupling of *tarH* overexpression and transporter activity is currently under investigation in our laboratory. Evidence for Agr-mediated control of WTA polymer length has been reported by Meredith and colleagues[62]. However, we could not detect differences in polymer length when we compared the WTA^{high} and WTA^{low} strains analysed here. Interestingly, screening for late-stage WTA biosynthesis inhibitors in large compound libraries[45,63,64] only identified TarG inhibitors, indicating again that WTA precursor export might be the rate-limiting step in the pathway. Furthermore, we demonstrate here for the first time that Agr control of WTA biosynthesis is mediated by Rot, an important repressor of several Agr targets[65]. The Agr effector RNAIII has been demonstrated to decrease *rot* mRNA stability and efficiently reduce Rot-mediated repression[66]. A defined consensus sequence for Rot binding in promoter regions of Rot-controlled genes has not been identified[67]. However, Rot seems to exhibit high affinity to AT-rich promoter regions[67]. In fact, the *tarH* promoter region is AT-rich, arguing for Rot-dependent control of the *tarH* promoter (Supplementary Fig. 15). In whole-cell lysates (in *agr*-negative background to ensure high Rot levels) of isogenic *rot* wt and mutant we could detect binding of Rot to the *tarH* promoter region. Our analysis clearly indicates that the WTA^{high} phenotype is mediated by high RNAIII levels, which facilitate a more efficient Rot derepression in WTA^{high} strains. In line with this explanation of strain-specific differences, we found that in a WTA^{low} strain, which is a functional *agr* mutant (SA113), mutation of *rot* leads to *tarH* expression levels and WTA amounts that are comparable to WTA^{high} strains. Measuring WTA levels over time we found that the WTA amounts for WTA^{high} and WTA^{low} strains only started to differ significantly at the onset of the stationary growth phase. We conclude that in *agr* mutants or low Agr-activity isolates, Rot activity is not decreased at the onset of the stationary phase as much as in WTA^{high} isolates. In addition, we detected a strong increase in the RNAIII level when we mutated *rot* in the WTA^{high} background, indicating an altered steady state of RNAIII amounts. These results are in line with a more efficient, RNAIII-mediated, Rot derepression in WTA^{high} strains.

We have shown before that WTA is able to activate CD4$^+$ T cells in an MHC II-dependent manner, which modulates the early development of skin abscesses in a mouse model[51]. Consequently, the increased amounts of WTA render the cell wall of CA-MRSA more immunologically active. In line with these findings, abscess induction correlated with the amount of WTA incorporated in the cell wall of *S. aureus* strains. This phenotype probably depends on the ability of WTA^{high} cell wall fractions to induce CD4$^+$ T cell proliferation and IFN-γ secretion more efficiently than WTA^{low} cell walls. This is in line with a recent study reporting that WTA-specific T cells can be detected in healthy humans[68], with a sub-fraction of these WTA-specific T cells exhibiting a robust IFN-γ response. In contrast, other reports implicate IL-17-producing γδT cells and TH17-dependent responses in controlling mouse[69] or rabbit[70] cutaneous *S. aureus* infection at the innate stage. However, the authors either studied dermonecrotic lesions and not defined skin abscesses, or monitored later time points. When we injected purified WTA mixed with cytodex beads s.c. into the flanks of mice, we detected only a weak peak of IL-17 in the early phases of abscess formation. The primary IL-17 peak occurred at later time points that coincided with abscess clearing. The earliest relevant cytokine we detected in this model was IFN-γ, which peaks early, even before IL-17 could be detected. In addition, abscess induction with WTA did not lead to severe necrotic skin lesions but to a self-clearing, defined abscess. Thus, we conclude that WTA modulates the very early phases of skin abscess formation by a CD4$^+$ T cell- and IFN-γ-dependent mechanism, while IL-17-dependent mechanisms play a host-protective role at later time points and contribute to the clearing of the abscess and wound healing. Another study provided evidence for a host protective role of IL-17/TH17 responses and an anti-protective role for IFN-γ/TH1 responses in *S. aureus* skin infections[71], arguing for an active role of *S. aureus* in early abscess formation as a mechanism supporting immune evasion. High WTA amounts might permit *S. aureus* to amplify early mechanisms of abscess formation, thereby creating a microenvironment that protects bacteria from host responses. In line with this idea, overexpression of *tar*H in a WTA^{low} strain (SA113), which turned the strain into a WTA^{high} strain, led to increased abscess-inducing activity (Fig. 6a). More strikingly, we could increase abscess formation and c.f.u.s in the abscess by injecting purified WTA together with the bacterial inoculums of WTA^{low} strains USA500 and SA113 (Supplementary Fig. 13). USA500 is a strong toxin producer, and the fact that purified WTA alone allows USA500 to reach higher c.f.u.s in the abscess clearly underlines that WTA and toxins play different roles in the process of abscess formation. We also tested the impact of important WTA tailoring modifications D-alanine and GlcNAc and could not detect differences in D-alanylation between the WTA^{high} and WTA^{low} strains. The GlcNAc tailoring modification was slightly increased in USA300; however, when we compared the wt to an isogenic *tarM/S* mutant that lacks all GlcNAc modifications, we could not detect a significant phenotype in the s.c. mouse model of abscess formation.

Taken together, we conclude that overexpression of WTA biosynthesis is a mechanism that certain CA-MRSAs exploit to gain virulence (Fig. 6b). Recent advances in the development of antimicrobial substances led to the conclusion that WTA is an ideal target for novel anti-infective strategies[42] and antibiotics[43,44], and we believe that our report will aid in the development of novel anti-staphylococcal strategies that can be especially helpful in combating highly virulent CA-MRSA.

Methods

Bacterial strains and growth conditions. The bacterial strains, plasmids and oligonucleotides used in this study are described in Supplementary Table 1. *S. aureus* strains were cultivated in B-Medium (for cell wall or WTA isolation and infection experiments) or in TSB (tryptic soy broth) medium (Difco Laboratories) and incubated at 37 °C with shaking. Resistant *S. aureus* were cultivated in media supplemented with appropriate antibiotics (tetracycline (5 μg ml^{-1}) or chloramphenicol (10 μg ml^{-1})). All strains were kept on blood agar plates to monitor toxin *agr* activity and toxin production.

Construction of *agr* deletion mutants. For deletion of *agr* (Supplementary Table 1), bacteriophage Φ11 containing *agr::tet(M)* was propagated in strain RN4220. Using standard methods, Φ11 was used to transduce *agr::tet(M)* from RN6911 (ref. 32) to different target strains. In this construct, the entire *agr* locus, including *agrDBCA* and RNAIII, has been deleted[32]. The deletion of *agr* was confirmed by PCR and transcription analysis (primer *rnaIIIfor* and *rnaIIIrev*).

Construction of a recombinant expression vector (pRB474) for *tarH* with Gibson cloning. The open reading frame of *tarH* was amplified and cloned into expression vector pRB474 using a modified Gibson cloning protocol[72]. Wild-type *tarH* gene was amplified by PCR (primers gib_pRB474_*tarH*_for and gib_pRB474_*tarH*_rev) from the genomic DNA of the corresponding strains. Oligonucleotide sequences are provided in Supplementary Table 1. Vector pRB474 was amplified by PCR with primers gib_pRB474_f and gib_pRB474_r to generate *tarH* insert overhangs. Vector and insert PCR products were digested for 1 h at 37 °C with 10 U of DpnI. Each of

© 2017 Macmillan Publishers Limited, part of Springer Nature. All rights reserved.

the DpnI-digested DNA samples (1 µl) was added to 15 µl of the Gibson master mix and incubated for 45 min at 50 °C. Gibson reaction mix (pRB474+*tarH*, 5 µl) was used to transform 50 µl of chemo-competent *Escherichia coli* DC10B or DH5α cells.

PAGE analysis of WTA. For PAGE analysis of WTA samples, a 26% and 0.75-mm-thick resolving gel was cast, as described recently[62]. WTA samples (100 nmol of phosphate per lane) were loaded onto gels and resolved for 24 h using a constant current of 40 mA per gel. WTA bands were visualized using the Alcian blue silver staining method. Briefly, the gels were fixed and stained with 0.005% (wt/vol) Alcian blue in EAW solution (40% ethanol and 5% acetic acid in water) at room temperature for several hours until the WTA ladder became visible. To intensify the staining pattern, the Bio-Rad silver stain kit (Bio-Rad) was used according to the manufacturer's instructions after oxidation of the gels with 0.7% $NaIO_4$ for 20 min.

Cell wall and WTA isolation and polymer analysis. Cell wall and WTA were isolated as described previously[38]. The instruments and devices used in the isolation process were depyrogenated by heat inactivation for 4 h at 240 °C. Bacteria were grown overnight in B-medium, supplemented with 0.2% glucose. WTA and cell wall extraction for immunological assays and *in vivo* experiments were performed on a large scale with a Euler cell mill (Euler) and a mini scale for WTA quantification with a FastPrep-24 Instrument (MP Biomedicals). Cell lysates were incubated overnight with DNase I (40 units ml^{-1}, Roche) and RNase A (80 units ml^{-1}, Sigma) at 37 °C and 200 r.p.m. followed by a proteinaseK digest (80 units per g cell wall, Applichem). Cell wall and WTA were dialysed against pyrogen-free water (Ambion). WTA amounts were quantified by determining the inorganic phosphate (P_i) content, as described previously[38,58].

D-Alanylation and GlcNAc amounts for the WTA polymers were quantified as described previously[73,74].

Purified, pyrogen-free cell wall and WTA for immunological assays and *in vivo* experiments were analysed for endotoxin with the Limulus amoebocyte lysate test (Charles River Laboratories), for protein via ultraviolet absorbance at 280 nm, for SDS–PAGE electrophoresis with silver stain, and for nucleic acids by agarose gel electrophoresis or a PicoGreen assay.

Gel shift assays with *tarH* promoter. Whole-cell protein extracts were prepared from over night cultures in TSB. Cells were washed in tris-EDTA buffer and lysed in a buffer containing 10 mM Tris, 1 mM EDTA, 50 mM KCl, 5 mM $MgCl_2$, 10% glycerol, pH 7.4, as described in ref. 57, supplemented with dithiothreitol (1 mM) and 1× complete proteinase inhibitor cocktail (Sigma). Protein extracts from isogenic strains with and without *rot* (all in *agr*-negative background to allow high Rot protein levels; USA300*Δagr* and USA300*ΔagrΔrot*) were mixed with infrared-dye labelled promoter probes (PCR amplification with labelled primers (DY-701 for *hla* and DY-781 for *rot*) purchased from Biomers GmbH, Supplementary Table 1) for *tarH* and *hla* (positive control) and incubated for 20 min at room temperature. The probes were 355 bp (*tar*H) and 299 bp (*hla*). Samples were directly run on a 3% agarose gel and imaged on a LI-COR Odyssey system with settings for 700 nm emission (*hla* promoter) and 800 nm (*rot* promoter).

Mouse model of subcutaneous abscess formation. Male Swiss Webster ND4 mice (4–6 weeks old) were obtained from Harlan. In the subcutaneous abscess model, 20 µg/100 µl purified cell wall WTA or live whole bacterial cells (as indicated in the figure legends) were mixed with equal volumes of sterile dextran beads (Cytodex 1, Sigma), and the mixture (0.2 ml) was injected into each flank of the mouse as described previously[75]. For controls, equal volumes of PBS were mixed with dextran beads. After 48 h, mice were euthanized, and the abscesses were excised and homogenized in 1 ml PBS (Gibco by Life Technologies) for c.f.u. determination or in 500 µl extraction buffer[76] for MPO measurement or cytokine determination. MPO is present in the azurophilic granules of neutrophils and is routinely used to assess inflammatory responses in tissues[77] as well as abscess formation. Measurements of single cytokines were performed, for example with mouse IL-17 and IFN-γ Quantikine ELISA Kits (R&D Biosystems). MPO activity was determined with a colorimetric assay[76] and was used as a quantitative measure of neutrophil infiltration. For assays where we injected purified WTA we screened for the production of a number of different cytokines by ELISA (R&D Systems Quantikine) at early (2 h) and late phases (48 h) at 20 µg per abscess (Supplementary Fig. 16a). While large amounts of IFN-γ were measurable very early, IL-17 production was primarily observed at later stages of abscess formation. We then elucidated the production of IFN-γ and IL-17 over time and in more detail. For c.f.u. counts, MPO measurements und cytokine assays, each abscess was treated as an independent *n*, as described previously (two abscesses per mouse).

T cell activation and IFN-γ cytokine production assay. Mononuclear cells were purified by density gradient centrifugation in Polymorphoprep (Axis-Shield) from blood drawn from different healthy human donors. $CD4^+$ T cells were purified with $CD4^+$ MACS enrichment columns (Milteny). Then, 2×10^5 T cells per ml were co-cultured with 1×10^5 irradiated APCs per ml and purified *S. aureus* cell wall (50 µg ml^{-1}), which was the optimal amount, as determined from titration experiments (Supplementary Fig. 16b). *S. aureus* enterotoxin A (SEA) (2 ng ml^{-1}) was used as a positive control, and T cells co-cultured with APCs alone were used as negative controls. Proliferation was assayed with a carboxyfluorescein succinimidyl ester dilution assay by fluorescence-activated cell scanning. The T cell stimulation index was calculated by normalizing to wells with APCs and T cells but no stimulating antigen. After stimulation, supernatants were collected by centrifugation (300*g*, 10 min, 4 °C) and stored at −80 °C until IFN-γ was assayed by ELISA (R&D Biosystems) according to the manufacturer`s instructions. Blocking antibodies were used in some experiments to evaluate the impact of HLA on WTA-dependent IFN-γ production. The antibodies used were HLA-DR clone L243 (Abcam), HLA-DQ clone SPV-L3 (Abcam), HLA-DP clone 1E3 Abnova, HLA-A,B,C clone W6/32 (Biolegend) and the isotype controls IgG2b clone 20116 (R&D Systems) and IgG2a clone ICIGG2A (Abcam).

RNA isolation *in vitro* and qRT–PCR. For RNA isolation, bacteria were grown overnight in TSB medium to the stationary growth phase (optical density at 600 nm (OD_{600}) of 10–14), and 1 ml was collected by centrifugation for 3 min at 10,000 r.p.m. and 4 °C. Bacteria were mechanically disrupted in 1 ml TRIzol reagent (Invitrogen/Life Technologies) with 0.5 ml zirconia-silica beads (diameter of 0.1 mm, Carl-Roth) in a high-speed homogenizer (FastPrep-24 Instrument, MP Biomedicals). RNA was further isolated as described in the manual provided by the manufacturer. Primers (obtained from Metabion) used for qRT–PCR are shown in Supplementary Table 1 and were designed using Primer3web (http://bioinfo.ut.ee/primer3). qRT–PCR was carried out using Brilliant II SYBR Green 1-Step Master Mix (Agilent). Relative quantifications were performed with a LightCycler480II instrument (Roche).

The transcriptional levels of target genes (*tarO/A/K/L/G/H/M/S*, *dlt operon*, *rot*, RNAIII) were normalized against the expression of *gyr*B as an internal control and in some assays normalized to expression in WTA^{low} strain SA113.

Ethics statement. Animal experiments were performed in strict accordance with the German regulations of the Society for Laboratory Animal Science (GV-SOLAS) and the European Health Law of the Federation of Laboratory Animal Science Associations (FELASA). The protocol was approved by the Regierungspräsidium Tübingen (permit no. H2/10). Human blood was collected from healthy volunteers who gave written informed consent for venipuncture in accordance with protocols approved by the University of Tübingen, Germany.

Statistical analysis. Statistical analyses were performed with Graphpad Prism (GraphPad Software, version 5.04) using appropriate statistical methods as indicated in the figure legends. *P* values ≤0.05 were considered significant. For all experiments *n* refers to the number of independent experiments (except for animal studies, where *n* refers to a single abscess, as described previously[51]). In all experiments, two technical replicates were used unless noted otherwise. For animal studies we used SPSS Sample Power V.3 or G-Power 3.1 to estimate the group size required for statistical significance. Power calculations were performed without assumption of a normal distribution and we used Wilcoxon–Mann–Whitney to evaluate the sample size for a first-degree error of 0.05 and a second degree error of 0.2. We did not fully blind or randomize animal experiments.

Data availability. The data that support the findings are available from the corresponding author upon request.

Received 25 April 2016; accepted 28 November 2016; published 23 January 2017; corrected 13 March 2017

References

1. DeLeo, F. R., Otto, M., Kreiswirth, B. N. & Chambers, H. F. Community-associated meticillin-resistant *Staphylococcus aureus*. *Lancet* **375,** 1557–1568 (2010).
2. Stryjewski, M. E. & Chambers, H. F. Skin and soft-tissue infections caused by community-acquired methicillin-resistant *Staphylococcus aureus*. *Clin. Infect. Dis.* **46(Suppl. 5),** S368–S377 (2008).
3. Fridkin, S. K. *et al.* Methicillin-resistant *Staphylococcus aureus* disease in three communities. *N. Engl. J. Med.* **352,** 1436–1444 (2005).
4. Purcell, K. & Fergie, J. Epidemic of community-acquired methicillin-resistant *Staphylococcus aureus* infections: a 14-year study at Driscoll Children's Hospital. *Arch. Pediatr. Adolesc. Med.* **159,** 980–985 (2005).
5. Hulten, K. G. *et al.* Three-year surveillance of community onset health care-associated *Staphylococcus aureus* infections in children. *Pediatr. Infect. Dis. J.* **25,** 349–353 (2006).
6. Liu, C. *et al.* A population-based study of the incidence and molecular epidemiology of methicillin-resistant *Staphylococcus aureus* disease in San Francisco, 2004–2005. *Clin. Infect. Dis.* **46,** 1637–1646 (2008).
7. Mediavilla, J. R., Chen, L., Mathema, B. & Kreiswirth, B. N. Global epidemiology of community-associated methicillin resistant *Staphylococcus aureus* (CA-MRSA). *Curr. Opin. Microbiol.* **15,** 588–595 (2012).
8. Macal, C. M. *et al.* Modeling the transmission of community-associated methicillin-resistant *Staphylococcus aureus*: a dynamic agent-based simulation. *J. Transl. Med.* **12,** 124 (2014).

© 2017 Macmillan Publishers Limited, part of Springer Nature. All rights reserved.

9. Moran, G. J. *et al.* Methicillin-resistant *S. aureus* infections among patients in the emergency department. *N. Engl. J. Med.* **355,** 666–674 (2006).
10. Baker, P., Cohen, B., Liu, J. & Larson, E. Incidence and risk factors for community-associated methicillin-resistant *Staphylococcus aureus* in New York City, 2006–2012. *Epidemiol. Infect.* **144,** 1014–1017 (2016).
11. Como-Sabetti, K. *et al.* Community-associated methicillin-resistant *Staphylococcus aureus*: trends in case and isolate characteristics from six years of prospective surveillance. *Public Health Rep.* **124,** 427–435 (2009).
12. Foster, T. J. Immune evasion by staphylococci. *Nat. Rev. Microbiol.* **3,** 948–958 (2005).
13. Rooijakkers, S. H., van Kessel, K. P. & van Strijp, J. A. Staphylococcal innate immune evasion. *Trends Microbiol.* **13,** 596–601 (2005).
14. Otto, M. Basis of virulence in community-associated methicillin-resistant *Staphylococcus aureus*. *Annu. Rev. Microbiol.* **64,** 143–162 (2010).
15. Voyich, J. M. *et al.* Insights into mechanisms used by *Staphylococcus aureus* to avoid destruction by human neutrophils. *J. Immunol.* **175,** 3907–3919 (2005).
16. Moran, G. J., Amii, R. N., Abrahamian, F. M. & Talan, D. A. Methicillin-resistant *Staphylococcus aureus* in community-acquired skin infections. *Emerg. Infect. Dis.* **11,** 928–930 (2005).
17. King, M. D. *et al.* Emergence of community-acquired methicillin-resistant *Staphylococcus aureus* USA 300 clone as the predominant cause of skin and soft-tissue infections. *Ann. Intern. Med.* **144,** 309–317 (2006).
18. Melles, D. C. *et al.* Panton–Valentine leukocidin genes in *Staphylococcus aureus*. *Emerg. Infect. Dis.* **12,** 1174–1175 (2006).
19. Voyich, J. M. *et al.* Is Panton–Valentine leukocidin the major virulence determinant in community-associated methicillin-resistant *Staphylococcus aureus* disease? *J. Infect. Dis.* **194,** 1761–1770 (2006).
20. Bubeck Wardenburg, J., Bae, T., Otto, M., Deleo, F. R. & Schneewind, O. Poring over pores: α-hemolysin and Panton–Valentine leukocidin in *Staphylococcus aureus* pneumonia. *Nat. Med.* **13,** 1405–1406 (2007).
21. Bubeck Wardenburg, J., Palazzolo-Ballance, A. M., Otto, M., Schneewind, O. & DeLeo, F. R. Panton–Valentine leukocidin is not a virulence determinant in murine models of community-associated methicillin-resistant *Staphylococcus aureus* disease. *J. Infect. Dis.* **198,** 1166–1170 (2008).
22. Otto, M. Community-associated MRSA: what makes them special? *Int. J. Med. Microbiol.* **303,** 324–330 (2013).
23. Wang, R. *et al.* Identification of novel cytolytic peptides as key virulence determinants for community-associated MRSA. *Nat. Med.* **13,** 1510–1514 (2007).
24. Kobayashi, S. D. *et al.* Comparative analysis of USA300 virulence determinants in a rabbit model of skin and soft tissue infection. *J. Infect. Dis.* **204,** 937–941 (2011).
25. Berube, B. J., Sampedro, G. R., Otto, M. & Bubeck Wardenburg, J. The *psmα* locus regulates production of *Staphylococcus aureus* alpha-toxin during infection. *Infect Immun.* **82,** 3350–3358 (2014).
26. Hanberger, H. *et al.* Increased mortality associated with methicillin-resistant *Staphylococcus aureus* (MRSA) infection in the intensive care unit: results from the EPIC II study. *Int. J. Antimicrob. Agents* **38,** 331–335 (2011).
27. Inoshima, I. *et al.* A *Staphylococcus aureus* pore-forming toxin subverts the activity of ADAM10 to cause lethal infection in mice. *Nat. Med.* **17,** 1310–1314 (2011).
28. Cheung, G. Y., Wang, R., Khan, B. A., Sturdevant, D. E. & Otto, M. Role of the accessory gene regulator agr in community-associated methicillin-resistant *Staphylococcus aureus* pathogenesis. *Infect. Immun.* **79,** 1927–1935 (2011).
29. Queck, S. Y. *et al.* RNAIII-independent target gene control by the *agr* quorum-sensing system: insight into the evolution of virulence regulation in *Staphylococcus aureus*. *Mol. Cell* **32,** 150–158 (2008).
30. Li, M. *et al.* Evolution of virulence in epidemic community-associated methicillin-resistant *Staphylococcus aureus*. *Proc. Natl Acad. Sci. USA* **106,** 5883–5888 (2009).
31. Novick, R. P. & Geisinger, E. Quorum sensing in staphylococci. *Annu. Rev. Genet.* **42,** 541–564 (2008).
32. Novick, R. P. *et al.* Synthesis of staphylococcal virulence factors is controlled by a regulatory RNA molecule. *EMBO J.* **12,** 3967–3975 (1993).
33. Bronesky, D. *et al. Staphylococcus aureus* RNAIII and its regulon link quorum sensing, stress responses, metabolic adaptation, and regulation of virulence gene expression. *Annu. Rev. Microbiol.* **70,** 299–316 (2016).
34. Miller, L. G. *et al.* Clinical and epidemiologic characteristics cannot distinguish community-associated methicillin-resistant *Staphylococcus aureus* infection from methicillin-susceptible *S. aureus* infection: a prospective investigation. *Clin. Infect. Dis.* **44,** 471–482 (2007).
35. Diep, B. A. *et al.* Complete genome sequence of USA300, an epidemic clone of community-acquired meticillin-resistant *Staphylococcus aureus*. *Lancet* **367,** 731–739 (2006).
36. Thurlow, L. R. *et al.* Functional modularity of the arginine catabolic mobile element contributes to the success of USA300 methicillin-resistant *Staphylococcus aureus*. *Cell Host Microbe* **13,** 100–107 (2013).
37. Weidenmaier, C. & Peschel, A. Teichoic acids and related cell-wall glycopolymers in Gram-positive physiology and host interactions. *Nat. Rev. Microbiol.* **6,** 276–287 (2008).
38. Weidenmaier, C. *et al.* Role of teichoic acids in *Staphylococcus aureus* nasal colonization, a major risk factor in nosocomial infections. *Nat. Med.* **10,** 243–245 (2004).
39. Baur, S. *et al.* A nasal epithelial receptor for *Staphylococcus aureus* WTA governs adhesion to epithelial cells and modulates nasal colonization. *PLoS Pathog.* **10,** e1004089 (2014).
40. Weidenmaier, C. *et al.* DltABCD- and MprF-mediated cell envelope modifications of *Staphylococcus aureus* confer resistance to platelet microbicidal proteins and contribute to virulence in a rabbit endocarditis model. *Infect. Immun.* **73,** 8033–8038 (2005).
41. Weidenmaier, C. *et al.* Lack of wall teichoic acids in *Staphylococcus aureus* leads to reduced interactions with endothelial cells and to attenuated virulence in a rabbit model of endocarditis. *J. Infect. Dis.* **191,** 1771–1777 (2005).
42. Lehar, S. M. *et al.* Novel antibody–antibiotic conjugate eliminates intracellular *S. aureus*. *Nature* **527,** 323–328 (2015).
43. Ling, L. L. *et al.* A new antibiotic kills pathogens without detectable resistance. *Nature* **517,** 455–459 (2015).
44. Santa Maria, J. P. Jr *et al.* Compound–gene interaction mapping reveals distinct roles for *Staphylococcus aureus* teichoic acids. *Proc. Natl Acad. Sci. USA* **111,** 12510–12515 (2014).
45. Wang, H. *et al.* Discovery of wall teichoic acid inhibitors as potential anti-MRSA β-lactam combination agents. *Chem. Biol.* **20,** 272–284 (2013).
46. Pasquina, L. W., Santa Maria, J. P. & Walker, S. Teichoic acid biosynthesis as an antibiotic target. *Curr. Opin. Microbiol.* **16,** 531–537 (2013).
47. Lee, S. H. *et al.* TarO-specific inhibitors of wall teichoic acid biosynthesis restore β-lactam efficacy against methicillin-resistant staphylococci. *Sci. Transl. Med.* **8,** 329ra332 (2016).
48. Mann, P. A. *et al.* Chemical genetic analysis and functional characterization of staphylococcal wall teichoic acid 2-epimerases reveals unconventional antibiotic drug targets. *PLoS Pathog.* **12,** e1005585 (2016).
49. Neuhaus, F. C. & Baddiley, J. A continuum of anionic charge: structures and functions of D-alanyl-teichoic acids in Gram-positive bacteria. *Microbiol. Mol. Biol. Rev.* **67,** 686–723 (2003).
50. Brown, S., Santa Maria, J. P. Jr & Walker, S. Wall teichoic acids of Gram-positive bacteria. *Annu. Rev. Microbiol.* **67,** 313–336 (2013).
51. Weidenmaier, C., McLoughlin, R. M. & Lee, J. C. The zwitterionic cell wall teichoic acid of *Staphylococcus aureus* provokes skin abscesses in mice by a novel CD4+ T-cell-dependent mechanism. *PLoS One* **5,** e13227 (2010).
52. Lazarevic, V. & Karamata, D. The *tagGH* operon of *Bacillus subtilis* 168 encodes a two-component ABC transporter involved in the metabolism of two wall teichoic acids. *Mol. Microbiol.* **16,** 345–355 (1995).
53. Schirner, K., Stone, L. K. & Walker, S. ABC transporters required for export of wall teichoic acids do not discriminate between different main chain polymers. *ACS Chem. Biol.* **6,** 407–412 (2011).
54. Bunce, C., Wheeler, L., Reed, G., Musser, J. & Barg, N. Murine model of cutaneous infection with Gram-positive cocci. *Infect. Immun.* **60,** 2636–2640 (1992).
55. Vuong, C., Gotz, F. & Otto, M. Construction and characterization of an agr deletion mutant of *Staphylococcus epidermidis*. *Infect. Immun.* **68,** 1048–1053 (2000).
56. Novick, R. P. Autoinduction and signal transduction in the regulation of staphylococcal virulence. *Mol. Microbiol.* **48,** 1429–1449 (2003).
57. Killikelly, A. *et al.* Structure-based functional characterization of repressor of toxin (Rot). A central regulator of *Staphylococcus aureus* virulence. *J. Bacteriol.* **197,** 188–200 (2015).
58. Rajagopal, M. & Walker, S. Envelope structures of Gram-positive bacteria. *Curr. Top. Microbiol. Immunol.* http://dx.doi.org.10.1007/82_2015_5021 (2016).
59. Peschel, A. *et al.* Inactivation of the *dlt* operon in *Staphylococcus aureus* confers sensitivity to defensins, protegrins, and other antimicrobial peptides. *J. Biol. Chem.* **274,** 8405–8410 (1999).
60. Winstel, V. *et al.* Wall teichoic acid glycosylation governs *Staphylococcus aureus* nasal colonization. *mBio* **6,** e00632-15 (2015).
61. Montgomery, C. P., Boyle-Vavra, S. & Daum, R. S. Importance of the global regulators *Agr* and *SaeRS* in the pathogenesis of CA-MRSA USA300 infection. *PLoS One* **5,** e15177 (2010).
62. Meredith, T. C., Swoboda, J. G. & Walker, S. Late-stage polyribitol phosphate wall teichoic acid biosynthesis in *Staphylococcus aureus*. *J. Bacteriol.* **190,** 3046–3056 (2008).
63. Lee, K., Campbell, J., Swoboda, J. G., Cuny, G. D. & Walker, S. Development of improved inhibitors of wall teichoic acid biosynthesis with potent activity against *Staphylococcus aureus*. *Bioorg. Med. Chem. Lett.* **20,** 1767–1770 (2010).
64. Swoboda, J. G. *et al.* Discovery of a small molecule that blocks wall teichoic acid biosynthesis in *Staphylococcus aureus*. *ACS Chem. Biol.* **4,** 875–883 (2009).
65. Geisinger, E., Adhikari, R. P., Jin, R., Ross, H. F. & Novick, R. P. Inhibition of *rot* translation by RNAIII, a key feature of *agr* function. *Mol. Microbiol.* **61,** 1038–1048 (2006).

© 2017 Macmillan Publishers Limited, part of Springer Nature. All rights reserved.

66. Boisset, S. *et al. Staphylococcus aureus* RNAIII coordinately represses the synthesis of virulence factors and the transcription regulator Rot by an antisense mechanism. *Genes Dev.* **21,** 1353–1366 (2007).
67. Zhu, Y. *et al.* Structure of *Rot*, a global regulator of virulence genes in *Staphylococcus aureus*. *Acta Crystallogr. D* **70,** 2467–2476 (2014).
68. Kolata, J. *et al.* The fall of a dogma? Unexpected high T cell memory response to *S. aureus* in humans. *J. Infect. Dis.* **212,** 830–838 (2015).
69. Cho, J. S. *et al.* IL-17 is essential for host defense against cutaneous *Staphylococcus aureus* infection in mice. *J. Clin. Invest.* **120,** 1762–1773 (2010).
70. Malachowa, N., Kobayashi, S. D., Sturdevant, D. E., Scott, D. P. & DeLeo, F. R. Insights into the *Staphylococcus aureus*–host interface: global changes in host and pathogen gene expression in a rabbit skin infection model. *PLoS One* **10,** e0117713 (2015).
71. Montgomery, C. P. *et al.* Protective immunity against recurrent *Staphylococcus aureus* skin infection requires antibody and interleukin-17A. *Infect. Immun.* **82,** 2125–2134 (2014).
72. Gibson, D. G. *et al.* Enzymatic assembly of DNA molecules up to several hundred kilobases. *Nat. Methods* **6,** 343–345 (2009).
73. Bertsche, U. *et al.* Increased cell wall teichoic acid production and D-alanylation are common phenotypes among daptomycin-resistant methicillin-resistant *Staphylococcus aureus* (MRSA) clinical isolates. *PLoS One* **8,** e67398 (2013).
74. Smith, R. L. & Gilkerson, E. Quantitation of glycosaminoglycan hexosamine using 3-methyl-2-benzothiazolone hydrazone hydrochloride. *Anal. Biochem.* **98,** 478–480 (1979).
75. Portoles, M., Kiser, K. B., Bhasin, N., Chan, K. H. & Lee, J. C. *Staphylococcus aureus* Cap5O has UDP-ManNAc dehydrogenase activity and is essential for capsule expression. *Infect. Immun.* **69,** 917–923 (2001).
76. Mullane, K. M., Kraemer, R. & Smith, B. Myeloperoxidase activity as a quantitative assessment of neutrophil infiltration into ischemic myocardium. *J. Pharmacol. Methods* **14,** 157–167 (1985).
77. van der Veen, B. S., de Winther, M. P. & Heeringa, P. Myeloperoxidase: molecular mechanisms of action and their relevance to human health and disease. *Antioxid. Redox Signal.* **11,** 2899–2937 (2009).

Acknowledgements

The authors thank I. Autenrieth and A. Peschel for discussions and critical reading of the manuscript. This research was supported by grants from the German Research Foundation (SFB) to C.We. (SFB766 and TR34), C.Wo. (SFB766 and TR34) and B.M.B. (TR34). The funders had no role in the design of the experiments, in the collection, analysis and interpretation of the data, in writing the manuscript, or in the decision to submit the manuscript for publication.

Author contributions

S.W., C.Wo., J.K., B.M.B., J.S. and C.We. planned the experiments. S.W., J.S., N.W., D.Ke., L.K., J.B., T.G., V.W. and C.We. performed the experiments. C.Wo., J.K., B.M.B., V.W. and D.Kr. supplied materials and strains. S.W., J.S. and C.We. wrote the manuscript. All authors read and approved the final manuscript.

Additional information

Supplementary information is available for this paper.

Reprints and permissions information is available at www.nature.com/reprints.

Correspondence and requests for materials should be addressed to C.We.

How to cite this article: Wanner, S. *et al.* Wall teichoic acids mediate increased virulence in *Staphylococcus aureus*. *Nat. Microbiol.* **2,** 16257 (2017).

Competing interests

The authors declare no competing financial interests.

© 2017 Macmillan Publishers Limited, part of Springer Nature. All rights reserved.

Corrigendum: Wall teichoic acids mediate increased virulence in *Staphylococcus aureus*

Stefanie Wanner, Jessica Schade, Daniela Keinhörster, Nicola Weller, Shilpa E. George, Larissa Kull, Jochen Bauer, Timo Grau, Volker Winstel, Henriette Stoy, Dorothee Kretschmer, Julia Kolata, Christiane Wolz, Barbara M. Bröker and Christopher Weidenmaier

Nature Microbiology **2,** 16257 (2017); published online 23 January 2017; corrected 13 March 2017

In the version of this Article originally published, the horizontal bars in Fig. 1a that indicate statistical differences were incorrectly placed. This has now been corrected in all versions of the Article, so that the horizontal bars indicate the statistical differences between strain 331865 and strains USA300, MW2 and 103.

© 2017 Macmillan Publishers Limited, part of Springer Nature. All rights reserved.

Publication 3

Inactivation of TCA cycle enhances *Staphylococcus aureus* persister cell formation in stationary phase.

Wang Y, Bojer MS, **George SE**, Wang Z, Jensen PR, Wolz C, Ingmer H

Scientific reports 2018 Jul 18;8(1):10849. doi: 10.1038/s41598-018-29123-0.

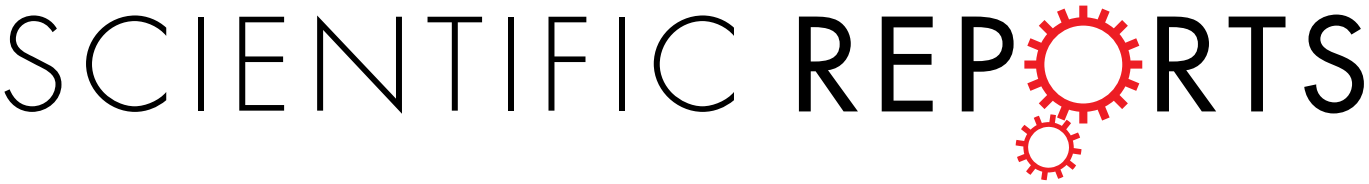

OPEN

Inactivation of TCA cycle enhances *Staphylococcus aureus* persister cell formation in stationary phase

Received: 26 October 2017
Accepted: 3 July 2018
Published online: 18 July 2018

Ying Wang[1], Martin Saxtorph Bojer[1], Shilpa Elizabeth George[2], Zhihao Wang[3], Peter Ruhdal Jensen[3], Christiane Wolz[2] & Hanne Ingmer[1]

Persister cells constitute a small subpopulation of bacteria that display remarkably high antibiotic tolerance and for pathogens such as *Staphylococcus aureus* are suspected as culprits of chronic and recurrent infections. Persisters formed during exponential growth are characterized by low ATP levels but less is known of cells in stationary phase. By enrichment from a transposon mutant library in *S. aureus* we identified mutants that in this growth phase displayed enhanced persister cell formation. We found that inactivation of either *sucA* or *sucB*, encoding the subunits of the α-ketoglutarate dehydrogenase of the tricarboxylic acid cycle (TCA cycle), increased survival to lethal concentrations of ciprofloxacin by 10–100 fold as did inactivation of other TCA cycle genes or *atpA* encoding a subunit of the F_1F_0 ATPase. In *S. aureus*, TCA cycle activity and gene expression are de-repressed in stationary phase but single cells with low expression may be prone to form persisters. While ATP levels were not consistently affected in high persister mutants they commonly displayed reduced membrane potential, and persistence was enhanced by a protein motive force inhibitor. Our results show that persister cell formation in stationary phase does not correlate with ATP levels but is associated with low membrane potential.

Persister cells are phenotypic variants present in the bacterial populations that in the absence of heritable mutations or antibiotic resistance genes display remarkable antibiotic tolerance. They are detected as survivors when exposed to very high antibiotic concentrations often reaching 100 times the minimal inhibitory concentration (MIC) and they are observed in both exponential and stationary growth phases for multiple bacterial species and with several antibiotics[1,2]. During exponential growth, persister cells (designated type II) arise at very low frequencies whereas upon entry into stationary growth phase the fraction of persister cells (type I) increases substantially[3,4]. Commonly, persister cells are considered to be in a state of dormancy and several mechanisms have been proposed to explain the phenomenon. In *Escherichia coli* and *Salmonella*, dormancy was previously proposed to be stochastically induced by the action of the toxin-antitoxin (TA) systems that compromise key cellular functions and are activated by ppGpp or by the SOS response[5–10]. However, this model was recently disproven[11,12]. In fact, conditions that halt transcription, translation or ATP synthesis dramatically increase persister frequency from 0.01% to up to 10–100%[13]. Particularly, the cellular ATP level is important as depletion of ATP with arsenate increases the number of persister cells both in *E. coli* and in the human pathogen, *Staphylococcus aureus*[4,14]. In the latter organism, neither the stringent response nor TA loci contribute to persistence but rather persister cells express stationary phase marker genes, such as the capsular polysaccharide operon, suggesting that they are cells that during exponential growth have prematurely entered stationary phase with low ATP levels[4].

Although the central role of bacterial metabolism in bacterial persistence has been documented by several reports, a uniform picture of the contribution has not emerged. In *E. coli*, fumarate accumulation and perturbations of the TCA cycle as well as the electron transport chain has been linked with increased persistence while others have found that inactivation of *sucB*, encoding α-ketoglutarate dehydrogenase and other genes of the TCA cycle reduced persister formation[15–17]. Tolerance to aminoglycosides is provided by low proton motive force (PMF) as persister cells are eradicated by conditions that enhance PMF and facilitates aminoglycoside uptake[18,19].

[1]Department of Veterinary and Animal Sciences, Faculty of Health and Medical Sciences, University of Copenhagen, Stigbøjlen 4, 1870, Frederiksberg C, Denmark. [2]Department of Medical Microbiology and Hygiene, Interfaculty Institute for Microbiology and Infection Medicine Tübingen (IMIT), University of Tübingen, Elfriede-Aulhorn-Straße 6, 72076, Tübingen, Germany. [3]National Food Institute, Technical University of Denmark, DK-2800 Kgs, Lyngby, Denmark. Correspondence and requests for materials should be addressed to H.I. (email: hi@sund.ku.dk)

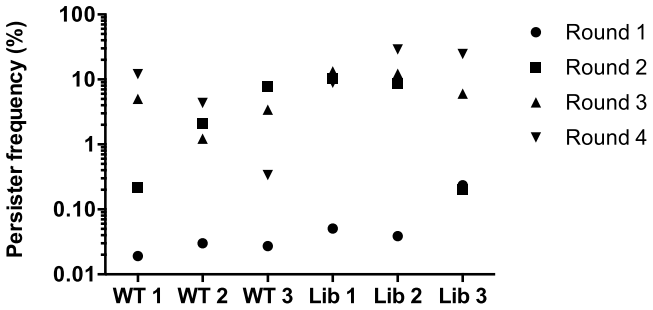

Figure 1. The enrichment of persisters with both *S. aureus* Newman wild type and transposon library. 24-hour culture of either wild type (WT 1–3) or Tnp library (Lib 1–3) was exposed to 100 × MIC of ciprofloxacin (MIC = 0.5 μg/ml) for another 24 hours before plating on TSA plates for CFU calculation. The same procedure was repeated consecutively for 4 times (Round 1–4) and the persister frequencies were recorded accordingly.

The varying contributions of metabolism to persister formation may in part be explained by different experimental setups but also by the significant differences in metabolism between organisms and growth conditions[13]. For example, in Gram-negative bacteria which are growing under laboratory conditions, such as *E. coli*, ATP is produced via oxidative phosphorylation driven by products generated in the TCA cycle while the low-passage counterpart produces ATP by substrate level phosphorylation; in the Gram-positive bacteria, *S. aureus*, the TCA cycle is repressed during exponential growth where glucose is metabolized to acetate with ATP generated by substrate level phosphorylation[20].

S. aureus is known to give rise to a diverse range of serious diseases such as endocarditis, osteomyelitis and chronic and re-occurring infections that are difficult to treat with antibiotics. The clinical relevance of persister cells has been demonstrated by infection of a chronic wound model with *S. aureus* that could be eradicated with an acyldepsipeptide antibiotic, ADEP4 that killed persister cells[21,22]. With most studies of persisters having focused on the exponential growth phase we set out to determine if the already high level of persisters observed for *S. aureus* in stationary growth phase may be increased even further and if so which genes are contributing. For this purpose, we have taken a transposon library approach to identify genes that either by inactivation or overproduction increase persister cell frequency in stationary phase[23]. During enrichment, we found that inactivation of either *sucA* or *sucB* encoding subunits of α-ketoglutarate dehydrogenase dramatically increased persister cell formation as did inactivation of other enzymes of the TCA cycle or *atpA* gene. Commonly, all the mutants with enhanced persister levels displayed reduced membrane potential that contributes to PMF indicating that in stationary phase membrane potential becomes critical for persister cell formation or survival.

Results

Inactivation of α-ketoglutarate dehydrogenase increases persister cell formation in stationary phase. With the aim of identifying genes that contribute to persister cell formation in stationary phase in *S. aureus*, we constructed a high-density transposon (Tnp) insertion library in strain Newman employing the bacteriophage-based mariner transposon delivery system that allowed both gene inactivation and gene overexpression from an outward-facing promoter in the transposon element[23,24]. The coverage of Tnp insertions were assessed in 10 random library isolates and the results revealed that the 10 isolates carrying insertions at 10 independent sites were evenly distributed throughout the genome indicating random Tnp insertion (see Supplementary Table S1).

Library clones with increased frequency of persister cells formation in stationary phase were identified by an enrichment strategy where the Tnp library cells were repeatedly exposed to the fluoroquinolone drug, ciprofloxacin at a lethal dose of 100 times MIC[25]. The survivors were collected and inoculated into fresh medium and allowed to reach stationary phase before repeated exposure to ciprofloxacin. This treatment was repeated four times in total for pooled library clones as well as for the wild type strain Newman (Fig. 1) with the starting CFU/ml indicated in Supplementary Table S2. The persister frequency of strain Newman was approximately 1% by the end of enrichment with a few samples reaching 5–10% while the percentage of persisters from the Tnp library cultures exhibited more than 1000-fold increase, from the initial 0.01% to more than 20% after the four rounds of enrichment (Fig. 1). The increase in the fraction of persisters seen for wild type cells after enrichment implies that spontaneous mutations may enhance persister formation. Genome sequencing of one randomly picked clone confirmed this notion as it carried more than 200 mutations compared to the wild type cells prior to passage (data not shown).

To determine if individual clones were enriched by repeated exposure of the Tnp library to high antibiotic concentrations, six colonies (named as L1-L6) were randomly picked by the end of the fourth round of enrichment to examine persister formation in individual clones. When treated with ciprofloxacin, all the six isolates exhibited persister frequencies between 20–60% compared to approximately 1% for the wild type (Fig. 2a). The transposon/chromosome junction was determined by sequencing and the result showed that in five of the six isolates (L2-L6) the transposon was inserted at one of three different locations within the *sucA* gene while in the last clone (L1) it was inserted in *sucB*. *sucA* and *sucB* encode subunits of α-ketoglutarate dehydrogenase, which is a key enzyme of the TCA cycle that catalyses the conversion of α-ketoglutarate to succinyl-CoA with the concomitant production of NADH and CO_2 in an irreversible reaction[26].

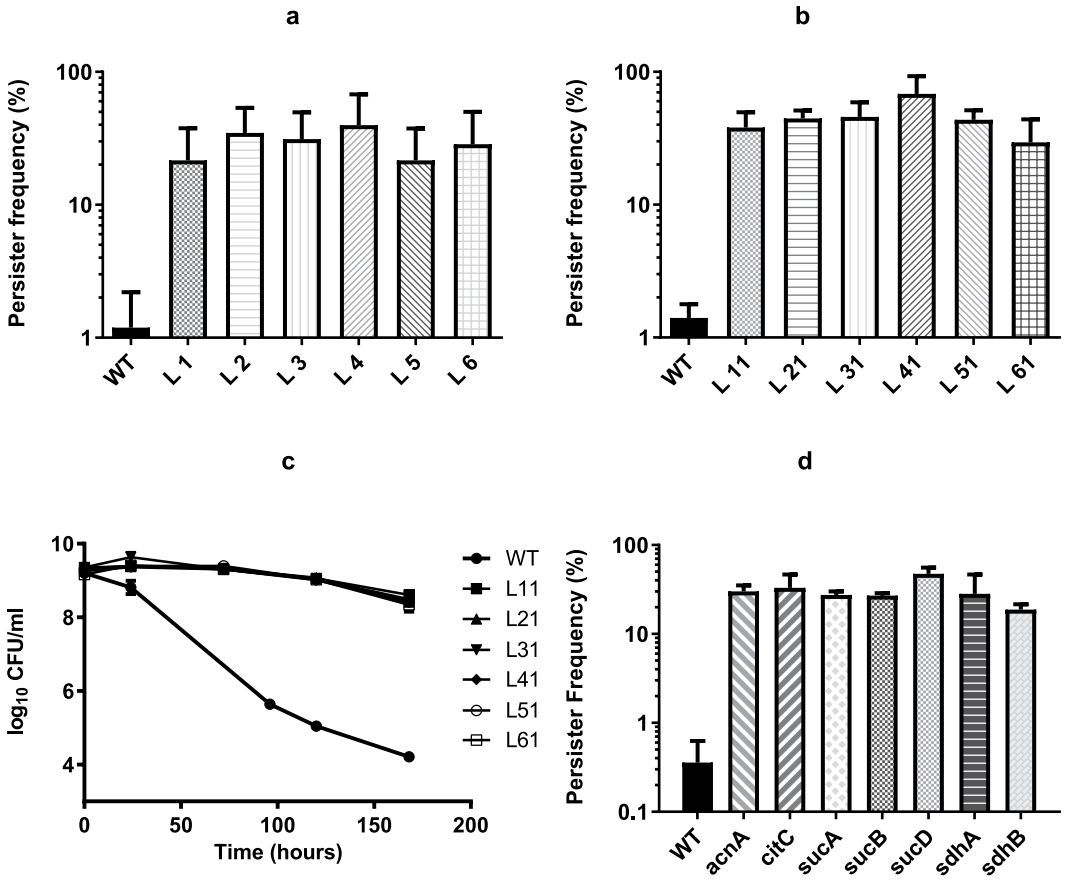

Figure 2. Persister frequency in the presence of ciprofloxacin or oxacillin. Persister frequency of 6 single colonies (L1-L6) of Tnp library (**a**) or their corresponding transductants (L11-L61) (**b**) in the presence of ciprofloxacin after persister enrichment was calculated by comparing the CFU calculation of 24-hour post and before the addition of 100 × MIC of ciprofloxacin (MIC = 0.5 µg/ml) (**c**) Survival of the transductants (L11-L61) challenged with 100 × MIC of oxacillin (MIC = 0.25 µg/ml) was recorded by CFU counting over 7 days. (**d**) Persister frequency of selected TCA cycle mutants (*acnA*, *citC*, *sucA*, *sucB*, *sucD*, *sdhA* and *sdhB*) when challenged with 100 × MIC of ciprofloxacin (MIC = 0.5 µg/ml). One wild type colony (WT) was included as control for all the experiments and starting CFU/ml are indicated in Supplementary Table S2. Three biological triplicates were included for each sample point and error bars represent standard deviation.

To rule out the possibility that secondary mutations within the library isolates contribute to the persister phenotype, the Tnp insertion mutations were transduced for all six clones to naïve wild type Newman cells to generate transductants, L11, L21-L61, carrying the individual mutations of the original library clones. All transductants yielded more than 30% persisters in comparison to 1% for the wild type when exposed to lethal concentrations of ciprofloxacin (Fig. 2b). To corroborate this finding and confirm that the enhanced persister cell formation is indeed due to inactivation of α-ketoglutarate dehydrogenase, an unmarked *sucA* deletion mutant (*ΔsucA*) was constructed. The *ΔsucA* mutant yielded more than 30% persisters when exposed to 100 times MIC of ciprofloxacin (see Supplementary Fig. S1). When the survival was followed for 48 hours after addition of ciprofloxacin, *ΔsucA* mutant exhibited improved survival compared to wild type which displayed the typical biphasic killing curve at the observed time points (see Supplementary Fig. S2). Additionally, the enhanced persister formation was also observed when the mutations were transduced into the *S. aureus* strains, SA564 and RN6607, which indicates that the current findings are not confined to strain Newman (see Supplementary Fig. S3). Further, we examined if the mutants influenced persister cell formation during exponential growth and found that in this growth phase the inactivation of *sucA* or *sucB* did not have any effect (data not shown) agreeing with the notion that in *S. aureus*, TCA cycle activity is low during exponential growth but de-repressed upon entry into stationary phase[20].

Persister cells have been observed with other antibiotics than ciprofloxacin and therefore we examined if inactivation of α-ketoglutarate dehydrogenase increased survival during treatment with lethal doses of oxacillin (Fig. 2c). Because there was no discernible differences in persister generation between wild type and library isolate transductants after a 24-hour treatment, the effect of oxacillin on bacterial survival was monitored over a 7-day period. The counting of colony forming unit (CFU/ml) showed that there was less than 1 log CFU reduction of the library isolate transductants while wild type dropped from 10^9 to 10^4 CFU/ml after the 7-day treatment with 100 × MIC of oxacillin. Furthermore, the MICs of all library transductants towards ciprofloxacin and

oxacillin were identical to that of wild type cells (see Supplementary Table S3), demonstrating that the increased persister cell formation is not a result of general changes in susceptibility to antibiotics. All together, these experiments show that inactivation of α-ketoglutarate dehydrogenase increases dramatically stationary phase persister cell formation in *S. aureus*.

Inactivation of TCA cycle genes increases persister cell formation in stationary phase. α-ketoglutarate dehydrogenase is an enzyme of the TCA cycle and to address if TCA cycle activity in general influences persister formation, we examined persister frequency of mutants obtained from a sequence-defined transposon mutant library carrying insertional inactivations of *sucD*, *sdhA*, *sdhB*, *acnA and citC*[27]. Importantly, all of these mutants exhibited increased persister frequency (20–60%) paralleling that observed for the *sucA* and *sucB* mutants, when compared with wild type cells (<1%) in stationary growth phase (Fig. 2d). While it is unclear why our enrichment strategy only identified *sucA* and *sucB* mutants and not mutants lacking other TCA cycle enzymes, it may be related to the observation that after 24-hour of cultivation, the optical density at 600 nm (OD_{600}) of *sucA* mutant cells was higher than observed for the other TCA cycle mutants (see Supplementary Fig. S4), indicating that this mutant may have a growth advantage. In summary, our results suggest that decreased TCA cycle activity increases *S. aureus* persister cell formation in stationary phase.

Increased persister cell formation is not caused by slow growth or low pH. The appearance of persister cells has been associated with arrested bacterial growth[28] but for the transductants carrying *sucA* or *sucB* inactivation we only observed slight differences in cell densities upon entry into stationary phase (see Supplementary Fig. S5). Similarly, long-term survival in stationary phase was not notably different between mutants and the wild type throughout a 7-day period (see Supplementary Fig. S5). In addition, the persister assay was repeated with bacterial cultures after 48-hour cultivation to ensure that all cells had entered stationary phase and again, the persister percentage of *sucA* mutant remained significantly higher than for wild type cells (see Supplementary Fig. S6), suggesting that any potential differences between strains in entry into stationary phase did not influence the results.

In contrast, we observed that culture supernatants of the TCA cycle mutants displayed lower pH (see Supplementary Table S4) and accumulated more acetate than wild type cells (Fig. 3a). This observation agrees with the fact that in *S. aureus*, the TCA cycle is required for post-exponential catabolism of acetate that has accumulated during exponential growth[20]. Similarly, the accumulation of acetate was also observed for all the transductants of library isolates (L11-L61) which have mutations of either *sucA* or *sucB* within TCA cycle (Fig. 3b). To examine if the enhanced persister cell formation was related to acidification of the growth medium, TSB medium without glucose was used to achieve comparable pH of supernatants from both *ΔsucA* and wild type cells in stationary phase (Fig. 4a). Importantly, in the absence of glucose where the pH of both mutant and wild type cultures was similar, the persister frequency of *ΔsucA* cells was still enhanced with 50% of the cells producing persisters while only 1% of wild type cells (Fig. 4b). These results show that low pH is not responsible for the increased persister cell formation in the TCA cycle mutants.

Membrane potential is associated with persister cell formation. Recently, it was demonstrated that *S. aureus* persisters generated during exponential growth are characterized by low ATP level[4]. However, when we assessed the ATP content we found that while the majority of the TCA cycle mutants (*sucA*, *sucB*, *sucD*, *sdhA* or *sdhB*, Fig. 5a) including the library isolate transductants (L11-L61, Fig. 5b) contained about 50% of the wild type ATP level, two mutants, namely *acnA* and *citC*, encoding aconitase and isocitrate dehydrogenase, respectively, had similar ATP levels as wild type cells (Fig. 5a) even though their ability to form persisters was remarkably higher than wild type cells (Fig. 2d). This phenomenon may be explained by the fact that some amino acids can feed into the TCA cycle at the point of α-ketoglutarate, and therefore, the inactivation of upstream enzymes, either aconitase (*acnA*) or isocitrate dehydrogenase (*citC*), may not affect the downstream metabolic activity of TCA cycle including ATP production[26].

During exponential growth ATP is generated by substrate level phosphorylation in *S. aureus*, but in stationary phase oxidative phosphorylation and the ATP synthase could contribute[20]. Therefore, we examined a mutant lacking *atpA* that encodes the α-subunit of F_1F_0 ATP synthase. As has been observed previously for other organisms we found that there was no significant reduction in ATP level of the *atpA* mutant when cultivated in rich medium (Fig. 6a) indicating that also in the post-exponential growth phase substrate level phosphorylation contributed to ATP production[29]. Strikingly, however, the inactivation of *atpA* increased persister formation approximately 1000-fold compared to wild type cells (Fig. 6b) underscoring the notion that ATP content is not decisive for *S. aureus* persister cell formation in stationary phase.

Inactivation of the TCA cycle is likely to reduce the production of reducing equivalents that enters the electron transport chain and contributes to the PMF[30]. Therefore, we speculated that membrane potential, which contributes to PMF, may be related to persister cell formation. Indeed, when monitoring membrane potential using the fluorescent probe, $DiOC_2(3)$ and flow cytometry we consistently found that all TCA cycle mutants which exhibited increased persister cell frequencies displayed reduced membrane potential (Fig. 7a). Importantly, also the membrane potential of the *atpA* mutant was decreased compared to wild type cells (Fig. 7a). This result may indicate that wild type *S. aureus* cells in the post-exponential growth phase maintains PMF by extruding protons through the F_1F_0 ATP synthase with hydrolysis of ATP. The critical role of PMF for persister cell formation was lastly confirmed by addition of the PMF inhibitor, carbonyl cyanide m-chlorophenylhydrazone (CCCP) as expected it enhanced persister cell formation (Fig. 7b)[31–33]. Collectively, our results suggest that in stationary phase, the reduced proton motive force (PMF) characterizes *S. aureus* persister cells.

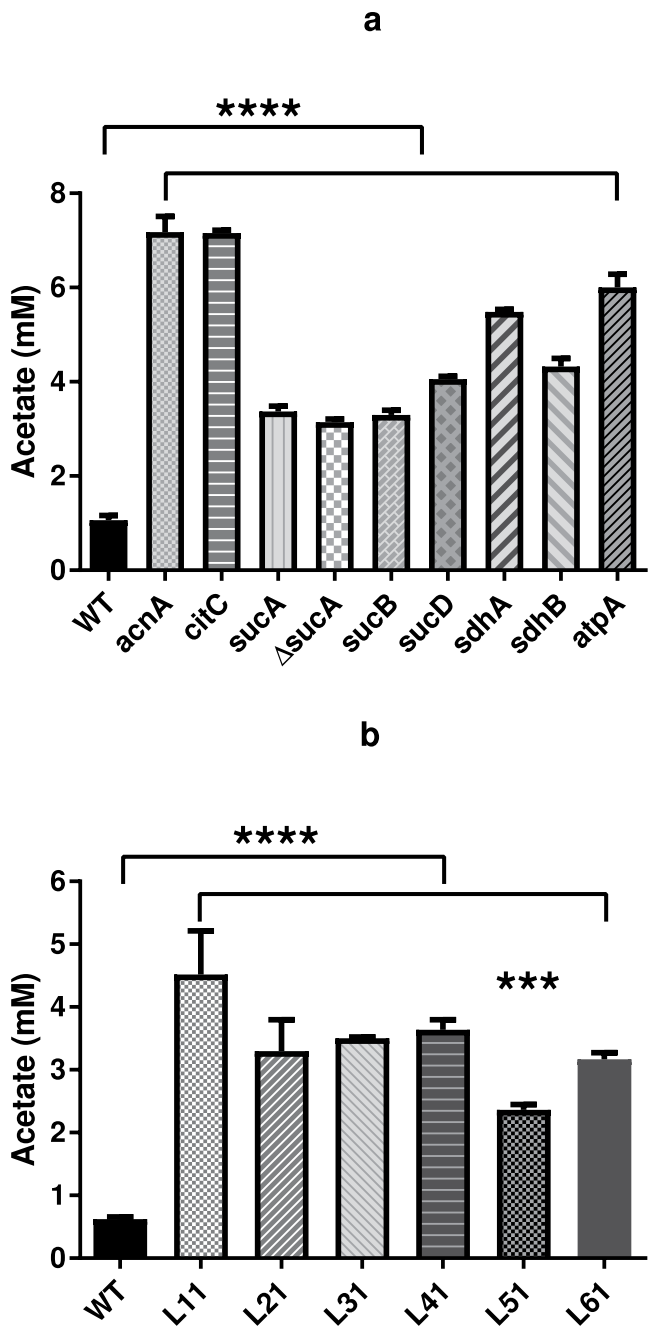

Figure 3. Acetate production by TCA cycle mutants (**a**) and transductants (L11-L61) (**b**). All strains were cultivated with TSB medium at 37 °C with shaking at 200 rpm and 1 ml of the culture was filtrated with 0.22 μm filter before the measurement with HPLC. The accumulation of acetate was calculated by comparing the concentration from early exponential phase (3-hour cultivation) and stationary phase (24-hour cultivation). There were 3 biological replicates for each sample and error bars represent standard deviation. The statistical comparison between wild type and mutants (**a**) or transductants (**b**) was determined with one way ANOVA followed by Dunnett's test. The asterisks indicate significant difference at $P < 0.05$.

***sucA* is expressed in stationary phase.** In *S. aureus* TCA cycle activity is de-repressed in stationary phase[20]. To examine if this de-repression correlates with expression of TCA cycle genes, we fused the *sucA* promoter to the *cfp* reporter gene and monitored expression in exponential and stationary phase single cells (Fig. 8). While essentially no expression was observed in exponentially growing cells, *sucA* was clearly expressed in stationary phase cells. Similar expression pattern was observed for the *cap* promoter, an established stationary phase marker that is expressed along with TCA cycle activity[34]. In addition, we observed that expression of *sucA* varied between individual cells. These results show that TCA cycle genes are expressed in stationary phase and that variation in expression of *sucA* and possibly of other TCA cycle genes occurs. Thus, we speculate that in wild

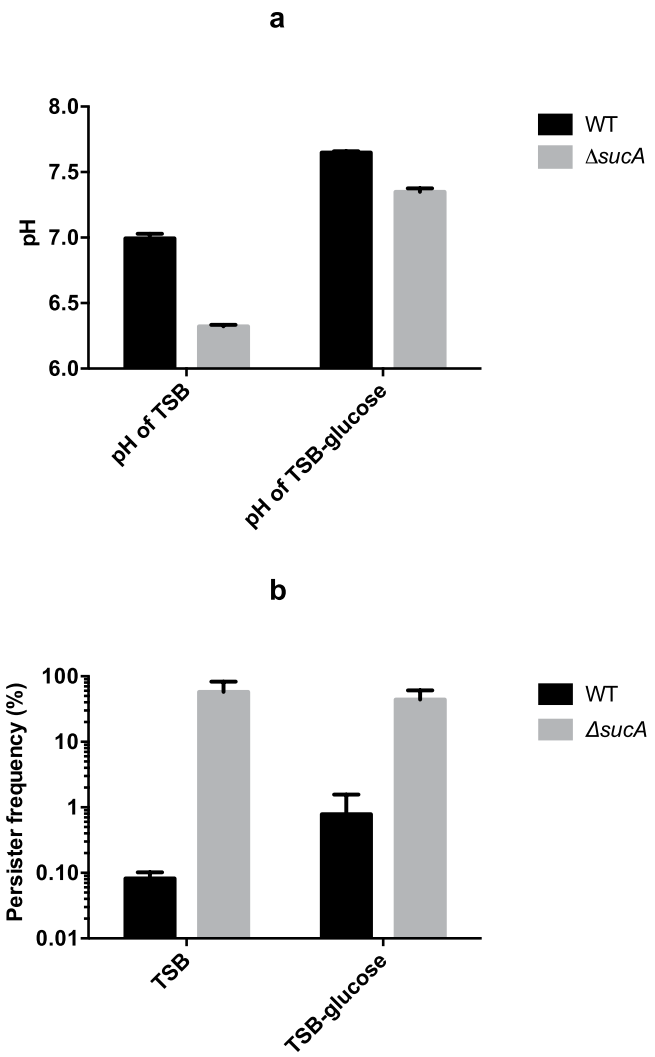

Figure 4. pH does not affect persister formation. (**a**) pH of cell-free supernatant. Wild type (WT) and *ΔsucA* were cultivated in TSB medium with or without glucose (TSB-glucose) for 24 hours and the pH of the supernatant was measured and compared; (**b**) the persister frequency of wild type (WT) and *ΔsucA* was calculated when cultivated with TSB medium or TSB medium without glucose (TSB-glucose). There were 3 biological replicates for each sample and error bars stand for standard deviation. Starting CFU/ml are indicated in Supplementary Table S2.

type cells, cell to cell variation in expression of TCA cycle genes in stationary phase determines persister cell formation.

Discussion

When searching for mutants that in stationary phase gave increased persister frequencies we identified insertion mutants of *sucA* and *sucB*, which encode the subunits of the α-ketoglutarate dehydrogenase, a key enzyme of the TCA cycle that converts α-ketoglutarate to succinyl-CoA[35]. Importantly, also mutants lacking other genes of the TCA cycle as well as *atpA* encoding a subunit of the F_1F_0 ATP synthase displayed elevated persister cell frequencies. In contrast to our findings, Wang *et al*. reported that reduced activity of the electron transport chain and the TCA cycle decreased the number of persister cells when challenged with the fluoquinolone, levofloxacin[36]. To address the basis for this inconsistency, we examined our strains using their reported protocol. The result presented in Supplementary Fig. S7 shows that with the experimental approach by Wang *et al*., the *sdhA* (as well as *sucA*) mutant survived levofloxacin equally well as the wild type cells within a 5 days period. In contrast, when the persister assay was repeated with our standard protocol and using levofloxacin, both mutants (*sucA* and *sdhA*) exhibited higher persister frequencies compared to wild type cells (data not shown). Thus, we conclude that while the difference is not due to the antibiotics (ciprofloxacin vs. levofloxacin); there is a difference between the outcomes from the two protocols. We do, however, not see the same effect from an *sdhA* mutant in our strain background when using Wang's persister assay protocol[36], suggesting that strain choice is also important. Moreover, we have replicated our findings in different strain backgrounds (strains SA564 or RN6607, see Supplementary Fig. S3), supporting the generality of our findings. We also noted that, in Wang's study[36], the persister assay

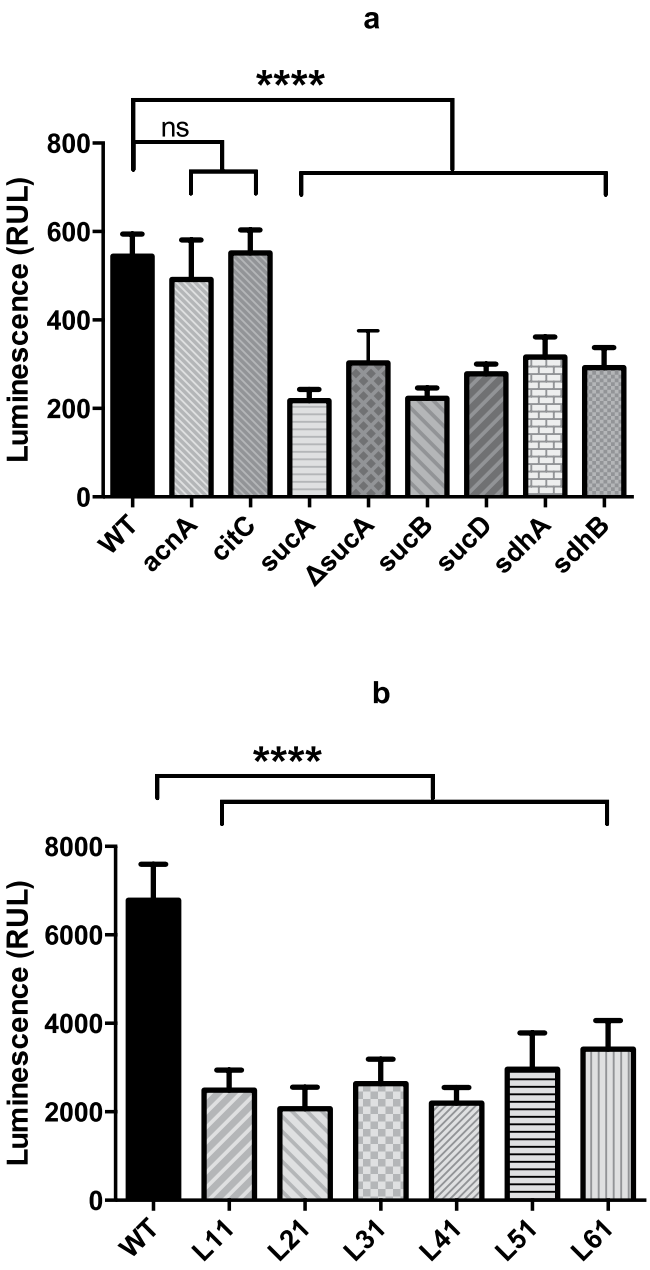

Figure 5. ATP is not the sole determinant of cellular persistence. (**a**) The ATP content of TCA cycle mutants (*acnA*, *citC*, *sucA*, *sucB*, *sucD*, *sdhA*, *sdhB* and *ΔsucA*) was measured after 24 hours of cultivation; (**b**) the ATP levels of wild type (WT) and transductants of Tnp library isolates (L11-L61) were measured after 24-hour cultivation. There were 3 biological replicates for each sample and 3 different reads of luminescence signal for each biological replicate. The statistical comparison between wild type and TCA cycle mutants (**a**) or Tnp isolate transductants (**b**) was determined with one way ANOVA followed by Dunnett's test. The error bars stand for standard deviation and the asterisks indicate significant difference at $P < 0.05$.

was carried out with static cultures in eppendorf tubes where the available oxygen is expected to be limited and rapidly depleted during cultivation. As an electron acceptor involved in electron transport chain, the scarcity of oxygen may restrict TCA cycle activity and oxidative phosphorylation, which could influence the outcome of their persister assay and potentially explain the differences compared to our results.

In the absence of antibiotics, a general link seems to exist between reduced TCA cycle activity and prolonged survival as inactivation of the aconitase resulted in extended stationary phase survival of *S. aureus*[37]. Also, small colony variants of *S. aureus* are resistant to aminoglycosides due to mutations in TCA cycle or electron transport chain genes and they display reduced membrane potential[38,39]. Recently, ATP content was reported to be a determining factor for whether or not exponentially growing cells become persisters[4,14]. However, in stationary phase cells of *S. aureus* we did not observe this correlation. In *S. aureus*, metabolism changes dramatically from exponential to stationary phase with the TCA cycle being inactive during exponential growth and ATP generated

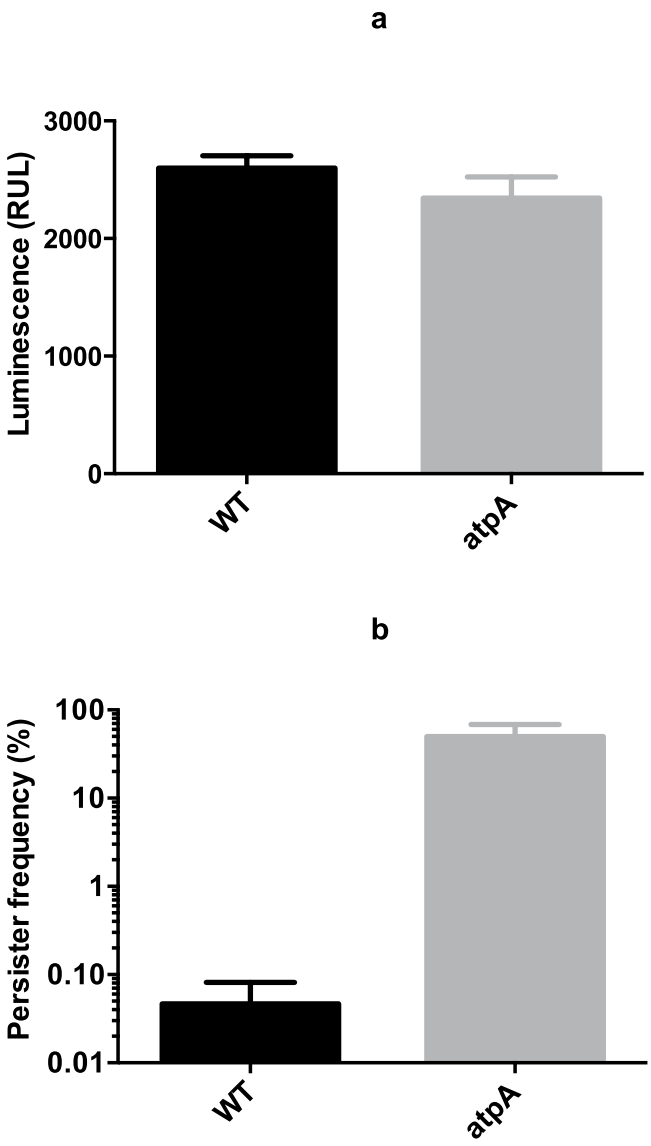

Figure 6. Comparison of ATP level (**a**) and persister frequency (**b**) between *S. aureus* Newman wild type (WT) and *atpA* mutant. For ATP measurement (**a**) 3 different reads of luminescence signal were taken for each biological replicate. Persister frequency (**b**) was tested with 100 × MIC of ciprofloxacin and the samples for ATP measurement were taken after 24 hours of incubation right before the addition of ciprofloxacin. There were 3 biological replicates for each sample and error bars indicate standard deviation. Starting CFU/ml are indicated in Supplementary Table S2.

by substrate level phosphorylation whereas in stationary phase cells TCA cycle activity is de-repressed as acetate is being catabolized[20,40]. Consequently, persisters formed in exponential and stationary phase may be different and the genes contributing in the two phases may also vary. However, for all mutants with increased stationary phase persister cell frequencies in response to ciprofloxacin we observed a lower membrane potential than for wild type cells. Reduced membrane potential may for the TCA cycle mutants arise from reduced flow of electron donors to the electron transport chain while for the *atpA* mutant it indicates that in *S. aureus* the ATP synthase is normally working in reverse and contributes to PMF by pumping out protons fuelled by ATP hydrolysis. This may be necessary to get rid of the protons that at low pH enter the cell together with acetate which has accumulated during exponential growth. Membrane potential has previously been linked with persister cell formation but primarily in response to aminoglycosides. In *Pseudomonas aeruginosa*, PMF was increased by mannitol and it leads to increased killing of biofilm associated persister cells by tobramycin while in both *E. coli* and *S. aureus*, aminoglycoside uptake was stimulated by increased PMF leading to enhanced killing of persister cells[18,19]. Our data indicate that reduced PMF in stationary phase may enhance persister formation not only in response to aminoglycosides but also to fluoroquinolones. In our experiments, however, the high-persister phenotype with β-lactam treatment was observed over a 7 days period instead of within 24 hours as was the case for ciprofloxacin, which indicates a difference in persister mechanism between the two antibiotic classes. Since β-lactam killing relies on active cell wall synthesis, such a difference could result from increased cell turn-over in the wild type

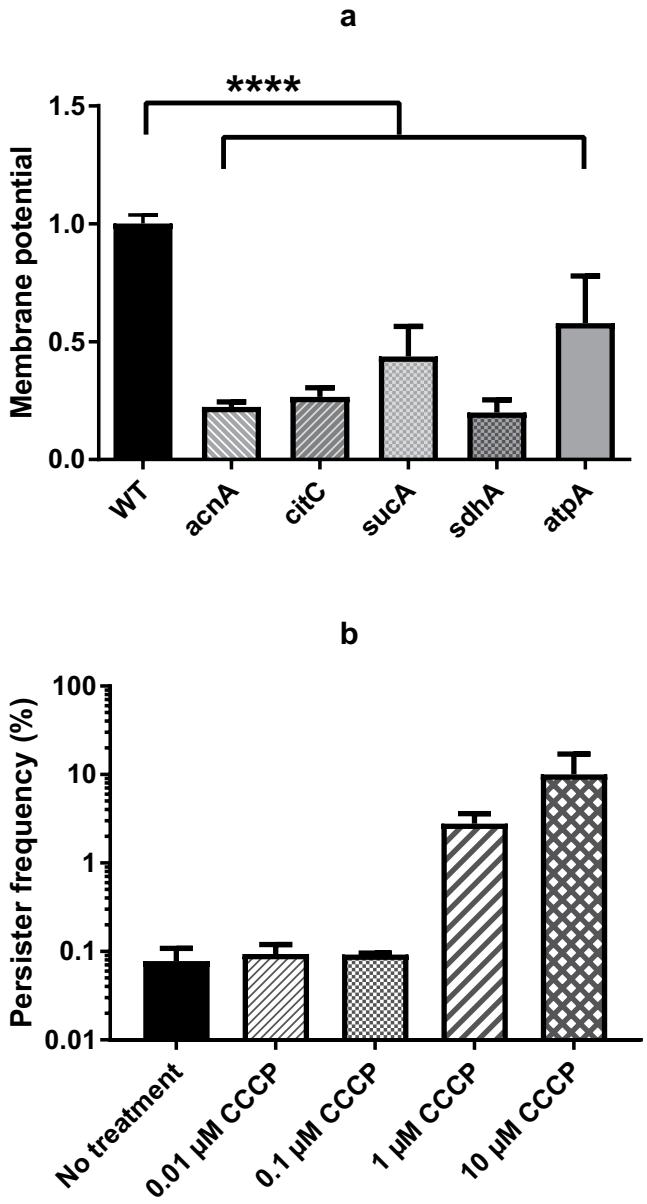

Figure 7. Measurement of membrane potential of selected mutants (**a**) and the persister formation in the presence of CCCP (**b**). (**a**) Membrane potential was measured for TCA cycle mutants (*acnA*, *citC*, *sucA* and *sdhA*) and *atpA* by flow cytometer after 30 minutes co-incubation with dye, $DiOC_2(3)$. (**b**) The persister frequency of *S. aureus* Newman wild type, challenged with 100 × MIC of ciproloxacin, was determined in the presence of CCCP, from 0.01 μM to 10 μM. There were biological triplicates for each sample and error bars represent standard deviation. Starting CFU/ml are indicated in Supplementary Table S2. The statistical comparison of membrane potential between wild type and selected TCA cycle mutants was determined with one way ANOVA followed by Dunnett's test and the asterisks indicate significant difference at $P < 0.05$ (**a**).

compared to the TCA cycle mutants. We speculate that mutations within TCA cycle contribute to the maintenance of *S. aureus* β-lactam persisters rather than their generation.

The exact mechanism by which the TCA cycle and PMF contribute to persister formation in *S. aureus* remains unclear. We found that expression of *sucA* is high and variable in stationary phase cells and correlates with the expression of *cap*, an established reporter of the stationary growth phase. Thus, we anticipate that in wild type populations, individual *S. aureus* cells with low expression of TCA cycle genes may be prone to form persisters. However, this is only in stationary phase, as in exponential phase where *sucA* is not expressed and TCA cycle is repressed, persister cells form at low frequency and TCA cycle inactivation does not influence this frequency. But how does reduced PMF lead to dormancy? In *Salmonella enterica*, the TacT toxin promotes persister formation by halting translation and its activity is modulated by the NAD^+-dependent CobB sirtuin deacetylase suggesting that NAD^+/NADH levels may influence persister formation[9,41]. However, for *S. aureus*, TA systems are not involved in persister cells formation indicating that alternative killing mechanisms should be sought[4]. Another

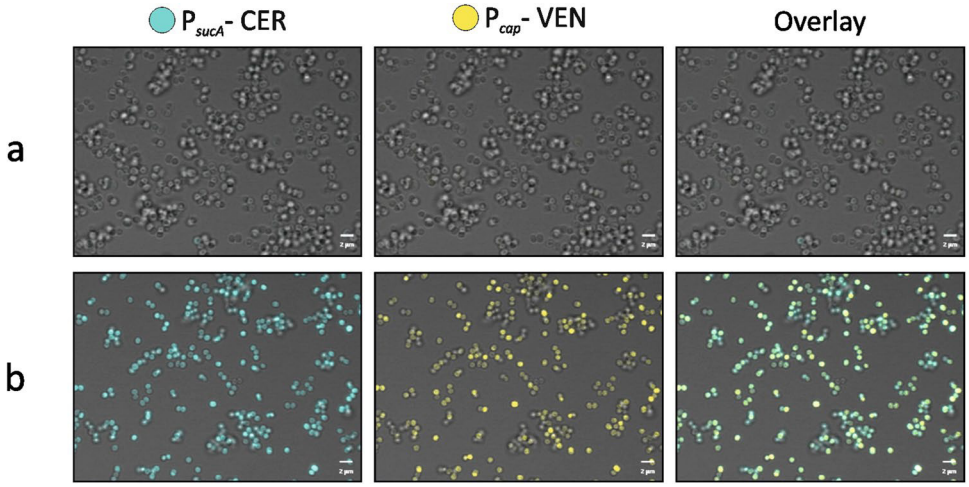

Figure 8. Expression of *sucA* in *S. aureus* Newman in exponential or stationary phase. The fluorescence expression of both P_{sucA} (CFP channel) and P_{cap} (YFP channel) in strain Newman was monitored at exponential (**a**) and stationary phase (**b**) respectively. The promoter activity of P_{sucA} appeared blue and P_{cap} activity appeared yellow.

possibility could be that the reduced membrane potential leads to a halt in cell wall synthesis as was recently shown in *Bacillus subtilis*[42]. Future analysis will be required to determine how reduced PMF leads to a persister state in *S. aureus*.

Methods

Strains, growth conditions and chemicals. A list of bacterial strains, plasmids and primers used in this study can be found in Supplementary Table S5. All the *S. aureus* strains, transposon library isolates and corresponding transductants, TCA cycle mutants and *atpA* mutant were all cultivated in Tryptic Soy Broth (TSB, Oxoid, Denmark) at 37 °C and 200 rpm of shaking in 12-ml centrifuge tube or plated on Tryptic Soy Agar (TSA, Oxoid, Denmark) at 37 °C of incubation unless otherwise indicated. All the plasmids and strains used for Tnp library construction were kindly provided by Timothy C. Meredith and supplemented glucose minimal medium (SGMM) was prepared as described previously[23]. TCA cycle mutants of *sucA*, *sucB*, *sucD*, *sdhA*, *sdhB*, *acnA* (NWMN-1263), *citC* and *atpA* were provided by bei Resources[27]. Ciprofloxacin, oxacillin, adenosine 5′-triphosphate disodium salt hydrate (ATP), carbonyl cyanidem-chlorophenylhydrazone (CCCP) and other mentioned chemicals were from Sigma-Aldrich (MO, USA). All restriction endonucleases and T4 ligase were from NEB BioLabs (MA, USA).

Construction of transposon library and identification of Tnp insertion sites. Transposon library was constructed in *S. aureus* Newman as reported previously[23,24]: (1) Tnp donor lysates were prepared by infecting TM43-45 with Ø11-FRT and the Tnp-plasmid packaging efficacy was determined by tittering these phage lysates on both RN4220 and TM19; (2) recipient strains were obtained by transforming plasmids pOrf5 Tnp^{+} or pOrf5 Tnp^{-} into *S. aureus* Newman; (3) the Tnp donor lysates were gently mixed with recipient strains in SGMM and incubated at 22 °C overnight; (4) the cells were pelleted and incubated with TSB medium for 2 hours at 30 °C before plated on TSA plates containing erythromycin (5 μg/ml). Subsequently, the plates were left at room temperature until visible growth of individual Tnp insertion mutants could be observed.

The identification of the Tnp insertion site of library isolates was performed as reported by Bae *et al.* by PCR amplification of the transposon/chromosome junction using primers Martn-F and Martn-ermR and an annealing temperature of 63 °C. After purification, the PCR products were sequenced with primer Martn-F[43].

Monitoring of P_{cap} and P_{sucA} activity and image acquisition. Approximately 10^8 bacterial cells were harvested and re-suspended in 1 ml of pre-chilled 1x phosphate buffered saline (PBS) containing 3.7% formaldehyde. After 15 minutes of gentle mixing at room temperature, 500 μl of the fixed bacterial suspension was transferred to each well of a 24-well cell culture plate (Greiner Bio-One, Germany) lined with 12 mm diameter round coverslips. After centrifugation at 600 *g* for 5 minutes, coverslips were mounted onto slides with 3 μl fluorescence mounting medium (DAKO, Denmark).

Image acquisition was performed in the confocal mode of an inverted Zeiss LSM 710 NLO microscope equipped with a spectral detector and employing Zeiss Plan-Apochromat 63x/1.40 oil DIC M27 objective (Zeiss, Germany). The following excitation wavelengths, laser sources and detection spectra were used for the promoter activity experiments, gpCerulean: 405 nm/diode laser/454–516 nm; gpVenus: 514 nm/argon laser/519–621 nm. Images were exported in the different channels or overlays as 16-bit tagged image files. The exported images were assembled with CorelDRAW X7 and adjusted for brightness and contrast.

Enrichment of the mutants with enhanced persistence. 1 μl of pooled wild type or Tnp library was inoculated into 2 ml TSB medium for incubation at 37 °C with shaking at 200 rpm in 12-ml centrifuge tube, after

24 hours, 1 ml of the culture was taken out to be treated by 100 × MIC of ciprofloxacin (MIC = 0.5 μg/ml) at 37 °C for another 24 hours in 12-ml centrifuge tube. The culture was washed and re-suspended with 1 ml FK buffer (9 g/l sodium chloride), and then certain dilutions were plated on TSA plates to be incubated at 37 °C for 24 hours. The plates with 100–200 colonies were eluted with FK buffer and 2 μl of the suspensions were inoculated in 2 ml fresh TSB medium which then undergone the same treatment of ciprofloxacin. This procedure was repeated for four times in a row to enrich persister cells.

Persister assay. 2 μl of overnight culture of library isolates, TCA cycle mutants or wild type was inoculated into 2 ml TSB medium and incubated at 37 °C with shaking at 200 rpm for 24 hours in 12-ml centrifuge tube, then 1 ml of the culture was challenged by 100 × MIC of ciprofloxacin for another 24 hours still at 37 °C in 12-ml centrifuge tube. The persister frequency was determined by calculating the ratio between the CFU/ml counting of 24-hour post and right before the addition of ciprofloxacin by plating and incubating known dilutions of the samples on TSA plates at 37 °C for 24 hours. Aliquots of *ΔsucA* mutant and parent strain cultures were taken at 1, 3, 5, 24 or 48 hours post the addition of ciprofloxacin and the dilutions were plated on TSA plate at 37 °C for 24 hours for CFU determination. The transductants of Tnp library isolates were also tested with 100 × MIC of oxacillin (MIC = 0.25 μg/ml) and the CFU/ml was determined over 7 days.

To evaluate the effect of medium acidification on persister generation, TSB medium with or without glucose (fisher scientific, MA, USA) was used for the cultivation and the persister frequencies were compared between the cultures with these two media. CCCP dissolved in DMSO was added into bacterial culture right before the treatment of ciprofloxacin to test the effect of PMF on persister generation.

Quantification of cellular ATP level. The ATP level of 24-hour cultures was tested with BacTiter-Glo™ Microbial Cell Viability Assay kit (Promega, WI, USA) according to manufacturer's instruction. 100 μl suspension of bacterial culture (10-fold diluted with TSB medium) was carefully mixed with equal volume of BacTiter-Glo™ Reagent and incubated at room temperature for 5 minutes before the luminescence was recorded with emission at 560 nm. The value of each sample was the average of three independent reads and there were 3 biological replicates for each individual sample.

Measurement of membrane potential. Membrane potential was assessed by *Bac*Light™ Bacterial Membrane Potential Kit (Life Technologies, CA, USA) where 24-hour cultures were re-suspended with 0.5 ml filtered PBS, mixed with 10 μl of fluorescent membrane potential indicator dye, $DiOC_2(3)$ and incubated at room temperature for 30 minutes. The fluorescent signals were recorded by BD Biosciences Accuri C6 flow cytometer (BD Biosciences, CA, USA) counting 50,000 cells with the threshold of 16,000 at medium flow rate. The ratio between channel F3 (red fluorescence) and F1 (green fluorescence) was calculated with CFlow® (BD Accuri, CA, USA) to indicate membrane potential.

Quantification of fermentation products. The concentration of acetate in the supernatant of cultures from both early exponential (3-hour cultivation) and stationary phase (24-hour cultivation) was determined by Ultimate 3000 HPLC system (Dionex, Sunnyvale, USA) equipped with an Aminex HPX-87H column (Bio-Rad, Hercules, USA) and a Shodex RI-101 detector (Showa Denko KK, Tokyo, Japan). The column oven temperature was set as 60 °C and the mobile phase consisted of sulfuric acid (5 mM) with a flow rate of 0.5 ml/minute.

Statistical analysis. Results were represented as the mean of biological triplicates with standard deviation besides for the ATP measurements there were 3 independent luminescent reads for each biological replicate. Statistical significance was analyzed using one way ANOVA followed by Dunnett test with $P < 0.05$ in GraphPad Prism 7 (GraphPad software Inc., CA, USA).

Data Availability. The datasets generated during and/or analysed during the current study are available from the corresponding author on reasonable request.

References

1. Fisher, R. A., Gollan, B. & Helaine, S. Persistent bacterial infections and persister cells. *Nat Rev Microbiol* **15**, 453–464, https://doi.org/10.1038/nrmicro.2017.42 (2017).
2. Van den Bergh, B., Fauvart, M. & Michiels, J. Formation, physiology, ecology, evolution and clinical importance of bacterial persisters. *FEMS Microbiol Rev* **41**, 219–251, https://doi.org/10.1093/femsre/fux001 (2017).
3. Balaban, N. Q., Merrin, J., Chait, R., Kowalik, L. & Leibler, S. Bacterial persistence as a phenotypic switch. *Science* **305**, 1622–1625, https://doi.org/10.1126/science.1099390 (2004).
4. Conlon, B. P. *et al.* Persister formation in Staphylococcus aureus is associated with ATP depletion. *Nat Microbiol* **1**, 16051, https://doi.org/10.1038/nmicrobiol.2016.51 (2016).
5. Germain, E., Roghanian, M., Gerdes, K. & Maisonneuve, E. Stochastic induction of persister cells by HipA through (p)ppGpp-mediated activation of mRNA endonucleases. *Proc Natl Acad Sci USA* **112**, 5171–5176, https://doi.org/10.1073/pnas.1423536112 (2015).
6. Maisonneuve, E., Castro-Camargo, M. & Gerdes, K. p)ppGpp controls bacterial persistence by stochastic induction of toxin-antitoxin activity. *Cell* **154**, 1140–1150, https://doi.org/10.1016/j.cell.2013.07.048 (2013).
7. Maisonneuve, E. & Gerdes, K. Molecular mechanisms underlying bacterial persisters. *Cell* **157**, 539–548, https://doi.org/10.1016/j.cell.2014.02.050 (2014).
8. Helaine, S. *et al.* Internalization of Salmonella by macrophages induces formation of nonreplicating persisters. *Science* **343**, 204–208, https://doi.org/10.1126/science.1244705 (2014).
9. Cheverton, A. M. *et al.* A Salmonella Toxin Promotes Persister Formation through Acetylation of tRNA. *Mol Cell* **63**, 86–96, https://doi.org/10.1016/j.molcel.2016.05.002 (2016).
10. Dorr, T., Vulic, M. & Lewis, K. Ciprofloxacin causes persister formation by inducing the TisB toxin in Escherichia coli. *PLoS Biol* **8**, e1000317, https://doi.org/10.1371/journal.pbio.1000317 (2010).

11. Harms, A., Fino, C., Sorensen, M. A., Semsey, S. & Gerdes, K. Prophages and Growth Dynamics Confound Experimental Results with Antibiotic-Tolerant Persister Cells. *MBio* **8**, https://doi.org/10.1128/mBio.01964-17 (2017).
12. Goormaghtigh, F. *et al*. Reassessing the Role of Type II Toxin-Antitoxin Systems in Formation of Escherichia coli Type II Persister Cells. *MBio* **9**, https://doi.org/10.1128/mBio.00640-18 (2018).
13. Wood, T. K., Knabel, S. J. & Kwan, B. W. Bacterial persister cell formation and dormancy. *Appl Environ Microbiol* **79**, 7116–7121, https://doi.org/10.1128/AEM.02636-13 (2013).
14. Shan, Y. *et al*. ATP-Dependent Persister Formation in Escherichia coli. *MBio* **8**, https://doi.org/10.1128/mBio.02267-16 (2017).
15. Kim, J. S. *et al*. Fumarate-Mediated Persistence of Escherichia coli against Antibiotics. *Antimicrob Agents Chemother* **60**, 2232–2240, https://doi.org/10.1128/AAC.01794-15 (2016).
16. Ma, C. *et al*. Energy production genes sucB and ubiF are involved in persister survival and tolerance to multiple antibiotics and stresses in Escherichia coli. *FEMS Microbiol Lett* **303**, 33–40, https://doi.org/10.1111/j.1574-6968.2009.01857.x (2010).
17. Orman, M. A. & Brynildsen, M. P. Inhibition of stationary phase respiration impairs persister formation in E. coli. *Nat Commun* **6**, 7983, https://doi.org/10.1038/ncomms8983 (2015).
18. Allison, K. R., Brynildsen, M. P. & Collins, J. J. Metabolite-enabled eradication of bacterial persisters by aminoglycosides. *Nature* **473**, 216–220, https://doi.org/10.1038/nature10069 (2011).
19. Barraud, N., Buson, A., Jarolimek, W. & Rice, S. A. Mannitol enhances antibiotic sensitivity of persister bacteria in Pseudomonas aeruginosa biofilms. *PLoS One* **8**, e84220, https://doi.org/10.1371/journal.pone.0084220 (2013).
20. Somerville, G. A. *Staphylococcus: Genetics and Physiology*. 107–118 (Caister Academic Press, 2016).
21. Conlon, B. P. *et al*. Activated ClpP kills persisters and eradicates a chronic biofilm infection. *Nature* **503**, 365–370, https://doi.org/10.1038/nature12790 (2013).
22. Conlon, B. P. Staphylococcus aureus chronic and relapsing infections: Evidence of a role for persister cells: An investigation of persister cells, their formation and their role in S. aureus disease. *Bioessays* **36**, 991–996, https://doi.org/10.1002/bies.201400080 (2014).
23. Wang, H., Claveau, D., Vaillancourt, J. P., Roemer, T. & Meredith, T. C. High-frequency transposition for determining antibacterial mode of action. *Nat Chem Biol* **7**, 720–729, https://doi.org/10.1038/nchembio.643 (2011).
24. Santiago, M. *et al*. A new platform for ultra-high density Staphylococcus aureus transposon libraries. *BMC Genomics* **16**, 252, https://doi.org/10.1186/s12864-015-1361-3 (2015).
25. Girgis, H. S., Harris, K. & Tavazoie, S. Large mutational target size for rapid emergence of bacterial persistence. *Proc Natl Acad Sci USA* **109**, 12740–12745, https://doi.org/10.1073/pnas.1205124109 (2012).
26. D L. Nelson, M. M. C. Lehninger Principles of Biochemistry. *W.H. Freeman*, 1328 (2008).
27. Fey, P. D. *et al*. A genetic resource for rapid and comprehensive phenotype screening of nonessential Staphylococcus aureus genes. *MBio* **4**, e00537–00512, https://doi.org/10.1128/mBio.00537-12 (2013).
28. Page, R. & Peti, W. Toxin-antitoxin systems in bacterial growth arrest and persistence. *Nat Chem Biol* **12**, 208–214, https://doi.org/10.1038/nchembio.2044 (2016).
29. Strahl, H. & Hamoen, L. W. Membrane potential is important for bacterial cell division. *Proc Natl Acad Sci USA* **107**, 12281–12286, https://doi.org/10.1073/pnas.1005485107 (2010).
30. Mitchell, P. & Moyle, J. Chemiosmotic hypothesis of oxidative phosphorylation. *Nature* **213**, 137–139 (1967).
31. Heytler, P. G. uncoupling of oxidative phosphorylation by carbonyl cyanide phenylhydrazones. I. Some characteristics of m-Cl-CCP action on mitochondria and chloroplasts. *Biochemistry* **2**, 357–361 (1963).
32. Cunarro, J. & Weiner, M. W. Mechanism of action of agents which uncouple oxidative phosphorylation: direct correlation between proton-carrying and respiratory-releasing properties using rat liver mitochondria. *Biochim Biophys Acta* **387**, 234–240 (1975).
33. Kwan, B. W., Valenta, J. A., Benedik, M. J. & Wood, T. K. Arrested protein synthesis increases persister-like cell formation. *Antimicrob Agents Chemother* **57**, 1468–1473, https://doi.org/10.1128/AAC.02135-12 (2013).
34. George, S. E. *et al*. Phenotypic heterogeneity and temporal expression of the capsular polysaccharide in Staphylococcus aureus. *Mol Microbiol* **98**, 1073–1088, https://doi.org/10.1111/mmi.13174 (2015).
35. Tretter, L. & Adam-Vizi, V. Alpha-ketoglutarate dehydrogenase: a target and generator of oxidative stress. *Philos Trans R Soc Lond B Biol Sci* **360**, 2335–2345, https://doi.org/10.1098/rstb.2005.1764 (2005).
36. Wang, W. *et al*. Transposon Mutagenesis Identifies Novel Genes Associated with Staphylococcus aureus Persister Formation. *Front Microbiol* **6**, 1437, https://doi.org/10.3389/fmicb.2015.01437 (2015).
37. Somerville, G. A. *et al*. Staphylococcus aureus aconitase inactivation unexpectedly inhibits post-exponential-phase growth and enhances stationary-phase survival. *Infect Immun* **70**, 6373–6382 (2002).
38. Kriegeskorte, A. *et al*. Staphylococcus aureus small colony variants show common metabolic features in central metabolism irrespective of the underlying auxotrophism. *Front Cell Infect Microbiol* **4**, 141, https://doi.org/10.3389/fcimb.2014.00141 (2014).
39. Vestergaard, M. *et al*. Novel Pathways for Ameliorating the Fitness Cost of Gentamicin Resistant Small Colony Variants. *Front Microbiol* **7**, 1866, https://doi.org/10.3389/fmicb.2016.01866 (2016).
40. Somerville, G. A. & Proctor, R. A. At the crossroads of bacterial metabolism and virulence factor synthesis in Staphylococci. *Microbiol Mol Biol Rev* **73**, 233–248, https://doi.org/10.1128/MMBR.00005-09 (2009).
41. VanDrisse, C. M., Parks, A. R. & Escalante-Semerena, J. C. A Toxin Involved in Salmonella Persistence Regulates Its Activity by Acetylating Its Cognate Antitoxin, a Modification Reversed by CobB Sirtuin Deacetylase. *MBio* **8**, https://doi.org/10.1128/mBio.00708-17 (2017).
42. Muller, A. *et al*. Daptomycin inhibits cell envelope synthesis by interfering with fluid membrane microdomains. *Proc Natl Acad Sci USA*, https://doi.org/10.1073/pnas.1611173113 (2016).
43. Bae, T. *et al*. Staphylococcus aureus virulence genes identified by bursa aurealis mutagenesis and nematode killing. *Proc Natl Acad Sci USA* **101**, 12312–12317, https://doi.org/10.1073/pnas.0404728101 (2004).

Acknowledgements

We would like to thank NARSA (University of Nebraska Medical Centre) and bei RESOURCES for providing mutants used in this study and TC Meredith for help with the Tnp library construction. Y. Wang, M.S. Bojer and H. Ingmer, were funded by the Danish National Research Foundation (DNRF-120); SEGeorge and C. Wolz, by the Deutsche Forschungsgemeinschaft (SFB766) and Z.H. Wang and P. R. Jensen, by the Danish Council for Strategic Research and the Danish Council for Technology and Innovation (0603-00522B).

Author Contributions

Y.W. designed and performed most of the experiments, wrote and edited the manuscript, M.S.B. designed and performed some experiments and wrote part of the manuscript, Z.H.W. and S.E.G. performed the experiments included in Figures 3 and 8 respectively, C.W. and P.R.J. conceived some experiments and wrote part of the manuscript, H.I. conceived the experiments, wrote and edited the manuscript. All authors reviewed the manuscript.

Additional Information

Supplementary information accompanies this paper at https://doi.org/10.1038/s41598-018-29123-0.

Competing Interests: The authors declare no competing interests.

Publisher's note: Springer Nature remains neutral with regard to jurisdictional claims in published maps and institutional affiliations.

Open Access This article is licensed under a Creative Commons Attribution 4.0 International License, which permits use, sharing, adaptation, distribution and reproduction in any medium or format, as long as you give appropriate credit to the original author(s) and the source, provide a link to the Creative Commons license, and indicate if changes were made. The images or other third party material in this article are included in the article's Creative Commons license, unless indicated otherwise in a credit line to the material. If material is not included in the article's Creative Commons license and your intended use is not permitted by statutory regulation or exceeds the permitted use, you will need to obtain permission directly from the copyright holder. To view a copy of this license, visit http://creativecommons.org/licenses/by/4.0/.

© The Author(s) 2018

Publication 4

Revisiting the regulation of the capsular polysaccharide biosynthesis gene cluster in *Staphylococcus aureus*.

Keinhörster D, Salzer A, Duque-Jaramillo A, **George SE**, Marincola G, Lee JC, Weidenmaier C, Wolz C.

Molecular Microbiology 2019 Jul 8. doi: 10.1111/mmi.14347.

Molecular Microbiology (2019) 0(0), 1–17 doi:10.1111/mmi.14347

Revisiting the regulation of the capsular polysaccharide biosynthesis gene cluster in *Staphylococcus aureus*

Daniela Keinhörster,[1] Andrea Salzer,[1] Alejandra Duque-Jaramillo,[1] Shilpa E. George,[1] Gabriella Marincola,[1†] Jean C. Lee,[2] Christopher Weidenmaier[1] and Christiane Wolz[1*]

[1] *Interfaculty Institute of Microbiology and Infection Medicine, University of Tübingen, Tübingen, Germany.*

[2] *Department of Medicine (Infectious Diseases), Brigham and Women's Hospital, Harvard Medical School, Boston, MA 02115, USA.*

Summary

Capsular polysaccharide (CP) biosynthesis in *Staphylococcus aureus* is tightly controlled resulting in a heterogeneous phenotype within a population and CP being mainly detectable in nongrowing cells. Expression of the corresponding biosynthesis gene cluster is driven by one promoter element (P_{cap}). Here, we demonstrate that P_{cap} contains a main SigB-dependent promoter. The SigB consensus motif overlaps with a previously described inverted repeat (IR) that is crucial for *cap* expression. The essentiality of the IR is derived from this region acting as a SigB binding site rather than as an operator site for the proposed *cap* activators RbsR and MsaB. Furthermore, P_{cap} contains an extensive upstream region harboring a weak SigA-dependent promoter and binding sites for *cap* repressors such as SaeR, CodY and Rot. Heterogeneous CP synthesis is determined by SigB activity and repressor binding to the upstream region. SigB dependency and regulation by the upstream repressors are also sufficient to explain the temporal gene expression pattern at the transcriptional level. However, CP synthesis remains growth phase-dependent even when transcription is rendered constitutive, suggesting additional post-transcriptional regulatory circuits. Thus, the interference of multiple repressors with SigB-dependent promoter activity as well as post-transcriptional mechanisms ensure the appropriate regulation of CP synthesis.

Accepted 3 July, 2019. *For correspondence. E-mail christiane.wolz@uni-tuebingen.de; Tel. +49 7071 2974648; Fax 00497071295937. Present address: †Institute for Molecular Infection Biology, University of Würzburg, Würzburg, Germany.

Introduction

Staphylococcus aureus is an opportunistic pathogen that asymptomatically colonizes parts of the human population, thereby increasing the risk of subsequent infections. Its capacity to cause a wide variety of diseases depends on secreted virulence factors as well as cell surface-attached proteins and polysaccharides (Gordon and Lowy, 2008; Weidenmaier and Lee, 2017; de Jong *et al.*, 2019). The capsular polysaccharide (CP) is one of these cell surface structures playing an important role in *S. aureus* pathogenesis and bacterial evasion of the host immune defenses (O'Riordan and Lee, 2004; Weidenmaier and Lee, 2017). Therefore, it is being discussed as a target for immunotherapy and as a vaccine candidate (Missiakas and Schneewind, 2016; Weidenmaier and Lee, 2017; Ansari *et al.*, 2019).

CP serotypes 5 and 8 are the two main CP serotypes produced by *S. aureus* strains (Arbeit *et al.*, 1984; Hochkeppel *et al.*, 1987; Roghmann *et al.*, 2005; Verdier *et al.*, 2007). Their structure is highly similar due to the closely related *cap5* and *cap8* gene clusters. These allelic operons consist of 16 genes, *cap5/8A* to *cap5/8P*, whose gene products are involved in CP biosynthesis, O-acetylation, transport and regulation (O'Riordan and Lee, 2004; Weidenmaier and Lee, 2017; Rausch *et al.*, 2019). The *cap* operon is thought to be mainly transcribed as a single large 17 kb transcript driven by one principal promoter element (P_{cap}), located upstream of *capA* (Sau *et al.*, 1997; Ouyang *et al.*, 1999). While *cap* gene clusters are extremely conserved across *S. aureus* genomes, not all clinically relevant isolates produce CP and acapsular variants may emerge during chronic infections. The loss of CP expression can typically be explained by mutations in any of the *cap* genes essential for CP synthesis or in the promoter region (Cocchiaro *et al.*, 2006; Tuchscherr *et al.*, 2010). For instance, the acapsular phenotype of strains from the USA300 lineage was attributed to conserved mutations in the *cap5* locus (Boyle-Vavra *et al.*, 2015). However, this assumption has been recently challenged

© 2019 The Authors. *Molecular Microbiology* John Wiley & Sons Ltd.
This is an open access article under the terms of the Creative Commons Attribution License, which permits use, distribution and reproduction in any medium, provided the original work is properly cited.

by the finding that USA300 strains might indeed produce CP during infection (Mohamed *et al.*, 2019). In addition to mutations that abolish its production, CP synthesis can also be switched off in response to environmental conditions via a complex regulatory network. Extensive *in vitro* and *in vivo* analyses have shown that *cap* expression is highly sensitive to changes in nutrients, pH, CO_2 and oxygen availability (Sutra *et al.*, 1990; Dassy *et al.*, 1991; Stringfellow *et al.*, 1991; Lee *et al.*, 1993; Poutrel *et al.*, 1995; Herbert *et al.*, 1997; Pohlmann-Dietze *et al.*, 2000; George *et al.*, 2015). Interestingly, CP synthesis was commonly found to be strictly growth phase-dependent and detectable only after post-exponential growth phase (Poutrel *et al.*, 1995; Dassy and Fournier, 1996; Pohlmann-Dietze *et al.*, 2000; Cunnion *et al.*, 2001; George *et al.*, 2015). In addition, not all bacteria in a population are CP-positive as revealed by flow cytometry and immunofluorescence (IF) of *in vitro*- and *in vivo*-grown bacteria (Poutrel *et al.*, 1997; Pohlmann-Dietze *et al.*, 2000; George *et al.*, 2015; Conlon *et al.*, 2016). As only nonencapsulated cells are able to adhere to endothelial cells (Pohlmann-Dietze *et al.*, 2000), while CP protects bacterial cells from phagocytosis (Karakawa *et al.*, 1988; Thakker *et al.*, 1998; Portoles *et al.*, 2001), it is likely that CP heterogeneity provides better adaptability of the population as a whole. So far, the underlying regulatory mechanisms of this particular expression pattern (early-Off/late-Heterogeneous) are only partially understood.

In general, P_{cap} activity correlates with CP synthesis, indicating that regulation occurs predominantly at the transcriptional level (Ouyang *et al.*, 1999; Meier *et al.*, 2007; Jansen *et al.*, 2013; Hartmann *et al.*, 2014; George *et al.*, 2015). Yet, the data to explain the molecular mechanisms of *cap* regulation are puzzling. The identified transcriptional start site (TSS) is not preceded by a classical sigma factor consensus sequence (Ouyang *et al.*, 1999); instead, several inverted and direct repeats were identified further upstream, among which a 10 bp inverted repeat (IR) was shown to be crucial for promoter activity (Ouyang *et al.*, 1999). It has been proposed that this IR functions as an operator site for the *cap* activators RbsR and MsaB (Lei and Lee, 2015; Batte *et al.*, 2016). RbsR also functions as a repressor of the *rbsUDK* operon involved in ribose uptake. While the presence of ribose relieves repression of the *rbsUDK* operon by RbsR, the presence and absence of ribose had no effect on *cap* expression (Lei and Lee, 2015). MsaB is described as a transcriptional factor with DNA binding capacity (Batte *et al.*, 2016) but is also annotated as cold-shock protein CspA, which exerts regulatory effects via RNA binding (Caballero *et al.*, 2018). In addition to RbsR and MsaB/CspA, there are several other transcription factors (MgrA, CcpA, RpiR, SpoVG, CcpE, XdrA, CodY, Rot), two-component regulatory systems (Agr, ArlRS, KdpDE, AirRS, SaeRS) and the alternative sigma factor B (SigB) known to be involved in the regulation of *cap* expression (O'Riordan and Lee, 2004; Weidenmaier and Lee, 2017). The role of these regulators was mainly deduced from the characterization of single regulatory mutants and, in most cases, it remains unclear how they affect *cap* expression. In particular, SigB and Agr are believed to act indirectly via other regulatory systems. For instance, the absence of a SigB consensus motif in front of the proposed TSS led to the hypothesis that SigB acts through the SigB-dependent *cap* regulators SpoVG, ArlRS and RbsR (Bischoff *et al.*, 2001; 2004; Meier *et al.*, 2007; Schulthess *et al.*, 2009; Lei and Lee, 2015). SigB is a central part of the general stress response, and is activated upon environmental stresses and toward stationary growth phase (Pane-Farre *et al.*, 2006). Its activity is regulated mainly at the post-translational level by a complex regulatory cascade involving RsbW, RsbV and RsbU, encoded within the *rsbUVWsigB* operon (Senn *et al.*, 2005).

For the quorum sensing system Agr, it was shown that Agr-mediated *cap* activation occurs via inactivation of the repressor Rot (George *et al.*, 2015). Rot is known to bind to several target genes; however, its binding motif is ill-defined (Killikelly *et al.*, 2015). Nevertheless, Rot as well as the DNA binding proteins CodY and SaeR are likely candidates for direct interference with the P_{cap} promoter element. CodY represses many metabolic and virulence genes, including the *cap* operon (Pohl *et al.*, 2009; Majerczyk *et al.*, 2010), and binding of CodY to the P_{cap} region has been demonstrated (Majerczyk *et al.*, 2010; Batte *et al.*, 2018; Lei and Lee, 2018). The two-component system (TCS) SaeRS regulates a number of virulence factors, with *cap* being one of the few genes repressed (Steinhuber *et al.*, 2003; Luong *et al.*, 2011; George *et al.*, 2015). With only a poorly conserved SaeR consensus sequence in P_{cap}, it remains unclear whether SaeR exerts its effect on *cap* expression indirectly or via direct promoter interaction.

All in all, despite a plethora of work published on *cap* regulation, results are yet inconclusive regarding P_{cap} architecture and the molecular interference of the different regulatory elements. Here, we redefined the P_{cap} promoter structure and reinvestigated the main players of *cap* expression. We identified a SigB consensus motif overlapping with the IR structure. In addition, we found a second weak SigA-dependent promoter in the P_{cap} upstream region, as well as binding sites for three *cap* repressors, CodY, Rot and SaeR, which interfere with SigB-dependent promoter activity. Thus, the early-Off/late-Heterogeneous *cap* expression pattern is a consequence of SigB activity together with repression mediated through the P_{cap} upstream region. However, negative regulation of CP synthesis in early growth phase is maintained through additional post-transcriptional mechanisms.

Results

P_{cap} contains SigA- and SigB-dependent promoters

Previous primer extension analysis of the 344 bp comprising P_{cap} revealed a TSS –17 bp upstream of the ATG start codon of *capA* (Ouyang *et al.*, 1999). However, RNA-Seq data indicate an alternative TSS further upstream, at position –41 from the *capA*-coding region (data not shown), consistent with recent whole genome analyses of TSSs in *S. aureus* (Mäder *et al.*, 2016; Prados *et al.*, 2016). To resolve this ambiguity, we employed 5′ rapid amplification of cDNA endings (5′ RACE) (Fig. 1A). Most of the clones (6/10) revealed a TSS at position –41 bp from the *capA* start codon, which is preceded by a putative SigB consensus sequence. This SigB promoter consists of a conserved SigB –35 motif (GTTTAA) and a –10 region harboring three mismatches (ATGTAA versus GGGTAT) (Homerova *et al.*, 2004). Remarkably,

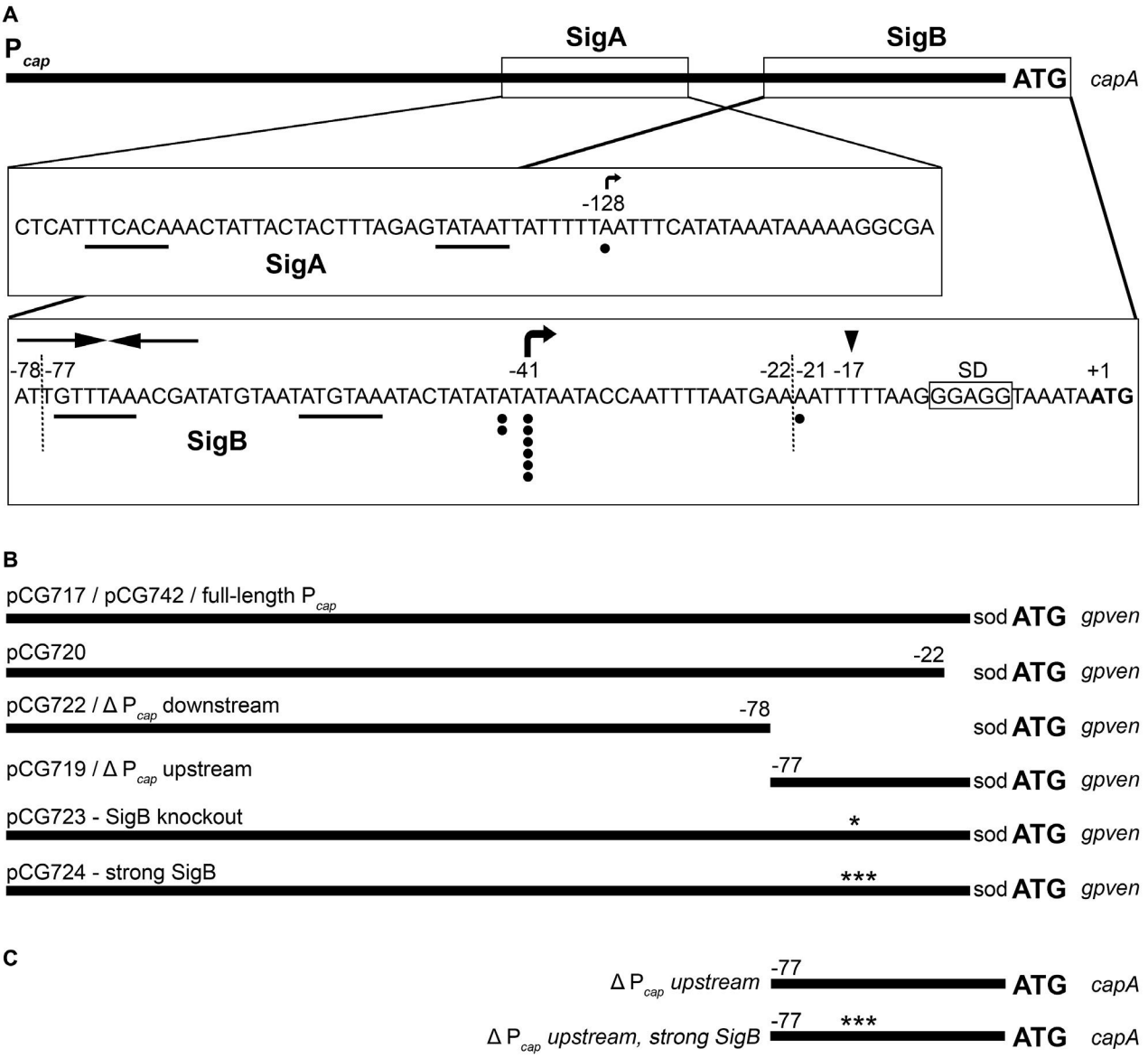

Fig. 1. P_{cap} promoter architecture and P_{cap} variants employed in this study.
A. P_{cap} (344 bp) in front of *capA* with magnified SigA and SigB promoters. Black dots represent the putative TSSs suggested by 10 analyzed 5′ RACE clones. Sigma factor –35 and –10 motifs are underlined, bent arrows indicate the corresponding TSSs. The TSS and inverted repeat (IR) structure proposed by Ouyang *et al.* (1999) are marked as black triangle and opposing arrows, respectively. Vertical dashed lines indicate sites of promoter truncation. Numbers mark positions with reference to the ATG of *capA*. The native Shine Dalgano (SD) sequence is labeled and indicated by a box.
B. P_{cap} promoter fusion variants in front of an artificial ribosomal binding site (sod) and *gpven* gene. Numbers show truncation sites and asterisks indicate point mutations (* –56:G → T; *** –58:A → G, –57:T → G, –52:A → T).
C. Genomic P_{cap} variants in front of *capA*. Numbers show truncation sites and asterisks indicate point mutations (*** –58:A → G, –57:T → G, –52:A → T).

© 2019 The Authors. *Molecular Microbiology* John Wiley & Sons Ltd.,

the SigB –35 consensus sequence is located within the IR that is crucial for P_{cap} activity (Ouyang *et al.*, 1999). The identified TSS confirmed our RNA-Seq data and the TSS prediction of Prados *et al.* (2016). In addition, 5′ RACE revealed one clone with a putative TSS at position –128 bp upstream of the *capA* start codon, which was also predicted by Prados *et al.* (2016). A conserved SigA consensus sequence was identified in front of this TSS containing canonical –35 and –10 regions. Interestingly, the TSS –17 bp upstream of the *capA* start codon proposed by Ouyang *et al.* (1999) was not detected. Though one 5′ RACE clone suggested a potential TSS in close proximity, at position –21, this was not preceded by a sigma factor consensus sequence, challenging the presence of a functional promoter. Using 5′ RACE and sequence analysis, we provide evidence for a dominant SigB-dependent promoter and an additional SigA-dependent promoter further upstream in the P_{cap} promoter element.

cap expression is mainly driven by direct SigB regulation

To analyze promoter activities, we constructed various P_{cap}-*gpven* promoter fusions (Fig. 1B), including deletions and variations of the putative SigA- and SigB-dependent promoters. Cloning the full-length P_{cap} in front of *gpven* and an artificial ribosomal binding site (Liese *et al.*, 2013) (pCG717) resulted in detectable *gpven* expression and was used as reference for all further experiments (Fig. 2A). Deletion of the downstream element containing the putative TSSs at position –17 (Ouyang *et al.*, 1999) and –21 in pCG720 did not influence *gpven* expression. This supports that there is no active promoter located in this region and that these putative TSSs may have been derived from RNA processing. A construct containing only the SigA-dependent promoter (pCG722) resulted in a low but detectable fluorescence signal, suggesting weak promoter activity. In contrast, a construct containing only the SigB-dependent promoter (pCG719) resulted in a strong promoter activity. This indicates dual promoter activity driving P_{cap} expression: a weak SigA-dependent promoter located in the upstream region plus a main SigB-dependent promoter further downstream. The deletion of the upstream region containing the SigA consensus sequence (pCG719) resulted in promoter activity higher than that of the full-length construct (pCG717). Taken together, these results suggest that despite containing a functional SigA-dependent promoter, the upstream region mainly functions as a repressive element.

To further prove that SigB is directly involved in *cap* activation, the expression of the full-length P_{cap} promoter fusion was measured in wild-type and a *sigB* mutant over time. In addition, constructs where the SigB –10 consensus sequence was mutated to either abolish (pCG723) or enhance (pCG724) SigB affinity were included (Fig. 2B). Deletion of *sigB* (data not shown) or a loss-of-function mutation in the SigB consensus sequence eliminated P_{cap} activity. In contrast, the strong SigB consensus motif further enhanced promoter activity in comparison to the native promoter. These results reveal that *cap* expression is mainly and directly driven by SigB activity.

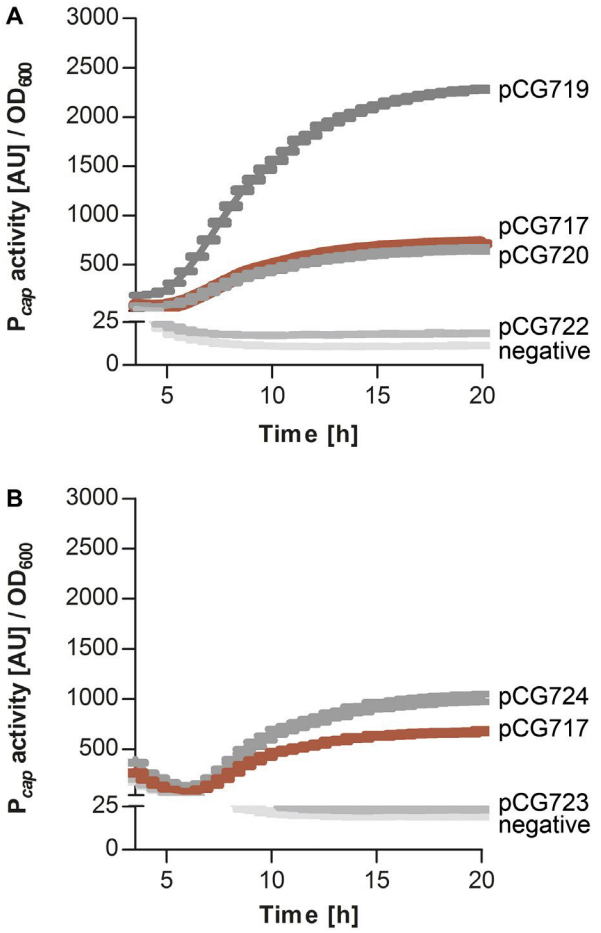

Fig. 2. SigB is the main driver of P_{cap} activity. Promoter activities of different truncated (A) or mutated (B) P_{cap} fusions in Newman wild-type. The different promoter fusion constructs are described in Fig. 1B. The promoter activity of the full-length P_{cap} promoter fusion (pCG717) serves as reference and is marked in red. Mean gpVenus intensity per OD_{600} plus standard deviation of biological triplicates is shown over time.

MsaB/CspA activates cap expression by modulating SigB activity

Interestingly, the crucial IR structure that in fact constitutes the SigB –35 motif was shown to be the binding site for two *cap* activators, RbsR and MsaB (Lei and Lee, 2015; Batte *et al.*, 2016). To elucidate whether and how these regulators interfere with SigB-dependent promoter activity, full-length P_{cap} promoter fusions were introduced

into *msa* and *rbsR* knockout mutants. Under our growth conditions, deletion of *rbsR* showed no effect on P_{cap} activity (Fig. S1).

In the *msa* mutant, P_{cap} promoter activity was lower than in the wild-type, supporting the finding that MsaB/CspA contributes to *cap* activation (Fig. 3A). We hypothesized that MsaB/CspA exerted its effect by modulating SigB activity. To test this hypothesis, we used the dual promoter fusion construct pCG742 to simultaneously measure P_{cap} and P_{asp23} activities. The P_{asp23} promoter is widely used as marker for SigB activity (Gertz *et al.*, 1999; Giachino *et al.*, 2001; Homerova *et al.*, 2004) and was cloned in front of *gpcer* (Liese *et al.*, 2013). We found P_{cap} and P_{asp23} activities to be highly correlated, in line with the assumption that both are controlled directly by SigB. The activity of both promoters was lower in a *msa* mutant (Fig. 3A and B). It was previously shown that MsaB/CspA could bind to *rsbVWsigB* transcript, likely leading to its stabilization (Caballero *et al.*, 2018). In this case, expression of *sigB* alone should lead to MsaB/CspA-independent regulation. Therefore, we expressed *sigB* from a constitutive promoter in a *rsbUVWsigB* mutant (const. *sigB*). By this means, we also circumvented post-transcriptional regulation of SigB by the RsbUVW phosphorelay. As expected, neither P_{cap} activity (Fig. 3A) nor P_{asp23} activity (Fig. 3B) was affected by *msa* deletion in this background. To exclude additional regulation by direct binding of MsaB/CspA to P_{cap}, we performed electrophoretic mobility shift assays (EMSAs) with purified MsaB/CspA protein. Even using high amounts of MsaB/CspA protein, no band shift was observed (Fig. S2). Thus, MsaB/CspA promotes *cap* expression via modulation of SigB activity and not by direct interaction with P_{cap}.

Upstream promoter region leads to P_{cap} repression

To follow up on the observation that the P_{cap} upstream region is of repressive function (Fig. 2A), we investigated the role of the known *cap* repressors CodY, Rot and Sae. Full-length (pCG717) and truncated (pCG719 and pCG722) P_{cap} promoter fusions were introduced in *codY*-, *rot*- or *sae*-negative background. Mutation of any of the three regulators resulted in a significant increase of full-length P_{cap} activity (Fig. 4A). The effect of the individual regulators is additive, since in the *sae codY rot* triple mutant, the promoter activity is further enhanced compared to the single mutants. If these repressors target the P_{cap} upstream region, their deletion should not affect promoter activity of a construct lacking this part of the promoter. Indeed, repressor mutations have no or only minor effects on promoter activity of construct pCG719 (Fig. 4B). Interestingly, promoter activity of the full-length construct in the triple mutant remained significantly below the level of the upstream-truncated construct (Fig. 4A and B). This indicates that, besides CodY, Sae and Rot, additional repressive factors are acting on the P_{cap} upstream region.

We further analyzed whether the repressors also affect the activity of the weak SigA-dependent promoter located in this region (Fig. 4C). Remarkably, neither Rot

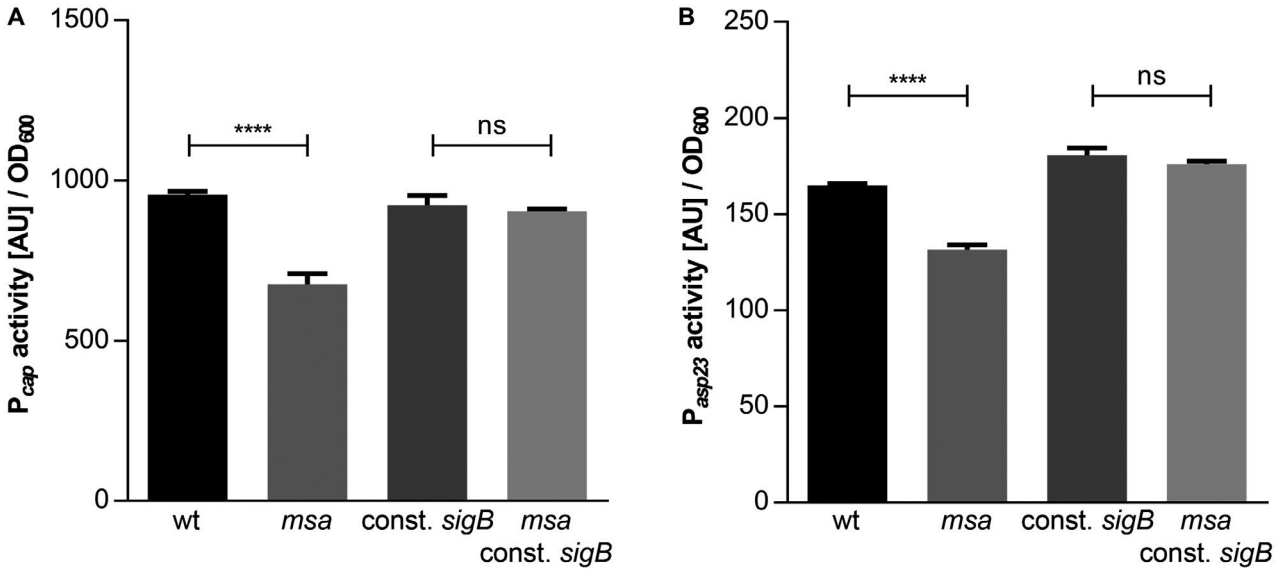

Fig. 3. MsaB/CspA activates *cap* expression by modulating SigB activity. Promoter activity of full-length P_{cap}-*gpven* (A) and P_{asp23}-*gpcer* (B) dual promoter fusion (pCG742, see Fig. 1B) in Newman wild-type and a *msa* mutant with or without constitutive *sigB* expression (const. *sigB*). gpCerulean (P_{asp23}) and gpVenus (P_{cap}) intensities are given per OD_{600} after 16 h of growth. Experiments were performed in biological triplicates, error bars represent the standard deviation. Statistical significance was obtained by ordinary one-way ANOVA followed by Tukey's multiple comparison test (ns: not significant, ****: $P < 0.0001$).

© 2019 The Authors. *Molecular Microbiology* John Wiley & Sons Ltd.,

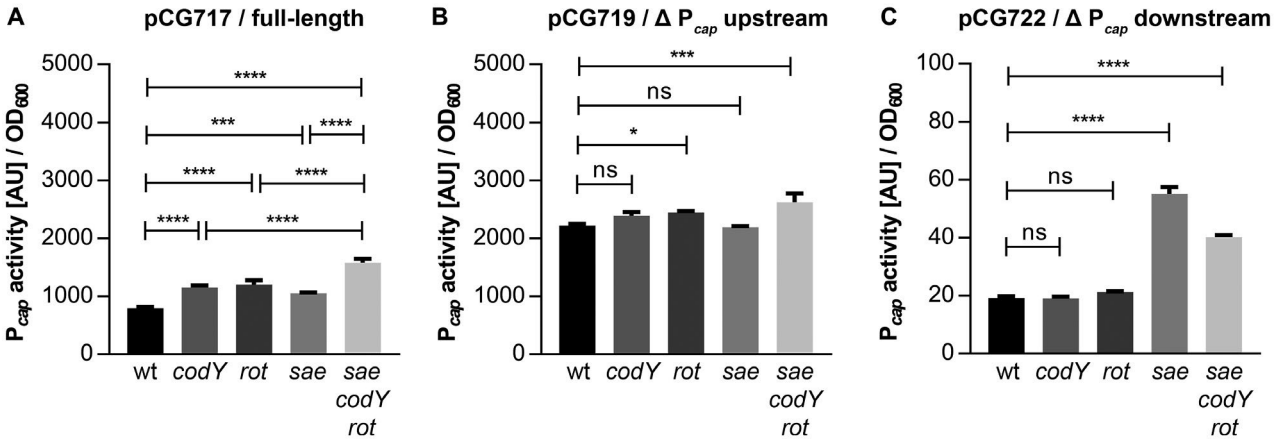

Fig. 4. CodY, Rot and Sae repress *cap* expression by interfering with the P_{cap} upstream region. Promoter activity of different P_{cap} truncations in Newman wild-type, *codY*, *rot*, *sae* single and triple mutants (A–C). The different promoter fusion constructs are described in Fig. 1B. gpVenus intensity is given per OD_{600} after 16 h of growth. Experiments were performed in biological triplicates, error bars represent the standard deviation. Statistical significance was determined by ordinary one-way ANOVA followed by Dunnett's multiple comparison test (ns: not significant, *: $P < 0.1$, ***: $P < 0.001$, ****: $P < 0.0001$).

nor CodY showed any influence on promoter activity in a construct only containing the upstream part of the promoter (pCG722). However, mutation of *sae* resulted in increased SigA-dependent promoter activity, even though it remained weak in comparison to the full-length promoter (pCG717). Hence, while all three repressors target the upstream region and affect SigB-dependent promoter activity, only Sae additionally represses the weak SigA-dependent promoter.

Sae, Rot and CodY repress P_{cap} by direct binding

We have demonstrated that Sae, Rot and CodY repress P_{cap}, but it remains unclear whether repression occurs through direct DNA–protein interaction or rather indirectly through the complex regulatory network. To elucidate the nature of the repressors, we performed EMSAs with purified SaeR, Rot and CodY proteins. As SaeR only binds DNA in its phosphorylated state (Sun *et al.*, 2010), we created a phosphomimetic SaeR with a D51E substitution. Incubation of increasing amounts of $SaeR^{D51E}$ with fluorescence-labeled P_{cap} upstream fragment (–78 to –344 from *capA*, see Fig. 1A) resulted in a retarded protein–DNA complex (Fig. 5A), which was not observed using the unphosphorylated native SaeR (Fig. 5B). Binding is consistent with a putative SaeR binding motif located between –79 bp and –94 bp upstreams of the *capA* start codon (Liu *et al.*, 2016). Specific binding to the P_{cap} upstream region was also found for Rot and CodY (Fig. 5C and D). These findings are in line with the promoter activities described above showing that Sae, Rot and CodY target the P_{cap} upstream region (Fig. 4A and B). Binding of CodY to the downstream fragment (+10 to –77 from *capA*, see Fig. 1A) is unspecific as band shifts are eliminated by specific and unspecific unlabeled competitors (Fig. S3D). However, it was previously found that CodY can interact with a region downstream (+160 to –152 from *capA*, see Fig. 1A) reaching into the *capA* coding sequence (Lei and Lee, 2018). This region was so far not included in our promoter activity assays or EMSAs. We could confirm CodY binding to this region, when using a 3′ extended downstream fragment (+160 to –77 from *capA*, see Fig. 1A) covering the *capA* coding region (Fig. S3E). Together, these results show that SaeR and Rot directly bind to the P_{cap} upstream region, whereas CodY can bind to two distinct sites, one within the P_{cap} upstream region and one further downstream reaching into the *capA*-coding region.

SigB-dependent regulation and various repressors targeting the upstream region contribute to temporal and heterogeneous CP synthesis

So far, we analyzed P_{cap} promoter activity using artificial promoter fusion constructs. To confirm that our findings translate into CP production, we used IF for CP detection. This also allows monitoring the onset of CP production and CP heterogeneity on the single cell level. Cultures were diluted thrice to ensure that all bacteria are actively dividing after inoculation and do not carry residual CP from stationary phase. Bacteria were analyzed throughout growth at different time points (T_0–T_4) (Fig. 6 and Table S1). On exponentially growing bacteria, no CP was detectable, but upon reaching stationary phase approximately 40% of the population became CP-positive, which is consistent with previous results (George *et al.*, 2015). With SigB

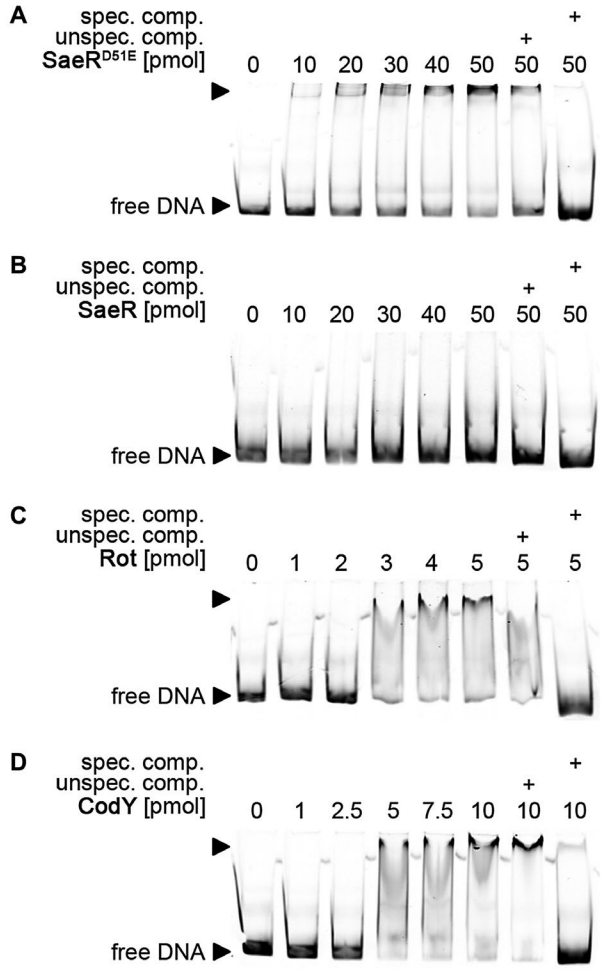

Fig. 5. CodY, Rot and SaeR bind directly to P_{cap} upstream region. Electrophoretic mobility shift assays of purified SaeR^{D51E} (A), SaeR (B), Rot (C) and CodY (D). Increasing amounts of protein were incubated with fluorescently labeled P_{cap} upstream region (–78 to –344 from *capA*, see Fig. 1A). As a control for specificity, shifts were subject to competition with the promoter of the 16 S rRNA gene (unspec. comp.) or unlabeled P_{cap} upstream region (–78 to –344 from *capA*, see Fig. 1A) (spec. comp.) in 100-fold excess. Representative pictures from at least three independently performed experiments are shown.

being a regulator of late genes, we first investigated the effect of constitutive *sigB* expression on CP synthesis during growth. Constitutive *sigB* expression in a *rsbUVWsigB*-negative background resulted in earlier onset of CP production and 50% CP-positive bacteria in stationary phase. In addition, we generated a P_{cap} mutant in which the upstream promoter region containing repressor binding sites was chromosomally deleted (ΔP_{cap} *upstream*, Fig. 1C). Also in this strain, CP production started earlier and 83% CP-positive cells could be detected in the late growth phase. Of note, the effect of the P_{cap} upstream region deletion was more profound than that of constitutive *sigB* expression. Furthermore, IF revealed that in bacteria from stationary phase, much of the heterogeneity is reduced in the ΔP_{cap} *upstream* strain and omitted in combination with constitutive *sigB* expression. Thus, it seems to be the combination of repression via transcriptional regulators and SigB-dependent promoter activity that is responsible for the heterogeneous CP expression pattern in stationary phase.

However, throughout all experiments, CP expression remained growth phase-dependent. We thought that this could be due to the weak SigB promoter of P_{cap}. Therefore, we additionally altered the SigB –10 region to the conserved SigB –10 motif on the chromosome in the P_{cap} upstream-truncated strain *(*ΔP_{cap} *upstream, strong SigB*, Fig. 1C*)*. Together with constitutive *sigB* expression, this shifted the onset of CP even further toward early growth phase. However, the majority of the bacterial population still remained CP-negative in early logarithmic growth phase.

The bacteria analyzed by IF also contained the dual promoter fusion construct pCG742 (P_{asp23}-*gpcer*, P_{cap}-*gpven*) which allowed us to simultaneously analyze SigB activity throughout growth on the single cell level (Fig. 7A). As expected, P_{asp23} and P_{cap} activities reached their maximum in stationary phase cells, confirming growth phase-dependent SigB activity. However, in contrast to P_{cap} activity (yellow), P_{asp23} (blue) activity was already detectable in some bacteria from the exponential growth phase. This indicates that SigB activity itself is also heterogeneous but is not sufficient to activate P_{cap} in the early growth phase.

CP synthesis is also controlled on the post-transcriptional level

To analyze whether growth phase dependency on the CP level correlates to *capA* transcript levels, *capA* mRNA was quantified by qRT-PCR at T_0–T_2 (Fig. 7B). As expected, in the wild-type strain, *capA* expression was strongly repressed in early growth phase. In contrast, constitutive *cap*A expression was achieved in a strain with upstream-deleted P_{cap} promoter, strong SigB consensus sequence and constitutive *sigB* expression (ΔP_{cap} *upstream, strong SigB*, const. *sigB)*, exceeding that of the wild-type. Of note, CP production is still growth phase-dependent under these conditions (Fig. 6), suggesting the existence of post-transcriptional mechanisms regulating CP synthesis.

P_{cap} regulation is conserved in different S. aureus *strains*

So far, all experiments have been performed in strain Newman which is special due to its hyperactive SaeRS system (Mainiero *et al.*, 2010). To validate our findings in a different *S. aureus* background, we chose the

© 2019 The Authors. *Molecular Microbiology* John Wiley & Sons Ltd.,

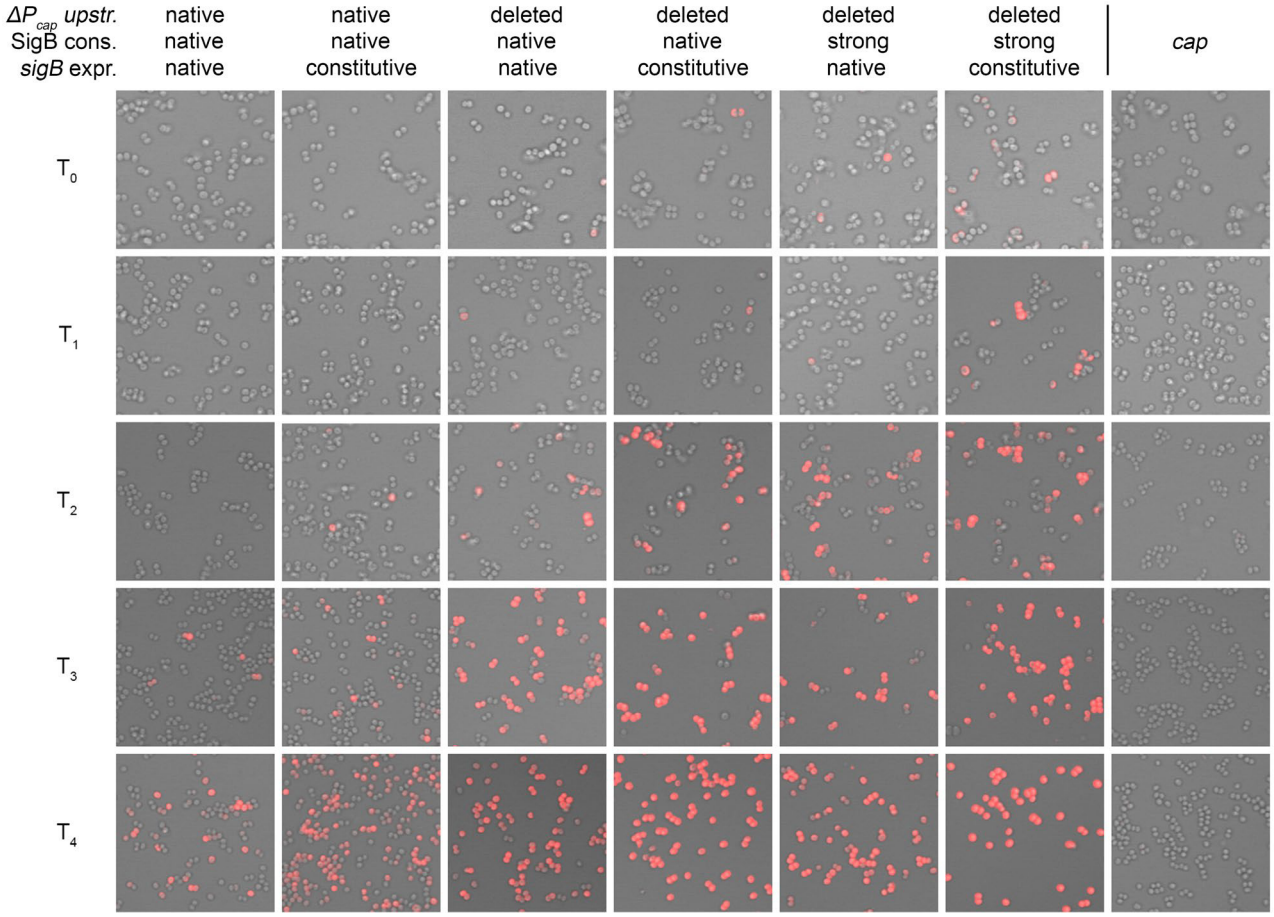

Fig. 6. SigB regulation and upstream repressors determine temporal and heterogeneous CP synthesis. Detection of CP production by bacteria from different growth phases via immunofluorescence. The wild-type strain Newman was mutated in order to delete the upstream region (ΔP_{cap} *upstr.*), to contain a strong SigB –10 consensus motif (SigB cons.) and/or constitutive *sigB* expression (*sigB* expr.) and grown to defined growth phase T_0–T_4. The different genomic P_{cap} variants are described in Fig. 1C. Representative pictures from at least three independent cultures are shown.

widely studied community-acquired methicillin-resistant *S. aureus* strain USA300 JE2. This strain has an acapsular phenotype due to three crucial mutations in the P_{cap} promoter region and in the coding regions of *cap5D* and *cap5E* (Boyle-Vavra *et al.*, 2015). Therefore, we first generated derivatives in which we either only repaired the mutation in P_{cap} (P_{cap} *repaired*) or all three mutations (*cap repaired*) (Fig. 8 and Table S2). In line with previous observations, the USA300 JE2 wild type shows an acapsular phenotype and the repair of the mutation in P_{cap} alone is not sufficient to enable CP production *in vitro* (Boyle-Vavra *et al.*, 2015). Only when all three mutations were repaired, USA300 JE2 was capable of producing CP, following the same peculiar expression pattern as strain Newman: CP-positive cells were observed toward late growth phase and CP expression was highly heterogeneous. Upon deletion of the P_{cap} upstream region and introduction of the fully conserved SigB consensus sequence (*cap repaired*, ΔP_{cap} *upstream, strong SigB*), CP-positive cells were detected earlier and, in late growth phase, all cells were CP-positive. Therefore, the CP expression pattern of USA300 *cap repair* and its regulation closely resembles that of Newman.

Discussion

CP protects *S. aureus* against phagocytosis, but also hampers adherence to endothelial cells and matrix proteins. It is believed that heterogeneity of CP expression has evolved to provide better adaptability of the bacterial population during infection and colonization (George *et al.*, 2015). Apart from this heterogeneous phenotype, CP production is strongly growth phase-dependent, with encapsulated cells found only toward stationary growth phase (George *et al.*, 2015). During the last decades, many regulatory proteins have been shown to have an impact on CP production, forming

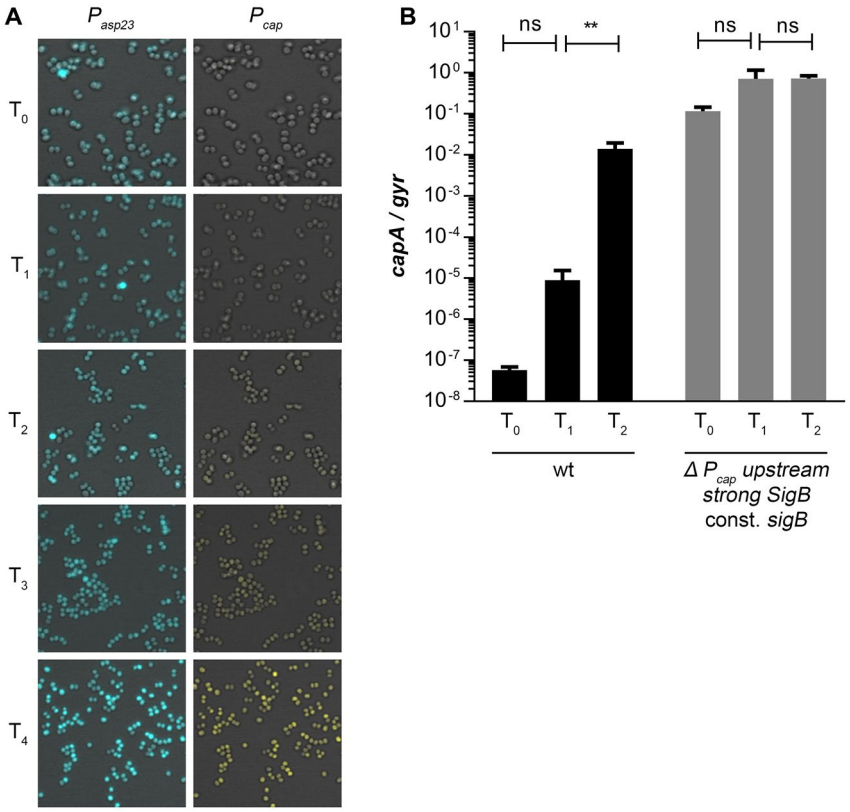

Fig. 7. *capA* transcription can be rendered constitutive.
A. Promoter activities of P_{asp23}-*gpcer* and full-length P_{cap}-*gpven* dual promoter fusion (pCG742, see Fig. 1B) in Newman wild-type. Bacteria cells were grown to defined growth phase T_0–T_4. Representative pictures from at least three independent cultures are shown.
B. Bacterial cells were harvested at different growth phases (T_0–T_2) and total RNA was isolated. *capA* transcripts in Newman wild-type and a P_{cap} upstream truncated strain with strong SigB –10 consensus sequence and additional constitutive *sigB* expression (Newman ΔP_{cap} *upstream, strong SigB*, const. *sigB*) were measured by qRT-PCR and normalized to *gyr*. The genomic P_{cap} variant is described in Fig. 1C. Experiments were performed in biological triplicates, error bars represent the standard deviation. Statistical significance was determined by ordinary one-way ANOVA followed by Tukey's multiple comparison test (ns: not significant, **: $P < 0.01$).

a complex regulatory network. However, to date, it is not known which regulator is mainly responsible for this peculiar expression pattern. Here, we revisited the role of important molecular determinants of P_{cap} activity, summarized in Fig. 9.

cap expression is mainly driven by SigB activity

We show that the main P_{cap} promoter is SigB-dependent. This is based on (i) 5′ RACE results revealing a new TSS downstream of a conserved SigB consensus sequence with minor mismatches in the –10 region; (ii) only very weak promoter activity in a *sigB* mutant or upon mutation of the –10 consensus sequence; (iii) higher P_{cap} activity when the SigB –10 region matches the proposed SigB consensus sequence; and (iv) correlation of P_{asp23} and P_{cap} promoter activity. Of note, the SigB –35 region is directly located within the IR which was shown to be crucial for *cap* expression (Ouyang *et al.*, 1999). Thus, the effects of previously reported mutations in this region can be simply explained by its function as a SigB binding site. A positive effect of SigB on *cap* expression was previously shown. However, it was believed to be mediated via the SigB-dependent *cap* activators SpoVG, ArlRS-MgrA and RsbR (Bischoff *et al.*, 2001; 2004; Meier *et al.*, 2007; Schulthess *et al.*, 2009; Lei and Lee, 2015). Our results highlight the importance of SigB for *cap* expression and clearly demonstrate that its main impact is through direct SigB-dependent promoter activation. Nevertheless, other SigB-dependent *cap* regulators may contribute to the fine tuning of *cap* expression and amplify SigB dependency.

MsaB/CspA activates cap expression by modulating SigB activity

It was previously shown that the SigB –35 consensus sequence functions as binding site for two *cap* activators RbsR and MsaB (Lei and Lee, 2015; Batte *et al.*, 2016). We did not observe an effect of RbsR on P_{cap} activity, neither in wild-type nor in a *sae*-negative

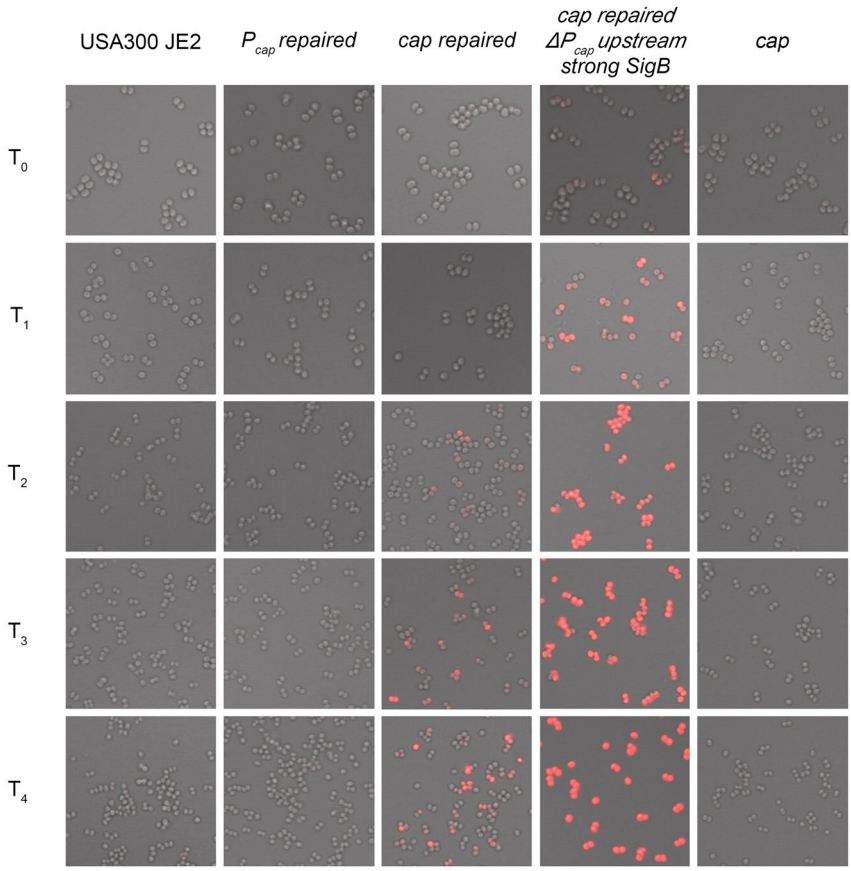

Fig. 8. CP production in strain USA300 JE2. Detection of CP in bacteria from different growth phases. USA300 JE2 wild-type and mutants in which either the mutation in P_{cap} alone (*P_{cap} repaired*) or in the whole *cap* locus (P_{cap}, *capD, capE; cap repaired*) are repaired were grown to defined growth phase T_0–T_4 and CP was detected by immunofluorescence. In addition, the effect of P_{cap} upstream truncation and a strong SigB –10 consensus sequence (*cap repaired, ΔP_{cap} upstream, strong SigB*) was analyzed. This genomic P_{cap} variant is described in Fig. 1C. Representative pictures of at least three independent cultures are shown.

background. RbsR likely functions as metabolic sensor, and thus the discrepancy with the results of Lei and Lee (Lei and Lee, 2015) could be due to differences in growth conditions.

We reproduced the activating effect of MsaB/CspA on *cap* expression, but demonstrated that it is mediated by modulation of SigB activity: *msa* deletion negatively affected P_{cap} and P_{asp23} activities and constitutive expression of *sigB* rendered both promoters insensitive to MsaB/CspA. Moreover, in contrast to Batte *et al.* (2016), no detectable MsaB/CspA binding to P_{cap} was observed, challenging the role of MsaB/CspA as a classical transcription factor. Indeed, it was recently shown that MsaB/CspA binds *rsbVWsigB* mRNA, thereby increasing transcript stability (Caballero *et al.*, 2018). Strong influence of MsaB/CspA on SigB activity is consistent with previous findings that MsaB/CspA increases expression of *sigB* and its target genes (Katzif *et al.*, 2005; Sahukhal and Elasri, 2014; Donegan *et al.*, 2019). With respect to direct P_{cap} regulation, our results indicate that under the conditions employed, the region containing the previously described IR motif functions instead as a promoter for the SigB holoenzyme.

Cap expression is modified by upstream SigA promoter and repressor binding sites

Upstream of the main SigB-dependent promoter we identified an additional weak SigA-dependent promoter with conserved SigA –35 and –10 consensus sequences. However, the SigA-dependent promoter seems to play a minor role in *cap* expression, with its activity being mainly detectable upon deletion of *sae*. The reason for such low promoter activity is unclear and might be due to suboptimal structure and spacing of the SigA consensus in P_{cap}. (Ruff *et al.*, 2015; Browning and Busby, 2016). Furthermore, the average activity of SigA promoters has been found to be generally lower than that of SigB promoters (Mäder *et al.*, 2016). However, for any given promoter sequence, changes in temperature, salt and solute

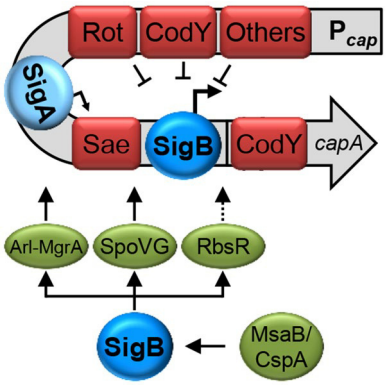

Fig. 9. Transcriptional regulation of *cap* expression. *Cap* expression is mainly driven from a SigB-dependent promoter. However, there is a second weak SigA-dependent promoter further upstream. In addition, the P_{cap} upstream region is targeted by the *cap* repressors SaeR, CodY, Rot and others. Of note, Rot and CodY only interfere with SigB-dependent promoter activity, whereas Sae is able to repress both. A predicted SaeR binding motif is located between the SigA- and SigB-dependent promoters. P_{cap} contains a second CodY binding site reaching into the coding region of *capA*. The depicted binding sites for the upstream regulators (relative to each other and the SigA promoter) are arbitrary and further studies are needed to localize these site(s) and their mechanisms of action. SigB activity is modulated by MsaB/CspA, promoting *sigB* transcript stability. Consequently, MsaB/CspA likely also affects indirect SigB-dependent P_{cap} activation through ArlRS-MgrA, SpoVG and RbsR. However, for RbsR we were unable to prove an activating effect on *cap* expression.

concentrations, as well as protein factors and ligands can affect its kinetics by 10–1000-fold or more (Ruff *et al.*, 2015). Therefore, we cannot rule out that under certain conditions the SigA-dependent promoter gets activated. This may be the case during infections with strains from the USA300 lineage. Among others, USA300 strains carry a point mutation within the SigB consensus motif of P_{cap}. Interestingly, strains harboring only this mutation seem to produce CP under infectious conditions (Mohamed *et al.*, 2019), which might be attributed to activation of the weak SigA-dependent promoter.

Besides containing a SigA-dependent promoter, we observed that the P_{cap} upstream region is of repressive function. *cap* repression was confirmed by promoter activity assays, suggesting that the main function of the upstream promoter region is to reduce SigB-dependent promoter activity. Indeed, there are many transcription factors and TCS known to repress *cap* indirectly via other regulators or directly through direct DNA binding. It is likely that the P_{cap} upstream region is targeted by many of these repressors. Here, we focused on the *cap* repressors SaeR, CodY and Rot for which a direct interaction with the P_{cap} upstream region was demonstrated by EMSAs. While Sae, CodY and Rot all interfered with SigB-dependent promoter activity, only Sae additionally repressed activity of the SigA-dependent promoter. This is in line with a predicted SaeR binding site located between the two promoters (Liu *et al.*, 2016). We hypothesize that the repression of SigB-dependent promoter activity occurs via steric interference, whereas the SigA-dependent promoter activity might be repressed via a roadblock mechanism. Nonetheless, the molecular mechanism for the long-distance effect of Rot and CodY on the SigB-dependent promoter activity remains to be elucidated. One may speculate that secondary structures of the promoter bring these two regulators in close proximity to the SigB consensus motif, allowing them to interfere with SigB binding. It is well known that DNA structural elements like supercoiling are involved in the control of bacterial gene expression (Dorman and Dorman, 2016), and *cap* expression was indeed shown to be supercoiling sensitive (Schröder *et al.*, 2014).

Of note, there are two CodY binding sites within the *cap* locus. One reaching into the coding region of *capA*, consistent with previous findings (Lei and Lee, 2018), and one in the P_{cap} upstream region. Functional assays using truncated promoter fusion constructs indicate that the upstream binding site alone is sufficient for *cap* repression.

SigB activity and upstream repressors determine temporal/heterogeneous CP synthesis

We showed that SigB-dependent regulation and the regulators targeting the upstream region contribute to the temporal pattern of CP production and to its phenotypic heterogeneity. Congruent with SigB being a known activator of late genes (Bischoff *et al.*, 2001; 2004; Pane-Farre *et al.*, 2006; Mäder *et al.*, 2016), we observed earlier onset of CP production and more CP-positive cells in stationary phase upon constitutive *sigB* expression in a *rsbUVWsigB*-negative background. However, the greater impact on temporal and heterogeneous CP production was observed upon deletion of the upstream promoter region resulting in single CP-positive cells already in early exponential growth phase and almost all cells being CP-positive in later growth. The effects of constitutive *sigB* expression and P_{cap} upstream deletion were additive, and only in combination the phenotypic heterogeneity could be completely abolished in stationary growth phase. This suggests that the regulators targeting the upstream region of P_{cap} are mainly responsible for heterogeneous CP production, with the residual heterogeneity resulting from variable SigB activity within cells. These data support the prediction by Sharon *et al.* stating that more transcription factor binding sites result in noisier promoters (Sharon *et al.*, 2014). A similar pattern of CP production was shown in the USA300 background, indicating a conserved regulatory mechanism.

Of note, even upon P_{cap} upstream deletion and constitutive *sigB* expression, CP synthesis remains growth

phase-dependent which is not reflected at the transcriptional level, indicating that further post-transcriptional levels of regulation are in place. These might be required as CP synthesis is linked to the metabolic status of the cell. For instance, UDP N-acetylglucosamine used for CP biosynthesis is mainly derived from gluconeogenesis, which naturally occurs when glucose becomes limited toward later growth phases (Sadykov *et al*., 2010). In addition, CP, peptidoglycan and wall teichoic acids synthesis make use of the universal bactoprenol carrier lipid, which could become limited in earlier growth phases (Campbell *et al*., 2012). This coordination of the different cell wall polymers synthesis was recently shown to involve reversible protein phosphorylation of the capsular biosynthesis gene products CapM and CapE (Rausch *et al*., 2019).

In summary, our results show that CP synthesis is tightly controlled at the transcriptional level. However, post-transcriptional mechanisms are also in place to avoid conflict between precursor usage by the CP synthesis machinery and the synthesis machinery of other cell wall glycopolymers in growing bacterial cells. Further in-depth studies are required to fully understand this regulation and to increase the potential of CP as prospective target for novel anti-infective strategies.

Experimental procedures

Bacterial strains and growth conditions

Strains and plasmids are listed in Tables S3 and S4. For overnight culture, strains were grown in lysogeny broth (LB) medium (low salt) with appropriate antibiotics (10 μg ml^{-1} chloramphenicol (Cm10), 10 μg ml^{-1} erythromycin, 50 μg ml^{-1} kanamycin, 3 μg ml^{-1} tetracycline) at 37°C and 200 rpm. Day cultures were inoculated from overnight cultures to an OD_{600} of 0.05 and were grown without antibiotics at 37°C and 200 rpm.

Growth curves and fluorescence measurements

Overnight cultures were diluted to an OD600 of 0.05 and 200 μl were loaded onto a 96-well U-bottom plate (Greiner Bio-One). Continuous absorbance and fluorescence were monitored with a TECAN Infinite 200 microplate reader every half an hour with shaking at 37°C. Absorbance was measured at 600 ± 9 nm; gpVenus was excited at 505 ± 9 nm and emission was measured at 535 ± 20 nm, and gpCerulean was excited at 434 ± 9 nm and emission was measured at 485 ± 20 nm. Optical densities measured in microplate reader are not linear over the extended growth cycle. To address this problem, we simultaneously measured dilutions of an overnight culture in the plate reader and the Ultrospec™ 2100 pro UV/Vis spectrophotometer (Pharmacia). From the plotted values, a conversion formula was calculated and used to correct the optical densities measured in the microplate reader.

Strain construction

All plasmids and oligonucleotides are listed in Tables S4 and S5, respectively. The transposon mutants Newman *rbsR* and Newman *sae rbsR* were constructed by phage transduction of the transposon insertions from the Nebraska transposon mutant NE425 to Newman and Newman-29 and then verified by PCR.

Strains Newman *msa*, Newman ΔP_{cap} *upstream*, Newman ΔP_{cap} *upstream, strong SigB*, USA300 P_{cap} *repaired*, USA300 *cap repaired* and USA300 ΔP_{cap} *upstream, strong SigB* were created using the temperature-sensitive pIMAY plasmid for allelic exchange (Monk *et al*., 2012). Corresponding homologous regions were PCR amplified as indicated in Table S5 and inserted into the *Eco*RI-linearized pIMAY backbone via Gibson assembly. The resulting plasmids were verified by PCR using primers piMAYcontrolfor and piMAYcontrolrev and sequencing, and then electroporated into strain RN4220 and transduced into the target strains. Allelic exchange was performed as described before (Monk *et al*., 2012) with few alterations. Briefly, a single colony was homogenized in 200 μl of TSB and 50 μl of serial dilutions (10^{-1}–10^{-3}) were plated on TSA-Cm10 and incubated overnight at 37°C. Large colonies were picked and subcultured on TSA-Cm10 at 37°C. Integrants were confirmed via PCR using primers piMAYcontrolfor and piMAYcontrolrev as well as a primer pair flanking the individual homologous regions (Table S5). One integrant colony was used to inoculate an overnight culture in 10 ml TSB grown at 28°C without chloramphenicol, and later plated on TSA containing 0.7–1 μg ml^{-1} anhydrotetracycline. After 48 h of growth at 28°C, colonies were picked on both blood and TSA-Cm10 plates and incubated at 37°C. Cm10-sensitive colonies were screened by PCR with the oligonucleotides mentioned above and by sequencing to identify clones containing the desired mutation.

The *rsbUVWsigB* mutants were obtained using the temperature-sensitive shuttle vector pBASE6 (Geiger *et al*., 2012). Replacement was introduced by creating PCR products using RN6390 as a template and primer pairs MazSIG-for and Hybrid-MazSIG-rev, as well as MazSIGrev and Hybrid-MazSIG-for for the homologous regions. The tetracycline resistance cassette was amplified from pCG75 using primers TetMfor and TetMrev. PCR products were linked using primers BglIIMazSIGfor and SalIMazSIGrev. The obtained amplicon was cloned into *Bgl*II and *Sal*I digested pBASE6. The resulting plasmid pCG331 was introduced into the restriction-deficient strain RN4220 and transduced into *S. aureus* target strains. Mutagenesis was performed as described elsewhere (Bae and Schneewind, 2006). The deletion was verified by PCR with oligonucleotides flanking the deleted region and within the resistance cassette.

For constitutive *sigB* expression under the control of the P_{SarA} promoter, the *sigB* gene including its native ribosomal binding site was amplified from Newman genomic DNA using primers pCG795gibfor and pCG795gibrev and inserted into *Eco*RI and *Asc*I digested pJL78. The resulting plasmid pCG795 was verified via PCR and sequencing prior to electroporation into strain RN9011 and transduction into target strains. Correct insertion into the SaPI site was verified via PCR using primers SaPIintfor and SaPIintrev.

The *sae codY rot* triple mutant was obtained by transduction of the Δ*codY::tetM* mutation from RN4220-21 (Pohl

et al., 2009) into Newman-29, followed by transduction of the *rot::bursa aurealis* transposon insertions from the Nebraska transposon mutant NE386.

For the generation of a *cap* mutant in USA300 JE2, pCG132 was transduced from RN4220 pCG132 (Jansen *et al*., 2013) into USA300 JE2 using phage Φ11.

Promoter fusion constructs

Two tandem sequences, each comprising a promoter of interest (P_{gene}) followed by a strong ribosomal binding site (RBS), genes encoding for fluorescent protein gpVenus (*gpven*) or gpCerulean (*gpcer*) (Liese *et al*., 2013) and a terminator (ter) sequence, were designed *in silico*. Restriction sites were designed to flank both promoter replacements. The entire cassette encompassing P_{cap}-RBS-*gpven*-ter–P_{tagH}-RBS-*gpcer*-ter was also flanked by restriction sites. The dual promoter–reporter protein fusion cassette was synthesized by Life Technologies GmbH and provided in a pUC18-like *E. coli* vector backbone (pMA-RQ, geneart plasmid). The dual promoter–reporter fusion cassette was subcloned into pCG246 (Helle *et al*., 2011) using restriction sites *Sph*I and *Nar*I. The resulting plasmid pCG570 was verified by restriction digestion (*Bam*HI) and using the primers pCG246for, pCG246rev, Pcap_rev and PtagHrev for sequencing. The plasmid pCG570 was introduced into RN4220 and then transduced into strain Newman.

Promoter truncations and mutations were generated with the Q5 Site-Directed Mutagenesis Kit from NEB according to the manufacturer's instructions. All primers used are enlisted in Table S5. For plasmids pCG742, pCG815 and pCG816, P_{tagH} was replaced with P_{asp23} via Gibson cloning. The *asp23* promoter region was amplified from Newman genomic DNA using primers pCG657gibfor and pCG657gibrev and inserted into *Bam*HI and *Eco*RI digested pCG717, pCG719 and pCG769.

RNA isolation

A day culture was inoculated from an overnight culture and grown to an OD_{600} of 0.3. The day culture was then used to inoculate a second day culture to an OD_{600} of 0.05, which was grown to an OD_{600} of 0.3 and used again for subculturing. When the third day culture reached an OD_{600} of 0.3, 10 ml of cell suspension was harvested (T_0). After additional 2 h (T_1) and 4 h (T_2) of growth, 5 ml of *S. aureus* cells were harvested. Cells were lysed in 1 ml TRIzol reagent (Life Technologies, Germany) with 0.5 ml of zirconia–silica beads (0.1 mm diameter) in a high-speed homogenizer. RNA was isolated as described in the instructions provided by the manufacturer of TRIzol (Life Technologies).

5′ Rapid Amplification of cDNA Endings (5′ RACE)

5′ RACE was performed as described previously (Marincola *et al*., 2012) using strain Newman pCG717. Briefly, isolated RNA from T_2 was treated with MICROBExpress (Ambion) in order to remove rRNAs. After treatment with Cap-Clip Phosphatase (Biozym) to remove pyrophosphate at the 5′ prime end of the native transcripts, a specific RNA 5′ adapter (Table S5) was ligated to the RNA. After phenol/chloroform extraction and ethanol precipitation, the RNA was subjected to reverse transcription using oligonucleotide YFPCFPpolymorrev. Nested PCR was performed using oligonucleotides Race2 and Racecapnestedrev (Table S5). The PCR amplicon was cloned into pCRII-TOPO (Invitrogen) following the manufacturer's instructions. Single clones were analyzed via PCR using primers Race2 and Racecapseqrev and the PCR products of 10 clones were sequenced with primer Racecapseqrev.

qRT-PCR

qRT-PCR to quantify *cap* and *gyr* mRNA was performed using the QuantiFast SYBR-Green RT-PCR kit (Qiagen). Standard curves were generated using 10-fold serial dilutions (10^4–10^8 copies) of specific *in vitro*-transcribed RNA standard molecules (Burian *et al*., 2010). The number of copies of each transcript was determined with the aid of the LightCycler software and *cap* mRNA was expressed in reference to copies of *gyrB*.

Protein expression

Plasmid pCWsae106 containing $SaeR^{D51E}$ was created by overlapping PCR employing the oligonucleotides saetetfor1 and 1680l29Gluok as well as 1684U31 and saetetfor1. The amplicon was inserted into pCR2.1. pCWsae106 was then transformed into RN4220 and transduced into strain Newman-29. Coagulase assays were performed to verify the function of the phosphomimetic $SaeR^{D51E}$. Strain Newman-29 pCWsae106 was used as a template to generate the insert for the $SaeR^{D51E}$ expression vector with the primers pCG791gibfor and pCG791gibrev. The amplicon was inserted into *Bam*HI-linearized pET15b via Gibson assembly. All other expression vectors were generated accordingly using primers and template DNA as indicated in Table S5. All vectors were verified via PCR and sequencing using primers pET15bfor and pET15brev.

A 10 ml LB culture containing 100 μg ml^{-1} ampicillin was inoculated with freshly transformed *E. coli* BL21 DE3 cells and incubated for 6 h at 37°C and 200 rpm. For the expression culture, 1 L LB medium supplemented with 100 μg ml^{-1} ampicillin and IPTG or D(+)-lactose monohydrate (for expression conditions see Table S6) was inoculated with 10 ml day culture and incubated at 16°C and 200 rpm overnight (16–18 h). Cells were harvested (20 min, 2000× *g*, 4°C) and resuspended in 30 ml ice-cold HisTrap binding buffer (20 mM Na_2HPO_4, 500 mM NaCl, 40 mM imidazole, pH 7.4, sterile filtered and degassed) supplemented with 10 μg ml^{-1} DNAse (Roth) and cOmplete protease inhibitor cocktail (Roche). Cells were lysed using a French press at 1000 psi. The lysate was centrifuged (236 982× *g*, 45 min, 4°C), and the clear supernatant was filtered (0.22 μm pore size) before being loaded onto a 1 ml HisTrap HP column (GE Healthcare Life Sciences) equilibrated with HisTrap binding buffer. Purification was performed with an ÄKTA purification system (GE Healthcare Life Sciences), and elution was carried out with an imidazole gradient to a final concentration of 500 mM.

For $SaeR^{D51E}$ batch purification using Ni-NTA agarose resin (Qiagen) equilibrated with HisTrap binding buffer was

performed. After incubation for 1 h at constant overhead rotation at 4°C the Ni-NTA agarose was centrifuged at 500× *g* for 2 min at 4°C and washed thrice with 37.5 ml HisTrap binding buffer. Elution was performed at increasing imidazole concentrations (250/300/350/500 mM).

Column and batch fractions were analyzed by SDS-PAGE, and the fractions containing the protein of interest were collected, concentrated and rebuffered into EMSA buffer (10 mM Tris-HCl, 50 mM KCl, 5 mM $MgCl_2$, 10% glycerol, pH 7.4) using Amicon® ultra centrifugal filters (ULTRACEL® 10K/30K) according to the instructions of the manufacturer. To determine the protein concentration of purified proteins, a Pierce™ BCA assay (Thermo Fisher) was performed following the manufacturer's protocol for a microplate procedure. The absorbance was measured with the TECAN Infinite 200 microplate reader. Purified proteins were stored in aliquots at –20°C.

Electrophoretic Mobility Shift Assay (EMSA)

The primers used for EMSAs are listed in Table S5. DNA probes were PCR amplified from strain Newman with fluorescently labeled primers (DY-781, absorption: 783 nm, emission: 800 nm) and purified with the innuPREP PCRpure Kit from Analytik Jena AG according to the manufacturer's instructions. In a volume of 20 µl, 30 fmol DNA probe were mixed with various amounts of protein. For competition experiments, unlabeled DNA fragment with a sequence identical to the labeled probe was used as a specific competitor and a 161 bp DNA fragment containing the promoter of the 16S rRNA gene was used as unspecific competitor. Competitors were obtained via ethanol precipitation after PCR and added in 100-fold excess. After incubation for 20 min at room temperature, samples were analyzed by nondenaturing native 6% TBE polyacrylamide gel electrophoresis at 75 V for 90 min in 1x TBE buffer. The fluorescently labeled DNA probes were visualized in the polyacrylamide gel with the Odyssey® infrared imaging system (LI-COR) and the Image Studio 4.0 software.

IF and promoter fusion microscopy

For synchronization, three subsequent day cultures were inoculated to an OD_{600} of 0.05, grown to an OD_{600} of 0.3 and subcultured twice. When the third subculture reached an OD_{600} of 0.3 (T_0) and after additional 2 h (T_1), 4 h (T_2), 6.5 h (T_3) and overnight growth (T_4) cells were harvested by centrifugation at 3800× *g* for 10 min at 4°C. Roughly 1.3×10^8 bacteria were suspended in 1 ml fixation solution (3.7% formaldehyde in 1x PBS) and incubated with gentle mixing for 15 min at room temperature. Wells of Ibi-treat µ-slide angiogenesis slides (ibidi®) were loaded with 32 µl of cell suspension and centrifuged at 600× *g* for 6 min. The cells were washed with 1 x PBS and protein A was blocked by incubation with pre-adsorbed human serum (diluted 1:10 in 1x PBS/0.1% Tween 20) for 1 h. After blocking, the slides were washed thrice for 5 min each with PBS/Tween 20 followed by incubation with rabbit serum raised against CP5 (1 h, diluted 1:200 in PBS/Tween 20). The slides were washed thrice with PBS/Tween 20 followed by incubation with the secondary antibody Cy3-conjugated F(ab)2 goat-anti-rabbit IgG (Dianova, Hamburg) (diluted 1:500 in PBS/Tween 20, 1 h). For generation of pre-adsorbed human serum and antibody generation, see (George *et al.*, 2015). After washing the cells thrice with PBS/Tween 20 each slide was finally mounted using ibidi® fluorescence mounting medium.

Microscopy images were acquired in the confocal mode of an inverted Zeiss LSM 710 NLO microscope equipped with a spectral detector and a Zeiss Plan-Apochromat 63x/1.40 oil DIC M27 objective and ZEN Black software. The following excitation wavelength, laser sources and detection spectra were used for IF: Cy3: Ex: 561 nm/DPSS laser/Em: 566–702 nm and for promotor activity measurement: gpVenus: Ex: 514 nm/argon laser/Em: 519–554 nm, gpCerulan: Ex: 405 nm/diode laser/Em: 454–516 nm. Additionally, a bright-field image was captured. The images were exported in the single channels or as overlays as 16-bit tagged image files after equal adjustment for gain and color intensity within one experiment. For each image about 100 bacteria as detected by bright field were randomly selected and CP-positive bacteria of the corresponding IF image enumerated. Mean percentage of CP-positive bacteria and standard deviations of three biological replicates is given in Tables S1 and S2.

Acknowledgements

The work was supported by grants from the Deutsche Forschungsgemeinschaft SFB766/A7 to CWo and CWe and GRK1708 to CWo. We thank Isabell Samp, Natalya Korn and Vittoria Bisanzio for excellent technical assistance. We thank Markus Bischoff for fruitful discussions and Jan Liese for providing plasmid pJL78. The mutants NE386 and NE425 from the Nebraska library were obtained through the Network on Antimicrobial Resistance in *Staphylococcus aureus* (NARSA) program. The authors have no conflict of interest to declare.

Author contributions

DK, SG and CWo have made major contributions to the conception and design of the study; DK, AS, ADJ, SG, GM, JL, CWe and CWo have made major contributions to the acquisition, analysis or interpretation of the data; DK and CWo have made major contributions to writing the manuscript.

References

Ansari, S., Jha, R.K., Mishra, S.K., Tiwari, B.R. and Asaad, A.M. (2019) Recent advances in *Staphylococcus aureus* infection: focus on vaccine development. *Infection and Drug Resistance*, **12**, 1243–1255.

Arbeit, R.D., Karakawa, W.W., Vann, W.F. and Robbins, J.B. (1984) Predominance of two newly described capsular polysaccharide types among clinical isolates of

Staphylococcus aureus. *Diagnostic Microbiology and Infectious Disease*, **2**(2), 85–91.
Bae, T. and Schneewind, O. (2006) Allelic replacement in *Staphylococcus aureus* with inducible counter-selection. *Plasmid*, **55**(1), 58–63.
Batte, J.L., Sahukhal, G.S. and Elasri, M.O. (2018) MsaB and CodY interact to regulate *Staphylococcus aureus* capsule in a nutrient-dependent manner. *Journal of Bacteriology*, **200**(17), e00294-00218.
Batte, J.L., Samanta, D. and Elasri, M.O. (2016) MsaB activates capsule production at the transcription level in *Staphylococcus aureus*. *Microbiology*, **162**(3), 575–589.
Bischoff, M., Dunman, P., Kormanec, J., Macapagal, D., Murphy, E., Mounts, W., *et al*. (2004) Microarray-based analysis of the *Staphylococcus aureus* sigmaB regulon. *Journal of Bacteriology*, **186**(13), 4085–4099.
Bischoff, M., Entenza, J.M. and Giachino, P. (2001) Influence of a functional sigB operon on the global regulators *sar* and *agr* in *Staphylococcus aureus*. *Journal of Bacteriology*, **183**(17), 5171–5179.
Boyle-Vavra, S., Li, X., Alam, M.T., Read, T.D., Sieth, J., Cywes-Bentley, C., *et al*. (2015) USA300 and USA500 clonal lineages of *Staphylococcus aureus* do not produce a capsular polysaccharide due to conserved mutations in the *cap5* locus. *MBio*, **6**(2), e02585-02514.
Browning, D.F. and Busby, S.J. (2016) Local and global regulation of transcription initiation in bacteria. *Nature Reviews Microbiology*, **14**(10), 638–650.
Burian, M., Wolz, C. and Goerke, C. (2010) Regulatory adaptation of *Staphylococcus aureus* during nasal colonization of humans. *PLoS ONE*, **5**(4), e10040.
Caballero, C.J., Menendez-Gil, P., Catalan-Moreno, A., Vergara-Irigaray, M., Garcia, B., Segura, V., *et al*. (2018) The regulon of the RNA chaperone CspA and its auto-regulation in *Staphylococcus aureus*. *Nucleic Acids Research*, **46**(3), 1345–1361.
Campbell, J., Singh, A.K., Swoboda, J.G., Gilmore, M.S., Wilkinson, B.J. and Walker, S. (2012) An antibiotic that inhibits a late step in wall teichoic acid biosynthesis induces the cell wall stress stimulon in *Staphylococcus aureus*. *Antimicrobial Agents and Chemotherapy*, **56**(4), 1810–1820.
Cocchiaro, J.L., Gomez, M.I., Risley, A., Solinga, R., Sordelli, D.O. and Lee, J.C. (2006) Molecular characterization of the capsule locus from non-typeable *Staphylococcus aureus*. *Molecular Microbiology*, **59**(3), 948–960.
Conlon, B.P., Rowe, S.E., Gandt, A.B., Nuxoll, A.S., Donegan, N.P., Zalis, E.A., *et al*. (2016) Persister formation in *Staphylococcus aureus* is associated with ATP depletion. *Nature Microbiology*, **1**(5), 16051.
Cunnion, K.M., Lee, J.C. and Frank, M.M. (2001) Capsule production and growth phase influence binding of complement to *Staphylococcus aureus*. *Infection and Immunity*, **69**(11), 6796–6803.
Dassy, B. and Fournier, J.M. (1996) Respiratory activity is essential for post-exponential-phase production of type 5 capsular polysaccharide by *Staphylococcus aureus*. *Infection and Immunity*, **64**(7), 2408–2414.
Dassy, B., Stringfellow, W.T., Lieb, M. and Fournier, J.M. (1991) Production of type 5 capsular polysaccharide by *Staphylococcus aureus* grown in a semi-synthetic medium. *Journal of General Microbiology*, **137**(5), 1155–1162.
Donegan, N.P., Manna, A.C., Tseng, C.W., Liu, G.Y. and Cheung, A.L. (2019) CspA regulation of *Staphylococcus aureus* carotenoid levels and sigma(B) activity is controlled by YjbH and Spx. *Molecular Microbiology*. https://doi.org/10.1111/mmi.14273.
Dorman, C.J. and Dorman, M.J. (2016) DNA supercoiling is a fundamental regulatory principle in the control of bacterial gene expression. *Biophysical Reviews*, **8**(3), 209–220.
Geiger, T., Francois, P., Liebeke, M., Fraunholz, M., Goerke, C., Krismer, B., *et al*. (2012) The stringent response of *Staphylococcus aureus* and its impact on survival after phagocytosis through the induction of intracellular PSMs expression. *PLoS Pathogens*, **8**(11), e1003016.
George, S.E., Nguyen, T., Geiger, T., Weidenmaier, C., Lee, J.C., Liese, J., *et al*. (2015) Phenotypic heterogeneity and temporal expression of the capsular polysaccharide in *Staphylococcus aureus*. *Molecular Microbiology*, **98**(6), 1073–1088.
Gertz, S., Engelmann, S., Schmid, R., Ohlsen, K., Hacker, J. and Hecker, M. (1999) Regulation of sigmaB-dependent transcription of *sigB* and *asp23* in two different *Staphylococcus aureus* strains. *Molecular and General Genetics*, **261**(3), 558–566.
Giachino, P., Engelmann, S. and Bischoff, M. (2001) Sigma(B) activity depends on RsbU in *Staphylococcus aureus*. *Journal of Bacteriology*, **183**(6), 1843–1852.
Gordon, R.J. and Lowy, F.D. (2008) Pathogenesis of methicillin-resistant *Staphylococcus aureus* infection. *Clinical Infectious Diseases*, **46**(Supplement 5), 350–359.
Hartmann, T., Baronian, G., Nippe, N., Voss, M., Schulthess, B., Wolz, C., *et al*. (2014) The catabolite control protein E (CcpE) affects virulence determinant production and pathogenesis of *Staphylococcus aureus*. *Journal of Biological Chemistry*, **289**(43), 29701–29711.
Helle, L., Kull, M., Mayer, S., Marincola, G., Zelder, M.E., Goerke, C., *et al*. (2011) Vectors for improved Tet repressor-dependent gradual gene induction or silencing in *Staphylococcus aureus*. *Microbiology*, **157**(Part 12), 3314–3323.
Herbert, S., Worlitzsch, D., Dassy, B., Boutonnier, A., Fournier, J.M., Bellon, G., *et al*. (1997) Regulation of *Staphylococcus aureus* capsular polysaccharide type 5: CO2 inhibition *in vitro* and *in vivo*. *Journal of Infectious Diseases*, **176**(2), 431–438.
Hochkeppel, H.K., Braun, D.G., Vischer, W., Imm, A., Sutter, S., Staeubli, U., *et al*. (1987) Serotyping and electron microscopy studies of *Staphylococcus aureus* clinical isolates with monoclonal antibodies to capsular polysaccharide types 5 and 8. *Journal of Clinical Microbiology*, **25**(3), 526–530.
Homerova, D., Bischoff, M., Dumolin, A. and Kormanec, J. (2004) Optimization of a two-plasmid system for the identification of promoters recognized by RNA polymerase containing *Staphylococcus aureus* alternative sigma factor B. *FEMS Microbiology Letters*, **232**(2), 173–179.
Jansen, A., Szekat, C., Schröder, W., Wolz, C., Goerke, C., Lee, J.C., *et al*. (2013) Production of capsular

polysaccharide does not influence *Staphylococcus aureus* vancomycin susceptibility. *BMC Microbiology*, **13**, 65.
de Jong, N.W.M., van Kessel, K.P.M. and van Strijp, J.A.G. (2019) Immune evasion by *Staphylococcus aureus*. *Microbiology Spectrum*, **7**(2), GPP3-0061-201.
Karakawa, W.W., Sutton, A., Schneerson, R., Karpas, A. and Vann, W.F. (1988) Capsular antibodies induce type-specific phagocytosis of capsulated *Staphylococcus aureus* by human polymorphonuclear leukocytes. *Infection and Immunity*, **56**(5), 1090–1095.
Katzif, S., Lee, E.H., Law, A.B., Tzeng, Y.L. and Shafer, W.M. (2005) CspA regulates pigment production in *Staphylococcus aureus* through a SigB-dependent mechanism. *Journal of Bacteriology*, **187**(23), 8181–8184.
Killikelly, A., Benson, M.A., Ohneck, E.A., Sampson, J.M., Jakoncic, J., Spurrier, B., *et al*. (2015) Structure-based functional characterization of repressor of toxin (Rot), a central regulator of *Staphylococcus aureus* virulence. *Journal of Bacteriology*, **197**(1), 188–200.
Lee, J.C., Takeda, S., Livolsi, P.J. and Paoletti, L.C. (1993) Effects of *in vitro* and *in vivo* growth conditions on expression of type 8 capsular polysaccharide by *Staphylococcus aureus*. *Infection and Immunity*, **61**(5), 1853–1858.
Lei, M.G. and Lee, C.Y. (2015) RbsR activates capsule but represses the *rbsUDK* operon in *Staphylococcus aureus*. *Journal of Bacteriology*, **197**(23), 3666–3675.
Lei, M.G. and Lee, C.Y. (2018) Repression of capsule production by XdrA and CodY in *Staphylococcus aureus*. *Journal of Bacteriology*, **200**(18), e00203-00218.
Liese, J., Rooijakkers, S.H., van Strijp, J.A., Novick, R.P. and Dustin, M.L. (2013) Intravital two-photon microscopy of host-pathogen interactions in a mouse model of *Staphylococcus aureus* skin abscess formation. *Cellular Microbiology*, **15**(6), 891–909.
Liu, Q., Yeo, W.S. and Bae, T. (2016) The SaeRS two-component system of *Staphylococcus aureus*. *Genes (Basel)*, **7**(10), 81.
Luong, T.T., Sau, K., Roux, C., Sau, S., Dunman, P.M. and Lee, C.Y. (2011) *Staphylococcus aureus* ClpC divergently regulates capsule via *sae* and *codY* in strain Newman but activates capsule via *codY* in strain UAMS-1 and in strain Newman with repaired *saeS*. *Journal of Bacteriology*, **193**(3), 686–694.
Mäder, U., Nicolas, P., Depke, M., Pane-Farre, J., Debarbouille, M., van der Kooi-Pol, M.M., *et al*. (2016) *Staphylococcus aureus* transcriptome architecture: from laboratory to infection-mimicking conditions. *PLoS Genetics*, **12**(4), e1005962.
Mainiero, M., Goerke, C., Geiger, T., Gonser, C., Herbert, S. and Wolz, C. (2010) Differential target gene activation by the *Staphylococcus aureus* two-component system *saeRS*. *Journal of Bacteriology*, **192**(3), 613–623.
Majerczyk, C.D., Dunman, P.M., Luong, T.T., Lee, C.Y., Sadykov, M.R., Somerville, G.A., *et al*. (2010) Direct targets of CodY in *Staphylococcus aureus*. *Journal of Bacteriology*, **192**(11), 2861–2877.
Marincola, G., Schafer, T., Behler, J., Bernhardt, J., Ohlsen, K., Goerke, C., *et al*. (2012) RNase Y of *Staphylococcus aureus* and its role in the activation of virulence genes. *Molecular Microbiology*, **85**(5), 817–832.
Meier, S., Goerke, C., Wolz, C., Seidl, K., Homerova, D., Schulthess, B., *et al*. (2007) sigmaB and the sigmaB-dependent *arlRS* and *yabJ-spoVG* loci affect capsule formation in *Staphylococcus aureus*. *Infection and Immunity*, **75**(9), 4562–4571.
Missiakas, D. and Schneewind, O. (2016) *Staphylococcus aureus* vaccines: deviating from the carol. *Journal of Experimental Medicine*, **213**(9), 1645–1653.
Mohamed, N., Timofeyeva, Y., Jamrozy, D., Rojas, E., Hao, L., Silmon de Monerri, N.C., *et al*. (2019) Molecular epidemiology and expression of capsular polysaccharides in *Staphylococcus aureus* clinical isolates in the United States. *PLoS ONE*, **14**(1), e0208356.
Monk, I.R., Shah, I.M., Xu, M., Tan, M.W. and Foster, T.J. (2012) Transforming the untransformable: application of direct transformation to manipulate genetically *Staphylococcus aureus* and *Staphylococcus epidermidis*. *mBio*, **3**(2), e00277-00211.
O'Riordan, K. and Lee, J.C. (2004) *Staphylococcus aureus* capsular polysaccharides. *Clinical Microbiology Reviews*, **17**(1), 218–234.
Ouyang, S., Sau, S. and Lee, C.Y. (1999) Promoter analysis of the *cap8* operon, involved in type 8 capsular polysaccharide production in *Staphylococcus aureus*. *Journal of Bacteriology*, **181**(8), 2492–2500.
Pane-Farre, J., Jonas, B., Förstner, K., Engelmann, S. and Hecker, M. (2006) The sigmaB regulon in *Staphylococcus aureus* and its regulation. *International Journal of Medical Microbiology*, **296**(4–5), 237–258.
Pohl, K., Francois, P., Stenz, L., Schlink, F., Geiger, T., Herbert, S., *et al*. (2009) CodY in *Staphylococcus aureus*: a regulatory link between metabolism and virulence gene expression. *Journal of Bacteriology*, **191**(9), 2953–2963.
Pohlmann-Dietze, P., Ulrich, M., Kiser, K.B., Döring, G., Lee, J.C., Fournier, J.M., *et al*. (2000) Adherence of *Staphylococcus aureus* to endothelial cells: influence of capsular polysaccharide, global regulator *agr*, and bacterial growth phase. *Infection and Immunity*, **68**(9), 4865–4871.
Portoles, M., Kiser, K.B., Bhasin, N., Chan, K.H. and Lee, J.C. (2001) *Staphylococcus aureus* Cap5O has UDP-ManNAc dehydrogenase activity and is essential for capsule expression. *Infection and Immunity*, **69**(2), 917–923.
Poutrel, B., Gilbert, F.B. and Lebrun, M. (1995) Effects of culture conditions on production of type 5 capsular polysaccharide by human and bovine *Staphylococcus aureus* strains. *Clinical and Diagnostic Laboratory Immunology*, **2**(2), 166–171.
Poutrel, B., Rainard, P. and Sarradin, P. (1997) Heterogeneity of cell-associated CP5 expression on *Staphylococcus aureus* strains demonstrated by flow cytometry. *Clinical and Diagnostic Laboratory Immunology*, **4**(3), 275–278.
Prados, J., Linder, P. and Redder, P. (2016) TSS-EMOTE, a refined protocol for a more complete and less biased global mapping of transcription start sites in bacterial pathogens. *BMC Genomics*, **17**(1), 849.
Rausch, M., Deisinger, J.P., Ulm, H., Müller, A., Li, W., Hardt, P., *et al*. (2019) Coordination of capsule assembly and

cell wall biosynthesis in *Staphylococcus aureus*. *Nature Communications*, **10**(1), 1404.
Roghmann, M., Taylor, K.L., Gupte, A., Zhan, M., Johnson, J.A., Cross, A., *et al*. (2005) Epidemiology of capsular and surface polysaccharide in *Staphylococcus aureus* infections complicated by bacteraemia. *Journal of Hospital Infection*, **59**(1), 27–32.
Ruff, E.F., Record, M.T. Jr. and Artsimovitch, I. (2015) Initial events in bacterial transcription initiation. *Biomolecules*, **5**(2), 1035–1062.
Sadykov, M.R., Mattes, T.A., Luong, T.T., Zhu, Y., Day, S.R., Sifri, C.D., *et al*. (2010) Tricarboxylic acid cycle-dependent synthesis of *Staphylococcus aureus* Type 5 and 8 capsular polysaccharides. *Journal of Bacteriology*, **192**(5), 1459–1462.
Sahukhal, G.S. and Elasri, M.O. (2014) Identification and characterization of an operon, *msaABCR*, that controls virulence and biofilm development in *Staphylococcus aureus*. *BMC Microbiology*, **14**, 154.
Sau, S., Sun, J. and Lee, C.Y. (1997) Molecular characterization and transcriptional analysis of type 8 capsule genes in *Staphylococcus aureus*. *Journal of Bacteriology*, **179**(5), 1614–1621.
Schröder, W., Bernhardt, J., Marincola, G., Klein-Hitpass, L., Herbig, A., Krupp, G., *et al*. (2014) Altering gene expression by aminocoumarins: the role of DNA supercoiling in *Staphylococcus aureus*. *BMC Genomics*, **15**, 291.
Schulthess, B., Meier, S., Homerova, D., Goerke, C., Wolz, C., Kormanec, J., *et al*. (2009) Functional characterization of the sigmaB-dependent *yabJ-spoVG* operon in *Staphylococcus aureus*: role in methicillin and glycopeptide resistance. *Antimicrobial Agents and Chemotherapy*, **53**(5), 1832–1839.
Senn, M.M., Giachino, P., Homerova, D., Steinhuber, A., Strassner, J., Kormanec, J., *et al*. (2005) Molecular analysis and organization of the sigmaB operon in *Staphylococcus aureus*. *Journal of Bacteriology*, **187**(23), 8006–8019.
Sharon, E., van Dijk, D., Kalma, Y., Keren, L., Manor, O., Yakhini, Z., *et al*. (2014) Probing the effect of promoters on noise in gene expression using thousands of designed sequences. *Genome Research*, **24**(10), 1698–1706.
Steinhuber, A., Goerke, C., Bayer, M.G., Döring, G. and Wolz, C. (2003) Molecular architecture of the regulatory locus *sae* of *Staphylococcus aureus* and its impact on expression of virulence factors. *Journal of Bacteriology*, **185**(21), 6278–6286.
Stringfellow, W.T., Dassy, B., Lieb, M. and Fournier, J.M. (1991) *Staphylococcus aureus* growth and type 5 capsular polysaccharide production in synthetic media. *Applied and Environment Microbiology*, **57**(2), 618–621.
Sun, F., Li, C., Jeong, D., Sohn, C., He, C. and Bae, T. (2010) In the *Staphylococcus aureus* two-component system *sae*, the response regulator SaeR binds to a direct repeat sequence and DNA binding requires phosphorylation by the sensor kinase SaeS. *Journal of Bacteriology*, **192**(8), 2111–2127.
Sutra, L., Rainard, P. and Poutrel, B. (1990) Phagocytosis of mastitis isolates of *Staphylococcus aureus* and expression of type 5 capsular polysaccharide are influenced by growth in the presence of milk. *Journal of Clinical Microbiology*, **28**(10), 2253–2258.
Thakker, M., Park, J.S., Carey, V. and Lee, J.C. (1998) *Staphylococcus aureus* serotype 5 capsular polysaccharide is antiphagocytic and enhances bacterial virulence in a murine bacteremia model. *Infection and Immunity*, **66**(11), 5183–5189.
Tuchscherr, L., Löffler, B., Buzzola, F.R. and Sordelli, D.O. (2010) *Staphylococcus aureus* adaptation to the host and persistence: role of loss of capsular polysaccharide expression. *Future Microbiology*, **5**(12), 1823–1832.
Verdier, I., Durand, G., Bes, M., Taylor, K.L., Lina, G., Vandenesch, F., *et al*. (2007) Identification of the capsular polysaccharides in *Staphylococcus aureus* clinical isolates by PCR and agglutination tests. *Journal of Clinical Microbiology*, **45**(3), 725–729.
Weidenmaier, C. and Lee, J.C. (2017) Structure and function of surface polysaccharides of *Staphylococcus aureus*. *Current Topics in Microbiology and Immunology*, **409**, 57–93.

Supporting Information

Additional supporting information may be found online in the Supporting Information section at the end of the article

Revisiting the regulation of the capsular polysaccharide biosynthesis gene cluster in *Staphylococcus aureus*

Daniela Keinhörster, Andrea Salzer, Alejandra Duque-Jaramillo, Shilpa E. George, Gabriella Marincola, Jean C. Lee, Christopher Weidenmaier and Christiane Wolz

Supplementary Information

Fig. S1. RbsR does not affect *cap* expression. Promoter activity of the full-length P_{cap} promoter fusion (pCG717, see Fig. 1B) in Newman wild-type and a *sae* mutant with or without additional *rbsR* mutation. gpVenus intensity is given per OD_{600} after 16 h of growth. Experiments were performed in biological triplicates, error bars represent the standard deviation. Statistical significance was determined by ordinary one-way ANOVA followed by Tukey's multiple comparison test (ns: not significant).

Fig. S2. MsaB/CspA does not function as a transcription factor. Electrophoretic mobility shift assays of purified MsaB/CspA. Increasing amounts of protein were incubated with fluorescently labelled full-length P_{cap} probe (+10 to -344 from *capA*, see Fig. 1A). As a control, competition with the promoter of the 16 S rRNA gene (unspec. comp.) or unlabelled probe (spec. comp.) in 100 fold excess was performed.

Fig. S3. SaeR, Rot and CodY do not bind to the P_{cap} downstream region. Electrophoretic mobility shift assays of purified $SaeR^{D51E}$ (A), SaeR (B), Rot (C) and CodY (D, E). Increasing amounts of protein were incubated with fluorescently labelled P_{cap} downstream region (+10 to -77 from *capA*, see Fig. 1A) (A-D) or a 3' extended downstream fragment reaching into the *capA* coding region (+160 to -152 from *capA*, see Fig. 1A) (E). As a control for specificity, shifts were subject to competition with the promoter of the 16 S rRNA gene (unspec. comp.) or unlabelled probe (spec. comp.) in 100 fold excess. Representative pictures from at least three independently performed experiments are shown.

Table S1. Mean percentage of CP-positive bacteria in Newman background. Mean percentage of CP-positive bacteria and standard deviations of three biological replicates is given.

Table S2. Mean percentage of CP-positive bacteria in USA300 JE background. Mean percentage of CP-positive bacteria and standard deviations of three biological replicates is given.

Table S3. Strains. Bacterial strains used in this study.

Table S4. Plasmids. Plasmids used in this study.

Table S5. Oligonucleotides. Oligonucleotides used in this study.

Table S6. Protein expression conditions. Conditions applied for protein expression.

Fig. S1

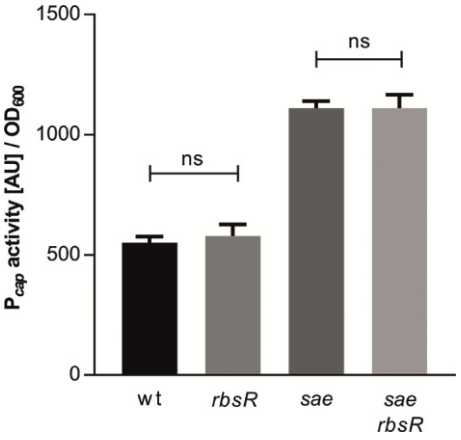

Fig. S2

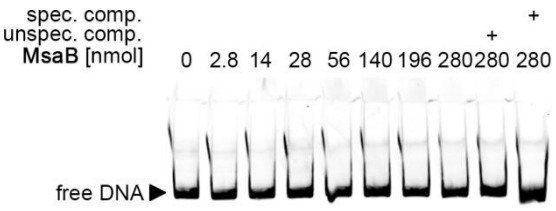

Fig. S3

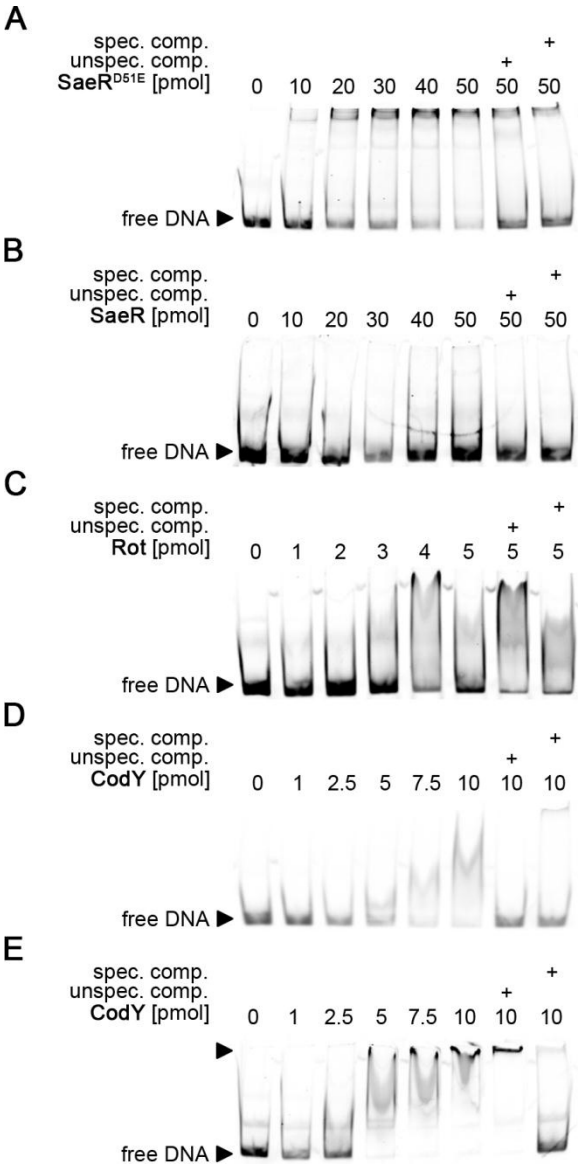
A
spec. comp.
unspec. comp.
SaeR^D51E [pmol]
0 10 20 30 40 50 + 50 + 50
free DNA
B
spec. comp.
unspec. comp.
SaeR [pmol]
0 10 20 30 40 50 + 50 + 50
free DNA
C
spec. comp.
unspec. comp.
Rot [pmol]
0 1 2 3 4 5 + 5 + 5
free DNA
D
spec. comp.
unspec. comp.
CodY [pmol]
0 1 2.5 5 7.5 10 + 10 + 10
free DNA
E
spec. comp.
unspec. comp.
CodY [pmol]
0 1 2.5 5 7.5 10 + 10 + 10
free DNA

Table S1. Mean percentage of CP-positive bacteria in Newman background. Mean percentage of CP-positive bacteria and standard deviations of three biological replicates is given.

	Newman wild-type	const. *sigB*	ΔP_{cap} *upstream*	ΔP_{cap} *upstream,* const. *sigB*	ΔP_{cap} *upstream strong SigB*	ΔP_{cap} *upstream strong SigB,* const. *sigB*
T_0	0 (± 0)	0 (± 0)	1.01 (± 1.75)	5.94 (± 5.92)	0.86 (± 1.48)	26.88 (± 7.08)
T_1	0 (± 0)	0.27 (± 0.46)	0.75 (± 0.65)	4.30 (± 1.95)	0.77 (± 0.75)	17.4 (± 0.44)
T_2	0 (± 0)	3.34 (± 1.35)	33.23 (± 5.20)	40.97 (± 7.59)	53.32 (± 16.14)	63.83 (± 7.37)
T_3	0.91 (± 0.89)	10.37 (± 3.10)	54.70 (± 5.54)	78.67 (± 7.16)	60.15 (± 7.41)	94.29 (± 7.72)
T_4	39.78 (± 3.41)	49.62 (± 7.46)	83.25 (± 8.89)	92.87 (± 5.91)	98.52 (± 0.22)	95.01 (± 4.33)

Table S2. Mean percentage of CP-positive bacteria in USA300 JE background. Mean percentage of CP-positive bacteria and standard deviations of three biological replicates is given.

	USA300 JE2	P_{cap} *repaired*	*cap repaired*	*cap repaired* ΔP_{cap} *upstream strong SigB*
T_0	0 (± 0)	0 (± 0)	0 (± 0)	9.57 (± 4.99)
T_1	0 (± 0)	0 (± 0)	0 (± 0)	58.87 (± 20.59)
T_2	0 (± 0)	0 (± 0)	9.87 (± 1.71)	94.85 (± 5.05)
T_3	0 (± 0)	0 (± 0)	25.65 (± 3.95)	95.24 (± 0.72)
T_4	0 (± 0)	0 (± 0)	41.40 (± 1.68)	99.38 (± 1.07)

Table S3. Strains. Bacterial strains used in this study.

Strain[1]	**Description**	**Reference**
E.coli		
OneShot, Top10	Competent *E. coli* for plasmid transformation	Invitrogen
DC10B	Competent *E. coli* DH10B*Δdcm* for plasmid transformation	NEB
BL21 DE3	T7 expression *E. coli* strain for protein overexpression	NEB

S. aureus		
RN4220	Restriction-deficient derivate of 8325-4	(Kreiswirth *et al.*, 1983)
RN6390	Laboratory strain related to 8325-4	(Peng *et al.*, 1988)
RN9011	RN4220 with SaPI-1integrase gene cloned in plasmid vector (ppRN7023)	(Charpentier *et al.*, 2004)
Newman	wild-type	(Duthie and Lorenz, 1952)
IK184 (*sigB)*	Newman, *ΔrsbUVWsigB::erm*	(Kullik *et al.*, 1998)
NE425	USA300, *rbsR*::*bursa aurealis*, Nebraska Transposon Mutant Library	(Fey *et al.*, 2013)
NE386	USA300, *rot*::*bursa aurealis*, Nebraska Transposon Mutant Library	(Fey *et al.*, 2013)
Newman *rbsR* (*rbsR*)	Newman*, rbsR::bursa aurealis*	this work
Newman-29 (*sae*)	Newman, *ΔsaePQRS::kana*	(Mainiero *et al.*, 2010)
Newman-29 *rbsR* *(sae rbsR)*	Newman, *ΔsaePQRS::kana, rbsR*::*bursa aurealis*	this work
Newman-784 (*msa*)	Newman, *ΔmsaABCR*	this work
Newman-331 (*rsbUVWsigB*)	Newman, *ΔmazEFrsbUVWsigB::tetM*	this work
Newman-331-795 (const. *sigB*)	Newman, *ΔmazEFrsbUVWsigB::tetM, SaPI::P_{sarA}-sigB*	this work
Newman-784-331-795 (*msa*, const. *sigB*)	Newman, *ΔmsaABCR, ΔmazEFrsbUVWsigB::tetM, SaPI:: P_{sarA}-sigB*	this work
Newman-21 (*codY*)	Newman, *ΔcodY::tetM*	(Pohl *et al.*, 2009)
Newman *rot* *(rot)*	Newman, *rot*::*bursa aurealis*	(George *et al.*, 2015)
Newman-29-21 *rot* (*sae codY rot*)	Newman, *ΔsaePQRS::kana, ΔcodY::tetM, rot*::*bursa aurealis*	this work
Newman-786 (*ΔP_{cap} upstream*)	Newman, *ΔP_{cap} upstream*	this work

Newman-786-331-795 (*ΔP$_{cap}$ upstream,* const. *sigB*)	Newman, *ΔP$_{cap}$ upstream, ΔmazEFrsbUVWsigB::tetM, SaPI:: P$_{sarA}$-sigB*	this work
Newman-740 (*ΔP$_{cap}$ upstream, strong SigB*)	Newman, *ΔP$_{cap}$ upstream strong sigB*	this work
Newman-740-331-795 (*ΔP$_{cap}$ upstream, strong SigB,* const. *sigB*)	Newman, *ΔP$_{cap}$ upstream strong sigB, ΔmazEFrsbUVWsigB::tetM, SaPI:: P$_{sarA}$-sigB*	this work
Newman-132 (*cap*)	Newman, pMUTIN integrated into capsule promoter P$_{cap}$	(Jansen *et al.*, 2013)
USA300 JE2	USA300 LAC cured of all 3 native plasmids	(Nuxoll *et al.*, 2012)
USA300-606 (*P$_{cap}$ repaired)*	USA300 JE2, *P$_{cap}$ repaired*	this work
USA300-cr (*cap repaired)*	USA300 JE2, *P$_{cap}$ & capDE repaired*	this work
USA300-740 (*cap repaired*, *ΔP$_{cap}$ upstream, strong SigB*)	USA300-cr, *ΔP$_{cap}$ upstream strong sigB*	this work
USA300-132 (*cap*)	USA300 JE2, pMUTIN integrated into capsule promoter P$_{cap}$	this work

[1]Strain designation used in the manuscript are indicated in brackets

Table S4. Plasmids. Plasmids used in this study.

Plasmids	Description	Reference
pCR2.1	Vector for cloning of Taq-amplified PCR products	Invitrogen
pJL78	P$_{sarA}$-sod-*gfpmut2*, integrative plasmid (SaPI site)	gift from Jan Liese
pCG75	pCR2.1 vector with a tet(M) resistant cassette of strain RN6911	(Geiger *et al.*, 2012)
pCG246	*cat bla*, *E. coli/Staphylococcus* shuttle vector, pCN47 derivative	(Helle *et al.*, 2011)
pCG570	Full-length P$_{cap}$-*gpven*, P$_{tagH}$-*gpcer* in pCG246 background	this work
pCG717	Full-length P$_{cap}$-*gpven*, P$_{tagH}$-*gpcer* in pCG570 background	this work
pCG742	P$_{cap}$-*gpven*, P$_{asp23}$-*gpcer* in pCG717 background	this work
pCG720	Downstream truncated (Δ(-1)-(-21) from *capA* ATG) P$_{cap}$-*gpven*, P$_{tagH}$-*gpcer* in pCG717 background	this work

pCG722	Downstream truncated (Δ(-1)-(-77) from *capA* ATG) P_{cap}-*gpven*, P_{tagH}-*gpcer* in pCG717 background	this work
pCG719	Upstream truncated (Δ(-78)-(-344) from *capA* ATG) P_{cap}-*gpven*, P_{tagH}-*gpcer* in pCG717 background	this work
pCG723	Mutated (G-56T from *capA* ATG) P_{cap}-*gpven*, P_{tagH}-*gpcer* in pCG717 background	this work
pCG724	Mutated (A-58G, T-57G, A-53T from *capA* ATG) P_{cap}-*gpven*, P_{tagH}-*gpcer* in pCG717 background	this work
pCG769	Upstream truncated (Δ(-78)-(-344) from *capA* ATG) P_{cap}-*gpven*, P_{tagH}-*gpcer* in pCG724 background	this work
pCG815	P_{cap}-*gpven*, P_{asp23}-*gpcer* in pCG719 background	this work
pCG816	P_{cap}-*gpven*, P_{asp23}-*gpcer* in pCG769 background	this work
pCG746	Mutated (G-73C from *capA* ATG) P_{cap}-*gpven*, P_{tagH}-*gpcer* in pCG717 background	this work
pBASE6	Suicide mutagenesis vector	(Geiger *et al.*, 2012)
pCG331	pBASE6 vector with flanking regions of *mazEFrsbUVWsigB* flanking *tetM*	this work
pIMAY	Temperature-sensitive plasmid for allelic exchange	(Monk *et al.*, 2012)
pCG784	pIMAY vector with flanking regions of *msaABCR*	this work
pCG786	pIMAY vector with flanking regions of P_{cap} *upstream*	this work
pCG740	pIMAY vector with flanking regions of P_{cap} *upstream* and a strong SigB consensus sequence	this work
pCG606	pIMAY vector with P_{cap} as in Newman wild-type	this work
pCG630	pIMAY vector with *capD* and *capE* as in Newman wild-type	this work
pCG795	Replacement of sod-*gfpmut2* with *sigB* plus native RBS in pJL78	this work
pET-15b	Vector for expression of N-terminal histidine-tagged proteins in *E. coli*	Novagen
pCG755	Protein expression plasmid for CodY based on pET-15b	this work
pCG756	Protein expression plasmid for Rot based on pET-15b	this work
pCG791	Protein expression plasmid for SaeR based on pET-15b	this work
pcwsae106	pCR2.1 vector containing $SaeR^{D51E}$	
pCG811	Protein expression plasmid for $SaeR^{D51E}$ based on pET-15b	this work
pCG812	Protein expression plasmid for MsaB based on pET-15b	this work

Table S5. Oligonucleotides. Oligonucleotides used in this study.

Purpose	Template	Name	Sequence[1]
5' RACE			
		RNA 5′ adapter	CTAGTACTCCGGTATTGCGGTACCCTTG TACGCCTGTTTTATA
		YFPCFPpolymorrev	TGTGTGAGTTATAGTTGTATTCCAATT
		Race2	GTATTGCGGTACCCTTGT
		Racecapnestedrev	GCATTGAAGACCATATCCAAGAGT
		Racecapseqrev	TTTCCAGTAGTGCAAATAAG
Transposon mutants			
	Newman *rbsR*	Tnbuster	GCTTTTTCTAAATGTTTTTTAAGTAAATC AAGTAC
		Tnupstream	CTCGATTCTATTAACAAGGG
		rbsRfor	CCACCTTGATATTCATTTGT
		rbsRrev	ACAATAAAAGTCATTCACGT
Promoter fusions			
pCG570		pCG246for	GCGTCAGACCCCGTAGAAAA
		pCG246rev	TCAAGTCCAACCAACTCGCT
		Pcap_rev	CGTACTTTCCAATATTTACCTCCCT
		PtagHrev	AAAACCTGTTGTAAAGTGTATAGAAGA
pCG717	pCG570	pCG717Q5mutfor	GTCGACTTAGGAGGATGATTATTTATG
		pCG717Q5mutrev	TTAAAAATTTTCATTAAAATTGGTATTAT ATATATAGTATTTAC
pCG720	pCG717	pCG717Q5mutfor	GTCGACTTAGGAGGATGATTATTTATG
		PcapRNASeqTSS+20 rev	TTAAAAATTTTCATTAAAATTGGTATTAT ATATATAGTATTTAC
pCG722	pCG717	pCG717Q5mutfor	GTCGACTTAGGAGGATGATTATTTATG
		pCG722Q5mutrev	ATTAATTACTTTTAAACCGCATTATTTTC
pCG719	pCG717	pCG632Q5mutfor	TGTTTAAACGATATGTAATATGTAAATAC
		pCG632Q5mutrev	TTATTGCTTATAATCATATGATGTTTG
pCG723	pCG717	pCG715Q5mutfor	TATGTAATATtTAAATACTATATATATAAT ACCAATTTTAATG
		pCG715Q5mutrev	TCGTTTAAACAATTAATTACTTTTAAAC
pCG724	pCG717	pCG669Q5mutfor	GATATGTAATgggtatATACTATATATATAA TACCAATTTTAATG
		pCG669Q5mutrev	GTTTAAACAATTAATTACTTTTAAACC

pCG769	pCG724	pCG769Q5mutfor	TGTTTAAACGATATGTAATGG
		pCG632Q5mutrev	TTATTGCTTATAATCATATGATGTTTG
pCG746	pCG717	pCG746Q5mutfor	ATTAATTGTTcAAACGATATGTAATATGT AAATAC
		pCG746Q5mutrev	TACTTTTAAACCGCATTATTTTC
pCG742	Newman wild-type	pCG657gibfor	TATCAAGCAAAGTGACAGGGATCCTGG ATTATACAAAGACTTCG
		pCG657gibrev	CATAAATAATCATCCTCCTAAGGAATTCT TGATGAATTAACTCCATCGA
pCG815	Newman wild-type	pCG657gibfor	TATCAAGCAAAGTGACAGGGATCCTGG ATTATACAAAGACTTCG
		pCG657gibrev	CATAAATAATCATCCTCCTAAGGAATTCT TGATGAATTAACTCCATCGA
pCG816	Newman wild-type	pCG657gibfor	TATCAAGCAAAGTGACAGGGATCCTGG ATTATACAAAGACTTCG
		pCG657gibrev	CATAAATAATCATCCTCCTAAGGAATTCT TGATGAATTAACTCCATCGA
Mutagenesis			
pCG331	RN6390	MazSIG-for	AGTAGCACGTCATTTAATGGAAA
		Hybrid-MazSIG-rev	TTGGGTTGCCTTTGTTTCTTGCTGACCA TATTATTTTAACA
		MazSIG-rev	ACCTTTCATTGGAGGTTGCAG
		Hybrid-MazSIG-for	CTACCTGTAACCTTCGAGTGTATAATGA AAAATCCATAT
		BglIIMazSIGfor	CCCAGATCTTGATAAAGCGATACAACAC
		SalIMazSIGrev	CCCGTCGACATCGCCTCTAAAATATAA
	pCG75	TetMfor	CAAGAAACAAAGGCAACCC
		TetMrev	CACTCGAAGGTTACAGGTA
pCG784	Newman wild-type	pCG784gibfor1	TATCGATAAGCTTGATATCGAGTTTGGA TTATCAATTCAATATGGCT
		pCG784gibrev1	GGTCTTTAATATTTCATGATGCTTGTTTA AAGTGTGG
		pCG784gibfor2	GCATCATGAAATATTAAAGACCCCTTCC ATACTTCA
		pCG784gibrev2	TGGATCCCCCGGGCTGCAGGGCTTTAA ATCAGCGATTAATGTTCGT
		pCG784seqfor	TGCAAAAGCCTTCTGTGTTT
		msaABCRoutfor	TCAATGGTAAACGCTACCCG
		msaABCRoutrev	GTGGATGGCTTTCTTTGAAACT
		piMAYcontrolfor	CCAGCCCCCTCACTACAT

		piMAYcontrolrev	ATCACCCGACGCACTTTG
pCG786	Newman wild-type	pCG740gibfor1	TATCGATAAGCTTGATATCGTGACGTTG CAATTATTGACCCT
		pCG740gibrev1	TCGTTTAAACATTATTGCTTATAATCATA TGATGTTTGA
		pCG786gibfor2	ATAAGCAATAATGTTTAAACGATATGTAA TATGT
		pCG786gibrev2	TGGATCCCCCGGGCTGCAGGTTCTCTA CATCTTCTTCATCT
		caphighseqrev	TATTACTTTGAACCTCTTGC
		caphighoutfor	ATTTTCAAGGTGCCTGCTCA
		cap5Aoutsiderev	TTGACATAAGTAGCAACCATCCTT
pCG740	Newman wild-type	pCG740gibfor1	TATCGATAAGCTTGATATCGTGACGTTG CAATTATTGACCCT
		pCG740gibrev1	TCGTTTAAACATTATTGCTTATAATCATA TGATGTTTGA
		pCG740gibfor2	ATAAGCAATAATGTTTAAACGATATGTAA TGGGTATATACTATATATATAATACC
		pCG740gibrev2	TGGATCCCCCGGGCTGCAGGTTCTCTA CATCTTCTTCATCTTTAATTCG
		caphighseqrev	TATTACTTTGAACCTCTTGC
		caphighoutfor	ATTTTCAAGGTGCCTGCTCA
		cap5Aoutsiderev	TTGACATAAGTAGCAACCATCCTT
pCG606	Newman wild-type	USA300Pcaprepgibfor	TCGATAAGCTTGATATCGGCACACTCAA TTGCGCATAA
		USA300Pcaprepgibrev	GATCCCCCGGGCTGCAGGATTCTTTCT CTACATCTTCTTCATCT
		USA300Pcaprepseqfor	TCAGAGAGATACAAACTAGACAATCA
		Pcapoutsidefor	AACGCATCAACTTTGGCTGG
		cap5Aoutsiderev	TTGACATAAGTAGCAACCATCCTT
pCG630	Newman wild-type	USA300cap5DErepgib for	TCGATAAGCTTGATATCGTGATTTTAATA GGTGGCTCAAGGT
		USA300cap5DErepgib rev	GATCCCCCGGGCTGCAGGACTATAATT TAAATCTCTGGAGTCTGCC
		USA300cap5Dseqrev	AGCTCCCATGACATTAGGCG
		USA300cap5Dseq2rev	TCGCTTCAACTTCATTACATTTCA
		USA300cap5Eseqrev	GGATACGCTGCCTTATCTGT
		USA300cap5DEoutfor	GCAGCTATATCACTATTCATATCGC
		cap5Eoutsiderev	TCAACGTCAATCTCTCCTATCTCA

pCG795		pCG795gibfor	GTATCGAGCAAGATGCATCGAATTCTGAAGTCACAGTATATAAAGAATC
		pCG795gibrev	ATTTATTATGCATTTAGAATAGGCGCGCCCTATTGATGTGCTGCTTC
		gfpcontrolfor	TTCTTTCCTGCGTTATCC
		pCNseqrev	CAAAATTATACATGTCAACGA
		SigB-DIG-rev	GTATGATTTCTCGTTCGC
		sapiintfor	CATTAACTTGAGGGAGTGGG
		sapiintrev	GGCAGAGGCCATATATCTG
Protein purification			
		pET15bfor	TGAGCGGATAACAATTCCCC
		pET15brev	CTCAAGACCCGTTTAGAGGC
pcwsae106	Newman wild-type	saetetfor1	CTTTGAATTCAGAGGTCGTAAGAACAGAGG
		1680l29gluok	CTTCTGGCATCATGATtTCAAGTACCATG
		1684U31	GTACTTGAAATCATGATGCCAGAAGTTAATG
		saetetrev	TATTGAATTCGAAGTTAAGGCACGTCCT
pCG755	Newman wild-type	pCG755gibfor	GCGGCAGCCATATGCTCGAGATGAGCTTATTATCTAAAACGAGAGAGT
		pCG755gibrev	TCGGGCTTTGTTAGCAGCCGTTATTTACTTTTTTCTAATTCATCT
pCG756	Newman wild-type	pCG756gibfor	GCGGCAGCCATATGCTCGAGATGAAAAAAGTAAATAACGACACTGT
		pCG756gibrev	TCGGGCTTTGTTAGCAGCCGTTACACAGCAATAATTGCGT
pCG791	Newman wild-type	pCG791gibfor	GCGGCAGCCATATGCTCGAGATGACCCACTTACTGATCGTGG
		pCG791gibrev	TCGGGCTTTGTTAGCAGCCGTTATCGGCTCCTTTCAAATT
pCG811	Newman sae::kana pCWsae106	pCG791gibfor	GCGGCAGCCATATGCTCGAGATGACCCACTTACTGATCGTGG
		pCG791gibrev	TCGGGCTTTGTTAGCAGCCGTTATCGGCTCCTTTCAAATT
pCG812	Newman wild-type	pCG812gibfor	GCGGCAGCCATATGCTCGAGATGAAACAAGGTACAGTTAAATGGT
		pCG812gibrev	TCGGGCTTTGTTAGCAGCCGTTATAGTTTAACAACGTTTGCAGCT

EMSA			
unspec. competitor	Newman wild-type	P16S1	TAAAATGTATAATTAATTCTTGTCGG
		P16S2	AGGATCAAACTCTCCATAAAAATTA
Upstream region	Newman wild-type	PcapGSlong800for	TCTATCTGATAATAATCATCTAACTCA, 5' modification DY-781
		PcapupstreamGS800 rev	ATTAATTACTTTTAAACCGCATTATTTTC 5' modification DY-781
		PcapGSlongfor	TCTATCTGATAATAATCATCTAACTCA
		pCG722Q5mutrev	ATTAATTACTTTTAAACCGCATTATTTTC
Downstream region	Newman wild-type	PcapdownstreamGS 800for	TGTTTAAACGATATGTAATATGTAAATAC 5' modification DY-781
		PcapGS800rev	TACTTTCCATTATTTACCTCCCT 5' modification DY-781
		pCG632Q5mutfor	TGTTTAAACGATATGTAATATGTAAATAC
		PcapGSrev	TACTTTCCATTATTTACCTCCCT
Downstream region into capA	Newman wild-type	PcapdownstreamGS 800for	TGTTTAAACGATATGTAATATGTAAATAC 5' modification DY-781
		capAGS800rev	GATTCACTAAAATTTGAGTATTAGCTT 5' modification DY-781
		pCG632Q5mutfor	TGTTTAAACGATATGTAATATGTAAATAC
		capAGSrev	GATTCACTAAAATTTGAGTATTAGCTT
Fulllength P_{cap}	Newman wild-type	PcapGSlong800for	TCTATCTGATAATAATCATCTAACTCA 5' modification DY-781
		PcapGS800rev	TACTTTCCATTATTTACCTCCCT 5' modification DY-781
		PcapGSlongfor	TCTATCTGATAATAATCATCTAACTCA
		PcapGSrev	TACTTTCCATTATTTACCTCCCT

[1] small letters indicate point mutation

Table S6. Protein expression conditions. Conditions applied for protein expression.

Protein	**Temperature**	**IPTG induction**	**Lactose induction**	**Purification method**
CodY	16°C	0.2 mM	-	column
Rot	16°C	-	12.5 g/L	column
SaeR	16°C	-	12.5 g/L	column
$SaeR^{D51E}$	16°C	1.0 mM, induction at OD_{600} 0.6	-	batch
MsaB/CspA	16°C	0.5 mM	-	column

References

Charpentier E., Anton A.I., Barry P., Alfonso B., Fang Y., Novick R.P. (2004) Novel cassette-based shuttle vector system for gram-positive bacteria. *Appl Environ Microbiol*, 70(10), 6076-6085.

Duthie E.S., Lorenz L.L. (1952) Staphylococcal coagulase; mode of action and antigenicity. *J Gen Microbiol*, 6(1-2), 95-107.

Fey P.D., Endres J.L., Yajjala V.K., Widhelm T.J., Boissy R.J., Bose J.L., Bayles K.W. (2013) A genetic resource for rapid and comprehensive phenotype screening of nonessential *Staphylococcus aureus* genes. *MBio*, 4(1), e00537-00512.

Geiger T., Francois P., Liebeke M., Fraunholz M., Goerke C., Krismer B.*, et al.* (2012) The stringent response of *Staphylococcus aureus* and its impact on survival after phagocytosis through the induction of intracellular PSMs expression. *PLoS Pathog*, 8(11), e1003016.

George S.E., Nguyen T., Geiger T., Weidenmaier C., Lee J.C., Liese J., Wolz C. (2015) Phenotypic heterogeneity and temporal expression of the capsular polysaccharide in *Staphylococcus aureus*. *Mol Microbiol*, 98(6), 1073-1088.

Helle L., Kull M., Mayer S., Marincola G., Zelder M.E., Goerke C.*, et al.* (2011) Vectors for improved Tet repressor-dependent gradual gene induction or silencing in *Staphylococcus aureus*. *Microbiology*, 157(Part 12), 3314-3323.

Jansen A., Szekat C., Schröder W., Wolz C., Goerke C., Lee J.C.*, et al.* (2013) Production of capsular polysaccharide does not influence *Staphylococcus aureus* vancomycin susceptibility. *BMC Microbiol*, 13, 65.

Kreiswirth B.N., Lofdahl S., Betley M.J., O'Reilly M., Schlievert P.M., Bergdoll M.S., Novick R.P. (1983) The toxic shock syndrome exotoxin structural gene is not detectably transmitted by a prophage. *Nature*, 305(5936), 709-712.

Kullik I., Giachino P., Fuchs T. (1998) Deletion of the alternative sigma factor sigmaB in *Staphylococcus aureus* reveals its function as a global regulator of virulence genes. *J Bacteriol*, 180(18), 4814-4820.

Mainiero M., Goerke C., Geiger T., Gonser C., Herbert S., Wolz C. (2010) Differential target gene activation by the *Staphylococcus aureus* two-component system *saeRS*. *J Bacteriol*, 192(3), 613-623.

Monk I.R., Shah I.M., Xu M., Tan M.W., Foster T.J. (2012) Transforming the untransformable: application of direct transformation to manipulate genetically *Staphylococcus aureus* and *Staphylococcus epidermidis*. *MBio*, 3(2), e00277-00211.

Nuxoll A.S., Halouska S.M., Sadykov M.R., Hanke M.L., Bayles K.W., Kielian T.*, et al.* (2012) CcpA regulates arginine biosynthesis in *Staphylococcus aureus* through repression of proline catabolism. *PLoS Pathog*, 8(11), e1003033.

Peng H.L., Novick R.P., Kreiswirth B., Kornblum J., Schlievert P. (1988) Cloning, characterization, and sequencing of an accessory gene regulator (*agr*) in *Staphylococcus aureus*. *J Bacteriol*, 170(9), 4365-4372.

Pohl K., Francois P., Stenz L., Schlink F., Geiger T., Herbert S.*, et al.* (2009) CodY in *Staphylococcus aureus*: a regulatory link between metabolism and virulence gene expression. *J Bacteriol*, 191(9), 2953-2963.

Publication 5

Function and regulation of *Staphylococcus aureus* wall teichoic acids and capsular polysaccharides.

Keinhörster D, **George SE**, Weidenmaier C, Wolz C.

Int J Med Microbiol. 2019 Jul 18:151333. doi: 10.1016/j.ijmm.2019.151333.

International Journal of Medical Microbiology 309 (2019) 151333

Contents lists available at ScienceDirect

International Journal of Medical Microbiology

journal homepage: www.elsevier.com/locate/ijmm

Function and regulation of *Staphylococcus aureus* wall teichoic acids and capsular polysaccharides

Daniela Keinhörster, Shilpa Elizabeth George, Christopher Weidenmaier*, Christiane Wolz*

Interfaculty Institute of Microbiology and Infection Medicine, University of Tübingen, Elfriede-Aulhorn-Str. 6, 72076 Tübingen, Germany

ARTICLE INFO

Keywords:
Staphylococcus aureus
Glycopolymers
Wall teichoic acids (WTA)
Capsular polysaccharides (CP)
Regulation
Heterogeneity

ABSTRACT

Staphylococcus aureus produces different secondary cell wall glycopolymers such as wall teichoic acids (WTA) and capsular polysaccharides (CP). These structures play an important role in *S. aureus* colonization, pathogenesis and bacterial evasion of the host immune defences. To fulfil their diverse functions, biosynthesis of both glycopolymers has to be tightly controlled. Regulation of WTA biosynthesis and modification is only partially understood. The transcription factor MgrA and the two-component systems (TCS) Agr, GraRS, and ArlRS control WTA export, chain-length and modification. CP synthesis is determined by transcriptional and post-transcriptional regulatory circuits. On the transcriptional level expression of the *capA-P* operon is mainly driven by the alternative Sigma factor B and modulated by several transcriptional factors and TCS. Post-transcriptional mechanisms are in place to avoid conflict between precursor usage by the CP synthesis machinery and the synthesis machinery of other cell wall glycopolymers. The complex interplay of these regulatory systems determines the peculiar, strictly temporal expression of CP in the late growth phase and the high degree of phenotypic heterogeneity. Differential expression of CP, WTA and its modification systems during infection and colonisation are likely important for disease development, immune escape and survival within the host.

1. Introduction

The cell envelope of *S. aureus* consists of peptidoglycan, secondary cell wall glycopolymers and proteins. This multicomponent composition affords protection against cellular immunity and antibiotics and is involved in staphylococcal virulence. Two major secondary cell wall glycopolymers are wall teichoic acids (WTA) and capsular polysaccharides (CP). Their synthesis and modification is highly variable, tightly regulated and plays a key role in host-cell interactions. Thus, they are considered promising targets for anti-infective therapies and vaccines (Weidenmaier and Lee, 2017; Ansari et al., 2019). Structure and function of WTA and CP were recently reviewed (O'Riordan and Lee, 2004; Xia et al., 2010; Brown et al., 2013; Winstel et al., 2014; Schade and Weidenmaier, 2016; Weidenmaier and Lee, 2017). Here, we briefly summarize the function and molecular make-up of the glycopolymers. We will mainly focus on the regulatory system controlling WTA and CP biosynthesis and implicated functional consequences.

2. Function and regulation of WTA

2.1. Structure and function

WTA is unique with respect to its multiple functions in cell wall biosynthesis and maintenance, cellular physiology, phage interaction, host cell adhesion, antibiotic resistance as well as immune regulation (Weidenmaier and Peschel, 2008; Weidenmaier and Lee, 2017; van Dalen et al., 2019). WTA is present in all *S. aureus* strains analysed so far where it is mostly composed of 30–50 ribitol-phosphate (RboP) repeating units (Brown et al., 2013; Weidenmaier and Lee, 2017). However, certain strains produce poly-glycerol-phosphate (GroP) WTA instead (Winstel et al., 2014). The RboP backbone is connected to the peptidoglycan via a disaccharide linkage unit that contains N-acetylglucosamine (GlcNAC) linked to N-acetylmannosamine followed by two glycerol-3-phosphates (GroP) (Brown et al., 2013; Weidenmaier and Lee, 2017). The RboP is attached to the last GroP of the linkage unit and the RboP repeating units are connected to each other via phophodiester linkages (Weidenmaier and Lee, 2017). In addition, the repeating units are modified with D-alanine and GlcNAc.

The D-alanyl modifications are connected via an ester linkage to position C2 of RboP by the DltABCD enzymes (Peschel et al., 1999;

* Corresponding authors.
E-mail addresses: chrisweidenmaier@googlemail.com (C. Weidenmaier), christiane.wolz@uni-Tuebingen.de (C. Wolz).

https://doi.org/10.1016/j.ijmm.2019.151333
Received 7 January 2019; Received in revised form 9 July 2019; Accepted 17 July 2019
1438-4221/ © 2019 Published by Elsevier GmbH.

Neuhaus and Baddiley, 2003). The repeating units exhibit a zwitterionic charge due to the presence of negatively charged phosphodiesters and positively charged D-alanine ester modifications (Weidenmaier et al., 2010). WTA D-alanylation leads to a more cationic charge of the bacterial surface which affects the interaction of cationic antimicrobial peptides (CAMP) with the bacterial surface and renders *S. aureus* non-susceptible to relatively high CAMP concentrations (Peschel et al., 1999).

Glycosylation modification occurs on position C4 of RboP via the predominant GlcNAc transferases TarM and TarS exhibiting α- and β-(1–4) glycosyltransferase activities, respectively (Brown et al., 2012; Koc et al., 2015; Sobhanifar et al., 2015, 2016). Depending on the *S. aureus* strain, the anomeric configuration of the glycosidic linkage of GlcNAc to RboP can either be α or β or a mixture of both anomers (Endl et al., 1983; Winstel et al., 2015). In addition to the C4 glycosylation, a recent study reported the presence of GlcNAc modifications on the C3 position of RboP units (Gerlach et al., 2018). This modification was detected in a number of CC5 and CC398 strains that harbour a prophage encoding an alternative WTA glycosyltransferase (TarP). Interestingly, the C3 GlcNAc modification leads to a less immunogenic WTA polymer. Strains with C3 modifications cannot be inactivated by dominant antibodies against the C4 modified WTA which allows such strains to escape the immune response of the host more efficiently (Gerlach et al., 2018).

2.2. Regulation of WTA synthesis and modification

Although WTA is a dominant surface epitope with multiple roles in host infection, regulation of WTA biosynthesis and modification remains poorly understood. This might be attributed to the fact that the genes involved in WTA biosynthesis (*tarO, tarAHGBXD, tarI'J'KFIJL, mnaA*) and modification (*dltXABCD, tarM, tarS, tarP*) are scattered throughout the genome (Fig. 1). With respect to the regulation of the WTA main chain biosynthesis, so far only a few reports shed light on possible mechanisms that affect WTA chain length and WTA amounts in the cell wall. Chain length is determined by the two RboP polymerases TarK and TarL, which produce WTA of different size with TarK producing up to 50% shorter polymers than TarL (K-WTA versus L-WTA). The Agr quorum sensing system was shown to modulate the ratios of K-WTA and L-WTA via repression of *tarK*. Thus, while under low Agr activity K-WTA and L-WTA are produced, L-WTA is the dominant form under high Agr activity (Meredith et al., 2008). Furthermore, a recent report indicated that altered Agr activity affects WTA biosynthesis and leads to strain specific changes in the amounts of WTA in the cell wall (Wanner et al., 2017). Highly virulent strains exhibit a higher Agr activity and show a consistently higher amount of WTA in their cell walls. This WTA_{high} phenotype is dependent on an increased expression of the *tarH* gene, which encodes for the energizing ATPase subunit of the TarG/H ABC transporter (Wanner et al., 2017). TarG/H is responsible for the transport of WTA over the cytoplasmic membrane. In line with prior reports (Swoboda et al., 2009; Campbell et al., 2012; Brown et al., 2013) it is postulated that the transport constitutes a rate limiting step of WTA biosynthesis. Expression of *tarH* is controlled by direct binding of the repressor Rot to the *tarH* promoter (Wanner et al., 2017). The intracellular effector of the Agr system, RNAIII anneals to target mRNAs including *rot* resulting in repression of translation initiation followed by de-repression of Rot-regulated target genes (Boisset et al., 2007). Additional evidence for a differential regulation of WTA biosynthesis under certain physiological conditions came from studies that implicated WTA in antibiotic resistance (Bertsche et al., 2011, 2013). These studies reported that cell wall stress mediated by different antibiotics can lead to a phenotype that is characterized by a significant increase in WTA amounts in the cell walls of antibiotic resistant strains. The mechanism leading to altered WTA synthesis remains to be elucidated. Regulation of WTA biosynthesis gene clusters *in vivo* has been sparsely analysed. Analyses of transcription during nasal colonisation

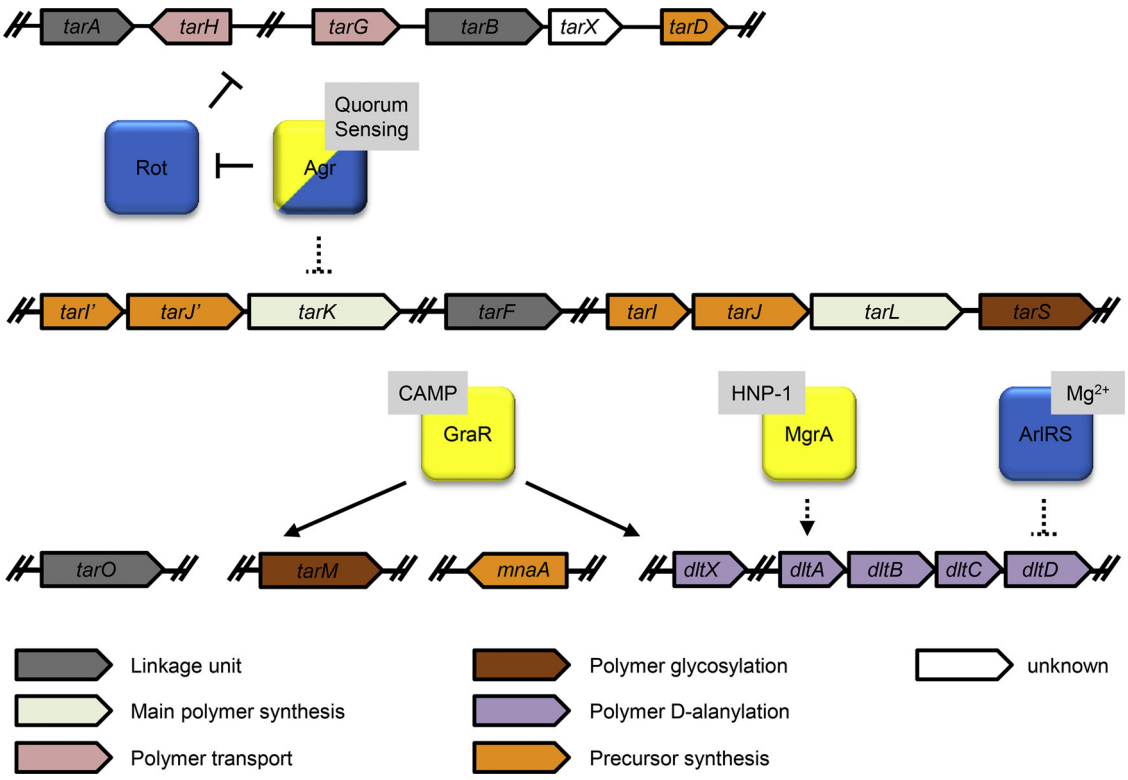

Fig. 1. Genetic organisation, function and regulation of genes involved in WTA biosynthesis and modification. Regulators in yellow indicate up-regulation, in blue down-regulation. Solid lines show direct interaction of the regulators with target genes, dashed lines mark unknown mechanisms of regulation. Signals controlling the activity of the regulators are shown in boxes. CAMP: cationic antimicrobial peptides, HNP: human neutrophil peptide.

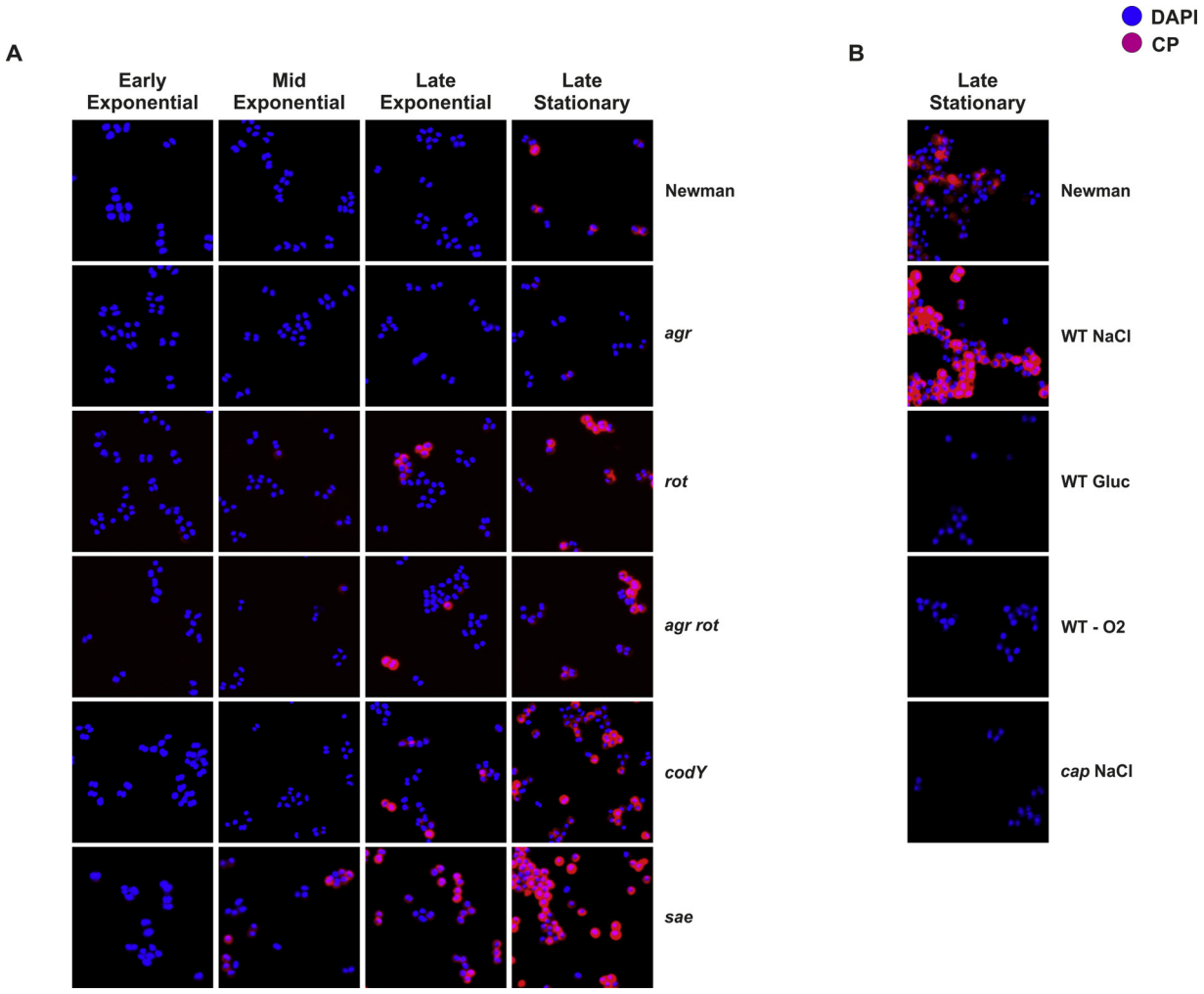

Fig. 2. Temporal and heterogeneous synthesis of CP influenced by (A) different regulators and (B) environmental conditions. CP was detected by immunofluorescence. (A) *S. aureus* strain Newman and isogenic mutants grown in LB medium to the indicated growth phase (modified from George et al., 2015). (B) *S. aureus* strain Newman grown in LB supplemented without or with 2 M NaCl, 1% glucose or grown anaerobically. A *cap* mutant strain was included as negative control (modified from George et al., 2015).

showed increased *tarO* expression at the onset of colonisation in an animal model (Burian et al., 2010).

Modification of WTA is sensitive to various environmental conditions. D-alanine ester content is regulated in response to physiological factors like salt concentration, temperature and pH (Neuhaus and Baddiley, 2003; Koprivnjak et al., 2006). For instance, Mg^{2+} induced *dlt* repression was shown to depend on the two-component system (TCS) ArlRS (Koprivnjak et al., 2006). In addition, the TCS GraRS is thought to directly up-regulate the expression of the *dlt*-operon and putative binding sites of the response regulator GraR have been identified upstream of the operon (Falord et al., 2011). GraS is involved in sensing of host-derived CAMP, but may also respond to other signals like oxidative stress (Falord et al., 2011). Recently, also the transcription factor MgrA was shown to positively regulate *dltA* expression, especially in response to human defense peptides (Li et al., 2019).

Regulation of the genes encoding for the GlcNAc glycosyltransferases TarM, TarS and TarP is only poorly studied. Recently, it was demonstrated that *S. aureus* is able to modify the phenotype of its WTA glycosylation pattern dependent on environmental conditions. The β-GlcNAc anomer was preferentially expressed at the expense of the α-GlcNAc anomer when grown on stress-inducing culture medium containing high NaCl concentration (Mistretta et al., 2019). Furthermore, while the inoculum used to infect animals produced almost exclusively α-GlcNAc WTA, bacteria recovered from infected organs produced only β-glycosylated WTA (Mistretta et al., 2019). The underlying molecular mechanisms remain elusive but may involve regulation by GraRS. A putative GraR binding site was predicted upstream of *tarM* and *tarM* expression was decreased in a *graRS* mutant (Falord et al., 2011). In another study TarS dependent GlcNAc modification of WTA was shown to play an important role in oxacillin resistance and interestingly only *tarS* but not *tarM* expression was strongly up-regulated by oxacillin (β-lactam) treatment (Brown et al., 2012). Again, the molecular mechanisms that confer this differential regulation remain unknown.

3. Function and regulation of CP

3.1. Structure and function

CP serves as essential virulence factor due to its anti-phagocytic properties which are important for immune evasion (Thakker et al., 1998; Nanra et al., 2013). However, depending on the infection setting either the presence or absence of CP has been reported to be advantageous for *S. aureus* (O'Riordan and Lee, 2004; Tuchscherr et al., 2010). CP enhances virulence in murine models of bacteraemia (Thakker et al., 1998; Watts et al., 2005), septic arthritis (Nilsson et al., 1997), abscess formation (Portoles et al., 2001), and surgical wound infection (McLoughlin et al., 2006). In contrast, in mammary gland infections

(Tuchscherr et al., 2005) and in catheter-induced endocarditis (Baddour et al., 1992; Nemeth and Lee, 1995) CP mutants are more virulent. This is likely because CP also inhibits the adherence of the underlying adhesins to their specific target molecule (Pohlmann-Dietze et al., 2000; Risley et al., 2007). CP-negative *S. aureus* strains are frequently isolated from patients with osteomyelitis, mastitis or cystic fibrosis, providing evidence that the loss of CP expression may be advantageous for *S. aureus* during chronic infection (Herbert et al., 1997; Lattar et al., 2009; Tuchscherr et al., 2010). The loss of CP expression can typically be explained by mutations in any of the genes essential for CP synthesis or in the promoter region (Cocchiaro et al., 2006; Tuchscherr et al., 2010). For instance, strains from the USA300 lineage are non-encapsulated due to conserved mutations in the *cap5* locus (Boyle-Vavra et al., 2015). However, this assumption has been recently challenged by the finding that USA300 strains might indeed produce CP during infection (Mohamed et al., 2019).

Amongst clinical *S. aureus* isolates the two serotypes 5 (CP5) and 8 (CP8) are the most prevalent (O'Riordan and Lee, 2004). The structure of CP5 and CP8 is very similar as they both consist of trisaccharide repeating units of D-N-acetyl mannosaminuronic acid, L-N-acetyl fucosamine, and D-N-acetyl fucosamine. The only difference lies in the linkages between the sugars and the site of O-acetylation of the mannosaminuronic acid residues, resulting in the different serotypes (Fournier et al., 1984, 1987; Moreau et al., 1990; Jones, 2005). Polymerized CP is covalently attached to the glycan strands of the peptidoglycan (Chan et al., 2014).

3.2. Influence of environmental signals on CP synthesis in vitro and in vivo

Expression of CP5 and CP8 is strongly dependent on environmental conditions (Sutra et al., 1990; Dassy et al., 1991; Stringfellow et al., 1991; Poutrel et al., 1995). CP production *in vitro* is enhanced under high-salt conditions (Pohlmann-Dietze et al., 2000; George et al., 2015), iron limitation and on solid medium (Lee et al., 1993) but inhibited by yeast extract, alkaline growth conditions, high glucose, low oxygen conditions and high CO_2 (Fig. 2B) (Dassy et al., 1991; Stringfellow et al., 1991; Herbert et al., 1997; George et al., 2015). Most of these environmental cues can be linked to the activity of several regulatory mechanisms described below. Furthermore, *in vitro* CP expression was widely shown to be low during exponential growth phase (Fig. 2A) (Poutrel et al., 1995; Dassy and Fournier, 1996; Pohlmann-Dietze et al., 2000; Cunnion et al., 2001; George et al., 2015; Conlon et al., 2016).

During infection and colonization CP synthesis is also highly variable. CP antigens were detectable in sera and infection sites of infected animals (Arbeit and Dunn, 1987; Arbeit and Nelles, 1987; Lee et al., 1993). However, *ex vivo* analysis of bacteria from cystic fibrosis patient revealed that CP is hardly expressed and only few bacteria are CP-positive. This was linked to the high CO_2 concentrations in the lungs (Herbert et al., 1997). Similar analysis revealed that during nasal colonization only part of the *S. aureus* population is CP-positive (George et al., 2015). Thus, not all bacteria in a population seem to express CP on their surface as confirmed by flow cytometry or immunofluorescence (Poutrel et al., 1997; Pohlmann-Dietze et al., 2000; Seidl et al., 2006; Meier et al., 2007; Jansen et al., 2013; Hartmann et al., 2014; George et al., 2015).

3.3. Regulation of CP

The proteins involved in CP5 or CP8 biosynthesis, O-acetylation, transport and regulation are encoded by 16 genes, *cap5/8A* to *cap5/8 P* (O'Riordan and Lee, 2004; Weidenmaier and Lee, 2017; Rausch et al., 2019). The *cap5* and *cap8* gene clusters are allelic (Goerke et al., 2005) and share a highly similar promoter element (P_{cap}) upstream of *capA* (Herbert et al., 2001). From here, the operon is mainly transcribed as single large 17 kb transcript (Sau et al., 1997; Ouyang et al., 1999). P_{cap} activity generally correlates with CP synthesis indicating that regulation occurs predominantly on the transcriptional level (Ouyang et al., 1999; Meier et al., 2007; Jansen et al., 2013; Hartmann et al., 2014; George et al., 2015).

For a long time the molecular architecture of P_{cap} remained puzzling due to a determined transcriptional start site (TSS) not being preceded by a classical consensus sequence for sigma factor A (SigA) or B (SigB) binding (Ouyang et al., 1999). Instead, within the *cap* promoter region a 10 bp inverted repeat (IR) was shown to be crucial for promoter activity (Ouyang et al., 1999). Recent re-analyses of the P_{cap} promoter structure revealed a different TSS preceded by a canonical SigB consensus motif overlapping with the IR structure (Keinhörster et al., 2019; Mäder et al., 2016; Prados et al., 2016). Thus, the previously observed activating effect of SigB on *cap* expression can be explained by direct SigB-dependent regulation. Other SigB-dependent *cap* activators may contribute to the fine tuning of *cap* expression and amplify SigB-dependency (Keinhörster et al., 2019; Bischoff et al., 2001, 2004; Meier et al., 2007; Schulthess et al., 2009; Lei and Lee, 2015).

Next to the main SigB-dependent promoter a weak SigA-dependent promoter was identified further upstream (Keinhörster et al., 2019). While it seems to play only a minor role for *cap* expression it cannot be ruled out that under certain conditions the SigA-dependent promoter gets activated. This may be the case during infections with CP-positive strains from the USA300 lineage which have a common mutation in the SigB binding motif (Mohamed et al., 2019). Besides containing a SigA-dependent promoter, the extended upstream region of P_{cap} is targeted by many transcriptional factors thereby modulating *cap* expression (see below) (Keinhörster et al., 2019).

The role of regulators affecting *cap* expression was mainly deduced from the characterization of single regulatory mutants and in most cases it remains unclear how *cap* expression is modulated. In particular, the following regulators likely act indirectly via other regulatory systems: Agr (Fig. 2A) (Dassy et al., 1993; Pohlmann-Dietze et al., 2000; Luong et al., 2002; van Wamel et al., 2002; George et al., 2015), SarA (Luong et al., 2002; van Wamel et al., 2002), MgrA (Gupta et al., 2013), ArlRS (Luong and Lee, 2006), CcpA (Seidl et al., 2006, 2009), RpiR (Zhu et al., 2011; Gaupp et al., 2016), ClpC (Luong and Lee, 2006; Graham et al., 2013), RsaA (Romilly et al., 2014), SbcDC (Luong and Lee, 2006; Chen et al., 2007) and SpdC (Poupel et al., 2018). However, there are also many regulators for which a binding to P_{cap} was demonstrated, indicating direct regulation. These are the activators SpoVG, RbsR and KdpE (Fig. 3, yellow) as well as the repressors CcpE, CodY, XdrA, Rot, SaeR and AirR (Fig. 3, blue) which are discussed in the following sections.

The ribose-responsive regulator RbsR (Lei and Lee, 2015) and the putative transcription factor MsaB (Batte et al., 2016) were proposed to activate *cap* expression by directly binding to the 10 bp IR of P_{cap} (now identified as canonical SigB binding motif (Keinhörster et al., 2019)). Interestingly, the presence or absence of ribose had no effect on *cap* expression in the wild type or the *rbsR* mutant (Lei and Lee, 2015). We could not confirm the effect of RbsR on P_{cap} activity (Keinhörster et al., 2019). However, RbsR likely functions as a metabolic sensor, and thus the discrepancy could be due to differences in growth conditions. *rbsR* expression itself is SigB-dependent and accordingly highest towards stationary growth phase (Lei and Lee, 2015). The *msaABCR* operon is involved in the regulation of virulence, biofilm development, antibiotic resistance and persister cell formation in *S. aureus*. Operon deletion and/or the deletion of *msaB* alone reduces *cap* transcription as well as CP production (Batte et al., 2016). However, MsaB is also annotated as cold-shock protein CspA, which exerts regulatory effects via RNA binding. It was shown that MsaB/CspA binds *rsbVWsigB* mRNA, thereby increasing transcript stability (Caballero et al., 2018). This is consistent with the observation that MsaB/CspA increases expression of *sigB* and its target genes (Katzif et al., 2005; Sahukhal and Elasri, 2014; Caballero et al., 2018; Donegan et al., 2019). We were able to reproduce the activating effect of MsaB/CspA on *cap* expression, but demonstrated that this is due to increased SigB activity. Moreover, no

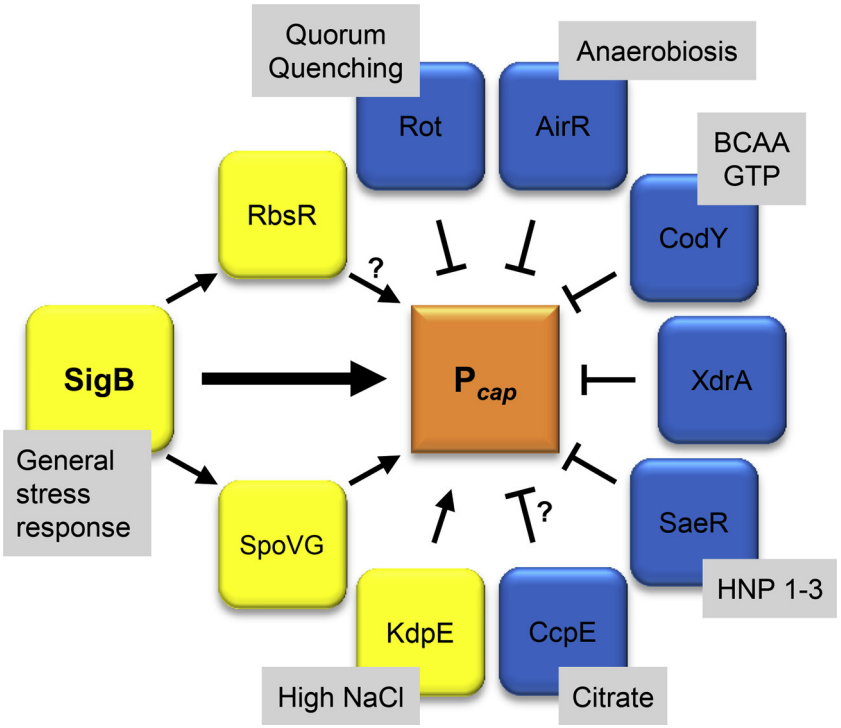

Fig. 3. Regulatory circuits known to directly impact *cap* expression. Regulators in yellow indicate up-regulation, in blue down-regulation of P_{cap} activity. Signals controlling activity of the regulators are shown in boxes. BCAA: branched-chain amino acids, HNP: human neutrophil peptides.

detectable MsaB/CspA binding to P_{cap} was observed (Keinhörster et al., 2019). Taken together, the role of the IR region as a target for other regulators besides SigB has to be questioned.

The transcription factor SpoVG regulates a number of virulence genes including *cap* via direct protein-DNA interaction (Meier et al., 2007; Schulthess et al., 2009, 2011; Jutras et al., 2013). The DNA-binding property of SpoVG is enhanced by phosphorylation via the protein kinase Stk1 (Bischoff et al., 2016). P_{cap} contains a conserved SpoVG binding motif in its extended upstream region and binding of phosphorylated SpoVG to the promoter was demonstrated (Jutras et al., 2013; Bischoff et al., 2016). *spoVG* expression itself is under the control of SigB. P_{cap} activity in a *spoVG* mutant is diminished but still growth phase-dependent (Meier et al., 2007).

KdpDE is a TCS which is inhibited by K^+, c-di-AMP and the auto-inducer AI-2 but activated by high Na^+ concentration (Zhao et al., 2010; Xue et al., 2011; Freeman et al., 2013; Price-Whelan et al., 2013; Moscoso et al., 2016). The direct interaction of the response regulator KdpE and P_{cap} was shown via electrophoretic mobility shift assays (EMSA) (Zhao et al., 2010). Thus, increased *cap* expression in response to high Na^+ is likely due to KdpDE and SigB activity (Pane-Farre et al., 2006; Price-Whelan et al., 2013).

Transcription of tricaboxylic acid cycle genes are controlled by CcpE (Hartmann et al., 2013). Additionally, *capA* levels were found to be decreased in a *ccpE* mutant throughout growth and less CP-positive cells were detected. EMSA failed to show that activation of *cap* is by direct DNA binding of CcpE to P_{cap}, suggesting an indirect regulatory mechanism (Hartmann et al., 2014; Batte et al., 2018). In contrast, in another study *capA* transcription was found up-regulated in a *ccpE* mutant in a citrate-dependent manner and direct CcpE-P_{cap} interaction was shown via EMSA (Ding et al., 2014). The reason for these discrepancies remains to be elucidated.

Regarding *cap* repression many regulators seem to primarily target the extended upstream region of P_{cap} and subsequently modulate the activity of the SigB-dependent promoter (Keinhörster et al., 2019). CodY is a repressor of several metabolic and virulence genes including *cap* (Fig. 2A), where it binds to a conserved consensus sequence (AATTTTCWGAAAATT) (Majerczyk et al., 2010). Binding and thus gene repression is enhanced in the presence of branched chain amino acids and GTP, making CodY most active under conditions of nutrient excess (e.g. early growth phase) (Pohl et al., 2009; Majerczyk et al., 2010). Protein-DNA interaction studies showed that CodY interacts with P_{cap} (Majerczyk et al., 2010; Batte et al., 2018; Lei and Lee, 2018) and footprint analysis revealed that CodY binding reaches into the *capA* coding region (Lei and Lee, 2018). We could show that CodY additionally binds to the upstream region of P_{cap} and that this region is essential and sufficient for the CodY repressive function (Keinhörster et al., 2019). In addition, CodY seems to be required for *cap* repression by XdrA. This transcription factor was shown to bind to P_{cap} with its binding region overlapping with the downstream binding site of CodY, reaching into the *capA* coding region (McCallum et al., 2010; Lei and Lee, 2018). Thus, the two proteins likely interact functionally or physically to repress *cap*. However, the mechanism of the CodY-XdrA interaction remains to be elucidated (Lei and Lee, 2018).

The transcription factor Rot is inactivated by RNAIII of the Agr system (Boisset et al., 2007) thereby being the mediator of the well-known Agr-dependent *cap* expression (Fig. 2A) (George et al., 2015). The DNA binding motif of Rot remains unresolved but was proposed to contain an 18 bp long section of AT-rich DNA (Killikelly et al., 2015). Rot specifically binds to the upstream region of $P_{cap,}$ interfering with SigB-dependent promoter activity (Keinhörster et al., 2019).

The TCS SaeRS is activated by α-defensins and required for the expression of many virulence factors (Geiger et al., 2008). *cap* is one of the few genes which is repressed by SaeRS (Fig. 2A) (Steinhuber et al., 2003; Luong et al., 2011; George et al., 2015). Regulation occurs by binding of phosphorylated response regulator SaeR to the consensus sequence ($GTTAAN_6GTTAA$) (Sun et al., 2010). In P_{cap} the poorly conserved SaeR binding site is located within the extended upstream region. Phosphorylated SaeR specifically binds to P_{cap} thereby repressing both SigB- and SigA-dependent promoter activities (Keinhörster et al., 2019).

The sensor kinase AirS of the TCS AirSR contains a redox active Fe-S cluster which can sense oxygen and redox signals. The oxidized AirS

phosphorylates the response regulator AirR influencing the expression of many regulatory genes as well as inhibiting *cap* under anaerobic conditions. Binding of AirR to P_{cap} was shown (Sun et al., 2012, 2013) but it remains open whether the binding site is also located within the extended upstream region.

On top of all these regulators controlling *cap* expression on the transcriptional level, post-transcriptional regulation is also important for the function of the CP synthesis machinery. The CapAB tyrosine kinase complex controls multiple enzymatic checkpoints through reversible phosphorylation in order to modulate the consumption of essential precursors that are also used in peptidoglycan biosynthesis (Rausch et al., 2019). Furthermore, CP biosynthesis was linked to tyrosine phosphorylation via the Ser/Thr kinase PknB, which can sense cellular lipid II levels (Hardt et al., 2017). PknB signaling serves to reduce CapAB autokinase activity and to reduce the CapM glycosyltransferase activity thereby leading to a shutdown of CP production (Rausch et al., 2019). This likely ensures a sufficient supply of precursors for peptidoglycan synthesis and WTA formation.

3.4. Heterogeneous and temporal CP expression

The most prominent feature of *cap* expression is the strict repression in growing bacteria and the highly heterogeneous expression in bacteria from stationary growth phase (George et al., 2015). In non-growing bacteria only a subpopulation of *S. aureus* is found to express CP. Changing environments or mutations in regulatory genes can shift the ratio of CP-positive bacteria or the onset of *cap* expression during the growth cycle (Fig. 2A and 2B).

On the transcriptional level the temporal and heterogeneous *cap* expression was shown to be determined by direct SigB-dependent regulation and regulators targeting the upstream region of P_{cap} (Keinhörster et al., 2019). Earlier onset of CP production and more CP-positive cells in stationary growth phase could be observed upon constitutive *sigB* expression (Keinhörster et al., 2019), which is consistent with SigB being a known activator of late genes (Bischoff et al., 2001, 2004; Pane-Farre et al., 2006; Mäder et al., 2016). An even more pronounced effect was observed upon chromosomal deletion of the P_{cap} upstream region (Keinhörster et al., 2019). This is in line with the absence of binding sites for the transcriptional repressors Rot and CodY; these being most active during exponential growth phase. In combination, P_{cap} upstream deletion and constitutive *sigB* expression resulted in constitutive *cap* expression and abolished heterogeneity of CP production in stationary phase (Keinhörster et al., 2019). However, CP synthesis remained growth phase-dependent even when *cap* gene expression was rendered constitutive. This is most likely due to the described post-transcriptional levels of regulation (Rausch et al., 2019). Together, the different regulatory circuits ensure that CP is only produced when needed e.g. for phagosomal escape and that a certain subpopulation is CP-negative to allow adherence to host cells. Furthermore they help to avoid conflict in precursor usage by machineries involved in either synthesis of CP or other glycopolymers in growing bacterial cells.

4. Conclusions

Biosynthesis of secondary cell wall glycopolymers has to be tightly controlled to ensure their diverse functions during infection. Further studies are required to unravel the regulatory network that governs WTA biosynthesis and modification. It can be anticipated that many regulatory pathways are involved, possibly resulting in a high degree of heterogeneity with regard to WTA quantity and modification at the single-cell level. So far there are limited tools available to study such variation. In contrast, regulation of CP is much more studied and several involved regulators were identified. CP synthesis is tightly controlled at the transcriptional level, and together with post-transcriptional mechanisms these regulatory circuits determine the peculiar temporal and heterogeneous CP expression. One can assume that such non-genetic variability contributes significantly to the evolutionary success of the species by increasing fitness of the bacterial population.

Acknowledgement

Our work was supported by grants from the German Research Council (DFG)SFB766/A7 to CWe and CWo. The authors have no conflict of interest to declare.

References

Ansari, S., Jha, R.K., Mishra, S.K., Tiwari, B.R., Asaad, A.M., 2019. Recent advances in *Staphylococcus aureus* infection: focus on vaccine development. Infect. Drug Resist. 12, 1243–1255.

Arbeit, R.D., Dunn, R.M., 1987. Expression of capsular polysaccharide during experimental focal infection with Staphylococcus aureus. J. Infect. Dis. 156 (6), 947–952.

Arbeit, R.D., Nelles, M.J., 1987. Capsular polysaccharide antigenemia in rats with experimental endocarditis due to Staphylococcus aureus. J. Infect. Dis. 155 (2), 242–246.

Baddour, L.M., Lowrance, C., Albus, A., Lowrance, J.H., Anderson, S.K., Lee, J.C., 1992. *Staphylococcus aureus* microcapsule expression attenuates bacterial virulence in a rat model of experimental endocarditis. J. Infect. Dis. 165 (4), 749–753.

Batte, J.L., Sahukhal, G.S., Elasri, M.O., 2018. MsaB and CodY interact to regulate *Staphylococcus aureus* capsule in a nutrient-dependent manner. J. Bacteriol. 200 (17), e00294–00218.

Batte, J.L., Samanta, D., Elasri, M.O., 2016. MsaB activates capsule production at the transcription level in Staphylococcus aureus. Microbiology 162 (3), 575–589.

Bertsche, U., Weidenmaier, C., Kuehner, D., Yang, S.J., Baur, S., Wanner, S., Francois, P., Schrenzel, J., Yeaman, M.R., Bayer, A.S., 2011. Correlation of daptomycin resistance in a clinical *Staphylococcus aureus* strain with increased cell wall teichoic acid production and D-alanylation. Antimicrob. Agents Chemother. 55 (8), 3922–3928.

Bertsche, U., Yang, S.J., Kuehner, D., Wanner, S., Mishra, N.N., Roth, T., Nega, M., Schneider, A., Mayer, C., Grau, T., Bayer, A.S., Weidenmaier, C., 2013. Increased cell wall teichoic acid production and D-alanylation are common phenotypes among daptomycin-resistant methicillin-resistant *Staphylococcus aureus* (MRSA) clinical isolates. PLoS One 8 (6), e67398.

Bischoff, M., Brelle, S., Minatelli, S., Molle, V., 2016. Stk1-mediated phosphorylation stimulates the DNA-binding properties of the *Staphylococcus aureus* SpoVG transcriptional factor. Biochem. Biophys. Res. Commun. 473 (4), 1223–1228.

Bischoff, M., Dunman, P., Kormanec, J., Macapagal, D., Murphy, E., Mounts, W., Berger-Bächi, B., Projan, S., 2004. Microarray-based analysis of the *Staphylococcus aureus* sigmaB regulon. J. Bacteriol. 186 (13), 4085–4099.

Bischoff, M., Entenza, J.M., Giachino, P., 2001. Influence of a functional sigB operon on the global regulators *sar* and *agr* in *Staphylococcus aureus*. J. Bacteriol. 183 (17), 5171–5179.

Boisset, S., Geissmann, T., Huntzinger, E., Fechter, P., Bendridi, N., Possedko, M., Chevalier, C., Helfer, A.C., Benito, Y., Jacquier, A., Gaspin, C., Vandenesch, F., Romby, P., 2007. *Staphylococcus aureus* RNAIII coordinately represses the synthesis of virulence factors and the transcription regulator Rot by an antisense mechanism. Genes Dev. 21 (11), 1353–1366.

Boyle-Vavra, S., Li, X., Alam, M.T., Read, T.D., Sieth, J., Cywes-Bentley, C., Dobbins, G., David, M.Z., Kumar, N., Eells, S.J., Miller, L.G., Boxrud, D.J., Chambers, H.F., Lynfield, R., Lee, J.C., Daum, R.S., 2015. USA300 and USA500 clonal lineages of *Staphylococcus aureus* do not produce a capsular polysaccharide due to conserved mutations in the *cap5* locus. MBio 6 (2), e02585–02514.

Brown, S., Santa Maria Jr., J.P., Walker, S., 2013. Wall teichoic acids of gram-positive bacteria. Annu. Rev. Microbiol. 67, 313–336.

Brown, S., Xia, G., Luhachack, L.G., Campbell, J., Meredith, T.C., Chen, C., Winstel, V., Gekeler, C., Irazoqui, J.E., Peschel, A., Walker, S., 2012. Methicillin resistance in *Staphylococcus aureus* requires glycosylated wall teichoic acids. Proc Natl Acad Sci U S A 109 (46), 18909–18914.

Burian, M., Rautenberg, M., Kohler, T., Fritz, M., Krismer, B., Unger, C., Hoffmann, W.H., Peschel, A., Wolz, C., Goerke, C., 2010. Temporal expression of adhesion factors and activity of global regulators during establishment of *Staphylococcus aureus* nasal colonization. J. Infect. Dis. 201 (9), 1414–1421.

Caballero, C.J., Menendez-Gil, P., Catalan-Moreno, A., Vergara-Irigaray, M., Garcia, B., Segura, V., Irurzun, N., Villanueva, M., Ruiz de Los Mozos, I., Solano, C., Lasa, I., Toledo-Arana, A., 2018. The regulon of the RNA chaperone CspA and its auto-regulation in Staphylococcus aureus. Nucleic Acids Res. 46 (3), 1345–1361.

Campbell, J., Singh, A.K., Swoboda, J.G., Gilmore, M.S., Wilkinson, B.J., Walker, S., 2012. An antibiotic that inhibits a late step in wall teichoic acid biosynthesis induces the cell wall stress stimulon in Staphylococcus aureus. Antimicrob. Agents Chemother. 56 (4), 1810–1820.

Chan, Y.G., Kim, H.K., Schneewind, O., Missiakas, D., 2014. The capsular polysaccharide of *Staphylococcus aureus* is attached to peptidoglycan by the LytR-CpsA-Psr (LCP) family of enzymes. J. Biol. Chem. 289 (22), 15680–15690.

Chen, Z., Luong, T.T., Lee, C.Y., 2007. The *sbcDC* locus mediates repression of type 5 capsule production as part of the SOS response in *Staphylococcus aureus*. J. Bacteriol. 189 (20), 7343–7350.

Cocchiaro, J.L., Gomez, M.I., Risley, A., Solinga, R., Sordelli, D.O., Lee, J.C., 2006. Molecular characterization of the capsule locus from non-typeable Staphylococcus

aureus. Mol. Microbiol. 59 (3), 948–960.
Conlon, B.P., Rowe, S.E., Gandt, A.B., Nuxoll, A.S., Donegan, N.P., Zalis, E.A., Clair, G., Adkins, J.N., Cheung, A.L., Lewis, K., 2016. Persister formation in *Staphylococcus aureus* is associated with ATP depletion. Nat. Microbiol. 1 (5), 16051.
Cunnion, K.M., Lee, J.C., Frank, M.M., 2001. Capsule production and growth phase influence binding of complement to Staphylococcus aureus. Infect. Immun. 69 (11), 6796–6803.
Dassy, B., Fournier, J.M., 1996. Respiratory activity is essential for post-exponential-phase production of type 5 capsular polysaccharide by Staphylococcus aureus. Infect. Immun. 64 (7), 2408–2414.
Dassy, B., Hogan, T., Foster, T.J., Fournier, J.M., 1993. Involvement of the accessory gene regulator (*agr*) in expression of type 5 capsular polysaccharide by *Staphylococcus aureus*. J. Gen. Microbiol. 139 (Pt 6), 1301–1306.
Dassy, B., Stringfellow, W.T., Lieb, M., Fournier, J.M., 1991. Production of type 5 capsular polysaccharide by *Staphylococcus aureus* grown in a semi-synthetic medium. J. Gen. Microbiol. 137 (5), 1155–1162.
Ding, Y., Liu, X., Chen, F., Di, H., Xu, B., Zhou, L., Deng, X., Wu, M., Yang, C.G., Lan, L., 2014. Metabolic sensor governing bacterial virulence in Staphylococcus aureus. Proc Natl Acad Sci U S A 111 (46), E4981–4990.
Donegan, N.P., Manna, A.C., Tseng, C.W., Liu, G.Y., Cheung, A.L., 2019. CspA regulation of *Staphylococcus aureus* carotenoid levels and sigma(B) activity is controlled by YjbH and Spx. Mol. Microbiol. https://doi.org/10.1111/mmi.14273.
Endl, J., Seidl, H.P., Fiedler, F., Schleifer, K.H., 1983. Chemical composition and structure of cell wall teichoic acids of staphylococci. Arch. Microbiol. 135 (3), 215–223.
Falord, M., Mäder, U., Hiron, A., Debarbouille, M., Msadek, T., 2011. Investigation of the *Staphylococcus aureus* GraSR regulon reveals novel links to virulence, stress response and cell wall signal transduction pathways. PLoS One 6 (7), e21323.
Fournier, J.M., Hannon, K., Moreau, M., Karakawa, W.W., Vann, W.F., 1987. Isolation of type 5 capsular polysaccharide from *Staphylococcus aureus*. Ann. Inst. Pasteur Microbiol. 138 (5), 561–567.
Fournier, J.M., Vann, W.F., Karakawa, W.W., 1984. Purification and characterization of *Staphylococcus aureus* type 8 capsular polysaccharide. Infect. Immun. 45 (1), 87–93.
Freeman, Z.N., Dorus, S., Waterfield, N.R., 2013. The KdpD/KdpE two-component system: integrating K(+) homeostasis and virulence. PLoS Pathog. 9 (3), e1003201.
Gaupp, R., Wirf, J., Wonnenberg, B., Biegel, T., Eisenbeis, J., Graham, J., Herrmann, M., Lee, C.Y., Beisswenger, C., Wolz, C., Tschernig, T., Bischoff, M., Somerville, G.A., 2016. RpiRc is a pleiotropic effector of virulence determinant synthesis and attenuates pathogenicity in Staphylococcus aureus. Infect. Immun. 84 (7), 2031–2041.
Geiger, T., Goerke, C., Mainiero, M., Kraus, D., Wolz, C., 2008. The virulence regulator Sae of *Staphylococcus aureus*: promoter activities and response to phagocytosis-related signals. J. Bacteriol. 190 (10), 3419–3428.
George, S.E., Nguyen, T., Geiger, T., Weidenmaier, C., Lee, J.C., Liese, J., Wolz, C., 2015. Phenotypic heterogeneity and temporal expression of the capsular polysaccharide in Staphylococcus aureus. Mol. Microbiol. 98 (6), 1073–1088.
Gerlach, D., Guo, Y., De Castro, C., Kim, S.H., Schlatterer, K., Xu, F.F., Pereira, C., Seeberger, P.H., Ali, S., Codee, J., Sirisarn, W., Schulte, B., Wolz, C., Larsen, J., Molinaro, A., Lee, B.L., Xia, G., Stehle, T., Peschel, A., 2018. Methicillin-resistant *Staphylococcus aureus* alters cell wall glycosylation to evade immunity. Nature 563 (7733), 705–709.
Goerke, C., Esser, S., Kümmel, M., Wolz, C., 2005. *Staphylococcus aureus* strain designation by *agr* and *cap* polymorphism typing and delineation of *agr* diversification by sequence analysis. Int. J. Med. Microbiol. 295 (2), 67–75.
Graham, J.W., Lei, M.G., Lee, C.Y., 2013. Trapping and identification of cellular substrates of the *Staphylococcus aureus* ClpC chaperone. J. Bacteriol. 195 (19), 4506–4516.
Gupta, R.K., Alba, J., Xiong, Y.Q., Bayer, A.S., Lee, C.Y., 2013. MgrA activates expression of capsule genes, but not the alpha-toxin gene in experimental *Staphylococcus aureus* endocarditis. J. Infect. Dis. 208 (11), 1841–1848.
Hardt, P., Engels, I., Rausch, M., Gajdiss, M., Ulm, H., Sass, P., Ohlsen, K., Sahl, H.G., Bierbaum, G., Schneider, T., Grein, F., 2017. The cell wall precursor lipid II acts as a molecular signal for the Ser/Thr kinase PknB of Staphylococcus aureus. Int. J. Med. Microbiol. 307 (1), 1–10.
Hartmann, T., Baronian, G., Nippe, N., Voss, M., Schulthess, B., Wolz, C., Eisenbeis, J., Schmidt-Hohagen, K., Gaupp, R., Sunderkötter, C., Beisswenger, C., Bals, R., Somerville, G.A., Herrmann, M., Molle, V., Bischoff, M., 2014. The catabolite control protein E (CcpE) affects virulence determinant production and pathogenesis of Staphylococcus aureus. J. Biol. Chem. 289 (43), 29701–29711.
Hartmann, T., Zhang, B., Baronian, G., Schulthess, B., Homerova, D., Grubmüller, S., Kutzner, E., Gaupp, R., Bertram, R., Powers, R., Eisenreich, W., Kormanec, J., Herrmann, M., Molle, V., Somerville, G.A., Bischoff, M., 2013. Catabolite control protein E (CcpE) is a LysR-type transcriptional regulator of tricarboxylic acid cycle activity in Staphylococcus aureus. J. Biol. Chem. 288 (50), 36116–36128.
Herbert, S., Newell, S.W., Lee, C., Wieland, K.P., Dassy, B., Fournier, J.M., Wolz, C., Döring, G., 2001. Regulation of *Staphylococcus aureus* type 5 and type 8 capsular polysaccharides by CO2. J. Bacteriol. 183 (15), 4609–4613.
Herbert, S., Worlitzsch, D., Dassy, B., Boutonnier, A., Fournier, J.M., Bellon, G., Dalhoff, A., Döring, G., 1997. Regulation of *Staphylococcus aureus* capsular polysaccharide type 5: CO2 inhibition *in vitro* and *in vivo*. J. Infect. Dis. 176 (2), 431–438.
Jansen, A., Szekat, C., Schröder, W., Wolz, C., Goerke, C., Lee, J.C., Türck, M., Bierbaum, G., 2013. Production of capsular polysaccharide does not influence *Staphylococcus aureus* vancomycin susceptibility. BMC Microbiol. 13, 65.
Jones, C., 2005. Revised structures for the capsular polysaccharides from *Staphylococcus aureus* Types 5 and 8, components of novel glycoconjugate vaccines. Carbohydr. Res. 340 (6), 1097–1106.
Jutras, B.L., Chenail, A.M., Rowland, C.L., Carroll, D., Miller, M.C., Bykowski, T., Stevenson, B., 2013. Eubacterial SpoVG homologs constitute a new family of site-specific DNA-binding proteins. PLoS One 8 (6), e66683.
Katzif, S., Lee, E.H., Law, A.B., Tzeng, Y.L., Shafer, W.M., 2005. CspA regulates pigment production in *Staphylococcus aureus* through a SigB-dependent mechanism. J. Bacteriol. 187 (23), 8181–8184.
Keinhörster, D., Salzer, A., Duque-Jaramillo, A., George, S.E., Marincola, G., Lee, J.C., Weidenmaier, C., Wolz, C., 2019. Revisiting the regulation of the capsular polysaccharide biosynthesis gene cluster in Staphylococcus aureus. Mol. Microbiol in press.
Killikelly, A., Benson, M.A., Ohneck, E.A., Sampson, J.M., Jakoncic, J., Spurrier, B., Torres, V.J., Kong, X.P., 2015. Structure-based functional characterization of repressor of toxin (Rot), a central regulator of *Staphylococcus aureus* virulence. J. Bacteriol. 197 (1), 188–200.
Koc, C., Gerlach, D., Beck, S., Peschel, A., Xia, G., Stehle, T., 2015. Structural and enzymatic analysis of TarM glycosyltransferase from *Staphylococcus aureus* reveals an oligomeric protein specific for the glycosylation of wall teichoic acid. J. Biol. Chem. 290 (15), 9874–9885.
Koprivnjak, T., Mlakar, V., Swanson, L., Fournier, B., Peschel, A., Weiss, J.P., 2006. Cation-induced transcriptional regulation of the *dlt* operon of *Staphylococcus aureus*. J. Bacteriol. 188 (10), 3622–3630.
Lattar, S.M., Tuchscherr, L.P., Caccuri, R.L., Centron, D., Becker, K., Alonso, C.A., Barberis, C., Miranda, G., Buzzola, F.R., von Eiff, C., Sordelli, D.O., 2009. Capsule expression and genotypic differences among *Staphylococcus aureus* isolates from patients with chronic or acute osteomyelitis. Infect. Immun. 77 (5), 1968–1975.
Lee, J.C., Takeda, S., Livolsi, P.J., Paoletti, L.C., 1993. Effects of *in vitro* and *in vivo* growth conditions on expression of type 8 capsular polysaccharide by *Staphylococcus aureus*. Infect. Immun. 61 (5), 1853–1858.
Lei, M.G., Lee, C.Y., 2015. RbsR activates capsule but represses the *rbsUDK* operon in *Staphylococcus aureus*. J. Bacteriol. 197 (23), 3666–3675.
Lei, M.G., Lee, C.Y., 2018. Repression of capsule production by XdrA and CodY in Staphylococcus aureus. J. Bacteriol. 200 (18), e00203–00218.
Li, L., Wang, G., Cheung, A., Abdelhady, W., Seidl, K., Xiong, Y.Q., 2019. MgrA governs adherence, host cell interaction, and virulence in a murine model of bacteremia due to Staphylococcus aureus. J. Infect. Dis. https://doi.org/10.1093/infdis/jiz219. jiz219.
Luong, T., Sau, S., Gomez, M., Lee, J.C., Lee, C.Y., 2002. Regulation of *Staphylococcus aureus* capsular polysaccharide expression by *agr* and *sarA*. Infect. Immun. 70 (2), 444–450.
Luong, T.T., Lee, C.Y., 2006. The *arl* locus positively regulates *Staphylococcus aureus* type 5 capsule via an mgrA-dependent pathway. Microbiology 152 (Pt 10), 3123–3131.
Luong, T.T., Sau, K., Roux, C., Sau, S., Dunman, P.M., Lee, C.Y., 2011. *Staphylococcus aureus* ClpC divergently regulates capsule via *sae* and *codY* in strain Newman but activates capsule via *codY* in strain UAMS-1 and in strain Newman with repaired *saeS*. J. Bacteriol. 193 (3), 686–694.
Mäder, U., Nicolas, P., Depke, M., Pane-Farre, J., Debarbouille, M., van der Kooi-Pol, M.M., Guerin, C., Derozier, S., Hiron, A., Jarmer, H., Leduc, A., Michalik, S., Reilman, E., Schaffer, M., Schmidt, F., Bessieres, P., Noirot, P., Hecker, M., Msadek, T., Völker, U., van Dijl, J.M., 2016. *Staphylococcus aureus* transcriptome architecture: from laboratory to infection-mimicking conditions. PLoS Genet. 12 (4), e1005962.
Majerczyk, C.D., Dunman, P.M., Luong, T.T., Lee, C.Y., Sadykov, M.R., Somerville, G.A., Bodi, K., Sonenshein, A.L., 2010. Direct targets of CodY in Staphylococcus aureus. J. Bacteriol. 192 (11), 2861–2877.
McCallum, N., Hinds, J., Ender, M., Berger-Bächi, B., Stutzmann Meier, P., 2010. Transcriptional profiling of XdrA, a new regulator of *spa* transcription in *Staphylococcus aureus*. J. Bacteriol. 192 (19), 5151–5164.
McLoughlin, R.M., Solinga, R.M., Rich, J., Zaleski, K.J., Cocchiaro, J.L., Risley, A., Tzianabos, A.O., Lee, J.C., 2006. CD4+ T cells and CXC chemokines modulate the pathogenesis of *Staphylococcus aureus* wound infections. Proc Natl Acad Sci U S A 103 (27), 10408–10413.
Meier, S., Goerke, C., Wolz, C., Seidl, K., Homerova, D., Schulthess, B., Kormanec, J., Berger-Bächi, B., Bischoff, M., 2007. sigmaB and the sigmaB-dependent *arlRS* and *yabJ-spoVG* loci affect capsule formation in *Staphylococcus aureus*. Infect. Immun. 75 (9), 4562–4571.
Meredith, T.C., Swoboda, J.G., Walker, S., 2008. Late-stage polyribitol phosphate wall teichoic acid biosynthesis in Staphylococcus aureus. J. Bacteriol. 190 (8), 3046–3056.
Mistretta, N., Brossaud, M., Telles, F., Sanchez, V., Talaga, P., Rokbi, B., 2019. Glycosylation of *Staphylococcus aureus* cell wall teichoic acid is influenced by environmental conditions. Sci. Rep. 9 (1), 3212.
Mohamed, N., Timofeyeva, Y., Jamrozy, D., Rojas, E., Hao, L., Silmon de Monerri, N.C., Hawkins, J., Singh, G., Cai, B., Liberator, P., Sebastian, S., Donald, R.G.K., Scully, I.L., Jones, C.H., Creech, C.B., Thomsen, I., Parkhill, J., Peacock, S.J., Jansen, K.U., Holden, M.T.G., Anderson, A.S., 2019. Molecular epidemiology and expression of capsular polysaccharides in *Staphylococcus aureus* clinical isolates in the United States. PLoS One 14 (1), e0208356.
Moreau, M., Richards, J.C., Fournier, J.M., Byrd, R.A., Karakawa, W.W., Vann, W.F., 1990. Structure of the type 5 capsular polysaccharide of Staphylococcus aureus. Carbohydr. Res. 201 (2), 285–297.
Moscoso, J.A., Schramke, H., Zhang, Y., Tosi, T., Dehbi, A., Jung, K., Gründling, A., 2016. Binding of cyclic di-AMP to the *Staphylococcus aureus* sensor kinase KdpD occurs via the universal stress protein domain and downregulates the expression of the Kdp potassium transporter. J. Bacteriol. 198 (1), 98–110.
Nanra, J.S., Buitrago, S.M., Crawford, S., Ng, J., Fink, P.S., Hawkins, J., Scully, I.L., McNeil, L.K., Aste-Amezaga, J.M., Cooper, D., Jansen, K.U., Anderson, A.S., 2013. Capsular polysaccharides are an important immune evasion mechanism for Staphylococcus aureus. Hum. Vaccin. Immunother. 9 (3), 480–487.
Nemeth, J., Lee, J.C., 1995. Antibodies to capsular polysaccharides are not protective against experimental *Staphylococcus aureus* endocarditis. Infect. Immun. 63 (2),

375–380.
Neuhaus, F.C., Baddiley, J., 2003. A continuum of anionic charge: structures and functions of D-alanyl-teichoic acids in gram-positive bacteria. Microbiol. Mol. Biol. Rev. 67 (4), 686–723.
Nilsson, I.M., Lee, J.C., Bremell, T., Ryden, C., Tarkowski, A., 1997. The role of staphylococcal polysaccharide microcapsule expression in septicemia and septic arthritis. Infect. Immun. 65 (10), 4216–4221.
O'Riordan, K., Lee, J.C., 2004. *Staphylococcus aureus* capsular polysaccharides. Clin. Microbiol. Rev. 17 (1), 218–234.
Ouyang, S., Sau, S., Lee, C.Y., 1999. Promoter analysis of the cap8 operon, involved in type 8 capsular polysaccharide production in *Staphylococcus aureus*. J. Bacteriol. 181 (8), 2492–2500.
Pane-Farre, J., Jonas, B., Förstner, K., Engelmann, S., Hecker, M., 2006. The sigmaB regulon in *Staphylococcus aureus* and its regulation. Int. J. Med. Microbiol. 296 (4-5), 237–258.
Peschel, A., Otto, M., Jack, R.W., Kalbacher, H., Jung, G., Götz, F., 1999. Inactivation of the *dlt* operon in *Staphylococcus aureus* confers sensitivity to defensins, protegrins, and other antimicrobial peptides. J. Biol. Chem. 274 (13), 8405–8410.
Pohl, K., Francois, P., Stenz, L., Schlink, F., Geiger, T., Herbert, S., Goerke, C., Schrenzel, J., Wolz, C., 2009. CodY in *Staphylococcus aureus*: a regulatory link between metabolism and virulence gene expression. J. Bacteriol. 191 (9), 2953–2963.
Pohlmann-Dietze, P., Ulrich, M., Kiser, K.B., Döring, G., Lee, J.C., Fournier, J.M., Botzenhart, K., Wolz, C., 2000. Adherence of *Staphylococcus aureus* to endothelial cells: influence of capsular polysaccharide, global regulator *agr*, and bacterial growth phase. Infect. Immun. 68 (9), 4865–4871.
Portoles, M., Kiser, K.B., Bhasin, N., Chan, K.H., Lee, J.C., 2001. *Staphylococcus aureus* Cap5O has UDP-ManNAc dehydrogenase activity and is essential for capsule expression. Infect. Immun. 69 (2), 917–923.
Poupel, O., Proux, C., Jagla, B., Msadek, T., Dubrac, S., 2018. SpdC, a novel virulence factor, controls histidine kinase activity in Staphylococcus aureus. PLoS Pathog. 14 (3), e1006917.
Poutrel, B., Gilbert, F.B., Lebrun, M., 1995. Effects of culture conditions on production of type 5 capsular polysaccharide by human and bovine *Staphylococcus aureus* strains. Clin. Diagn. Lab. Immunol. 2 (2), 166–171.
Poutrel, B., Rainard, P., Sarradin, P., 1997. Heterogeneity of cell-associated CP5 expression on *Staphylococcus aureus* strains demonstrated by flow cytometry. Clin. Diagn. Lab. Immunol. 4 (3), 275–278.
Prados, J., Linder, P., Redder, P., 2016. TSS-EMOTE, a refined protocol for a more complete and less biased global mapping of transcription start sites in bacterial pathogens. BMC Genomics 17 (1), 849.
Price-Whelan, A., Poon, C.K., Benson, M.A., Eidem, T.T., Roux, C.M., Boyd, J.M., Dunman, P.M., Torres, V.J., Krulwich, T.A., 2013. Transcriptional profiling of *Staphylococcus aureus* during growth in 2 M NaCl leads to clarification of physiological roles for Kdp and Ktr K+ uptake systems. MBio 4 (4), e00407–00413.
Rausch, M., Deisinger, J.P., Ulm, H., Müller, A., Li, W., Hardt, P., Wang, X., Li, X., Sylvester, M., Engeser, M., Vollmer, W., Müller, C.E., Sahl, H.G., Lee, J.C., Schneider, T., 2019. Coordination of capsule assembly and cell wall biosynthesis in Staphylococcus aureus. Nat. Commun. 10 (1), 1404.
Risley, A.L., Loughman, A., Cywes-Bentley, C., Foster, T.J., Lee, J.C., 2007. Capsular polysaccharide masks clumping factor A-mediated adherence of *Staphylococcus aureus* to fibrinogen and platelets. J. Infect. Dis. 196 (6), 919–927.
Romilly, C., Lays, C., Tomasini, A., Caldelari, I., Benito, Y., Hammann, P., Geissmann, T., Boisset, S., Romby, P., Vandenesch, F., 2014. A non-coding RNA promotes bacterial persistence and decreases virulence by regulating a regulator in Staphylococcus aureus. PLoS Pathog. 10 (3), e1003979.
Sahukhal, G.S., Elasri, M.O., 2014. Identification and characterization of an operon, *msaABCR*, that controls virulence and biofilm development in *Staphylococcus aureus*. BMC Microbiol. 14, 154.
Sau, S., Sun, J., Lee, C.Y., 1997. Molecular characterization and transcriptional analysis of type 8 capsule genes in Staphylococcus aureus. J. Bacteriol. 179 (5), 1614–1621.
Schade, J., Weidenmaier, C., 2016. Cell wall glycopolymers of Firmicutes and their role as nonprotein adhesins. FEBS Lett. 590 (21), 3758–3771.
Schulthess, B., Bloes, D.A., Francois, P., Girard, M., Schrenzel, J., Bischoff, M., Berger-Bächi, B., 2011. The sigmaB-dependent *yabJ-spoVG* operon is involved in the regulation of extracellular nuclease, lipase, and protease expression in Staphylococcus aureus. J. Bacteriol. 193 (18), 4954–4962.
Schulthess, B., Meier, S., Homerova, D., Goerke, C., Wolz, C., Kormanec, J., Berger-Bächi, B., Bischoff, M., 2009. Functional characterization of the sigmaB-dependent *yabJ-spoVG* operon in *Staphylococcus aureus*: role in methicillin and glycopeptide resistance. Antimicrob. Agents Chemother. 53 (5), 1832–1839.
Seidl, K., Müller, S., Francois, P., Kriebitzsch, C., Schrenzel, J., Engelmann, S., Bischoff, M., Berger-Bächi, B., 2009. Effect of a glucose impulse on the CcpA regulon in Staphylococcus aureus. BMC Microbiol. 9, 95.
Seidl, K., Stucki, M., Ruegg, M., Goerke, C., Wolz, C., Harris, L., Berger-Bächi, B., Bischoff, M., 2006. *Staphylococcus aureus* CcpA affects virulence determinant production and antibiotic resistance. Antimicrob. Agents Chemother. 50 (4), 1183–1194.
Sobhanifar, S., Worrall, L.J., Gruninger, R.J., Wasney, G.A., Blaukopf, M., Baumann, L., Lameignere, E., Solomonson, M., Brown, E.D., Withers, S.G., Strynadka, N.C., 2015. Structure and mechanism of *Staphylococcus aureus* TarM, the wall teichoic acid alpha-glycosyltransferase. Proc Natl Acad Sci U S A 112 (6), E576–585.
Sobhanifar, S., Worrall, L.J., King, D.T., Wasney, G.A., Baumann, L., Gale, R.T., Nosella, M., Brown, E.D., Withers, S.G., Strynadka, N.C., 2016. Structure and mechanism of *Staphylococcus aureus* TarS, the wall teichoic acid beta-glycosyltransferase involved in methicillin resistance. PLoS Pathog. 12 (12), e1006067.
Steinhuber, A., Goerke, C., Bayer, M.G., Döring, G., Wolz, C., 2003. Molecular architecture of the regulatory locus *sae* of *Staphylococcus aureus* and its impact on expression of virulence factors. J. Bacteriol. 185 (21), 6278–6286.
Stringfellow, W.T., Dassy, B., Lieb, M., Fournier, J.M., 1991. *Staphylococcus aureus* growth and type 5 capsular polysaccharide production in synthetic media. Appl. Environ. Microbiol. 57 (2), 618–621.
Sun, F., Ji, Q., Jones, M.B., Deng, X., Liang, H., Frank, B., Telser, J., Peterson, S.N., Bae, T., He, C., 2012. AirSR, a [2Fe-2S] cluster-containing two-component system, mediates global oxygen sensing and redox signaling in Staphylococcus aureus. J. Am. Chem. Soc. 134 (1), 305–314.
Sun, F., Li, C., Jeong, D., Sohn, C., He, C., Bae, T., 2010. In the *Staphylococcus aureus* two-component system *sae*, the response regulator SaeR binds to a direct repeat sequence and DNA binding requires phosphorylation by the sensor kinase SaeS. J. Bacteriol. 192 (8), 2111–2127.
Sun, H., Yang, Y., Xue, T., Sun, B., 2013. Modulation of cell wall synthesis and susceptibility to vancomycin by the two-component system AirSR in *Staphylococcus aureus* NCTC8325. BMC Microbiol. 13, 286.
Sutra, L., Rainard, P., Poutrel, B., 1990. Phagocytosis of mastitis isolates of *Staphylococcus aureus* and expression of type 5 capsular polysaccharide are influenced by growth in the presence of milk. J. Clin. Microbiol. 28 (10), 2253–2258.
Swoboda, J.G., Meredith, T.C., Campbell, J., Brown, S., Suzuki, T., Bollenbach, T., Malhowski, A.J., Kishony, R., Gilmore, M.S., Walker, S., 2009. Discovery of a small molecule that blocks wall teichoic acid biosynthesis in Staphylococcus aureus. ACS Chem. Biol. 4 (10), 875–883.
Thakker, M., Park, J.S., Carey, V., Lee, J.C., 1998. *Staphylococcus aureus* serotype 5 capsular polysaccharide is antiphagocytic and enhances bacterial virulence in a murine bacteremia model. Infect. Immun. 66 (11), 5183–5189.
Tuchscherr, L., Löffler, B., Buzzola, F.R., Sordelli, D.O., 2010. *Staphylococcus aureus* adaptation to the host and persistence: role of loss of capsular polysaccharide expression. Future Microbiol. 5 (12), 1823–1832.
Tuchscherr, L.P., Buzzola, F.R., Alvarez, L.P., Caccuri, R.L., Lee, J.C., Sordelli, D.O., 2005. Capsule-negative *Staphylococcus aureus* induces chronic experimental mastitis in mice. Infect. Immun. 73 (12), 7932–7937.
van Dalen, R., De La, Cruz, Diaz, J.S., Rumpret, M., Fuchsberger, F.F., van Teijlingen, N.H., Hanske, J., Rademacher, C., Geijtenbeek, T.B.H., van Strijp, J.A.G., Weidenmaier, C., Peschel, A., Kaplan, D.H., van Sorge, N.M., 2019. Langerhans cells sense *Staphylococcus aureus* wall teichoic acid through langerin to induce inflammatory responses. MBio 10 (3), e00330–00319.
van Wamel, W., Xiong, Y.Q., Bayer, A.S., Yeaman, M.R., Nast, C.C., Cheung, A.L., 2002. Regulation of *Staphylococcus aureus* type 5 capsular polysaccharides by *agr* and *sarA in vitro* and in an experimental endocarditis model. Microb. Pathog. 33 (2), 73–79.
Wanner, S., Schade, J., Keinhörster, D., Weller, N., George, S.E., Kull, L., Bauer, J., Grau, T., Winstel, V., Stoy, H., Kretschmer, D., Kolata, J., Wolz, C., Bröker, B.M., Weidenmaier, C., 2017. Wall teichoic acids mediate increased virulence in Staphylococcus aureus. Nat. Microbiol. 2, 16257.
Watts, A., Ke, D., Wang, Q., Pillay, A., Nicholson-Weller, A., Lee, J.C., 2005. *Staphylococcus aureus* strains that express serotype 5 or serotype 8 capsular polysaccharides differ in virulence. Infect. Immun. 73 (6), 3502–3511.
Weidenmaier, C., Lee, J.C., 2017. Structure and function of surface polysaccharides of Staphylococcus aureus. Curr. Top. Microbiol. Immunol. 409, 57–93.
Weidenmaier, C., McLoughlin, R.M., Lee, J.C., 2010. The zwitterionic cell wall teichoic acid of *Staphylococcus aureus* provokes skin abscesses in mice by a novel CD4+ T-cell-dependent mechanism. PLoS One 5 (10), e13227.
Weidenmaier, C., Peschel, A., 2008. Teichoic acids and related cell-wall glycopolymers in gram-positive physiology and host interactions. Nat. Rev. Microbiol. 6 (4), 276–287.
Winstel, V., Kühner, P., Salomon, F., Larsen, J., Skov, R., Hoffmann, W., Peschel, A., Weidenmaier, C., 2015. Wall teichoic acid glycosylation governs *Staphylococcus aureus* nasal colonization. MBio 6 (4), e00632.
Winstel, V., Xia, G., Peschel, A., 2014. Pathways and roles of wall teichoic acid glycosylation in Staphylococcus aureus. Int. J. Med. Microbiol. 304 (3-4), 215–221.
Xia, G., Kohler, T., Peschel, A., 2010. The wall teichoic acid and lipoteichoic acid polymers of Staphylococcus aureus. Int. J. Med. Microbiol. 300 (2-3), 148–154.
Xue, T., You, Y., Hong, D., Sun, H., Sun, B., 2011. The *Staphylococcus aureus* KdpDE two-component system couples extracellular K+ sensing and Agr signaling to infection programming. Infect. Immun. 79 (6), 2154–2167.
Zhao, L., Xue, T., Shang, F., Sun, H., Sun, B., 2010. *Staphylococcus aureus* AI-2 quorum sensing associates with the KdpDE two-component system to regulate capsular polysaccharide synthesis and virulence. Infect. Immun. 78 (8), 3506–3515.
Zhu, Y., Nandakumar, R., Sadykov, M.R., Madayiputhiya, N., Luong, T.T., Gaupp, R., Lee, C.Y., Somerville, G.A., 2011. RpiR homologues may link *Staphylococcus aureus* RNAIII synthesis and pentose phosphate pathway regulation. J. Bacteriol. 193 (22), 6187–6196.

Publication 6

Oxidative stress drives the selection of quorum sensing mutants in the *Staphylococcus aureus* population.

George SE, Hrubesch J, Breuing I, Vetter N, Korn N, Hennemann K, Bleul L, Willmann M, Ebner P, Götz F, Wolz C

PNAS 2019 Sep 17;116(38):19145-19154. doi: 10.1073/pnas.1902752116

Oxidative stress drives the selection of quorum sensing mutants in the *Staphylococcus aureus* population

Shilpa Elizabeth George[a], Jennifer Hrubesch[a], Inga Breuing[a], Naisa Vetter[a], Natalya Korn[a], Katja Hennemann[a], Lisa Bleul[a], Matthias Willmann[a], Patrick Ebner[a], Friedrich Götz[a], and Christiane Wolz[a,1]

[a]Interfaculty Institute of Microbiology and Infection Medicine, University of Tübingen, Tübingen 72076, Germany

Edited by Richard P. Novick, New York University School of Medicine, New York, New York, and approved August 14, 2019 (received for review February 15, 2019)

Quorum sensing (QS) is the central mechanism by which social interactions within the bacterial community control bacterial behavior. QS-negative cells benefit by exploiting public goods produced by the QS-proficient population. Mechanisms to keep the balance between producers and nonproducers within the population are expected but have not been elucidated for peptide-based QS systems in gram-positive pathogens. The Agr system of *Staphylococcus aureus* comprises the secretion and sensing of an autoinducing peptide to activate its own expression via the response regulator AgrA as well as the expression of a regulatory RNAIII and *psmα/psmß* coding for phenol-soluble modulins (PSMs). *Agr* mutants can be monitored on blood agar due to their nonhemolytic phenotype. In vitro evolution and competition experiments show that they readily accumulate in a process that is accelerated by ciprofloxacin, while the wild type (WT) is retained in the population at low numbers. However, *agr* mutants possess a fitness advantage only under aerobic conditions. Under hypoxia, Agr activity is increased but without the expected fitness cost. The Agr-imposed oxygen-dependent fitness cost is not due to a metabolic burden but due to the reactive oxygen species (ROS)-inducing capacity of the PSMs and RNAIII-regulated factors. Thus, selection of mutants is dictated by the QS system itself. Under aerobic conditions, emergence of *agr*-negative mutants may provide the population with a fitness advantage while hypoxia favors QS maintenance and even affords increased toxin production. The oxygen-driven tuning of the Agr system might be of importance to provide the pathogen with capabilities crucial for disease progression.

quorum sensing | oxidative stress | Agr | *Staphylococcus aureus* | PSMs

Bacterial QS is based on the secretion of a diffusible signal molecule which, upon reaching a critical concentration, activates a cognate receptor leading to changes in gene expression. Receptor activation facilitates the density-dependent production of extracellular products. These molecules have been termed "public goods" because they can benefit neighboring cells including nonproducers in the population. The production of the QS signal as well as the production of the public goods is assumed costly for the producer (1). QS deficient mutants, often called "cheaters," have been reported to evolve during infections caused by different bacteria (2–7). The social traits of QS have been extensively studied in proteobacteria that utilize mainly acyl-homoserine lactones as autoinducers and intracellular receptor molecules as transcriptional regulators. Laboratory models have shown that several mechanisms to control cheaters have evolved in these organisms (3, 8). In gram-positive species, such as *S. aureus*, short modified oligopeptides function as autoinducers, and histidine kinases function as receptors. However, QS systems in gram-positive pathogens have been sparsely studied from an evolutionary perspective (9–11).

The QS Agr system present in the Staphylococci is well studied on the molecular level (12–15). The system is composed of AgrA, AgrB, AgrC, and AgrD encoded by the *agrBDCA* operon and the divergently transcribed RNAIII molecule (depicted in Fig. 1*C*). The autoinducing peptide (AIP) is encoded by *agrD*. Extracellular AIP results in autophosphorylation of the histidine kinase AgrC and phosphotransfer to the response regulator AgrA. Phosphorylated AgrA triggers transcription of its own operon (*agrBDCA*) as well as the divergently transcribed regulatory RNAIII. Many extracellular virulence factors, such as hemolysins are under the control of RNAIII (15). Of note, RNAIII also encodes a small peptide, Hld (16, 17). The response regulator AgrA also binds to the promoters of the *psm* operons, *psm*α and *psm*β coding for the PSMs; PSMα1–4 and PSMβ1–2, respectively (depicted in Fig. 1*C*) (18). Hld and PSMs are a family of amphipathic α-helical peptides that have multiple roles in staphylococcal pathogenesis and contribute a large extent to the pathogenic success of virulent staphylococci (19). They are cytotoxic, stimulate inflammatory responses, and contribute to biofilm dissemination (20). However, PSMs and Hld may also interfere with bacteria. Hld and proteolytically processed derivatives of PSMα1 and PSMα2 possess antimicrobial activity against *Streptococccus pyogenes* (21, 22). They also interact with the producer's own membrane and promote the release of membrane vesicles from the cytoplasmic membrane via an increase in membrane fluidity (23, 24). Recently, PSMs were also shown to reduce persister formation (25, 26). The antibacterial effect of PSMs is further supported by the necessity for the producer to protect itself from PSMs by the specific PSM transporter (Pmt) export system (27).

Significance

The QS Agr system of the pathogen *S. aureus* is a social trait based on bacterial population density that orchestrates the expression of toxins crucial for virulence. Paradoxically, Agr-defective mutants are selected during infection. We studied the selection and fitness of *agr* mutants under infection-relevant conditions, such as antibiotic stress and hypoxia. Under aerobic growth, the Agr-controlled PSM toxins are produced. These are toxic for Staphylococci and select for *agr* mutants, which are nonproducers. Contrastingly, hypoxia favors QS maintenance and even allows hyperactivation of the system without imposing a fitness burden. We propose that changing oxygen environments encountered during infection not only alters the virulence potential, but also the course of microbial evolution of the *S. aureus* community.

Author contributions: S.E.G. and C.W. designed research; S.E.G., J.H., I.B., N.V., N.K., K.H., L.B., and P.E. performed research; M.W., P.E., and F.G. contributed new reagents/analytic tools; S.E.G., J.H., I.B., N.V., P.E., F.G., and C.W. analyzed data; and S.E.G. and C.W. wrote the paper.

The authors declare no conflict of interest.

This article is a PNAS Direct Submission.

Published under the PNAS license.

[1]To whom correspondence may be addressed. Email: christiane.wolz@med.uni-tuebingen.de.

This article contains supporting information online at www.pnas.org/lookup/suppl/doi:10.1073/pnas.1902752116/-/DCSupplemental.

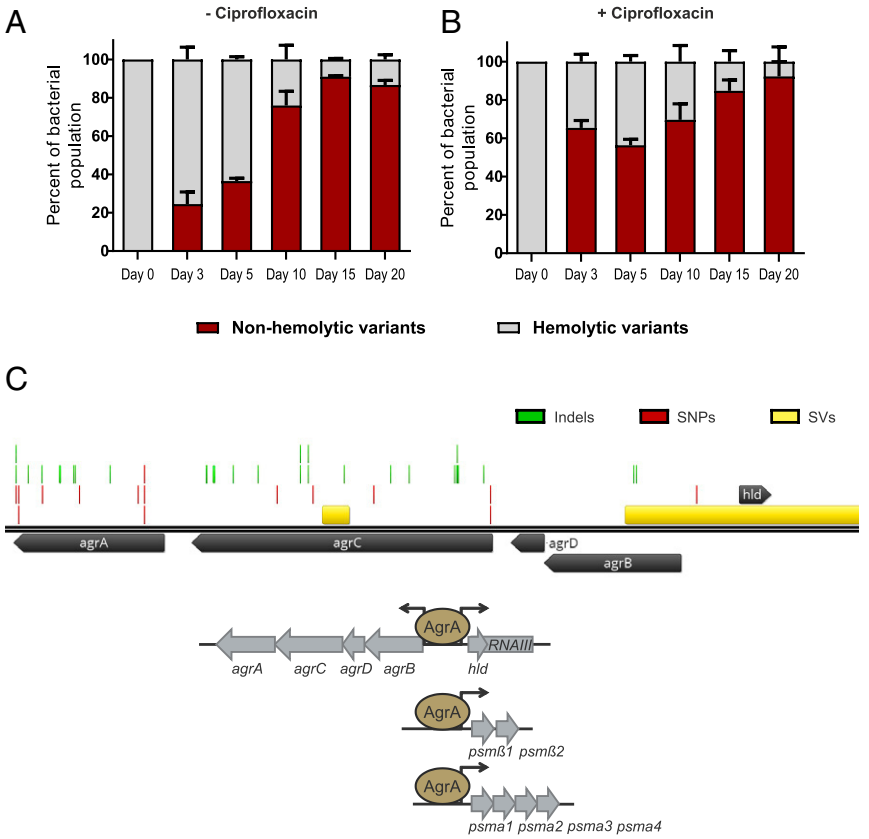

Fig. 1. Evolution of *agr* mutants in vitro. Long-term evolution of HG001 (*A*) without and (*B*) with sub-minimum inhibitory concentration (MIC) of ciprofloxacin (0.125 μg/mL). Percentage of nonhemolytic and hemolytic subpopulations was determined based on colony phenotype on blood agar. (*C*) Representation of the mutations occurring within the *agr* locus after evolution in an aerobic environment. Mutations comprise single residue insertions or deletions (indels), single nucleotide polymorphisms (SNPs), or larger deletions, i.e., structural variants (SVs). The *agr* locus comprises the *agrBDCA* operon and the divergently transcribed RNAIII molecule which also encodes δ-hemolysin (Hld). The autoinducing peptide (AIP) is encoded by *agrD*. Accumulation of extracellular AIP results in autophosphorylation of the histidine kinase AgrC and phosphotransfer to the response regulator AgrA. Phosphorylated AgrA triggers transcription of its own operon (*agrBDCA*) as well as RNAIII. AgrA also binds to the promoters of the *psm* operons, *psm*α and *psm*β coding for the PSMs; PSMα1–4 and PSMβ1–2, respectively.

Agr has been proven to be important for virulence in several animal models (5, 6, 7). Recently, Agr activity was also shown to be required for colonization of the human gastrointestinal tract (28). Many reports emphasize that Agr-dependent factors, such as α-hemolysin (29) and PSMs (19) are major virulence determinants. Correspondingly, the highly virulent community-acquired methicillin-resistant *S. aureus* (MRSA) strains, such as MW2 and USA300, are characterized by high Agr activity (30). However, several lineages of healthcare-acquired MRSA (haMRSA) strains and many clinical isolates were shown to have low or no Agr activity (5, 30). Agr-defective mutants also accumulate within the host, e.g., during chronic infections (31–33) or during persistent bacteremia (34–36) and were even linked to higher mortality in bacteremic patients (37). The use of certain antibiotics, such as fluoroquinolones seems to select for *agr* mutants not only in vitro (11, 38), but also during treatment (39). Of note, *agr*-positive and *agr*-negative strains often coexist in clinical samples (40, 41) or in animal models (42) suggesting that there are mechanisms at play keeping producer and cheater in balance. Thus, there is now compelling evidence for the Janus-faced role of Agr during different stages of colonization or infection. The selection pressures and mechanisms that shape the bacterial population; either tilting toward a net Agr function or dysfunction have not been defined. Here, we used an in vitro model to analyze the evolution and fixation of QS mutants in *S. aureus* populations under infection-relevant conditions, such as antibiotic stress and hypoxia. We find that *agr* mutants possess a fitness advantage only under aerobic conditions. Under hypoxia, Agr activity is increased but without a fitness cost. This Agr-imposed oxygen-dependent fitness cost is not due to a metabolic burden of QS but linked to oxidative stress.

Results

Evolution of *agr* Mutants In Vitro. We set up an experimental system in which the selection of QS mutants can be monitored over time due to their characteristic nonhemolytic phenotype. We also employed ciprofloxacin, a known inducer of the SOS system to accelerate the mutation rate (38). Cultures were transferred daily for 20 d in the presence or absence of subinhibitory concentrations of ciprofloxacin. While nonhemolytic variants accumulated readily in both treated and untreated cultures, ciprofloxacin accelerated the accumulation of variants (Fig. 1 *A* and *B*). After only 3 transfers (Day 3), the nonhemolytic variant subpopulation accounted for ∼24% of the untreated cultures while in treated cultures, this subpopulation accounted for ∼65% of the total population. Interestingly, the WT population did not get completely outcompeted or lost from the population. Indeed, after 15 transfers, both subpopulations seemed to reach a "steady state" with about 10% of the WT maintained.

Nonhemolytic variants isolated from independent cultures (42 isolates in total) after 3, 18, or 20 transfers were resequenced. All nonhemolytic variants were found to contain mutations within the *agr* locus (Fig. 1*C*), mostly within *agrA* and *agrC*. Interestingly,

with the exception of 1 isolate that bore a large deletion spanning RNAIII/*hld* and *agrB*, we did not detect SNPs or indels in other loci that influence hemolysis, i.e., *hla*, *hld*, *psm*, and *sae*. Thus, the Agr system imposes a strong fitness cost.

Fitness Advantage of *agr* Mutants. We compared growth characteristics of the WT against various *agr* mutants (Fig. 2*A*). We selected 1 representative *agr* deficient isolate which bore a single point mutation in AgrA^{R165H} without additional SNPs elsewhere in the genome. The point mutation lies in the C-terminal DNA-binding domain of AgrA and likely affects the ability to bind to target promoter regions. For comparison, we included an *agr*-deletion mutant in which the entire *agr*/RNAIII locus was deleted and a strain in which a single amino acid exchange in the histidine–kinase domain (AgrC^{R238H}) rendered the enzyme constitutively active (43, 44).

The *agr* mutants in which the Agr function had been abrogated had similar growth rates as the WT but differed in the final yield reached in the stationary phase. This is in line with the understanding that QS and thereby Agr is active only once the critical threshold of cell density is reached (*SI Appendix*, Fig. S1). Accordingly, constitutive expression independent of QS should already impose a fitness cost in the exponential phase. We could confirm that the growth of the constitutive *agrC*^{R238H} mutant (doubling time 31.36 ± 0.2139 min, $n = 3$) is slightly retarded compared to WT (doubling time 29.18 ± 0.5663 min, $n = 3$; $P < 0.05$) (Fig. 2*A*).

We postulated that, in the constitutive *agrC*^{R238H} derivative, Agr should impose a higher burden thereby accelerating the accumulation of *agr* mutants. *agrC*^{R238H} cultures accumulated nonhemolytic variants after fewer transfers compared to the WT (Fig. 2*B*). After 3 transfers, the percentage of nonhemolytic variants that accumulated within the untreated *agrC*^{R238H} population was comparable to that in ciprofloxacin-treated WT cultures and far exceeded that in untreated WT cultures. Interestingly, in contrast to the long-term experiment using the WT strain (Fig. 1 *A* and *B*), the Agr-functional ancestor was not maintained in the *agrC*^{R238H} population as far as the limit of detection of the test system.

Fitness Cost Associated with the Various Nodes of the Agr System. The production of QS signaling molecules has been considered

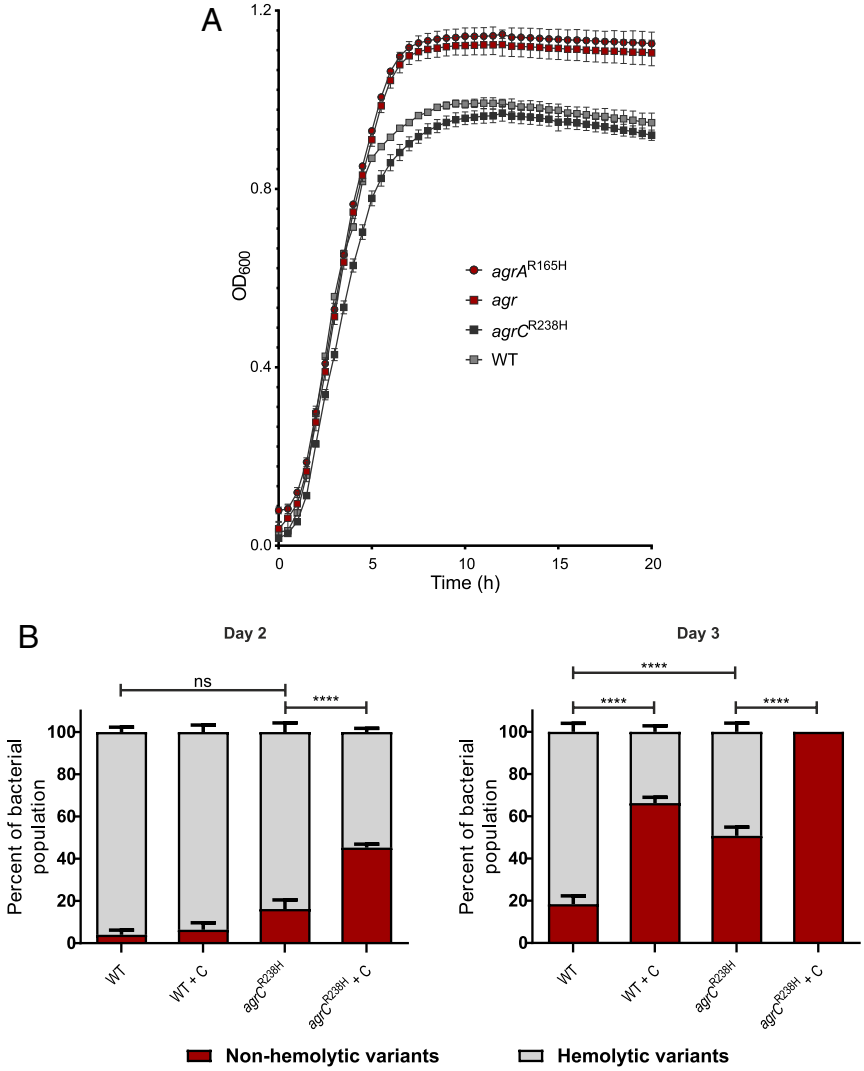

Fig. 2. Fitness advantage of *agr* mutants. (*A*) Aerobic growth of HG001, *agr*, *agrC*$_{R238H}$ (constitutive *agr*), and *agrA*^{R165H} in tryptic soy broth (TSB). Error bars represent SD ($n = 3$). (*B*) HG001 and *agrC*^{R238H} evolved for 2 and 3 d with and without sub-MIC of ciprofloxacin (0.125 μg/mL). Percentage of nonhemolytic and hemolytic subpopulations was determined based on colony phenotype on blood agar. Error bars indicate SEM ($n = 3$). Statistical significance determined by two-way ANOVA with Tukey's posttest. *$P \leq 0.05$, **$P \leq 0.01$, ***$P \leq 0.001$, and ****$P \leq 0.0001$.

to be costly thereby imposing a metabolic burden (1, 45). To test whether this holds true for staphylococcal AIPs, we created a signal nonproducing *agrD* mutant. Such a mutant would be expected to have a fitness advantage relative to the WT. We performed competition experiments between *agr* mutants (full deletion or *agrD*) and the WT. Strains were labeled with the fluorescent protein Venus and competed at a 1:1 ratio with the WT labeled with the fluorescent protein Cerulean (Fig. 3*A*). After 2 subcultures, the percentage of WT and mutant subpopulations was assessed. As expected, in the pairing with the *agr* full deletion, the WT was outcompeted, and the culture reached higher bacterial density. However, the *agrD* mutant did not outcompete the WT. This shows that the *agrD* mutant was functionally complemented by the AIPs produced by the WT and that the synthesis of AIP itself does not exert a fitness burden. Venus-labeled WT in coculture with WT labeled with Cerulean remained in a stable 1:1 ratio and, thus, confirmed that the fitness traits of the competing strains were not influenced by either of the fluorescent proteins themselves.

Therefore, downstream consequences of Agr signaling must drive the selection of *agr* mutations. This might occur in possibly 2 ways: either through the production of the regulatory RNAIII, which is a key virulence determinant and controls the expression of several virulence and metabolic genes, or through the production of the cytolytic PSM peptides which are directly controlled by AgrA (18). To identify which specific node of the Agr system imposes the fitness disadvantage, we compared the growth of mutants bearing deletions of either RNAIII or *psm*α/*psm*β genes. Surprisingly, the *psm* deletion was sufficient to confer the same growth advantage as the complete *agr* deletion (Figs. 2*A* and 3*B*). Deletion of RNAIII had only a slight effect on growth compared to WT. We next analyzed the accumulation of nonhemolytic variants in these backgrounds. Of note, mutations in RNAIII or *psms* result in an altered hemolytic phenotype but are still clearly distinguishable from nonhemolytic *agr* mutants. Interestingly, both deletions abrogated the accumulation of nonhemolytic variants in bacterial populations (Fig. 3*C*). This was confirmed in a constitutive $agrC^{R238H}$ background. No mutants were selectable in a *psm*α *psm*β double mutant. *psm*α deletion

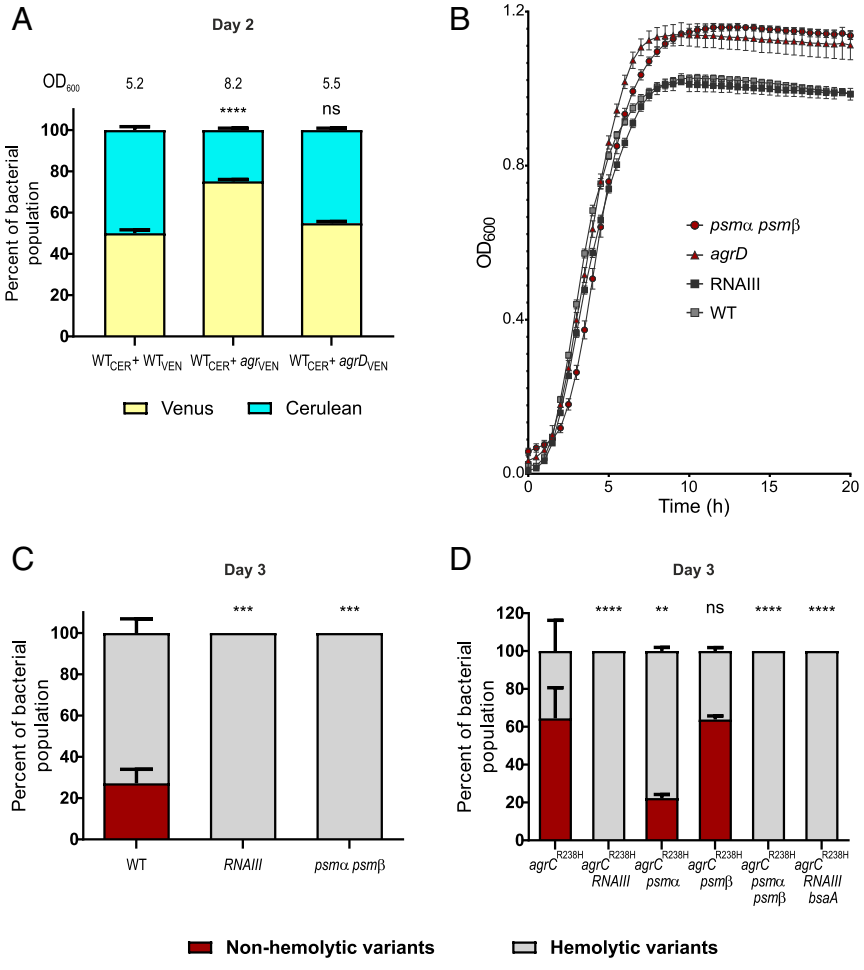

Fig. 3. Fitness cost associated with the various nodes of the Agr system. (*A*) HG001 bearing P*sarA*-Cerulean was competed for 2 d with either *agr* or *agrD* bearing P*sarA*-Venus, starting at a ratio of 1:1. The final bacterial yield in each culture (OD_{600}) is indicated. Percentage of each bacterial subpopulation was measured based on fluorescence. Error bars indicate SEM ($n = 3$). Statistical significance determined by one-way ANOVA with Tukey's posttest. Asterisks indicate statistical significance in comparison to the WT population ($WT_{CER} + WT_{VEN}$). (*B*) Aerobic growth of HG001, RNAIII, *agrD*, and *psm*α *psm*β in TSB. Error bars represent SD ($n = 3$). (*C*) HG001, RNAIII, and *psm*α *psm*β evolved for 3 d. Error bars indicate SEM ($n = 5$). Asterisks indicate statistical significance in comparison to the WT. (*D*) HG001 $agrC^{R238H}$, $agrC^{R238H}$ *RNAIII*, $agrC^{R238H}$ *psm*α, $agrC^{R238H}$ *psm*β, $agrC^{R238H}$ *psm*α *psm*β, and $agrC^{R238H}$ *RNAIII bsaA* evolved for 3 d. Error bars indicate SEM ($n = 3$). Asterisks indicate statistical significance in comparison to HG001 $agrC^{R238H}$. (*C* and *D*) Percentage of nonhemolytic and hemolytic subpopulations was determined based on colony phenotype on blood agar. Statistical significance determined by two-way ANOVA with Tukey's posttest. $*P \leq 0.05$, $**P \leq 0.01$, $***P \leq 0.001$, and $****P \leq 0.0001$.

alone was sufficient to significantly reduce the accumulation of nonhemolytic variants (Fig. 3*D*), indicating that PSMα is more active compared to PSMβ. In conclusion, the fitness advantage of an *agr* mutant can be attributed to the loss of PSMs and/or loss of RNAIII.

Agr Mutants Are Selected Only under Aerobic Growth Conditions. Different environmental cues are known to modulate Agr activity (14). Oxygen concentrations vary greatly across different tissues (46) affecting bacterial growth and signaling. There are conflicting results whether Agr is more (47) or less (48) active under hypoxia. We analyzed the Agr-associated fitness cost under different oxygen conditions (Fig. 4*A*). Surprisingly, *agr* mutants did not accumulate in cultures transferred under low oxygen conditions. With 5–15% oxygen (microaerophilic), the mutation frequency was significantly decreased compared to normoxic conditions. Under hypoxic or anaerobic growth, nonhemolytic variants were not selected. We next performed a long-term evolution experiment under anaerobic conditions. Even after 20 transfers with ciprofloxacin, no *agr* mutants were detectable (Fig. 4*B*). To ascertain these observations, we performed a competition experiment under aerobic and anaerobic conditions wherein the WT was competed with the streptomycin-resistant $agrA^{R165H}$ mutant starting at 1:1, 9:1 and 1:9 ratios (Fig. 4 *C* and *D* and *SI Appendix*, Fig. S3). Within 20 transfers, the $agrA^{R165H}$ mutant accumulated rapidly under aerobic growth conditions irrespective of the initial ratio. Competition of a *psm* mutant or a RNAIII mutant with the WT strain confirmed that both PSMs and RNAIII confer a fitness disadvantage over time (*SI Appendix*, Fig. S2). Under anaerobic growth, the relative starting ratios of the WT and $agrA^{R165H}$ mutants remained stable for 20 transfers (Fig. 4*D*). These results were unaltered in a competition experiment with the streptomycin-resistant WT and an unmarked $agrA^{R165H}$ mutant (*SI Appendix*, Fig. S3). Thus, both evolution and competition experiments show that Agr imposes a fitness burden only under aerobic growth.

Increased Agr Activity in Low Oxygen Environments. Growth under hypoxic conditions resulted in significantly lower final bacterial densities. However, the *agr* mutant no longer has a growth advantage under hypoxia (Fig. 5*A*). We reasoned that, perhaps, due to the lower cell density, the QS system might just not be active under low oxygen conditions. In contrast to this assumption, we found that Agr activity is even higher under hypoxic conditions. This was shown on the transcriptional level wherein both the Agr target genes *RNAIII* and *psmα* were significantly increased throughout growth under hypoxia compared to aerobic conditions (Fig. 5*B*). Interestingly, the transcription of *pmt* was not significantly influenced by hypoxia (*SI Appendix*, Fig. S4).

Next we analyzed whether the increased transcription of *RNAIII* and *psmα* is accompanied by Agr-dependent changes in hemolysis. Increased expression of hemolysis could be verified after anaerobic growth on blood agar plates (Fig. 5*C*). The hemolytic zone relative to the size of single colonies was significantly higher ($P < 0.005$) in anaerobic (20.3 ± 5.002) compared to aerobic (4.204 ± 0.2803) grown bacteria. Microtitration of supernatants from bacterial cultures using red blood cells confirmed the higher hemolytic activity under low oxygen (*SI Appendix*, Fig. S5). Moreover, under hypoxia, the RNAIII encoded

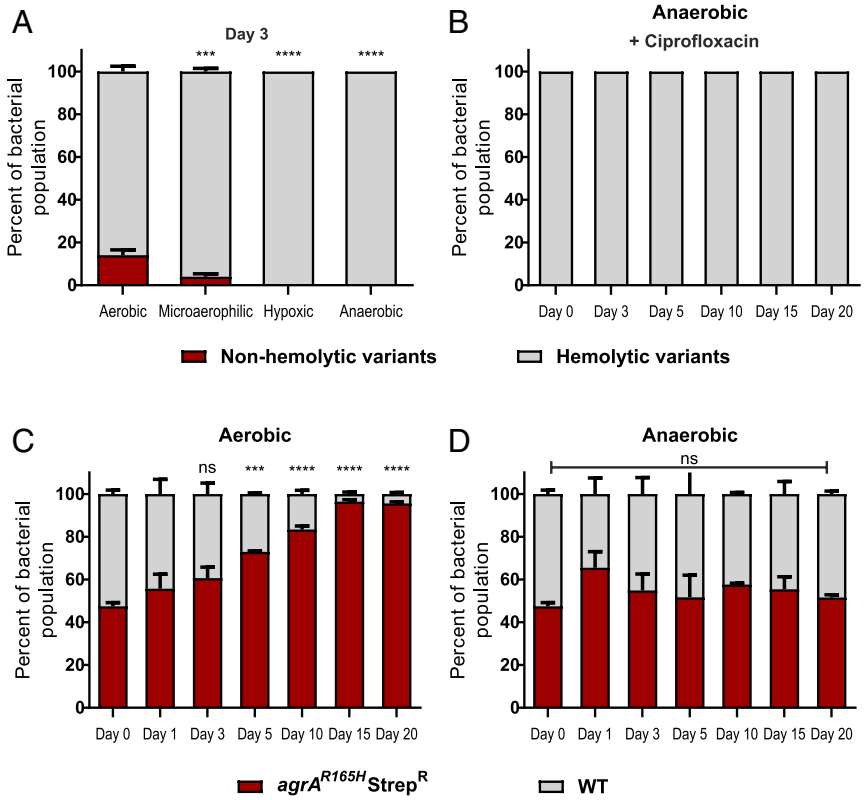

Fig. 4. Agr mutants are selected only under aerobic growth conditions. (*A*) HG001 evolved for 3 d under aerobic, microaerophilic, hypoxic, and anaerobic environments. Error bars indicate SEM ($n = 3$). Asterisks indicate statistical significance in comparison to the aerobic condition. (*B*) Long-term evolution of HG001 under anaerobic conditions with ciprofloxacin (*C* and *D*) HG001 was competed for 20 d with streptomycin-resistant $agrA^{R165H}$, starting at a ratio of 1:1 under (*C*) aerobic or (*D*) anaerobic conditions. Percentage of each bacterial subpopulation was determined based on colony phenotype on blood agar. Error bars indicate SEM ($n = 3$). Asterisks indicate statistical significance in comparison to Day 0. Statistical significance determined by (*A*) two-way ANOVA (*C* and *D*) repeated measures two-way ANOVA with Tukey's posttest. $^*P \leq 0.05$, $^{**}P \leq 0.01$, $^{***}P \leq 0.001$, and $^{****}P \leq 0.0001$.

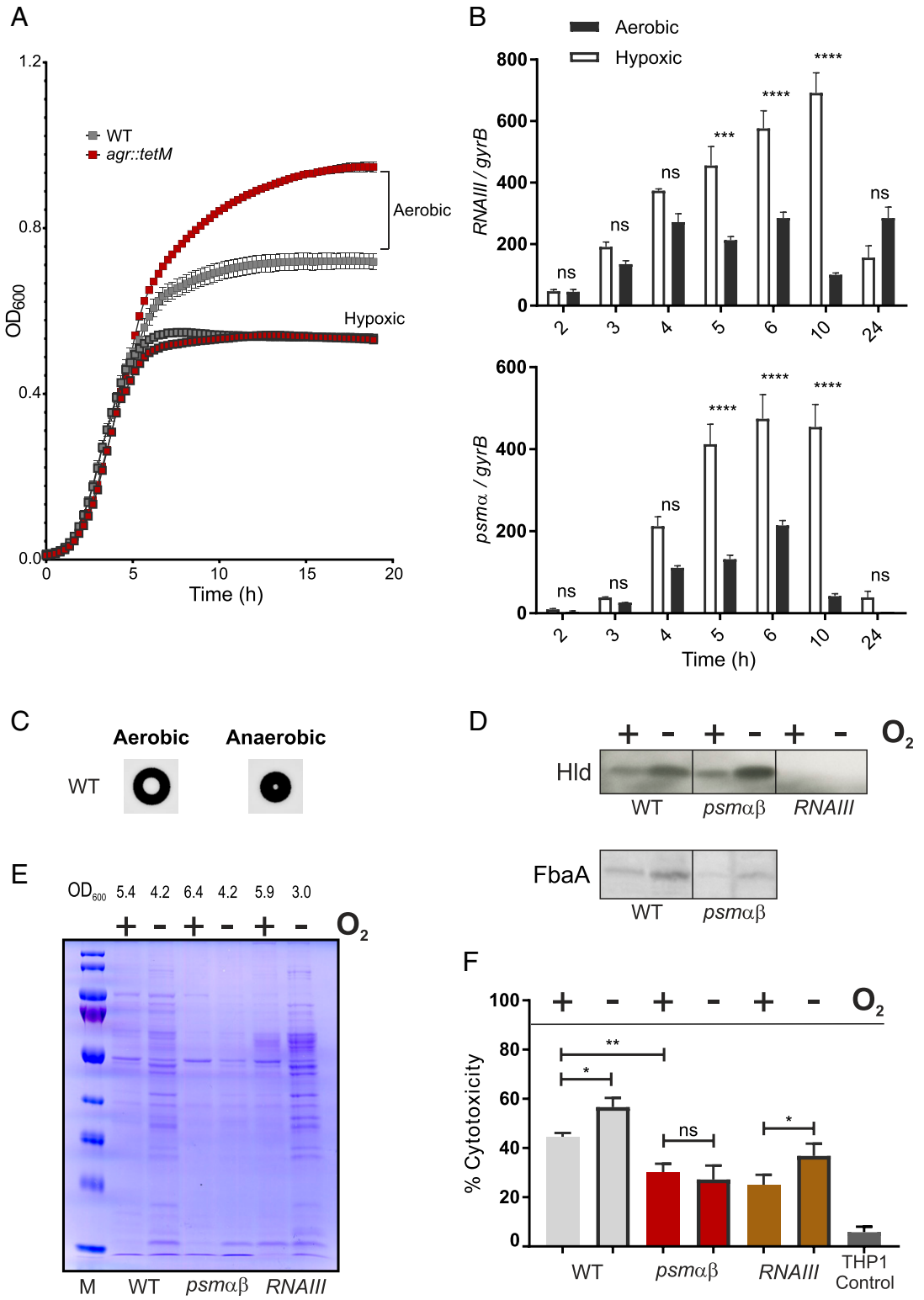

Fig. 5. Increased Agr activity in low oxygen environments. (*A*) Growth of HG001 and *agr::tetM* under aerobic and hypoxic environments. Error bars represent SD ($n = 3$). (*B*) Bacteria were harvested at different time points (2–6, 10, 24 h) during growth. Total RNA from strain HG001 was isolated. *RNAIII* or *psm*α mRNA was quantified by qRT-PCR with reference to *gyrB*. Error bars indicate SEM ($n = 3$). Statistical significance determined by repeated measures two-way ANOVA with Bonferroni's posttest. (*C*) Colony morphology and hemolysis zone of HG001 grown on blood agar under aerobic and anaerobic environments. (*D–F*) Bacterial supernatants from cultures (HG001, *psm*α *psm*β, and RNAIII) grown either aerobically or under hypoxic conditions were analyzed by (*D*) Western blot for Hld and aldolase (FbaA) and (*E*) SDS-PAGE for extracellular proteome (loading control for Western blots). The final bacterial yield in each culture (OD_{600}) is indicated. (*F*) Bacterial supernatants were analyzed for a cytotoxic potential against THP1 macrophages. Percentage of cytotoxicity shown was normalized to the Triton control. Error bars indicate SD ($n = 6$). Statistical significance determined by one-way ANOVA with Tukey's posttest. $^{*}P \leq 0.05$, $^{**}P \leq 0.01$, $^{***}P \leq 0.001$, and $^{****}P \leq 0.0001$.

peptide Hld was found to be more abundant in the supernatants (Fig. 5*D*) consistent with the increased transcription of RNAIII. The release of cytoplasmic proteins and lipoproteins into the extracellular milieu was shown previously to be dependent on PSMs (49, 50). Accordingly, fewer proteins are detectable in the supernatants of the *psm* mutant (Fig. 5*E*). Of note, this effect was mainly seen under hypoxia. There was also an increased level of the cytoplasmic protein aldolase in the secretome under hypoxia (Fig. 5*D*). Aldolase was previously used as a marker protein for excretion of cytoplasmic proteins (49).

These data demonstrate that Agr activity is clearly higher under hypoxia without imposing a fitness cost. Furthermore, the data indicate that the metabolic burden imposed by the synthesis of RNAIII or PSMs does not explain the fitness differences. If this was the case, we would expect the fitness differences between WT and *agr* mutants under hypoxia to be higher and not lower. To solve this conundrum, we speculated that PSMs may be inactivated under hypoxic conditions, e.g., through proteolytic cleavage and, thus, cannot impose a selection pressure. We, therefore, tested the cytotoxicity of bacterial culture supernatants on THP1 cells (Fig. 5*F*). There was a significant increase in cytotoxicity of supernatants from WT and RNAIII mutants grown under hypoxia. This was abrogated in a *psm*αβ mutant, indicating that PSMs produced under hypoxia are not inactive with regard to their cytotoxic effects.

PSMs Induce ROS and Possess Antimicrobial Activity under Aerobic Conditions. We next hypothesized that the bacterial cells are themselves not susceptible to PSMs under low O_2. In an aerobic environment, PSMα3 resulted in a concentration-dependent growth defect wherein as low as 10 μg/mL affected bacterial yield; while up to 50 μg/mL had no effect under hypoxia (Fig. 6*A*). Therefore, under hypoxia, the Agr system is highly active with increased secretion of toxic PSMs. However, bacteria seem to be protected from their antimicrobial effects under these conditions.

We speculated that PSMs may induce ROS under aerobic conditions contributing to the toxicity. Indeed, we found significantly higher levels of ROS in the WT compared to the *psm*αβ or *agr* mutant (Fig. 6*B*). Thus, under hypoxia cytotoxic PSM production is enhanced without harming the producer suggesting that the selection of *agr* mutants under aerobic conditions is to avoid PSM-mediated ROS production. Indeed, addition of 2,2'-bipyridyl and thiourea to block hydroxyl radical accumulation could completely prevent selection of *agr* mutants in the constitutive $agrC^{R238H}$ background (Fig. 6*C*).

However, we also found that RNAIII deletion was sufficient to prevent selection of *agr* mutants (Fig. 3*C*), although ROS production

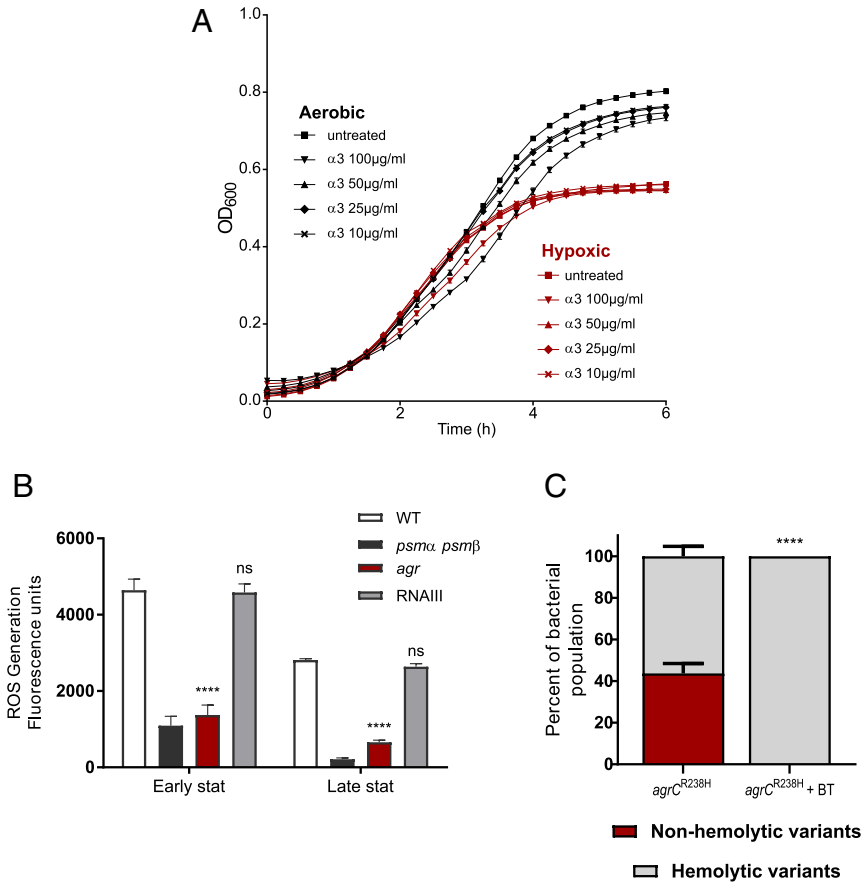

Fig. 6. PSMs induce ROS and possess antimicrobial activity under aerobic conditions. (*A*) Different concentrations of PSMα3 (100, 50, 25, and 10 μg/mL) were added to bacterial cultures of HG001 *agr*. Growth under aerobic and hypoxic environments was monitored. Error bars indicate SEM ($n = 3$). Bacterial yield compared to the untreated control was significant only under aerobic growth (****$P \leq 0.0001$) and not under hypoxia. (*B*) Early and late stationary phase cultures of HG001, *psm*α *psm*β, *agr*, and RNAIII were compared for ROS levels. Error bars indicate SEM ($n = 3$). Asterisks indicate statistical significance in comparison to HG001. (*C*) HG001 $agrC^{R238H}$ evolved for 3 d in the presence of antioxidants (1 mM 2,2'-bipyridyl and 100 mM thiourea). Percentage of nonhemolytic and hemolytic subpopulations was determined based on colony phenotype on blood agar. Error bars indicate SEM ($n = 3$). Asterisks indicate statistical significance in comparison to the HG001 $agrC^{R238H}$. Statistical significance determined by (*A*) one-way ANOVA with Tukey's posttest and (*B* and *C*) two-way ANOVA with Bonferroni's posttest. *$P \leq 0.05$, **$P \leq 0.01$, ***$P \leq 0.001$, and ****$P \leq 0.0001$.

was comparable to the WT (Fig. 6*B*). The glutathione peroxidase BsaA was reported to be derepressed in *agr* mutants, thus, enabling bacteria to survive oxidative stress (51). We, therefore, tested whether *bsaA* deletion would increase the selection pressure in a RNAIII mutant (Fig. 3*D*). However, this was not the case. Moreover, we could not confirm that *agrA* or RNAIII deletion significantly increases *bsaA* expression under our growth conditions (*SI Appendix*, Fig. S6). Taken together, these results suggest that other RNAIII-regulated factors are involved in the protective effect against ROS in a RNAIII mutant.

Discussion

The social trait of QS sensing in proteobacteria has been widely studied and, depending on the model organism analyzed, different mechanisms to balance the relationship between QS-positive bacteria and QS-negative cheaters have been discovered (2, 3, 8). To gain insight into such processes in peptide-based QS systems, we employed evolution and competition experiments. We investigated conditions and factors driving the evolution and selection of QS-negative *S. aureus* mutants and found the antimicrobial activity of the QS-dependent PSMs to be a major driver for the evolution of QS mutants. Thus, a QS-controlled gene product PSMα can drive the selection of QS mutants. This demarcates the Agr system from other QS systems that are described to have evolved mechanisms to avoid cheating (8, 52).

Fitness Advantage of *agr* Mutants. We show that under aerobic conditions *agr* mutants possess a fitness advantage and grow to higher cell densities compared to the WT. A*gr* mutants were shown to outcompete the WT consistent with previous in vitro (11) and in vivo reports (9). Interestingly, the WT is not lost from the population but remains in the culture at low numbers (Fig. 1). This is likely because the AIP concentration falls below the threshold for Agr activation. Accordingly, a constitutive AIP producer in which AIP synthesis is uncoupled from QS is lost from the population after prolonged coculture (Fig. 2*B*). When producers are scarce, the autoregulatory properties of the system restrict AgrA activity and thereby maintain the producer in the population (*SI Appendix*, Fig. S1). Other mechanisms to inactivate Agr during infection, e.g., through hemoglobin (53), lipoproteins (54), oxidants (55), or microbial interference (28, 56, 57) may similarly function to maintain producer–cheater homeostasis.

QS Fitness Cost Is Not due to Metabolic Burden. It was proposed that the fitness advantage of QS mutants is due to the costs associated with producing a QS signal and/or the regulated public goods (1, 8, 45). The metabolic cost to just produce AIP in *S. aureus* was estimated to be high with 184 ATP for a single AgrD preprotein AIP (1). However, our data show that that the fitness advantage of *agr* mutants is independent of the assumed metabolic burden. First, an AIP nonproducer showed a fitness advantage in monoculture but interestingly not in competition with an AIP producer. Thus, AIP synthesis itself does not impose a fitness burden. Second, the syntheses of downstream targets (public goods) are also unlikely to drive evolution of *agr* mutants based on the metabolic burden to produce them. This is based on our observation that, under anaerobic conditions, significantly more public goods, such as PSMs or RNAIII regulated factors, are synthesized (Fig. 5). However, under this specific condition, the increased Agr activity has no impact on the fitness monitored either by growth (Fig. 5*A*) or in competition experiments (Fig. 4*D*). Of note, also for other QS systems, experimental evidence for the assumption that QS cheaters arise because of the metabolic cost is limited (45) and warrants revisiting. This observation conforms to the idea that the function and not production of a factor downstream of QS signaling imposes the fitness burden under aerobic conditions.

Increased Agr Activity under Hypoxia. Here, we demonstrated that Agr activity is increased during hypoxic growth, despite lower bacterial cell densities. Hypoxia results in significantly enhanced transcription of the main AgrA targets (RNAIII and *psm*), Hld synthesis, PSM-mediated protein release, and cell toxicity (Fig. 5). The results confirm recent data from Wilde et al. (47). It has been shown that oxidizing conditions induce disulphide bond formation of AgrA involving the conserved cysteine Cys-199 (51). Of note, the same residue also reacts with nitric oxide (58). Both oxidation and *S*-nitrosylation of Cys-199 were shown to inhibit DNA binding of AgrA to its cognate promoters. Therefore, under aerobic conditions, AgrA function might be partially inhibited through oxidation.

Agr/PSM Does Not Impose a Fitness Cost under Hypoxia Due to Diminished ROS Formation. Under aerobic conditions, the fitness cost could be linked to PSM expression. Under hypoxia, the higher level of PSMs does not affect fitness since bacteria are protected from the antimicrobial activity of PSMs. We could further show that PSM synthesis results in increased ROS formation (Fig. 6*B*). This explains the fitness burden of *psm*-positive strains under aerobic conditions only. However, it does not explain the fitness advantage of the RNAIII mutant. *AgrA* mutants were previously found to be more resistant toward certain kinds of oxidative stress which was linked to higher expression of the glutathione peroxidase BsaA (51, 59). The role of BsaA could not be confirmed here. However, other ROS protective factors might be up-regulated in the RNAIII mutant to compensate for PSM toxicity.

Conclusion and Outlook: Role of Agr QS In Vivo. Several epidemiological and virulence studies indicate that Agr activity is required only under certain infection settings (5, 42). Nevertheless, Agr activity is maintained in most colonizing isolates despite the obvious fitness disadvantage. This indicates that, on the population level, several mechanisms may have evolved to maintain the balance. The Agr system was found to be inactive during nose colonization (60), possibly due to Agr interference imposed by other staphylococci (57) in the skin microbiome. Many of the globally spreading haMRSA strains are characterized by low Agr activity (30) which could also be seen as a strategy to avoid *agr* mutant selection.

Aerobic growth conditions and the clinically relevant quinolone antibiotic ciprofloxacin accelerates the selection of *agr* mutants. Ciprofloxacin leads to induction of the SOS response and, thus, an increased mutation rate. However, ciprofloxacin might also favor *agr* mutations because they are better adapted to survive oxidative stress imposed by the antibiotic (59). Thus, ROS formation by the bacterium's own products (PSMs), ciprofloxacin, or other infection-related stresses, such as phagocytosis may favor the selection of QS mutants. PSMs have been shown to disrupt membrane potential via depolarization (49) which might be a trigger for ROS accumulation. Bacteria have evolved mechanisms to dampen Agr activity under such conditions by, e.g., AgrA oxidation/nitrosylation (51, 58) or inactivation of the AIP (55). Hypoxic conditions in contrast favor the maintenance of the WT population and even allow the hyperactivation of the system without imposing a fitness burden.

S. aureus is a major skin pathogen and the oxygen-driven tuning of the Agr system might especially be of importance to provide the pathogen with different features beneficial for disease progression. Under high O_2 conditions, such as at the skin surface, *agr* mutants are selected (33), and one may also speculate that this might be the source for *agr* mutants often found in bacteremic patients (34–36). On the other hand, Agr activity is crucial for pathogenicity in skin abscesses (42). Here, *S. aureus* is entrapped in a hypoxic environment in which the bacteria can now afford to increase Agr activity without the accompanied

fitness disadvantage. The increase in Agr-regulated toxins, such as PSMs may, thus, function to facilitate escape from the abscess. In this manner, the environmental oxygen might act to alter the bacterial perception of a self-inflicted insult, such as the PSMs in order to change the course of microbial evolution.

Materials and Methods

More information on the methods used in this study is available in *SI Appendix*.

Bacterial Strains and Growth Conditions. Strains and plasmids are listed in *SI Appendix*, Table S1. All *S. aureus* strains were grown in tryptic soy broth (TSB), and antibiotics at 3 μg/mL tetracycline, 10 μg/mL erythromycin, 150 μg/mL streptomycin, or 10 μg/mL chloramphenicol, were added to the respective resistant strains in the overnight cultures. For evolution experiments under aerobic or anaerobic environments, bacteria were transferred daily to an optical density OD_{600} of 0.05 with or without subinhibitory concentration of ciprofloxacin (0.125 μg/mL). All strains tested had the same minimum inhibitory concentration (MIC) of 0.25 μg/mL as determined by Etest (bioMérieux). For evolution experiments with antioxidants, the combination of 2,2′-bipyridyl and thiourea was used as described (59) but at lower concentrations of 1 and 100 mM, respectively. Cultures were evaluated on columbia agar with sheep blood (Oxoid) at indicated intervals (2, 3, 5, 10, 15, and 20 d) to determine the percentage of nonhemolytic variants that had accumulated within the population. For growth under anaerobic conditions, the cultures were incubated in an anaerobic jar with an anaerobic gas pack (Oxoid AnaeroGen, Thermo Scientific). This pack reduces ambient oxygen to below 0.1% within 2.5 h and increases carbon dioxide to 13% within 24 h. For hypoxic growth, the corks were replaced with rubber stoppers similar to that described previously (47). For growth under a microaerophilic environment, the Campy Pouch system (BD Diagnostics) was used to create an oxygen concentration of 5–15%.

Bacterial Competition. Bacterial strains were set up in competition in a 1:1 or 1:9 or 9:1 ratio at an initial OD_{600} of 0.05. The culture was transferred (1% v/v) daily to fresh media. At the end of the competition experiment, the 2 subpopulations were measured by their respective markers by resistance to streptomycin (150 μg/mL) or fluorescence (P*sarA*-Cerulean or P*sarA*-Venus).

Fluorescence of competing bacterial strains were measured in an automated reader (Tecan Infinite 200 PRO). For Venus, an excitation wavelength of 505 nm with a bandwidth of 9 nm and emission wavelength of 535 nm with a bandwidth of 20 nm were used. For Cerulean, an excitation wavelength of 434 nm with a bandwidth of 9 nm and emission wavelength of 485 nm with a bandwidth of 20 nm were used.

Growth Curves. Growth curves were generated using an automated reader (Tecan Infinite 200 PRO). Overnight cultures were diluted to an OD_{600} of 0.05. Measurements were made using either a 24-well flat-bottom or a 96-well U-bottom plate format (Greiner) with 1 mL and 100 μL culture volumes, respectively. In order to create a hypoxic environment, wells in the 96-well plates were sealed with an adhesive optical film (BZO Seal film; Biozym). Plates were incubated at 37 °C with a 3 mm orbital shaking amplitude. The OD_{600} was measured every 15 or 30 min.

Toxins and Cytoplasmic Proteins in Bacterial Supernatants. Overnight cultures were subcultured to OD_{600} 0.05 and then grown for ∼22 h under aerobic or hypoxic conditions. Bacterial supernatants were harvested and filtered using a 0.45 μm filter (Millipore) and analyzed for cytotoxic potential, hemolytic activity, extracellular toxins, and proteome analysis.

ROS Measurement. ROS measurements were performed as described (61) with the following modifications: 10×PBS pH7.4 (without calcium and magnesium; Gibco) was used to stop the reaction to yield the final dichlorofluorescin (DCF) reagent (2′,7′-DCF diacetate). Bacteria were harvested from overnight cultures (late stationary) or after 6 h of growth (early stationary). A 1 OD_{600} equivalent of bacteria was resuspended in 100 μL of DCF reagent and incubated for 40 min. Fluorescence was measured using an automated reader (Tecan Infinite 200 PRO) where an excitation wavelength of 488 nm with a bandwidth of 9 nm and emission wavelength of 515 nm with a bandwidth of 20 nm were used.

Statistical Analyses. All statistical analyses are based on biological replicates as detailed in the figure legends. Data were analyzed with one-way or two-way ANOVA. Tukey's or Bonferroni's posttests were used as appropriate. *P* values ≤0.05 were considered significant. All data show the mean and SEM except the cytotoxicity assay where mean and SD are depicted.

ACKNOWLEDGMENTS. We thank Vittoria Bisanzio, Isabell Samp, Janina Bayer, Alexander Mathias Ott, and Petra Horvatek for technical assistance. We thank Jan Liese for the gift of plasmids. The work was supported by Grants from the Deutsche Forschungsgemeinschaft TR766/A7, TR156/A01, and GRK1708 to C. W. and by infrastructural funding from the Deutsche Forschungsgemeinschaft (DFG), Cluster of Excellence EXC 2124 "Controlling Microbes to Fight Infections."

1. L. Keller, M. G. Surette, Communication in bacteria: An ecological and evolutionary perspective. *Nat. Rev. Microbiol.* **4**, 249–258 (2006).
2. M. Whiteley, S. P. Diggle, E. P. Greenberg, Progress in and promise of bacterial quorum sensing research. *Nature* **551**, 313–320 (2017).
3. R. G. Abisado, S. Benomar, J. R. Klaus, A. A. Dandekar, J. R. Chandler, Bacterial quorum sensing and microbial community interactions. *MBio* **9**, e01749-18 (2018). Erratum in: *MBio* **9**, e02331-17 (2018).
4. Ö. Özkaya, K. B. Xavier, F. Dionisio, R. Balbontín, Maintenance of microbial cooperation mediated by public goods in single and multiple traits scenarios. *J. Bacteriol.* **199**, JB.00297-17 (2017).
5. B. Shopsin, R. Copin, "Staphylococcus aureus adaptation during infection" in *Antimicrobial Resistance in the 21st Century*, I. W. Fong, D. Shlaes, K. Drlica, Eds. (Springer International Publishing, Cham, 2018), pp. 431–459.
6. K. Y. Le, M. Otto, Quorum-sensing regulation in staphylococci-an overview. *Front. Microbiol.* **6**, 1174 (2015).
7. K. L. Painter, A. Krishna, S. Wigneshweraraj, A. M. Edwards, What role does the quorum-sensing accessory gene regulator system play during Staphylococcus aureus bacteremia? *Trends Microbiol.* **22**, 676–685 (2014).
8. K. L. Asfahl, M. Schuster, Social interactions in bacterial cell-cell signaling. *FEMS Microbiol. Rev.* **41**, 92–107 (2017).
9. E. J. G. Pollitt, S. A. West, S. A. Crusz, M. N. Burton-Chellew, S. P. Diggle, Cooperation, quorum sensing, and evolution of virulence in Staphylococcus aureus. *Infect. Immun.* **82**, 1045–1051 (2014).
10. W. Paulander *et al*., The agr quorum sensing system in Staphylococcus aureus cells mediates death of sub-population. *BMC Res. Notes* **11**, 503 (2018).
11. W. Paulander *et al*., Antibiotic-mediated selection of quorum-sensing-negative Staphylococcus aureus. *MBio* **3**, e00459-12 (2013).
12. R. P. Novick, E. Geisinger, Quorum sensing in staphylococci. *Annu. Rev. Genet.* **42**, 541–564 (2008).
13. B. Wang, T. W. Muir, Regulation of virulence in Staphylococcus aureus: Molecular mechanisms and remaining puzzles. *Cell Chem. Biol.* **23**, 214–224 (2016).
14. J. S. Kavanaugh, A. R. Horswill, Impact of environmental cues on staphylococcal quorum sensing and biofilm development. *J. Biol. Chem.* **291**, 12556–12564 (2016).
15. D. Bronesky *et al*., Staphylococcus aureus RNAIII and its regulon link quorum sensing, stress responses, metabolic adaptation, and regulation of virulence gene expression. *Annu. Rev. Microbiol.* **70**, 299–316 (2016).
16. L. Janzon, S. Löfdahl, S. Arvidson, Identification and nucleotide sequence of the delta-lysin gene, hld, adjacent to the accessory gene regulator (agr) of Staphylococcus aureus. *Mol. Gen. Genet.* **219**, 480–485 (1989).
17. L. Janzon, S. Arvidson, The role of the delta-lysin gene (hld) in the regulation of virulence genes by the accessory gene regulator (agr) in Staphylococcus aureus. *EMBO J.* **9**, 1391–1399 (1990).
18. S. Y. Queck *et al*., RNAIII-independent target gene control by the *agr* quorum-sensing system: Insight into the evolution of virulence regulation in *Staphylococcus aureus*. *Mol. Cell* **32**, 150–158 (2008).
19. G. Y. Cheung, H. S. Joo, S. S. Chatterjee, M. Otto, Phenol-soluble modulins–critical determinants of staphylococcal virulence. *FEMS Microbiol. Rev.* **38**, 698–719 (2014).
20. A. Peschel, M. Otto, Phenol-soluble modulins and staphylococcal infection. *Nat. Rev. Microbiol.* **11**, 667–673 (2013).
21. A. L. Cogen *et al*., Selective antimicrobial action is provided by phenol-soluble modulins derived from Staphylococcus epidermidis, a normal resident of the skin. *J. Invest. Dermatol.* **130**, 192–200 (2010).
22. H. S. Joo, G. Y. Cheung, M. Otto, Antimicrobial activity of community-associated methicillin-resistant Staphylococcus aureus is caused by phenol-soluble modulin derivatives. *J. Biol. Chem.* **286**, 8933–8940 (2011).
23. K. Schlatterer *et al*., The mechanism behind bacterial lipoprotein release: Phenol-soluble modulins mediate toll-like receptor 2 activation via extracellular vesicle release from Staphylococcus aureus. *MBio* **9**, e01851-18 (2018).
24. X. Wang, C. D. Thompson, C. Weidenmaier, J. C. Lee, Release of Staphylococcus aureus extracellular vesicles and their application as a vaccine platform. *Nat. Commun.* **9**, 1379 (2018).
25. M. S. Bojer, S. Lindemose, M. Vestergaard, H. Ingmer, Quorum sensing-regulated phenol-soluble modulins limit persister cell populations in *Staphylococcus aureus*. *Front. Microbiol.* **9**, 255 (2018).
26. T. Xu *et al*., The agr quorum sensing system represses persister formation through regulation of phenol soluble modulins in *Staphylococcus aureus*. *Front. Microbiol.* **8**, 2189 (2017).

27. S. S. Chatterjee *et al*., Essential Staphylococcus aureus toxin export system. *Nat. Med.* **19**, 364–367 (2013).
28. P. Piewngam *et al*., Pathogen elimination by probiotic Bacillus via signalling interference. *Nature* **562**, 532–537 (2018).
29. B. J. Berube, J. Bubeck Wardenburg, Staphylococcus aureus α-toxin: Nearly a century of intrigue. *Toxins (Basel)* **5**, 1140–1166 (2013).
30. R. Wang *et al*., Identification of novel cytolytic peptides as key virulence determinants for community-associated MRSA. *Nat. Med.* **13**, 1510–1514 (2007).
31. C. Goerke *et al*., Direct quantitative transcript analysis of the agr regulon of *Staphylococcus aureus* during human infection in comparison to the expression profile *in vitro*. *Infect. Immun.* **68**, 1304–1311 (2000).
32. C. M. Suligoy *et al*., Mutation of agr is associated with the adaptation of *Staphylococcus aureus* to the host during chronic osteomyelitis. *Front. Cell. Infect. Microbiol.* **8**, 18 (2018).
33. G. Soong *et al*., Methicillin-resistant Staphylococcus aureus adaptation to human keratinocytes. *MBio* **6**, e00289-15 (2015).
34. V. G. Fowler, Jr *et al*., Persistent bacteremia due to methicillin-resistant Staphylococcus aureus infection is associated with agr dysfunction and low-level in vitro resistance to thrombin-induced platelet microbicidal protein. *J. Infect. Dis.* **190**, 1140–1149 (2004).
35. S. G. Giulieri *et al*., Genomic exploration of sequential clinical isolates reveals a distinctive molecular signature of persistent Staphylococcus aureus bacteraemia. *Genome Med.* **10**, 65 (2018).
36. B. C. Young *et al*., Severe infections emerge from commensal bacteria by adaptive evolution. *eLife* **6**, e30637 (2017).
37. M. L. Schweizer *et al*., Increased mortality with accessory gene regulator (agr) dysfunction in Staphylococcus aureus among bacteremic patients. *Antimicrob. Agents Chemother.* **55**, 1082–1087 (2011).
38. W. Schröder, C. Goerke, C. Wolz, Opposing effects of aminocoumarins and fluoroquinolones on the SOS response and adaptability in Staphylococcus aureus. *J. Antimicrob. Chemother.* **68**, 529–538 (2013).
39. J. M. Butterfield *et al*., Predictors of agr dysfunction in methicillin-resistant Staphylococcus aureus (MRSA) isolates among patients with MRSA bloodstream infections. *Antimicrob. Agents Chemother.* **55**, 5433–5437 (2011).
40. C. Goerke *et al*., High phenotypic diversity in infecting but not in colonizing *Staphylococcus aureus* populations. *Environ. Microbiol.* **9**, 3134–3142 (2007).
41. K. E. Traber *et al*., *Agr* function in clinical *Staphylococcus aureus* isolates. *Microbiology* **154**, 2265–2274 (2008).
42. L. He, K. Y. Le, B. A. Khan, Resistance to leukocytes ties benefits of quorum sensing dysfunctionality to biofilm infection. *Nat. Microbiol.* **4**, 1114–1119 (2019).
43. S. E. George *et al*., Phenotypic heterogeneity and temporal expression of the capsular polysaccharide in Staphylococcus aureus. *Mol. Microbiol.* **98**, 1073–1088 (2015).
44. E. Geisinger, T. W. Muir, R. P. Novick, *Agr* receptor mutants reveal distinct modes of inhibition by staphylococcal autoinducing peptides. *Proc. Natl. Acad. Sci. U.S.A.* **106**, 1216–1221 (2009).
45. A. Ruparell *et al*., The fitness burden imposed by synthesising quorum sensing signals. *Sci. Rep.* **6**, 33101 (2016).
46. A. Carreau, B. El Hafny-Rahbi, A. Matejuk, C. Grillon, C. Kieda, Why is the partial oxygen pressure of human tissues a crucial parameter? Small molecules and hypoxia. *J. Cell. Mol. Med.* **15**, 1239–1253 (2011).
47. A. D. Wilde *et al*., Bacterial hypoxic responses revealed as critical determinants of the host-pathogen outcome by TnSeq analysis of Staphylococcus aureus invasive infection. *PLoS Pathog.* **11**, e1005341 (2015).
48. E. Stevens, M. Laabei, S. Gardner, G. A. Somerville, R. C. Massey, Cytolytic toxin production by Staphylococcus aureus is dependent upon the activity of the protoheme IX farnesyltransferase. *Sci. Rep.* **7**, 13744 (2017).
49. P. Ebner *et al*., Non-classical protein excretion is boosted by PSMα-induced cell leakage. *Cell Rep.* **20**, 1278–1286 (2017).
50. D. Hanzelmann *et al*., Toll-like receptor 2 activation depends on lipopeptide shedding by bacterial surfactants. *Nat. Commun.* **7**, 12304 (2016).
51. F. Sun *et al*., Quorum-sensing agr mediates bacterial oxidation response via an intramolecular disulfide redox switch in the response regulator AgrA. *Proc. Natl. Acad. Sci. U.S.A.* **109**, 9095–9100 (2012).
52. M. Wang, A. L. Schaefer, A. A. Dandekar, E. P. Greenberg, Quorum sensing and policing of Pseudomonas aeruginosa social cheaters. *Proc. Natl. Acad. Sci. U.S.A.* **112**, 2187–2191 (2015).
53. M. Pynnonen, R. E. Stephenson, K. Schwartz, M. Hernandez, B. R. Boles, Hemoglobin promotes Staphylococcus aureus nasal colonization. *PLoS Pathog.* **7**, e1002104 (2011).
54. P. R. Hall *et al*., Nox2 modification of LDL is essential for optimal apolipoprotein B-mediated control of agr type III Staphylococcus aureus quorum-sensing. *PLoS Pathog.* **9**, e1003166 (2013).
55. J. M. Rothfork *et al*., Inactivation of a bacterial virulence pheromone by phagocyte-derived oxidants: New role for the NADPH oxidase in host defense. *Proc. Natl. Acad. Sci. U.S.A.* **101**, 13867–13872 (2004).
56. A. E. Paharik *et al*., Coagulase-negative staphylococcal strain prevents Staphylococcus aureus colonization and skin infection by blocking quorum sensing. *Cell Host Microbe* **22**, 746–756.e5 (2017).
57. M. R. Williams *et al*., Quorum sensing between bacterial species on the skin protects against epidermal injury in atopic dermatitis. *Sci. Transl. Med.* **11**, eaat8329 (2019).
58. R. Urbano *et al*., Host nitric oxide disrupts microbial cell-to-cell communication to inhibit staphylococcal virulence. *Cell Host Microbe* **23**, 594–606.e7 (2018).
59. K. Kumar, J. Chen, K. Drlica, B. Shopsin, Tuning of the lethal response to multiple stressors with a single-site mutation during clinical infection by *Staphylococcus aureus*. *MBio* **8**, e01476-17 (2017).
60. M. Burian, C. Wolz, C. Goerke, Regulatory adaptation of *Staphylococcus aureus* during nasal colonization of humans. *PLoS One* **5**, e10040 (2010).
61. H. Y. Kim, J. Go, K. M. Lee, Y. T. Oh, S. S. Yoon, Guanosine tetra- and pentaphosphate increase antibiotic tolerance by reducing reactive oxygen species production in *Vibrio cholerae*. *J. Biol. Chem.* **293**, 5679–5694 (2018).

PNAS
www.pnas.org

Supplementary Information for

Oxidative stress drives the selection of quorum sensing mutants in the *Staphylococcus aureus* population

Shilpa Elizabeth George, Jennifer Hrubesch, Inga Breuing, Naisa Vetter, Natalya Korn, Katja Hennemann, Lisa Bleul, Matthias Willmann, Patrick Ebner, Friedrich Götz, Christiane Wolz

Interfaculty Institute of Microbiology and Infection Medicine, University of Tübingen, Germany

Christiane Wolz
Email: christiane.wolz@med.uni-tuebingen.de

This PDF file includes:

Supplementary text
Figs. S1 to S6
Tables S1 to S2
References for SI reference citations

www.pnas.org/cgi/doi/10.1073/pnas.1902752116

Supplementary Information Text

Materials and Methods

Strain Construction.

Plasmids and oligonucleotides used are listed in Tables S1 and S2, respectively. The *agr*-constitutive strain (HG001 *agrC*^{R238H}) and the *agrBCDA-hld* deletion mutant (HG001 *agr*) were constructed as described before using mutagenesis plasmids pCG383 and pCG391, respectively(1). The marker-less RNAIII deletion mutant (HG001 RNAIII) and AIP deletion mutant (HG001 *agrD*) were obtained using the temperature sensitive mutagenesis vector pIMAY (2). For RNAIII deletion, flanking regions were amplified using the oligonucleotides RNAIIIGibmutfor, RNAIIIGibdeletionrev and RNAIIIGibdeletionfor, RNAIIIGibmutrev. Both amplicons were cloned into pIMAY by Gibson assembly. The resulting plasmid pCG591 was transformed into RN4220 and then transduced into *S. aureus* strain HG001 or HG001-*agrC*^{R238H}. Allelic exchange and chromosomal deletion was performed as described (2). The deletion was verified by PCR using oligonucleotides flanking the deleted region.

For the 23bp AIP deletion within *agrD* (HG001 *agrD*), flanking regions were amplified using the oligonucleotides agrDmutgibfor, agrDdelgibrev and agrDdelgibfor, agrDmutgibrev. After integrating these amplicons by Gibson assembly into the pIMAY vector, the resulting plasmid pCG595 was transformed into RN4220. Subsequent to transduction into strain HG001, mutagenesis was performed. The deletion was verified by PCR using oligonucleotides spanning the deleted region and by sequencing the region of interest. Fluorescent derivatives of strains were created by introducing the plasmids pJL92 or pJL94 into RN4220 and then φ11-phage-mediated transduction into final strains; HG001, HG001 *agr* and HG001 *agrD*. Deletions in *psmα*, *psmβ* or both were also transduced from RN4220 background into final *S. aureus* strain HG001 *agrC*^{R238H}. The *bsaA* gene containing a transposon insertion was similarly transduced from the USA300 JE2 background (NE1730) into the HG001 *agrC*^{R238H} RNAIII double mutant. All transductants were verified by PCR using oligonucletetides spanning the mutations.

Spontaneous streptomycin-resistant derivatives of strains were selected by plating overnight cultures on TSA agar plates containing either streptomycin 150 μg/ml or 500 μg/ml. Colonies were screened for an unaltered phenotype on blood agar and by re-streaking on streptomycin-containing agar plates to confirm resistance. Colonies were confirmed to be unaltered in their growth characteristics relative to the original strain.

Re-Sequencing.

Bacterial isolates from evolution experiments were grown in TSB and $5x10^9$ cells were harvested. Genomic DNA was isolated using a standard kit (Qiagen, genomic tip 100/G) with modifications

to the protocol as follows. In the cell lysis step, Lysostaphin at a final concentration of 75 µg/ml was added. After cell lysis, proteinase K was added at a final concentration of 0.57 mg/ml. Precipitated DNA which was spooled using a glass rod was re-suspended in 200 µl nuclease-free water.

DNA quality was checked by agarose gel electrophoresis and UV spectrometer. Genomic DNA from bacterial isolates with an OD 260/280≥1.8, OD260/230≥1.2 and a concentration of at least 10 ng/µl was sent to GATC Biotech (Konstanz, Germany). Library preparation was performed by GATC Biotech using an automated library preparation protocol and sequenced on an Illumina HiSeq 2500 in a 250 bp paired-end mode. Bad quality bases were trimmed and adaptors removed using Trimmomatic (version 0.35)(3) with default criteria to generate high quality fastq files. After a subsequent quality control check using FastQC (version 0.11.5), we used SPANDx (version 3.1)(4) for indel calling with default options except a low depth criterion of 40. For SNP calling, we used BWA-MEM (version 0.6.2) (5) for mapping and subsequently SAMtools (version 1.2) (6) for SNP detection and filtering. Three non-haemolytic isolates that were not identified to be *agr* mutants by the SNP and indel calling pipeline were re-confirmed by PCR and sequencing.

RNA Isolation and Quantification.

Overnight HG001 cultures were inoculated into fresh medium at OD_{600} 0.05 and then grown under aerobic and hypoxic conditions. Bacteria were harvested at various time-points post-inoculation; 2, 3, 4, 5, 6, 10 and 24 h. For transcript analysis, approximately 10^9 *S. aureus* cells were lysed in 1 ml TRIzol reagent (Life Technologies, Germany) with 0.5 ml of zirconia-silica beads (0.1 mm diameter) in a high-speed homogenizer. RNA was isolated as described in the instructions provided by the manufacturer of TRIzol (Life Technologies). To quantify *bsaA* expression, bacterial strains were grown to OD_{600} of 3 and harvested for RNA isolation. qRT-PCR to quantify *gyrB*, *RNAIII*, *psmα*, *pmt* and *bsaA* mRNAs were performed using the Quanti Fast SYBR-Green RT-PCR kit (Qiagen) and standard curves generated (for all except for *pmt* and *bsaA*) using 10-fold serial dilutions (10^4 to 10^8 copies) of specific in vitro transcribed RNA standard molecules (7). The number of copies of each sample transcript was determined with the aid of the LightCycler software and the mRNA expressed in reference to copies of *gyrB*.

To quantify *agr* expression in co-culture, wild type and $agrA^{R165H}$ strains were set up in 1:1 or 1:9 ratios as in competition experiments. These cultures were grown to OD_{600} of 3 and harvested for RNA isolation. qRT-PCR was performed to quantify *RNAIII* mRNA expressed in reference to gyrB, and normalized to the wild type pure culture.

Protein and Western Blot Analysis.

Equal volumes of bacterial supernatants were precipitated with TCA. RunBlue LDS sample buffer (Expedeon) containing additional 100mM DTT was added to the samples and then heated for 10 min at 95°C. Samples were loaded onto 16% SDS-PAGE gel (Expedeon) for electrophoresis and either stained with Coommassie or transferred to polyvinylidene difluoride (PVDF) membrane (Biorad) by wet transfer in Tris-Glycine-SDS buffer (TGS buffer, Expedeon). Membrane was blocked with 5% non-fat dried milk powder in 1x Tris-buffered saline containing 0.05% Tween20 for 1 h, before incubation with primary rabbit anti-Hld antibody (Abgent), followed by goat anti-rabbit HRP-conjugated secondary antibody. Membrane blot was developed using Pierce ECL Western Blotting Substrate (Thermo Scientific). Western blot analysis for aldolase (FbaA) was performed as described before (8).

Cytotoxicity Assay.

Cytotoxicity assay was performed as described (9) with the exception that $1x10^5$ THP1 cells were seeded in 96-well cell culture plates in a final volume of 100 µl. Differentiated THP1 macrophages were treated with 200 µl of each bacterial supernatant. THP1 cells with medium was used as negative control and THP1 cells treated with 1xPBS containing 1% TritonX-100 was used as a positive control. Cytotoxic potential of the samples was determined from THP1-cell supernatants after 3 h using Cytotoxicity detection Kit (Roche) following instructions of the manufacturer.

Analysis of Colony Haemolysis under Aerobic and Anaerobic Growth.

Bacterial colonies growing under either aerobic or anaerobic conditions on agar containing 5% sheep blood were analysed for haemolysis after ~ 15 h of growth in either environment. Images of bacterial colonies on agar plates were analysed in Fiji (10). The colonies on each image were circumscribed and so also the zone of haemolysis which included the area occupied by the colony. The area corresponding to these regions of interest was used to calculate the haemolytic zone relative to the size of single colonies.

Haemolysis Assay.

Haemolytic activities of bacterial culture supernatants were measured as described (11). Serial dilutions of culture supernatants were incubated with sheep red blood cells for 4 h at 37 °C. Subsequently the absorbance of the assay supernatants was measured at 430nm.

Toxicity of PSMs.

The synthetic PSM peptide PSMα3 was synthesized in its N-formylated form by and purchased from Apeptide (Shanghai, China). The peptide had a purity of at least 95%. The synthetic PSM

peptide was dissolved in 50% DMSO and aliquots were stored at -20°C. Different concentrations of PSMα3 (100, 50, 25, 10 μg/ml) was added to HG001 *agr* bacteria (adjusted to OD_{600} 0.1). Growth was measured using an automated reader (Tecan Infinite 200 PRO).

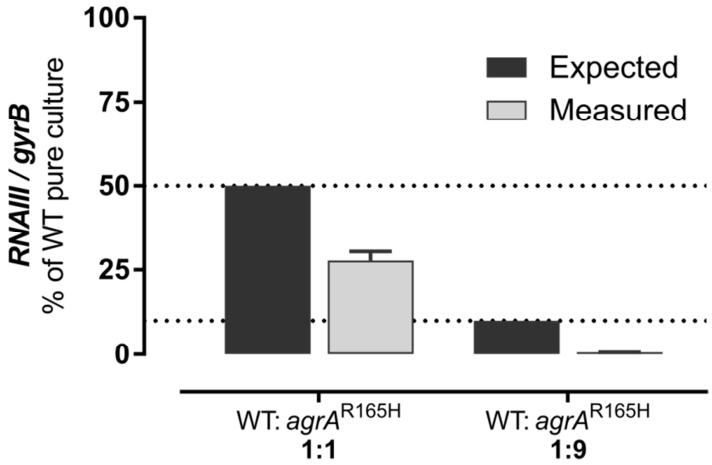

Figure S1. Agr activity depends on critical mass of producers in the population.

Wild type was co-cultured under aerobic environment with *agrA*^{R165H} starting at 1:1 and 1:9 ratios. At OD_{600} of 3, total RNA was isolated. *RNAIII* mRNA was quantified by qRT-PCR with reference to *gyrB* and then normalized to wild type pure culture. Error bars indicate SEM (n = 3).

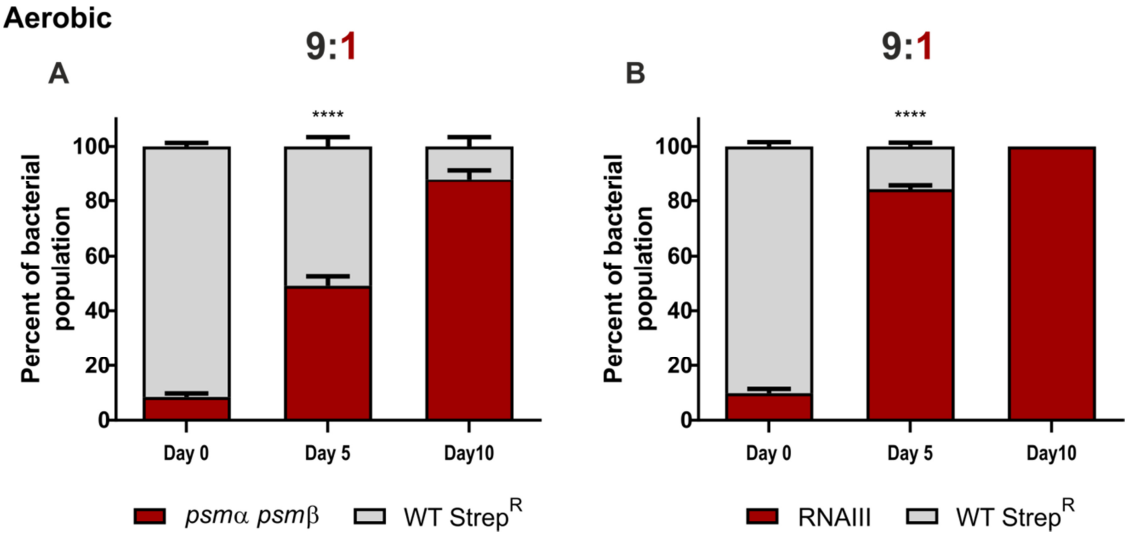

Figure S2. PSM and RNAIII mutants have a fitness advantage in co-culture with the wild type. Streptomycin-resistant HG001 was competed for 10 days with (A) *psmα psmβ* or (B) RNAIII starting at a ratio of 9:1 under aerobic conditions. Percentage of each bacterial sub-population was determined based on streptomycin resistance. Error bars indicate SEM (n = 3). Asterisks indicate statistical significance in comparison to Day 0. Statistical significance determined by repeated measures two-way ANOVA with Tukey's post-test. *P ≤ 0.05, **P ≤ 0.01, ***P ≤ 0.001, ****P ≤ 0.0001.

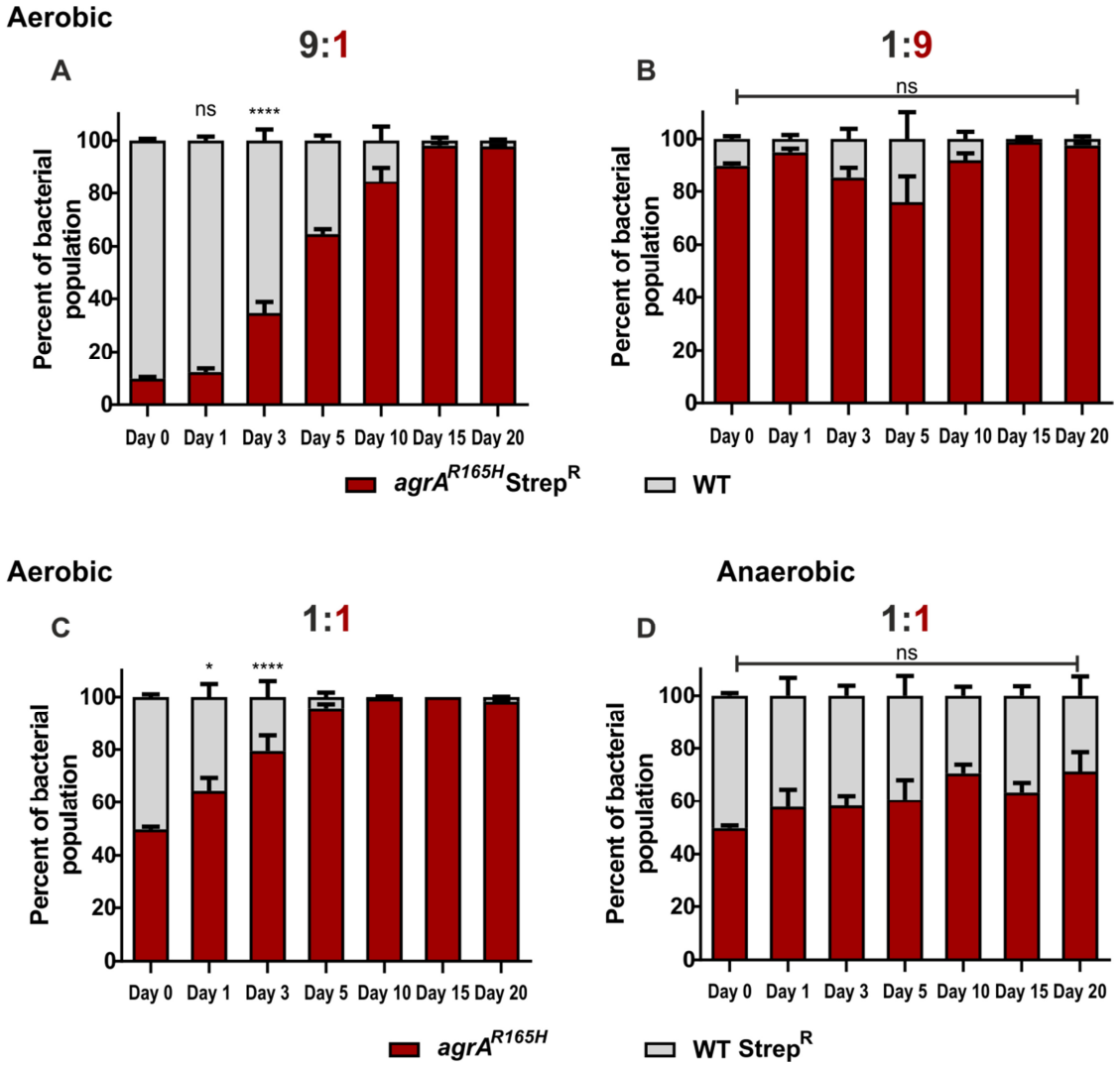

Figure S3. Competition under aerobic and anaerobic conditions. Wild type was competed for 20 days under aerobic environment with the streptomycin-resistant *agrA*^{R165H} starting at (A) 9:1 and (B) 1:9 ratios. (C and D) Streptomycin-resistant wild type was competed for 20 days with the *agrA*^{R165H} starting at 1:1 ratio under (C) aerobic and (D) anaerobic environments. Error bars indicate SEM (n = 3). Asterisks indicate statistical significance in comparison to Day 0. Statistical significance determined by repeated measures two-way ANOVA with Tukey's post-test. *P ≤ 0.05, **P ≤ 0.01, ***P ≤ 0.001, ****P ≤ 0.0001.

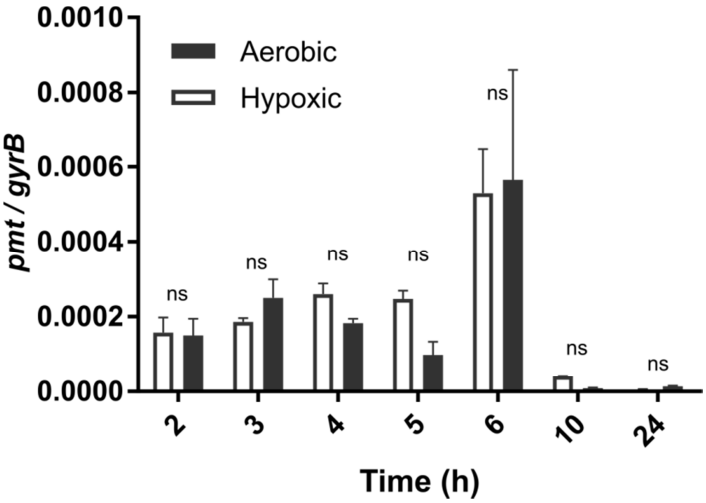

Figure S4. Transcription levels of PSM transporter not influenced by hypoxia.

HG001 cultures were harvested at different time-points (2, 3, 4, 5, 6, 10, 24 h) during growth under aerobic and hypoxic environments. Total RNA was isolated. Relative levels of *pmt* mRNA was determined by qRT-PCR with reference to *gyrB*. Error bars indicate SEM (n = 3). Statistical significance determined by repeated measures two-way ANOVA with Bonferroni's post-test. *P ≤ 0.05, **P ≤ 0.01, ***P ≤ 0.001, ****P ≤ 0.0001.

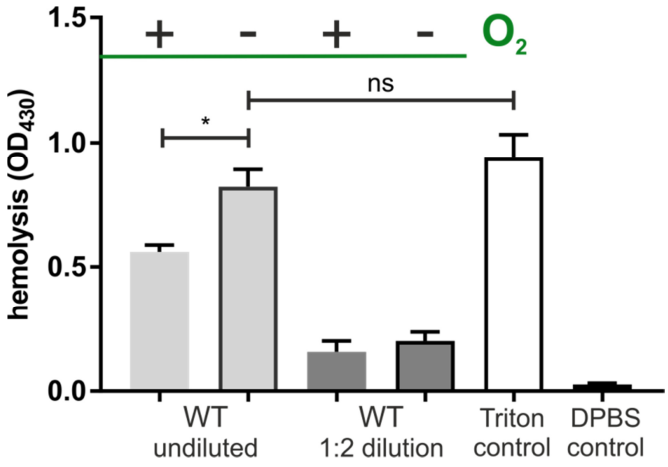

Figure S5. Increased haemolytic activity in low oxygen environments.

Serial dilutions of bacterial supernatants from HG001 cultures grown either aerobically or under hypoxic conditions were analysed for haemolytic activity using sheep blood. Negative control, DPBS; positive control, 1% Triton-X100 in DPBS. Of note, these values were not adjusted for bacterial density. Error bars indicate SEM (n = 3). Statistical significance determined by one-way ANOVA with Tukey's post-test. *P ≤ 0.05, **P ≤ 0.01, ***P ≤ 0.001, ****P ≤ 0.0001.

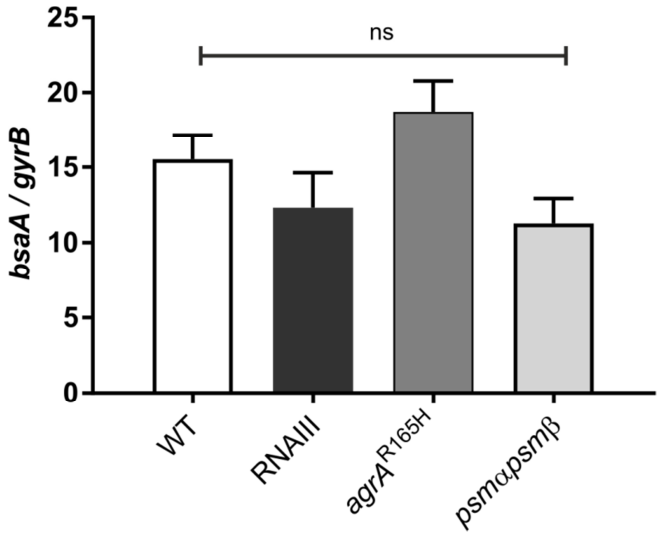

Figure S6. Transcription levels of *bsaA* not influenced by *agr* or RNAIII deletion.

Bacterial strains HG001, RNAIII, $agrA^{R165H}$ and *psmα psmβ* cultures were grown aerobically till OD_{600} of 3 and harvested. Total RNA was isolated. Relative levels of *bsaA* mRNA was determined by qRT-PCR with reference to *gyrB*. Error bars indicate SEM (n = 3). Statistical significance determined by one-way ANOVA with Tukey's post-test. *P ≤ 0.05, **P ≤ 0.01, ***P ≤ 0.001, ****P ≤ 0.0001.

Table S1. Bacterial strains and plasmids.

Strain or plasmid	Description	Reference
Strains		
E. coli		
One Shot TOP10	Competent *E. coli* for plasmid transformation	Invitrogen
S. aureus		
RN4220	Restriction-deficient *S. aureus* strain	(12)
HG001	*rsbU*-repaired derivative of RN1 (=8325)	(13)
HG001 Strep^R	HG001, spontaneous streptomycin resistance	This work
agrA^{R165H}	HG001, Agr defective isolate	This work
agrA^{R165H} Strep^R	HG001, Agr defective isolate, spontaneous streptomycin resistance	This work
agr::tetM	HG001, *agr*::*tetM*	(14)
agr	HG001, Δ*agr*, markerless deletion of *agrBDCA* and *hld*	This work
agrC^{R238H}	HG001 with constitutively on *agrC, agrC*^{R238H}	This work
psmα	HG001 *psmα1-4::tetM*	(14)
psmβ	HG001 *psmβ1-2::ermC*	(14)
psmα psmβ	HG001 *psmα1-4::tetM, psmβ1-2::ermC*	(14)
RN4220 *psmα*	RN4220 *psmα1-4::tetM*	(14)
RN4220 *psmβ*	RN4220 *psmβ1-2::ermC*	(14)
agrD	HG001 agrD ΔAIP	This work
RNAIII	HG001, ΔRNAIII	This work
agrC^{R238H} RNAIII	*agrC*^{R238H}, ΔRNAIII	This work
agrC^{R238H} *psmα*	*agrC*^{R238H}, *psmα1-4::tetM*	This work
agrC^{R238H} *psmβ*	*agrC*^{R238H}, *psmβ1-2::ermC*	This work
agrC^{R238H} *psmα psmβ*	*agrC*^{R238H}, *psmα1-4::tetM, psmβ1-2::ermC*	This work
WT_{CER}	HG001, pJL92, chloro^R	This work
WT_{VEN}	HG001, pJL94, chloro^R	This work
agr_{VEN}	HG001, Δ*agr*, pJL94, chloro^R	This work
$agrD_{VEN}$	HG001 agrD, pJL94, chloro^R	This work
NE1730	USA300 JE2, *bsaA*::*bursa aurealis*, Nebraska Transposon Mutant Library	(15)
agrC^{R238H} RNAIII *bsaA*	*agrC*^{R238H}, ΔRNAIII, *bsaA*::*bursa aurealis*	This work

Plasmids		
pBASE6	Suicide mutagenesis vector	(14)
pIMAY	Suicide mutagenesis vector, Allelic exchange plasmid	(2)
pCG383	pBASE6 vector *agrC*-mutation , $agrC^{R238H}$	(1)
pCG391	pBASE6 vector with regions flanking RNAIII	(1)
pCG591	pIMAY vector with regions flanking AIP I within *agrD*	This work
pCG595	pIMAY vector with regions flanking AIP I within *agrD*	This work
pJL92	P*sarA-cerulean*, cat194 (based on pJL76 with exchanged resistance cassette)	Gift from Jan Liese, (16)
pJL94	P*sarA-venus*, cat194 (based on pJL77 with changed exchanged resistance cassette)	Gift from Jan Liese, (16)

Table S2. Oligonucleotides.

Description/Purpose	Template	Name	Sequence
RNAIII deletion	USA300 JE2	RNAIIIGibmutfor	TCGATAAGCTTGATATCGTTTTTCATTTATTAAACATTTAGCTGA
		RNAIIIGibdeletionrev	TTAATATAACTGTTGGAAAAGGTCAAAAAATT
		RNAIIIGibdeletionfor	CCTTTTCCAACAGTTATATTAAAACATGCTAAAAGCA
		RNAIIIGibmutrev	GATCCCCCGGGCTGCAGGCTTCTATTATGATGCCTAATTGAATGA
	HG001 RNAIII	agr2742	GCGAAGTCATAATCAACAAAA
		agr114	AATGCTGAAGTAGATGTA
		pIMAYcontrolfor	CCAGCCCCCTCACTACAT
		pIMAYcontrolrev	ATCACCCGACGCACTTTG
agrD mutant (AIP deletion)	HG001	agrDmutgibfor	TCGATAAGCTTGATATCGGCAATATAATGATAAAAGATTGTACT
		agrDdelgibrev	ACTTCATCCAGCTGCGATGTTACCAATGT
		agrDdelgibfor	ATCGCAGCTGGATGAAGTTGAAGTACCAAAAGA
		agrDmutgibrev	GATCCCCCGGGCTGCAGGATATTTCATCTCTTTAAGGAGAA
	HG001 *agrD*	agr1801	ACCAGTTTGCCACGTATC
		agr2742	GCGAAGTCATAATCAACAAAA
		pIMAYcontrolfor	CCAGCCCCCTCACTACAT
		pIMAYcontrolrev	ATCACCCGACGCACTTTG
		HG001AIPfor	AGTACTTGTGACTTCATAATGGA
		agr3258	CGAATGTATTCTGAAAGTGTC
		agr1523	AAATTAAACAACTCATCA
		HG001AIPrev	TCCATTATGAAGTCACAAGTACT
gyr-qt RT PCR		gyr297	TTAGTGTGGGAAATTGTCGATAAT
		gyr574	AGTCTTGTGACAATGCGTTTACA
RNAIII-qt RT PCR		agr1189	CGATGTTGTTTACGATAGC
		agr1436	CGACACAGTGAACAAATTC
psmα-qt RT PCR		psm2715	TCATCGCTGGCATCATTA
		psm2391	CATCGTTTTGTCCTCCTG
pmt-qt RT PCR		pmtLCfor	TTTGTTAAGGAGCAAGATAGTTCTATTTT
		pmtLCrev	AACATTACTTAATTCTATGGCATTCATGA
bsaA mutant	HG001 $agrC^{R238H}$ RNAIII *bsaA*	bsaAfor	AATACAAAGATCAAGGGTTTGTAATTCTA
		bsaArev	AACTTAGTGAAATTCCATTTGATTTTCTC
		tnbuster	GCTTTTTCTAAATGTTTTTTAAGTAAATCAAGTAC

SI References

1. George SE, *et al.* (2015) Phenotypic heterogeneity and temporal expression of the capsular polysaccharide in Staphylococcus aureus. *Molecular microbiology* 98(6):1073-1088.
2. Monk IR, Shah IM, Xu M, Tan M-W, & Foster TJ (2012) Transforming the untransformable: application of direct transformation to manipulate genetically Staphylococcus aureus and Staphylococcus epidermidis. *mBio* 3(2):e00277-00211.
3. Bolger AM, Lohse M, & Usadel B (2014) Trimmomatic: a flexible trimmer for Illumina sequence data. *Bioinformatics* 30(15):2114-2120.
4. Sarovich DS & Price EP (2014) SPANDx: a genomics pipeline for comparative analysis of large haploid whole genome re-sequencing datasets. *BMC Research Notes* 7(1):618.
5. Li H & Durbin R (2010) Fast and accurate long-read alignment with Burrows–Wheeler transform. *Bioinformatics* 26(5):589-595.
6. Li H, *et al.* (2009) The Sequence Alignment/Map format and SAMtools. *Bioinformatics* 25(16):2078-2079.
7. Burian M, Wolz C, & Goerke C (2010) Regulatory adaptation of *Staphylococcus aureus* during nasal colonization of humans. *PloS one* 5(4):e10040.
8. Ebner P, *et al.* (2017) Non-classical Protein Excretion Is Boosted by PSMalpha-Induced Cell Leakage. *Cell reports* 20(6):1278-1286.
9. Munzenmayer L, *et al.* (2016) Influence of Sae-regulated and Agr-regulated factors on the escape of Staphylococcus aureus from human macrophages. *Cellular microbiology* 18(8):1172-1183.
10. Schindelin J, *et al.* (2012) Fiji: an open-source platform for biological-image analysis. *Nature methods* 9(7):676-682.
11. Cheung GY, *et al.* (2010) Staphylococcus epidermidis strategies to avoid killing by human neutrophils. *PLoS pathogens* 6(10):e1001133.
12. Kreiswirth BN, *et al.* (1983) The toxic shock syndrome exotoxin structural gene is not detectably transmitted by a prophage. *Nature* 305(5936):709-712.
13. Herbert S, *et al.* (2010) Repair of global regulators in *Staphylococcus aureus* 8325 and comparative analysis with other clinical isolates. *Infection and immunity* 78(6):2877-2889.
14. Geiger T, *et al.* (2012) The stringent response of *Staphylococcus aureus* and its impact on survival after phagocytosis through the induction of intracellular PSMs expression. *PLoS pathogens* 8(11):e1003016.
15. Fey PD, *et al.* (2013) A genetic resource for rapid and comprehensive phenotype screening of nonessential Staphylococcus aureus genes. *mBio* 4(1):e00537-00512.
16. Liese J, Rooijakkers SH, van Strijp JA, Novick RP, & Dustin ML (2013) Intravital two-photon microscopy of host-pathogen interactions in a mouse model of *Staphylococcus aureus* skin abscess formation. *Cellular microbiology* 15(6):891-909.

Acknowledgements

My deepest thanks to,

- My supervisor, Prof. Christiane Wolz for the close mentoring and guidance. Thank you for encouraging and nurturing my interest in different projects and methods. Thank you for providing the opportunity and freedom to learn from and collaborate with the larger scientific community especially through the conferences and workshops that I have had the privilege to attend.
- My second supervisor Prof. Andreas Peschel for taking the time to review my work.
- Former and current members of the AG Wolz for the highs (and lows) over the years. Thanks for the support and a great working environment. Thank you Petra, Vitty, Carina, Esther, Janina, Andrea, Lisa, Daniela, Fabio, Isa and Christina for the great time both in and out of the lab.
- Ellen and Gabriela for their support during my early days in Tübingen.
- Natalya for your friendship and the tremendous support throughout my PhD.
- The students and collaboration partners that I have had the privilege and joy to work with. Thank you Inga, Jenny, Esther, Mandy, Ale, Rosa, Naisa, Katja, Aylin, Alex and Anna.
- Colleagues and group leaders within the RTG1708 (Bacterial Survival Strategies) as well as the SFB766 (Bacterial Cell Envelope) for the great learning opportunities, lively interaction and providing both encouragement as well as criticism.
- My dearest family – for their unwavering support and faith.